

Université du Québec  
INRS - Institut Armand-Frappier  
Centre en Recherche de Santé Humaine

**IDENTIFICATION PAR BANQUE PHAGIQUE  
DE PEPTIDES AYANT UN POTENTIEL THÉRAPEUTIQUE  
ANTI-CANCÉREUX**

Par  
Mikhail Popkov

Thèse présentée pour l'obtention  
du grade de Philosophiae doctor (Ph.D.)  
en virologie et immunologie

Membres du jury: Daniel Oth, président  
Rosemonde Mandeville, directeur de recherche  
Claude Perreault, Hôpital Maisonneuve, jury externe  
Richard Béliveau, UQAM, jury externe

Hiver 2001

© droits réservés de Mikhail Popkov, 2001

## RÉSUMÉ SUBSTANTIEL

En dépit des progrès considérables apportés au cours des trente dernières années au diagnostic et au traitement du cancer, les statistiques indiquent que les thérapies actuelles ne procurent qu'une probabilité de survie de cinq (5) ans dans environ 40% des cas. Actuellement, la méthode de choix pour le traitement de la majorité des cas de cancer est la chirurgie, suivie de la radiothérapie et de la chimiothérapie. Cependant, ces traitements ne permettent pas de traiter certains des cancers les plus fréquents en plus de causer des effets secondaires sévères reliés à leur utilisation. Plusieurs raisons peuvent expliquer l'échec de ces traitements. D'abord certaines tumeurs ne peuvent être traitées en raison de leur localisation ou de leur dispersion métastatique, mais également à cause de leur faible sensibilité à la radiothérapie ou à la chimiothérapie. En outre, ces méthodes ne sont certainement pas idéales pour le traitement des néoplasies considérant la morbidité qui leur est associée.

En conséquence, de nombreuses autres approches ont été tentées dans le but d'améliorer le taux de survie des patients à haut risque de récurrence. Ces approches incluent l'immunothérapie seule ou en combinaison avec la chimiothérapie.

L'hypothèse de l'utilisation du système immunitaire pour éradiquer une tumeur n'est pas nouvelle. Il y a plus de cent ans, William Coley (en 1893) était le premier à publier une étude montrant qu'une activation non-spécifique du système immunitaire à l'aide de toxines bactériennes pouvait causer une régression tumorale (sarcome métastatique). Les bienfaits de la «toxine de Coley» demeurent encore controversés mais il reste que ce chercheur avait clairement démontré une régression tumorale ainsi qu'une survie prolongée chez certains patients. Les efforts héroïques de Coley lui ont valu le titre de « Père de l'Immunothérapie », bien avant que les principes fondamentaux de l'immunologie ne soient élucidés.

Avec les progrès récents accomplis dans l'élucidation du mécanisme d'action du système immunitaire et le développement de la technologie des hybridomes, le concept stipulant que l'immunothérapie représente un outil thérapeutique valable pour le traitement du cancer est devenu une réalité. L'avènement des anticorps monoclonaux (AcMo) a permis le développement de thérapies ciblant directement la tumeur, que ce

soit par le biais de mécanismes effecteurs anticorps-dépendant ou d'immunoconjugués (par exemple, une drogue, un isotope ou une toxine couplé à un anticorps). Au cours des quinze ou vingt dernières années, les AcMo sont passés du laboratoire aux essais cliniques pour le traitement d'un grand nombre de cancers variés. Plusieurs AcMo sont maintenant en phase clinique avancée et pourraient être introduits sur le marché au cours des prochaines années. Ces résultats sont sans nul doute impressionnants; toutefois, l'utilisation des AcMo comporte encore plusieurs contraintes physiques, biologiques et immunologiques pouvant limiter leur utilité clinique.

Le travail décrit dans cette thèse porte sur l'identification de molécules peptidiques pouvant être utilisées dans la thérapie anti-cancer. Cette étude a débuté à une période où les progrès en biologie moléculaire (banques peptidiques aléatoires ou BPAs) permettaient de développer des outils permettant de surmonter plusieurs difficultés. Les BPAs exprimées à la surface de phages filamenteux sont des outils versatiles pour identifier des épitopes détectés par des anticorps monoclonaux et autres molécules de liaison. Les séquences d'épitope, obtenues à partir du criblage de ces banques avec des anticorps, montrant de surcroît une divergence de séquence significative avec l'antigène originel, sont appelées mimotopes. Les mimotopes peptidiques sont d'un intérêt considérable à cause de leur utilisation potentielle pour le développement de vaccins anti-cancer. Toutefois, il y a encore peu de données disponibles sur le potentiel des mimotopes à induire une réponse humorale pouvant reconnaître l'antigène originel. De même, il y a encore peu d'information disponible sur le mécanisme d'action des anticorps anti-mimotope.

Bien que l'expression sur un phage (phage display) mène à plusieurs applications, le but de ce projet de doctorat était de découvrir des mimotopes pouvant être reconnus par l'AcMo murin BCD-F9 et d'utiliser ces mimotopes comme outil d'immunothérapie dans un modèle de xénogreffe sur souris nue. Bien que le travail présenté porte principalement sur le traitement du fibrosarcome humain, les concepts peuvent être appliqués à tous les types de tumeurs. Les implications de la découverte des mimotopes dans la compréhension des mécanismes d'action de la glycoprotéine-P (P-gp) sont aussi décrites.

Nous avons démontré que l'épitope reconnu par l'AcMo BCD-F9 n'était pas restreint aux lignées cellulaires de cancer du sein. Les observations décrites dans cette étude suggèrent que cet épitope est aussi présent en plus ou moins grande quantité à la surface de plusieurs d'autres lignées cellulaires néoplasiques: carcinome du colon, sarcome, lymphome et leucémie. Leur réactivité commune avec BCD-F9 implique que ces lignées cellulaires partagent un antigène de surface ou expriment différentes molécules portant des épitopes à réactivité croisée.

La réactivité de l'AcMo BCD-F9 avec le fibrosarcome humain HT-1080 nous a permis d'utiliser cette lignée cellulaire pour l'étude des propriétés anti-tumorales de BCD-F9 dans un modèle expérimental animal. Nos résultats ont montré que l'inoculation i.v. répétée de BCD-F9 à des souris nues CD-1, chez lesquelles les cellules HT-1080 étaient transplantées, réduisait de manière significative la croissance tumorale chez les animaux transplantés par voie s.c.. Ce même traitement abrogeait complètement le développement de métastases pulmonaires des souris transplantées par voie i.v.. Nos études *in vitro* de la lyse BCD-F9-dépendante de cellules HT-1080 ont confirmé que la cytotoxicité cellulaire anticorps-dépendante (ADCC) et la cytotoxicité anticorps-dépendante médiée par le complément (ADCMC) peuvent être impliquées dans l'activité anti-tumorale observée chez les animaux traités avec le BCD-F9. Le large spectre de lignées néoplasiques reconnues par BCD-F9 suggère que cet AcMo pourrait être un agent immunothérapeutique efficace. À cet égard, il serait intéressant de répéter avec d'autres cellules tumorales humaines les expériences examinant l'effet de BCD-F9 sur la croissance du fibrosarcome HT-1080 et les métastases en originant.

Nous avons également utilisé l'AcMo BCD-F9 pour identifier à l'aide des BPAs des peptides pouvant simuler l'épitope reconnaissant cet anticorps. Le phage choisi exprimait le peptide GRRPGGWWMR, qui pouvait se lier à l'AcMo BCD-F9. L'immunisation de lapins avec ce peptide-mimotope synthétique induisait des anticorps polyclonaux (AM-F9) capables de bloquer la liaison d'AcMo BCD-F9 aux cellules tumorales HT-1080. À l'aide d'un modèle de métastases pulmonaires agressives, nous avons démontré que l'administration i.v. de l'AM-F9 prolongeait significativement la survie de souris nues CD-1 inoculées i.v. avec des cellules de fibrosarcome humain HT-1080.



Ces observations initiales ont été suivies d'une autre étude examinant les propriétés de l'antisérum AM-F9. Nous avons démontré que le traitement avec AM-F9 inhibait de manière significative la croissance des cellules tumorales HT-1080 inoculées s.c. à des souris nues CD-1. Nous avons aussi étudié l'activité anti-tumorale de l'AM-F9 *in vitro* à l'aide d'essais ADCMC et ADCC. Nous avons démontré que, dans ce modèle, l'ADCMC jouait vraisemblablement un rôle majeur dans la lyse des cellules tumorales. Ces observations suggèrent que les mimotopes peptidiques induisent une réponse anti-tumorale bénéfique et peuvent ainsi être utilisés pour l'immunothérapie.

Les mimotopes peptidiques sont aussi importants pour la simulation de la liaison de substances non-protéiques, telles que des drogues chimiothérapeutiques à faible poids moléculaire. Nous avons donc utilisé les banques de phages pour identifier des ligands peptidiques pouvant se lier aux drogues MDR, simulant de ce fait l'activité de liaison de la P-gp. Nous avons démontré que les phages exprimant des peptides, contenant la séquence canonique WXXW, se liaient à des drogues de type MDR (vinblastine, doxorubicine, vérapamil et génistéine) avec la même sélectivité que la P-gp mais n'interagissaient pas avec des drogues de type non-MDR, telles que l'arabinosylcytosine (Ara-C) et le melphalan. Nous avons aussi démontré qu'un anticorps polyclonal obtenu contre le phage exprimant le peptide VCDWWGWGIC pouvait reconnaître de manière spécifique la P-gp dans la fraction membranaire de cellules MCF-7ADR à phénotype MDR. Les séquences se liant aux drogues MDR que nous avons identifiées dans ce travail fournissent un outil important pour le design et le criblage de nouveaux agents chimiothérapeutiques.

University of Québec  
INRS - Institute Armand-Frappier  
Human Health Center

**THE IDENTIFICATION (PHAGE DISPLAY)  
OF PEPTIDE MOLECULES WITH POTENTIAL APPLICATION IN  
ANTI-CANCER THERAPY**

By  
Mikhail Popkov

A dissertation submitted in partial fulfillment  
of the requirements for the degree of Doctor of Philosophy (Ph.D.)  
in Virology and Immunology

Committee members: Daniel Oth, president  
Rosemonde Mandeville, supervisor  
Claude Perreault, Hôpital Maisonneuve, external member  
Richard Béliveau, UQAM, external member

Winter 2001

© Copyright Mikhail Popkov, 2001

## ACKNOWLEDGMENTS

As I sit to write this page, I remember more and more people that should be thanked for helping to bring this work to completion, and I find I almost don't know where to start; even less do I know where to end!

I would like to express my sincere gratitude to my supervisor, Dr. Rosemonde Mandeville, for her scientific guidance, encouragement, enthusiasm, understanding, kindness and financial support through my education. Most of all, I value the freedom that Rosemonde gave me to explore new avenues and to make mistakes. I thank her for providing me with the knowledge, the skills and the example to do good science.

I would also like to thank Dr. Suzanne Lemieux and Yvette Lusignan for their time, efforts, many valuable suggestions and fruitful scientific collaboration during the last year of my Ph.D. study.

I have been extremely fortunate to work with learn from Dr. Valery Alakhov who is not only wonderful partner in the work presented in this thesis but great friend.

I am especially grateful to Dr. Michel Houde for his boundless help in numerous situations, in particular for his help with articles' discussions and French writing.

Dr. Viatcheslav Medvedkine was kind enough to help me with computer modeling.

I am indebted to the past lab members Ginette Mercier, Salwa Sidrac-Ghali, Norman Rocheleau, Luisette Labrie for their support, advice and assistance.

I would like to express my gratitude to fellow graduate students, Benoit, Pierre-Olivier, Monica, Anna-Karine, Annik, Isabelle, Maxime, Katie, Annie, and Jackie for their friendship and help in numerous situations, for making graduate school a more enjoyable place, and for not smacking me when I was grumpy; and many others for their encouragement and support while in Montreal.

I would also like to thank my thesis committee. Dr. Richard Béliveau and Dr. Claude Perreault have graciously served as my external committee members and provided valuable insight and encouragement. Dr. Daniel Oth not only served as the president on my committee, but also had a huge impact on my graduate career in his role as the Ph. D. program's director.

Many thanks to the Ph. D. program at IAF for opening my eyes to the various frontiers of science through their courses and instructions.

Thanks to various funding agencies, including NSERC, FCAR, and INRS – Institut Armand-Frappier for making all of this work possible, whether they knew it or not.

Most of all, I would like to thank my wife Ludmila and my daughters Natasha and Christina for their love, support, and for sharing the frustrations and joys of these past five years.

## TABLE OF CONTENTS

Résumé substantiel.....	iv
Acknowledgments.....	v
Table of Contents.....	vii
List of Figures.....	x
List of Tables.....	xii
List of Abbreviations.....	xiii
Abstract.....	xv
 Introduction.....	 1
References.....	4
 Chapter 1: Literature review	
 1. Therapeutic antibodies.....	 7
Introduction.....	7
Antigenic targets.....	8
Effector functions.....	9
Types of monoclonal antibodies.....	12
Clinical applications.....	13
Conclusion.....	15
 2. Random peptide libraries.....	 16
Introduction.....	16
Epitope definition.....	16
Display system.....	17
Affinity selection.....	20
Epitope discovery.....	22
Mimotope discovery.....	23
Immunogenic mimics and vaccine design.....	25
Conclusion.....	26
 3. Multidrug resistance.....	 27
Introduction.....	27
Structure of P-gp.....	28
Drug-binding site.....	31
Conclusion.....	33
 4. References.....	 34
 Chapter 2: Inhibition of Tumor Growth and Metastasis of Human Fibrosarcoma Cells HT-1080 by Monoclonal Antibody BCD-F9	
 Résumé traduit.....	 52

Abstract .....	54
Introduction.....	55
Materials and methods .....	57
Results.....	62
Discussion .....	65
References.....	68
 Chapter 3: Epitope-Specific Antibody Response to HT-1080 Fibrosarcoma Cells by Mimotope Immunization	
Résumé traduit .....	79
Abstract .....	81
Introduction.....	82
Materials and methods .....	84
Results.....	88
Discussion .....	91
References.....	94
 Chapter 4: Immunotherapy with Anti-Mimotope Polyclonal Antibodies in a Nude Mouse Xenograft Model	
Résumé traduit .....	105
Abstract .....	107
Introduction.....	108
Results.....	110
Discussion .....	114
Materials and methods .....	117
References.....	121
 Chapter 5: Multidrug Resistance Drug-Binding Peptides Generated by Using a Phage Display Library	
Résumé traduit .....	135
Summary .....	137
Introduction.....	138
Materials and methods .....	140
Results.....	144
Discussion .....	149
References.....	152
 Chapter 6: General Discussion	
Mimotope discovery .....	166
Immunotherapy .....	168
Antibody-dependent cytotoxicity.....	169
Elucidation of drug-binding site .....	171

References.....	174
Conclusion .....	178
Appendix A: List of Communications.....	181
Appendix B: Copies of Articles.....	183

## LIST OF FIGURES

### Chapter 1

Figure 1.1. Anti-tumor activity of naked mAbs.....	10
Figure 1.2. Schematic depiction of various formats of antibody. ....	14
Figure 1.3. Schematic representation of a filamentous phage .....	18
Figure 1.4. The principle of epitope mapping using phage RPLs.....	21
Figure 1.5. Schematic model of the human P-gp and its functional domains.....	29

### Chapter 2

Figure 2.1. Reactivity of mAb BCD-F9 with various neoplastic cell lines and PBMC .....	71
Figure 2.2. Characterization of the BCD-F9-reactive antigen .....	72
Figure 2.3. Antitumor activity of BCD-F9 in HT-1080-xenografted nude mice	73
Figure 2.4. Prolonged survival time of HT-1080 tumor-bearing mice after treatment with BCD-F9 .....	74
Figure 2.5. Tumor histology .....	75
Figure 2.6. Capacity of mAb BCD-F9 to kill HT-1080 cells by ADCMC.....	76
Figure 2.7. Capacity of mAb BCD-F9 to kill HT-1080 tumor cells by ADCC..	77

### Chapter 3

Figure 3.1. Selection of phages that bind to mAb BCD-F9 .....	99
Figure 3.2. Binding of Ala phage mutants and phage $\gamma 2$ to mAb BCD-F9 .....	100
Figure 3.3. Inhibition of BCD-F9 binding to HT-1080 cells by phages and by synthetic peptides .....	101
Figure 3.4. Inhibition of binding of the BCD-F9 mAb to HT-1080 cells by polyclonal antisera.....	102
Figure 3.5. Survival analysis of HT-1080 tumor-bearing nude mice .....	103

### Chapter 4

Figure 4.1. Inhibition of xenograft tumor growth in CD-1 nude mice inoculated with AM-F9 anti-mimotope antiserum .....	126
Figure 4.2. Susceptibility of HT-1080 cells to ADCMC .....	127
Figure 4.3. Phenotypic characterization of NK and LAK cells from normal and athymic CD-1 mice .....	128
Figure 4.4. Susceptibility of HT-1080 cells to NK and LAK cell-mediated lysis .....	129
Figure 4.5. Susceptibility of HT-1080 tumor cells to ADCC .....	130
Figure 4.6. Flow cytometric analysis of thioglycollate-elicited peritoneal cells .....	131
Figure 4.7. Identification of peritoneal cells mediating antibody-dependent lysis of tumor targets.....	132



Figure 4.8. Effect of NK cell-depletion on AM-F9-mediated inhibition of xenograft tumor growth in CD-1 nude mice .....	133
--	-----

## Chapter 5

Figure 5.1. Selection of phages that bind to doxorubicin-BSA .....	158
Figure 5.2. Displacement assay of binding of various anti-cancer drugs with V6 phage.....	159
Figure 5.3. Immunoblot analysis.....	160
Figure 5.4. HPLC of VCDWWGWGIC peptide .....	161
Figure 5.5. Inhibition of V6 phage binding to doxorubicin by the VCDWWGWGIC peptide.....	162
Figure 5.6. Molecular structure of VCDWWGWGIC peptide predicted by SYBYL Molecular Graphics (version 6.1a).....	163
Figure 5.7. Molecular docking of anti-cancer drug molecules into the tryptophane envelope of VCDWWGWGIC peptide .....	164

## Chapter 6

Figure 6.1. Schematic 3-D representation of the human P-glycoprotein.....	173
---	-----

**LIST OF TABLES****Chapter 1**

Table 1.1. Tumor antigens .....	8
---------------------------------	---

**Chapter 5**

Table 5.1. Peptide sequences and binding characteristics of affinity-purified clones .....	156
Table 5.2. Molecular ion masses and isotopic compositions of reduced and oxidized forms of VCDWWG WGIC peptide determined by mass spectrometry .....	157

## LIST OF ABBREVIATIONS

<b>A:</b>	Ala, Alanine
<b>ABC:</b>	ATP-binding cassette
<b>ADCC:</b>	antibody-dependent cellular cytotoxicity
<b>ADCMC:</b>	antibody-dependent complement-mediated cytotoxicity
<b>Ag:</b>	antigen
<b>BSA:</b>	bovine serum albumin
<b>C:</b>	Cys, Cysteine
<b>CCA:</b>	cell cycle arrest
<b>CDRs:</b>	complementarity-determining regions
<b>CFA:</b>	complete Freund's adjuvant
<b>D:</b>	Asp, Aspartic acid
<b>DNA:</b>	Deoxyribonucleic acid
<b>E:</b>	Glu, Glutamic acid
<b>EGF:</b>	epidermal growth factor
<b>ELISA:</b>	enzyme-linked immunosorbent assay
<b>F:</b>	Phe, Phenylalanine
<b>FBS:</b>	fetal bovine serum
<b>FcγR:</b>	Fcγ receptor
<b>FITC:</b>	fluorescein isothiocyanate
<b>Fmoc:</b>	9-fluorenylmethoxycarbonyl
<b>G:</b>	Gly, Glycine
<b>H:</b>	His, Histidine
<b>h:</b>	hour(s)
<b>HAMAs:</b>	human anti-mouse antibodies
<b>HBsAg:</b>	Hepatitis B surface antigen
<b>I:</b>	Ile, Isoleucine
<b>IFA:</b>	incomplete Freund's adjuvant
<b>IgG:</b>	immunoglobulin G
<b>i.v.:</b>	intravenous (injection)
<b>K:</b>	Lys, Lysine
<b>kDa:</b>	kilodalton
<b>KLH:</b>	keyhole limpet hemocyanin
<b>L:</b>	Leu, Leucine
<b>M:</b>	Met, Methionine
<b>mAbs:</b>	monoclonal antibodies
<b>MAC:</b>	membrane attack complex
<b>MDR:</b>	multidrug resistance
<b>MFI:</b>	mean fluorescence intensity
<b>min:</b>	minute(s)
<b>ml:</b>	milliliters
<b>mM:</b>	millimolar
<b>MRC:</b>	minimal residual cancer
<b>N:</b>	Asn, Asparagine

<b>NK:</b>	natural killer
<b>NHL:</b>	Non-Hodgkin's lymphoma
<b>P:</b>	Pro, Proline
<b>PBMC:</b>	peripheral blood mononuclear cells
<b>PBS:</b>	phosphate-buffered saline
<b>PE:</b>	phycoerythrin
<b>P-gp:</b>	P-glycoprotein
<b>PTX:</b>	<i>Bordetella pertussis</i> toxin
<b>Q:</b>	Gln, Glutamine
<b>R:</b>	Arg, Arginine
<b>RPLs:</b>	random peptide libraries
<b>s.c.:</b>	subcutaneous (injection)
<b>S:</b>	Ser, Serine
<b>SD:</b>	standard deviation
<b>SDS:</b>	sodium dodecyl sulfate
<b>SEM:</b>	standard error of mean
<b>T:</b>	Thr, Threonine
<b>TBS:</b>	Tris-buffered saline
<b>TGF-<math>\alpha</math>:</b>	transforming growth factor- $\alpha$
<b>TM:</b>	transmembrane
<b>TNF:</b>	Tumor necrosis factor
<b>TRAIL:</b>	TNF-related apoptosis-inducing ligand
<b>Tris:</b>	Tris(hydroxymethyl)aminomethane
<b>V:</b>	Val, Valine
<b>W:</b>	Trp, Tryptophan
<b>Y:</b>	Tyr, Tyrosine
<b><math>\mu</math>g:</b>	micrograms
<b><math>\mu</math>l:</b>	microliters
<b><math>\mu</math>M:</b>	micromolar

## ABSTRACT

The advent of mAbs has allowed the development of tumor directed therapies utilizing antibody-dependent effector mechanisms and immunoconjugates (e.g. drug, isotope and toxin coupled antibodies) against human malignancies. Random peptide libraries displayed on the surface of filamentous phage are a versatile tool for identifying protein epitopes detected by monoclonal antibodies and other binding molecules. Epitope sequences derived by screening these libraries with antibodies, which show significant sequence divergence from the native antigens, are also referred to as mimotopes. Peptide mimotopes are of considerable interest because of their potential for use in anti-cancer vaccine development. However, there are limited data on whether mimotopes so derived can induce a humoral response that recognizes native antigens. Also, at the present time, very little information is available on the mechanism of action of any of the anti-mimotope antibodies. To this end, we constructed phage epitope libraries and screened them with a mouse monoclonal antibody BCD-F9 (mAb). Hereafter, we report that (1) the phage that was selected encoded for the unique sequence GRRPGGWWMR representing the peptide capable of binding to the BCD-F9 mAb. (2) Polyclonal antibodies (AM-F9) generated by immunization of rabbits with this synthetic peptide specifically bound to HT-1080 cells and inhibited the binding of the BCD-F9 antibody to these cells. (3) Using an aggressive lung metastatic model, we demonstrated that AM-F9 administered i.v. significantly prolonged the life span of CD-1 nude mice inoculated i.v. with HT-1080 human fibrosarcoma cells. (4) We also showed that the administration of AM-F9 to CD-1 nude mice inoculated s.c. with HT-1080 cells led to a significant inhibition of tumor growth. (5) We also investigated the anti-tumor activity of AM-F9 in vitro in ADCMC and ADCC assays, and demonstrated that, in this model, ADCMC is likely to be a major mechanism responsible for tumor cell killing. These results indicate that peptide mimotopes can potentially be used as a novel immunotherapy to induce a beneficial antitumor response.

Peptide mimotopes are also of importance in mimicking the binding of non-proteineous substances such as, for example, low molecular chemotherapeutic drugs. We used therefore phage display libraries to generate peptide ligands that can bind MDR

drugs mimicking, in this respect, the drug binding activity of P-glycoprotein. We showed that (6) the phages expressing the peptides, which contain the core consensus motif WXXW, bound MDR type drugs (vinblastine, doxorubicin, verapamil, and genistein) with the same selectivity as P-glycoprotein and did not interact with non-MDR type drugs, such as arabinosylcytosine (Ara-C) and melphalan. (7) Most importantly, we showed that monospecific antibody obtained against the phage expressing VCDWWGWGIC peptide could specifically recognize P-glycoprotein in the membrane fraction of MDR phenotype MCF-7ADR cells. The MDR drug-binding sequences generated during this work could provide an important tool for design and screening of new chemotherapeutical agents.

## **INTRODUCTION**

Cancer now affects a large percentage of the population and although it can occur at any stage in the life of individual, most patients are middle-aged or older (1). Despite considerable advances in the diagnosis and therapy of cancer over the last 30 years, the statistics indicate that current cancer therapies only provide a 40 % probability that a patient diagnosed with cancer today will be alive in 5 years time (2).

At the present time, the accepted method for treating majority of the cancer clinical cases relies on the surgery, following by use of radiation or chemotherapeutic agents. These approaches fail to cure many of the most prevalent cancers, and often have serious adverse effects associated with their use. There are numerous reasons for the failure of these treatments; tumors that cannot be resected because of their location or metastatic spread, and poor sensitivity to radiation and/or chemotherapy. The severe morbidity that is often associated with the use of chemotherapy and radiotherapy often makes them less than an ideal form of therapy. Therefore, a number of other approaches have been tried in an effort to improve survival rates among patients at high risk for recurrence of tumor. These include immunotherapy alone or in combination with chemotherapy.

The idea of using the immune system to eradicate tumor is not new. Over 100 years ago, William Coley (in 1893) first reported on the ability to induce tumor regressions (metastatic sarcoma) by nonspecific activation of the immune system in response to bacterial toxins (3). The overall benefit of "Coley's Toxin" remains controversial, but there were clearly patients who showed tumor regression with prolonged survival. Coley's heroic efforts earned him the title of "Father of Immunotherapy", long before the principles of immunology were recognized.

With recent advances in our understanding of the immune system, and the development of hybridoma technology (4), the concept of immunotherapy being a useful therapeutic intervention for the treatment of cancer is becoming a reality. Over the last two and one half decades, monoclonal antibodies (mAbs) have moved from the laboratory to clinical trials for the treatment of various malignancies. (5-9). Several mAbs are currently entering advanced clinical trials and should appear on the market in the next few years (7,10,11). Indeed, the first mAb for cancer therapy was approved in the U.S. in 1997 (12).



Although these results are undoubtedly impressive, the use of mAbs, however, revealed many physical, biological, and immunological factors that have limited their clinical utility. This study was initiated at a time when advances in molecular biology (phage display) have provided tools to overcome many of these difficulties. While phage display has many diverse applications, the aim of this doctoral project was the discovery of mimotopes recognized by mAb BCD-F9 and their use in the immunotherapy in a nude mouse xenograft model. The work is presented as it relates mainly to the treatment of human fibrosarcoma, however, the concepts can be readily generalized to all tumor types. The implications of mimotope discovery in the understanding of the mechanism of action and function of P-glycoprotein (P-gp) are also described.

This thesis is divided into 6 chapters. The first chapter of this doctoral project presents a concise literature review concerning therapeutic antibodies, random peptide libraries (RPLs), and multidrug resistance. The results obtained during the course of this study are presented as 4 scientific articles, which have been published or submitted for publication. That replaces the Materials and Methods, Results, and Discussion sections of the classical doctoral thesis. It should be noted that these 4 chapters are formatted according to the particular journal's specifications as they were submitted with two minor exemptions. The position of figure legends and the format of references are presented in the classical doctoral format as means of standardizing the thesis presentation. Finally, the thesis ends with a general discussion and conclusion, reflecting a brief analysis of the major results obtained during the course of this research project.

## References

1. Hoel, D. G., D. L. Davis, A. B. Miller, E. J. Sondik, and A. J. Swerdlow. 1992. "Trends in cancer mortality in 15 industrial countries 1969-1986". J. Natl. Cancer Inst., vol. 84, p. 313-320.
2. Ries, L. A. G., P. A. Wingo, D. S. Miller, H. L. Howe, H. K. Weir, H. M. Rosenberg, S. W. Vernon, K. Cronin, and B. K. Edwards. 2000. "The annual report to the nation on the status of cancer, 1973-1997, with a special section on colorectal cancer". Cancer, vol. 15, p. 2398-2424.
3. Coley, W. B. 1893. "The treatment of malignant tumors by repeated inoculation of Erisipelas: with a report of ten original cases". Am. J. Med. Sci., vol. 105, p. 487-511.
4. Kohler, G. and C. Milstein. 1975. "Continuous cultures of fused cells secreting antibody of predicted specificity". Nature, vol. 256, p. 495-496.
5. Dillman, R. O. 1994. "Antibodies as cytotoxic therapy". J. Clin. Oncol., vol. 12, p. 1497-1514.
6. Vitetta, E. S. and J. W. Uhr. 1994. "Monoclonal antibodies as agonist: an expanded role for their use in cancer therapy". Cancer Res., vol. 54, p. 5301-5309.
7. von Mehren, M. and L. M. Weiner. 1996. "Monoclonal antibody-based therapy". Curr. Opin. Oncol., vol. 8, p. 493-498.
8. Jurcic, J. G., D. A. Scheinberg, and A. N. Houghton. 1997. "Monoclonal antibody therapy of cancer". In H. M. Pinedo, D. L. Longo, and B. A. Chabner (eds.). Cancer Chemotherapy and Biological Modifiers Annual 17. Amsterdam: Elsevier Science, p. 196-216.
9. Maloney, D. J. and O. W. Press. 1998. "Newer treatments for non-Hodgkin's lymphoma: monoclonal antibodies". Oncology, vol. 10, p. 63-76.
10. Kossman, S. E., D. A. Scheinberg, J. G. Jurcic, J. Jimenez, and P. C. Caron. 1999. "A phase I trial of humanized monoclonal antibody HuM195 (anti-CD33) with low-dose interleukin 2 in acute myelogenous leukemia". Clin. Cancer Res., vol. 5, p. 2748-2755.
11. Kaminski, M. S., K. R. Zasadny, I. R. Francis, M. C. Fenner, C. W. Ross, A. W. Milik, J. Estes, M. Tuck, D. Regan, S. Fisher, S. D. Glenn, and R. L. Wahl. 1996. "Iodine-131-anti-B1 radioimmunotherapy for B-cell lymphoma". J. Clin. Oncol., vol. 14, p. 1974-1981.

12. Anderson, D. R., A. Grillo-Lopez, C. Varns, K. S. Chambers, and N. Hanna. 1997. "Targeted anticancer therapy using rituximab, a chimeric anti-CD20 antibody (IDEC-C2B2) in the treatment of non-Hodgkin's B-cell lymphoma". Biochem. Soc. Trans., vol. 25, p. 705-708.

## **CHAPTER 1**

### **Literature Review**

# 1. THERAPEUTIC ANTIBODIES

## 1.1 Introduction

The discovery by Kohler and Milstein, in 1975, of a method of producing rodent mAbs of defined specificity by *in vitro* hybridization of immune spleen cells and myeloma cells allows the isolation of large amounts of pure and specific antibodies, thus intensifying the efforts in the use of antibodies for the detection, diagnosis and treatment of cancer as well as other diseases (1).

Although originally used in their natural form, mAbs are now used as fragments, chemically modified, chimeric and humanized forms. In addition, mAbs have been coupled to a variety of “warheads” such as toxins, drugs, enzymes, radionuclides, cytokines, superantigens, and drug-filled liposomes. Their applications extend to the fields of immunohistochemistry, isotopic and non-isotopic immunoassays, imaging of infarcts, atherosclerotic plaques, and cancers, immunotherapy of autoimmune diseases, graft-versus-host diseases, and asthma, prevention and reversal of allograft rejection, and most importantly the diagnosis and therapy of cancers (2-8).

The potential use of mAbs as powerful therapeutic tools in the treatment of cancer lies in their ability to recognize and specifically bind to the target antigens expressed by tumor cells. The variable regions (Fab) determine their antigen-binding specificity, whereas their constant regions (Fc) convey their capacity to interact with immune effector cells and classical pathway of the complement system (9). Since antibodies are clearly able to function *in vivo* after passive or active immunization, particularly against infectious disease, the question may be asked as to the therapeutic efficacy of passively administered mAbs against cancer. Passive immunization with antibodies may have an advantage in the initiation of tumor destruction, since it can occur within minutes to hours of antibody infusion. The use of specific mAbs that are capable of activating natural killer (NK) cells through antibody-dependent cellular cytotoxicity (ADCC) appears to be a method of treatment coming into favor. The present review is limited to antibodies that are used in an unconjugated or “naked” form as passive immunotherapy or as vaccines.

## 1.2 Antigenic Targets

There are a number of terminologies to define tumor antigens. The most accurate description overall is tumor-associated antigens which involves a number of oncofetal developmental antigens which may be expressed, e.g. CEA. Some antigens are more specific to tumors than normal cells, such as tumour specific antigens, which can include exogenous viruses that drive the tumor e.g. EBV and lymphoma, HPV and cancer of the cervix. Although a full description of the tumor antigens is beyond the scope of this review, Table 1 lists some examples from several hundred antigens described to date (10,11).

**Table 1.1. Tumor Antigens**

---

**Tumour-associated antigens (wide spectrum of affinity and tolerance)**

- 1. Cancer testes antigens** - restricted to primitive germs cells of the testes and following activation of expression in a number of tumors: MAGE-1-3, GAGE, BAGE, RAGE, PAGE, NY-ESO-1, ORF1-2, and many similar others
  - 2. Differentiation antigens** - normal tissues with altered expression on tumor cells: MART-1/Melan-A, gp100, tyrosinase, TRP-1-2, HER2/neu, CEA, MUC
- 

**Tumour-specific antigens (high affinity and no tolerance)**

- 1. Viral antigens** - associated with tumour pathogenesis: EBV - lymphoma, HPV - cervix, HBV/HCC - hepatoma (liver cancer)
  - 2. Mutation antigens** - specific tumor and not other tissues: ras, p53 bcr/abl, CDK4, MUM-1,  $\beta$ -CATENIN, Caspase 8
- 

In oncology, tumor-associated antigens are usually considered as good targets for the delivery of anti-cancer therapy, and mAbs directed at such antigens are increasingly being considered as important biological reagents. There is also a general consensus that most of the target antigens are essentially normal structures that are expressed in higher density, in an overt fashion, and in an atypical tissular context on tumor cells. A variety

of cell surface proteins have been used as targets for mAbs. In the case of cancer cells, the only truly tumor-specific antigens described are the clonally expressed receptor idiotypes on B-cell lymphomas. Unfortunately, the use of anti-Id mAbs to treat lymphoid cancer is limited by the need to create custom-made mAbs against the tumor for an individual patient or a small group of patients (12).

Accordingly, most investigators have used differentiation antigens, growth factor receptors, oncofetal antigens, unique carbohydrate antigens, or altered normal antigens as targets for immunotherapy (2,13,14). Such antigens are tumor selective rather than tumor specific, that is, they are present in higher densities on tumor cells when compared to normal cells. Unfortunately, antigen expression on tumors is neither uniform nor static, and heterogeneity is the rule rather than the exception. This property of tumor cells provides a potential mechanism for resistance, mainly because a small percentage of tumor cells will always lack the target antigen. Moreover, antigenic modulation, or the down-regulation of antigen expression after mAb binding (via internalization), could also provide another mechanism for resistance (11). Accordingly, affinity binding, molecular size, antibody form, and antigen expression on the tumor cells are among the features that can now be manipulated to increase the effectiveness of these antibodies for tumor targeting (15).

### **1.3 Effector Functions**

Different unconjugated or “naked” mAbs can induce antitumor activity by mechanisms that include the activation of the effector cells of the immune system, and/or the fixation of the complement (Figure 1.1). The former, called ADCC, depends on the ability of lymphocytes, macrophages, and granulocytes to recognize the Fc region of the tumor cell-bound antibody (Figure 1.1A). The latter, called antibody-dependent complement-mediated cytotoxicity (ADCMC), involves activation of the complement membrane attack complex (MAC, C5b-9) that eventually punches holes in the plasma membrane of the target cells (Figure 1.1B). Unfortunately, one of the inherent weaknesses of using murine mAbs to treat humans is their inability to effectively activate human ADCC or ADCMC mainly because of structural differences between the Fc portions of the mouse and the human immunoglobulins (16). Of the different subclasses

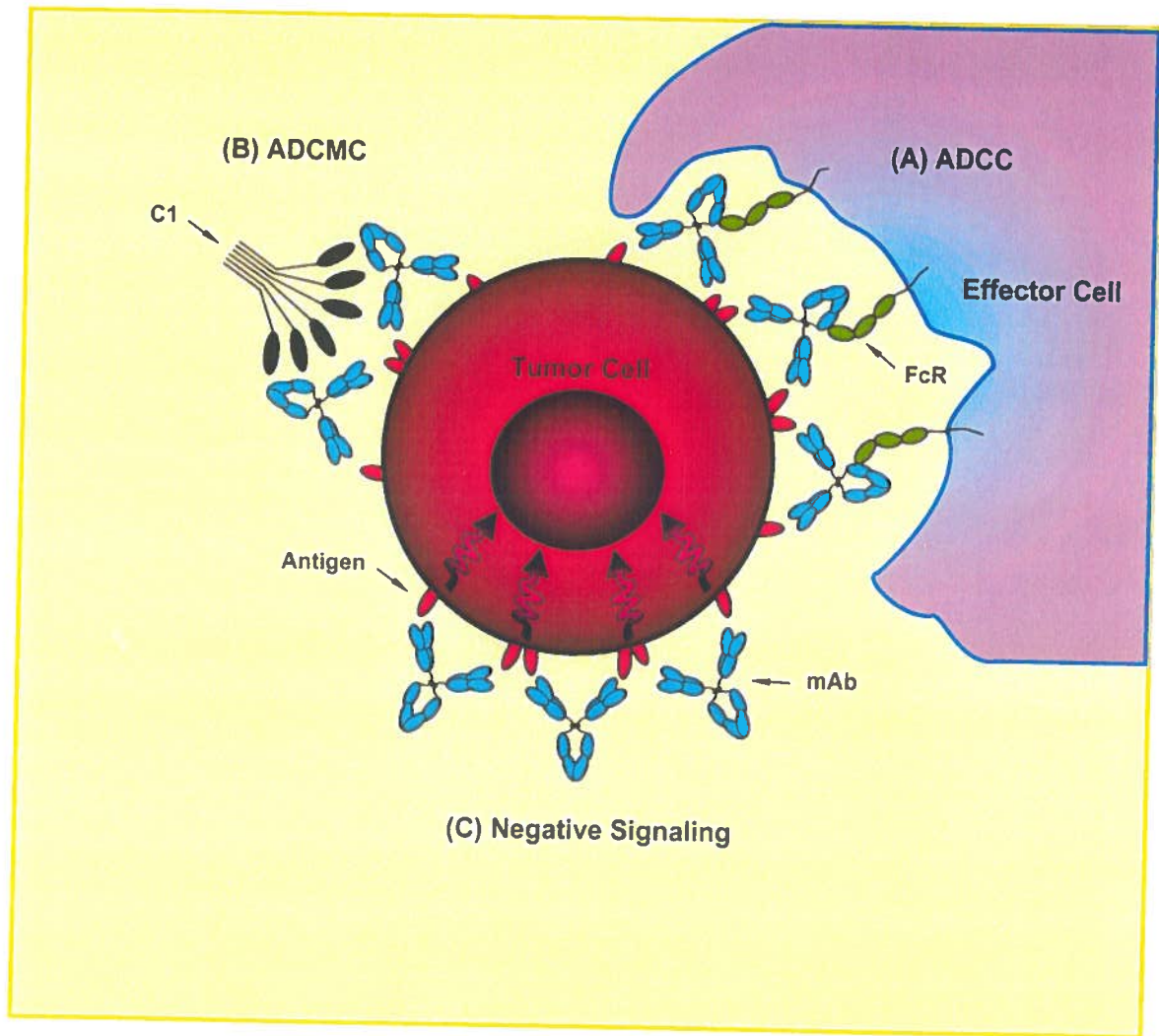


**Figure 1.1. Mechanisms of mAb-Mediated Killing.**

(A) ADCC: After binding to the membrane of the targeted cell, the Fc portion of the mAb binds to Fc receptors on effector cells such as NK cells, or macrophages. This triggers their lytic machinery leading to death of the tumor cell. (B) ADCMC: mAbs bind to the membrane of the tumor cell. The first component of C binds to the Fc portion of the mAb, and complement activation is initiated. This leads to disruption of the cell membrane, resulting in lysis of the cell. (C) Negative signaling: Hypercrosslinking of a membrane component by the mAbs activates intracellular signaling pathways in the tumor cell that result in CCA or apoptosis.



of mouse IgG, IgG2a appears to be the most efficient immunoglobulin subclass in mediating human ADCC, whereas IgG3 mediates potent complement-mediated cytotoxicity (17,18). Human IgG1 and IgG3 subclasses are activators of the complement system and efficient mediators of ADCC (19). However, regardless of its subclass, each mAb has a potentially different ability in the complement activation (20).

Recently, it has been shown that mAbs can exert antigrowth activity by signaling G<sub>0</sub>/G<sub>1</sub> cell cycle arrest (CCA) or apoptosis (Figure 1.1C). The best example of such a mAb is anti-Fas ligand that signals apoptosis in all Fas<sup>+</sup> cells (21,22). However, because of its ubiquitous expression, administration of anti-Fas antibody is lethal. Tumor necrosis factor (TNF)-related apoptosis-inducing ligand (TRAIL) is a more recently identified member of the TNF superfamily that has been shown to selectively kill neoplastic cells by engaging two cell-surface receptors, DR4 and DR5 (23,24). Mitsiades et al. have found that in most cases of thyroid carcinoma cell lines were resistant to Fas cross-linking, yet sensitive to TRAIL, thus concluding that targeting TRAIL receptors may provide a potential new therapeutic modality for thyroid cancer (25). Other mAbs can induce CCA or apoptosis, particularly when used as homodimers that hypercrosslink their antigenic targets (26). Both anti-CD19 and anti-CD22 induce CCA in several Burkitt lymphoma cell lines both *in vitro* and in mice xenografted with human tumors (27,28). Anti-Id mAbs are also thought to be effective therapeutic agents mainly because of their ability to negatively signal tumor cells leading to CCA and apoptosis. This was demonstrated by an increased tyrosine phosphorylation in tumors from responding patients (29).

A further mechanism of antitumor activity of mAbs is receptor blockade, since many tumor cells acquire autonomy with respect to growth factor dependence (30). Cytostatic or cytotoxic effects can result from the binding of a mAb to growth factors or cellular growth factor receptors. Such binding blocks the relevant receptor and could interrupt autocrine feedback loops (31). For example, many adult carcinomas depend, in part, on the autocrine or paracrine effects of epidermal growth factor (EGF) or transforming growth factor- $\alpha$  (TGF- $\alpha$ ). As a result, a large number of anti-EGF receptor mAbs demonstrates antitumor activity in cancers of the breast, vulva, cervix, and in squamous cell carcinomas (31). Other mAbs targeting various cell surface growth factor

receptors have also been shown to effectively induce CCA or apoptosis in tumor cells (32-34).

#### **1.4 Types of Monoclonal Antibodies**

The majority of mAbs is murine in origin and so are immunogenic to humans leading to the development of human anti-mouse antibodies (HAMAs) (13,18). The development of HAMA usually occurs within 1 to 4 weeks and frequently results in an accelerated clearance of subsequently administered mAb (35). This can also result in toxic side effects, such as serum sickness or anaphylaxis.

It has proven difficult to generate human mAbs and, as a result, genetic engineering methods have been applied to construct antibodies that resemble human immunoglobulins but retain the antigen-binding characteristics of murine mAbs (36). The genes encoding the murine Fab variable regions were combined with the genes encoding Fc constant regions of the human immunoglobulins to create chimeric mAbs. Such molecules maintain the antigen specificity of the murine antibody while displaying the effector properties of the human Fc portion (37). In order to reduce further the immunogenicity of the antibody, the murine antigen-binding complementarity-determining regions (CDRs) have been combined with human V-region framework determinants to produce molecules that very closely resemble human immunoglobulins (humanized antibodies) (38,39). However, even when humanized, the Fc region of an antibody has several disadvantages, including nonspecific uptake by Fc receptors and poor pharmacokinetics (40).

To overcome these limitations in the use of mAbs, fragments of antibodies can be prepared by an enzymatic digestion that cleaves off the Fc portion and results in the creation of a bivalent antigen-binding  $F(ab')_2$  fragment or a monovalent Fab fragment that contains intact immunoglobulin-binding sites (41,42). Additionally, single-chain antigen-binding proteins scFvs, consisting of the variable regions of the heavy  $V_H$  and light  $V_L$  chains joined by a peptide linker, can be produced by gene cloning (43). In general, all these molecules retain the antigen-binding specificity of the parental mAb but have more rapid plasma clearance and reduced immunogenicity (44). Their significantly smaller size results in easier penetration of solid tumor sites and more rapid equilibrium

with the extra-vascular space. Therefore, clinically, antibody fragments appear to be more appropriate for delivering cytotoxic molecules to the tumor area (45). Various mAb constructs are diagrammed in Figure 1.2.

### 1.5 Clinical Applications

Clinical trials with mAbs began in the late 1970s, primarily in patients with hematological malignancies. The first successful results were obtained using anti-Id mAbs, where impressive, long-lasting responses were induced in patients with Non-Hodgkin's lymphoma (NHL) (12). Other successful results were reported using anti-IL-2 receptor mAbs in T-cell acute lymphocytic leukemia (13,46). A major and important demonstration of the efficacy of a mAb in minimal residual cancer (MRC) was achieved using an anti-epithelial cell mAb in patients with Stage III colorectal cancers. Following surgical resection, mAb therapy reduced the overall death rate by 30% and decreased the recurrence rate by 27% even in the absence of chemotherapy (47).

Experience with unlabeled mAbs has clearly demonstrated that therapy is rarely associated with toxicity even when HAMAs are present, although in rare instances circulating immune complexes can lead to serum sickness and organ damage. Humanized and chimeric mAbs were much less immunogenic in patients. Murine/human chimeric or humanized mAbs have been developed for the treatment of NHL, renal cell carcinoma, ovarian carcinoma, breast cancer, melanoma, and neuroblastoma (48). Efficacy has been seen in clinical trials using antibodies that target tumor cell surface antigens such as B-cell idiotypes, CD-20 on malignant B cells, CD33 on leukemic blasts, and HER2/neu on breast cancer. Unconjugated immunoglobulins directed against CD20 (Rituximab) induce partial and complete responses in up to 50% of patients with advanced, indolent non-Hodgkin's lymphoma. When such antibodies are conjugated to radionuclides, complete and overall response rates are between 80 and 100% (49). Conjugates composed of anti-CD33 antibodies and the chemotherapeutic agent calicheamicin, show promising activity in patients with relapsed or refractory acute myelogenous leukemia. Treatment of patients with advanced breast cancer using anti-HER2/neu antibody (Transtuzumab) leads to objective responses in some patients with overexpression of the HER2/neu oncoprotein. These exciting results provide a basis for further refinement of the existing approaches to

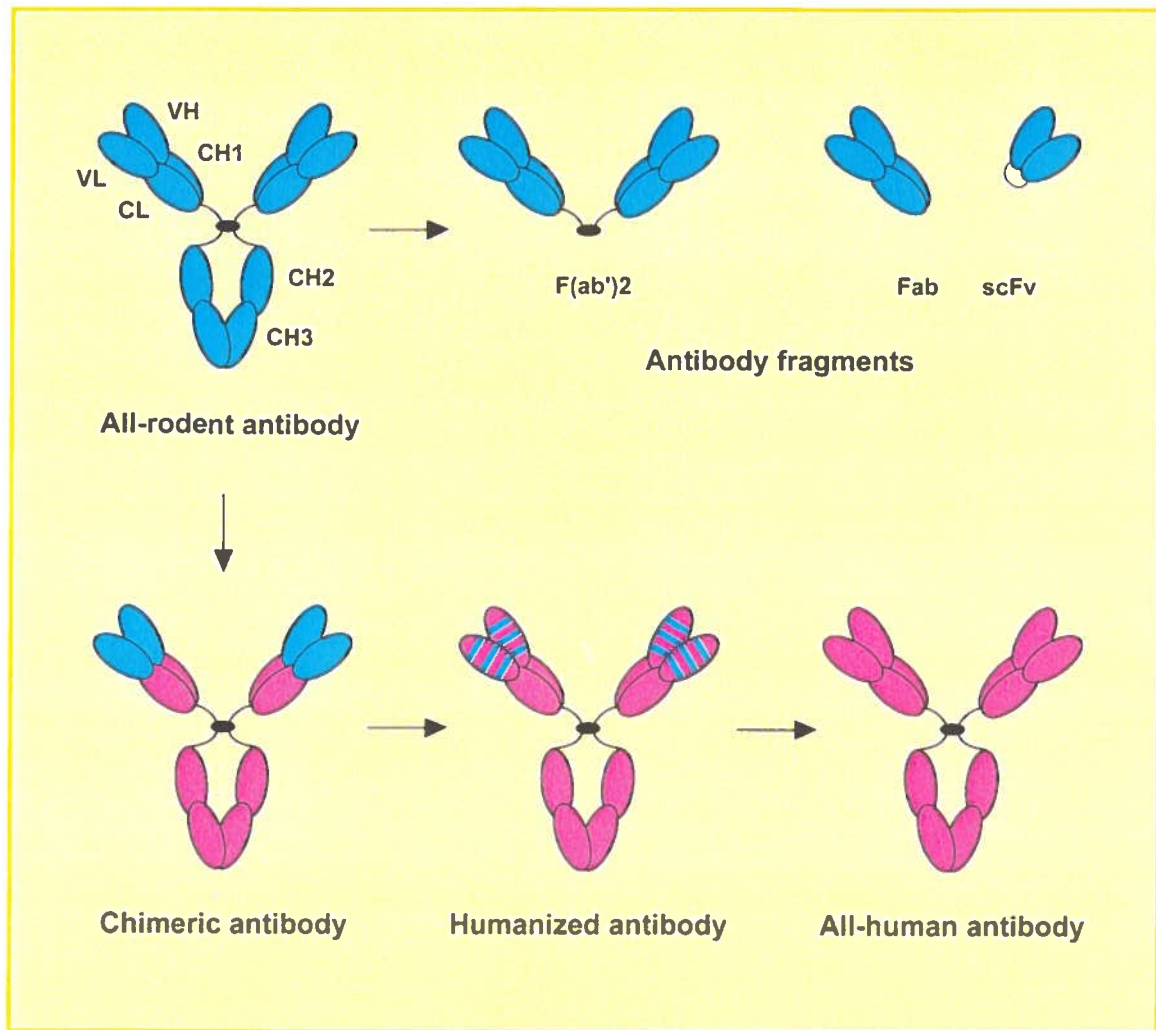


**Figure 1.2. Schematic Depiction of Various Formats of Antibody.**

develop new antibody-based cancer therapy (48). Ongoing Phase II and III trials with a variety of mAbs should lead to the approval and marketing of several drugs in the next 5 years.

### **1.6 Conclusion**

In summary, mAbs are currently widely used for diagnostic purposes. However, advances in hybridoma technology and gene-splicing techniques have led to the formation of chimeric mAbs, which exhibit enhanced antitumor activity, decreased immunogenicity and a very favorable toxicity profile (50). Radiolabelled mAbs can induce durable remissions in lymphoma with toxicity limited largely to bone marrow suppression. Standard treatment options for B-cell lymphoma will soon include antibody-based therapies. A large number of genetically engineered human mAbs are presently in phase I, II and III clinical trials for cancer therapy (51). Further basic and clinical research is needed so we can understand more thoroughly the mechanisms responsible for the observed antitumor effects, and explore more extensively the best approach for their clinical use.

## **2. RANDOM PEPTIDE LIBRARIES**

### **2.1 Introduction**

In the past few years, rapid advances have added new dimensions to the experimental strategies used to identify and characterize the binding of ligands to receptors (52,53). These new technologies are based on a common theme: the preparation of mixtures (repertoires) of very large numbers of molecules (peptides, oligonucleotides, or others) that have randomized sequences or structures. Among the “genetic” repertoires, the system that has received most attention, primarily because of its simplicity and versatility, is the so-called “phage display of peptides”, which is based on the unique properties of the filamentous phage strains M13, fd, and f1. While phage display has many diverse applications, the present review describes the construction of different RPLs and their use in the discovery of mimotopes (peptides that bear no sequence similarity to the antigen recognized by mAbs). The implications of mimotope identification with regards to the discovery and the development of novel drugs and vaccines will also be discussed.

### **2.2 Epitope Definition**

The use of combinatorial repertoires has greatly facilitated the mapping of both continuous and discontinuous epitopes, and the discovery of novel ligands or mimotopes (54-56). Classical epitope mapping requires a set of overlapping synthetic peptides spanning a region of the antigen, or a set of deletions obtained by genetic manipulation of the antigen-coding gene. If a peptide is found to react with the antibody, the epitope is declared to be linear or continuous. By contrast, if a reacting peptide could not be identified, by default, the epitope is declared to be discontinuous, and deemed to be made up of amino acids that are closely located in space, but far away in the primary sequence.

This distinction, apart from its validity as an operational definition, is clearly an oversimplification. Actually, epitopes defined structurally on the basis of the three-dimensional structure of the antigen-antibody complex were found to be composed of stretches of contiguous amino acids, as well as by amino acids that are distant in the primary sequences (57). Accordingly, “complete” epitope (i.e., the ensemble of all amino

acids that make contact with the antigen-binding sites) are probably all discontinuous to some degree. However, as a result of the indirect techniques used for defining them, epitopes are classified as continuous if the amount of binding energy involving only contiguous amino acids is sufficient, by itself, for the formation of an antigen-antibody complex.

Sometimes, the consensus sequence of selected peptides cannot be found in the sequence of the natural antigen. In these cases, it is possible that the peptides (mimotopes) are mimics of discontinuous stretches of natural epitopes (58-60). A new generation of anti-cancer vaccines could simply consist of a cocktail of mimotopes, perhaps including peptides that mimic the carbohydrate moiety of glycoproteins or complex epitopes, selected using tumor-specific mAbs. The phage itself is an excellent immunogen, even when injected without adjuvant, eliciting a T-cell-dependent response against the displayed epitope (61,62).

### 2.3 Display System

Phage display is a biological system that facilitates the cloning and rapid selection of peptides from RPLs. Filamentous phages are flexible rods about 1  $\mu\text{m}$  long and 6 nm in diameter, composed mainly (87% by mass) of a tube of helically arranged molecules of the 50-residue major coat protein pVIII; there are 2700 copies in wild-type virions, encoded by a single phage gene VIII. Inside this tube lies the single-stranded viral DNA. At one tip of the particle there are five copies each of the minor coat proteins pIII and pVI (genes III and VI, respectively); minor coat proteins pVII and pIX (genes VII and IX) are at the other tip (63).

In 1985, Smith showed that the genome of a filamentous phage fd could easily be manipulated to obtain phage particles displaying foreign epitopes on their surface (64). Foreign peptide sequences can be fused to the N-terminus of either pIII (65-67), a minor coat protein present as 5 copies at one tip of the virion, or the major coat protein pVIII (59,68) (Figure 1.3). The displayed epitopes are recognized by the corresponding antibodies. This observation stimulated further research in this area, and has culminated in the use of the phage-display technology in a variety of applications (69-71).

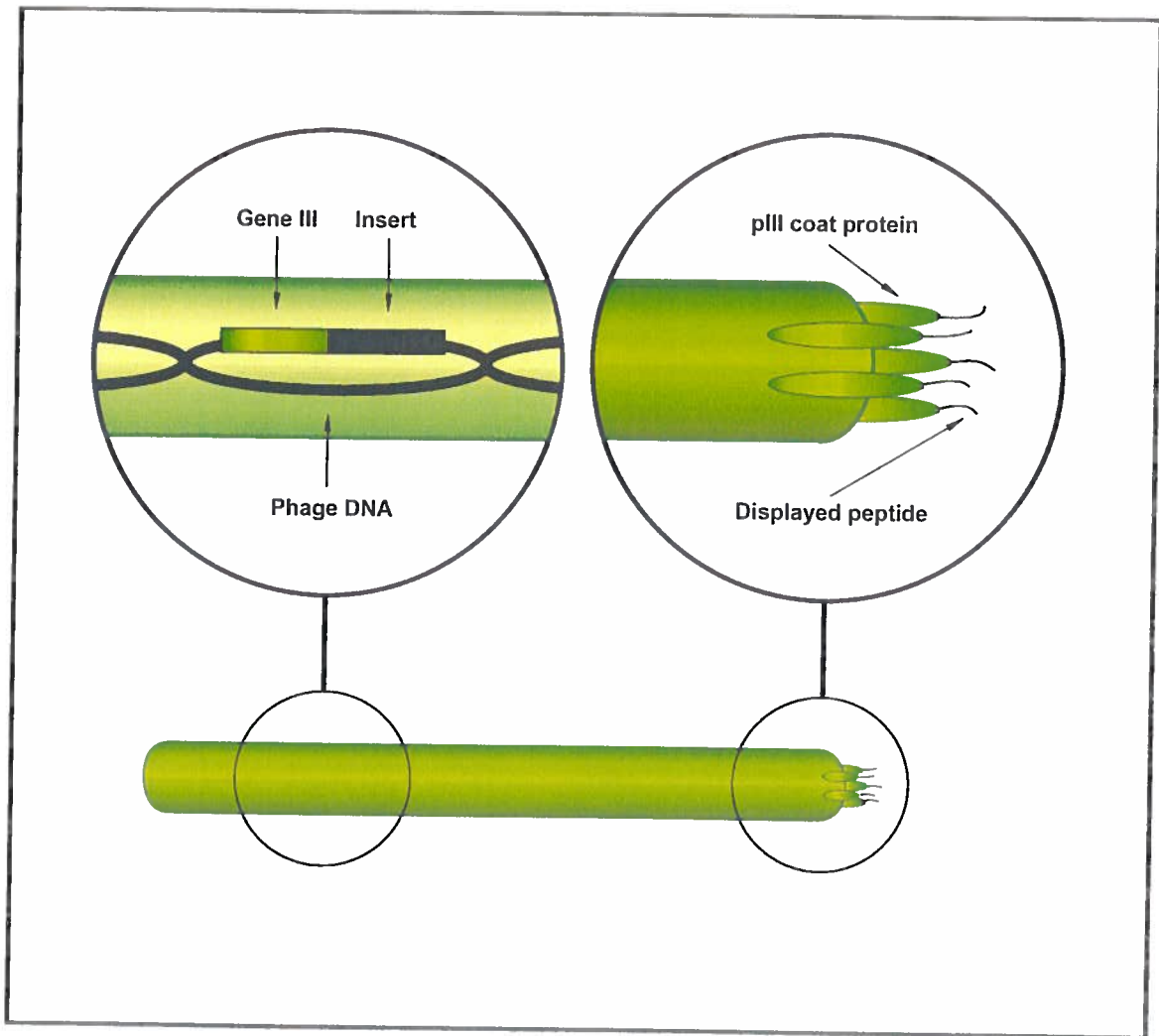


**Figure 1.3. Schematic Representation of the Filamentous Phage.**

The insert DNA is fused to the N-terminus of gene III resulting in the display of foreign peptide fused to the phage coat protein pIII. DNA can also be fused to gene VIII to allow the display of peptides on pVIII (not shown).



RPLs have been constructed by cloning random oligonucleotide sequences in frame with the genes encoding the capsid proteins; consequently, each phage displays a different peptide as a fusion protein on its surface. Displayed peptides are able to bind their ligand and are thus selectable by affinity purification. In contrast to the chemical combinatorial approach, the power of the biological system lies in the ability to propagate clones through multiple rounds of selection. This is particularly useful since modified selective pressure or additional diversity can be introduced in each round. Moreover, once made, biological libraries can be endlessly regenerated. As noted by George Smith, phage display is a practical realization of “*in vitro* evolution of chemicals” (63).

A wide range of RPLs has been constructed. These libraries differ in the length and in the form of displayed peptides. In “linear” libraries, no structural constraints are imposed on the peptide, allowing the peptide to adopt many different conformations. Peptide flexibility can also be improved by engineering constant residues into the flanking regions of the peptide. For example, glycine, alanine or proline residues have been introduced as peptide linkers to optimize the peptide presentation on the phage (65-67,72,73). To increase the diversity of the library, peptides ranging from 6-mer to 43-mer have been displayed (65,67,74,75). Long peptides are more likely to assume a folded structure that may be required for binding to a target molecule. A long peptide can also be considered as a series of overlapping smaller peptides with variable adjacent amino acids, thus increasing the structural diversity. For example, a 38-mer peptide contains 32 overlapping 7-mer sequences, each with different flanking regions. This further means that all possible 7-mer can now be represented in a 38-mer library whose size is only  $10^8$  which is 32-fold smaller than that required for a normal 7-mer library (75).

In an earlier review of epitope mapping of mAbs using RPLs, it was reported that approximately half of all the mAbs used failed to select specific sequences (76,77). The major cause of this problem was attributed to the difficulty of mimicking discontinuous epitopes with linear, unconstrained peptides. To overcome these problems, “constrained” RPLs were constructed by placing two cysteine residues on both sides of the random peptide sequence (59,78,79). This results in the formation of a disulfide bond and the presentation of peptide in a loop form. It is also possible to place the cysteine residues at different sites within the random peptides to introduce internal constraints (75,80).

There are several advantages in using conformationally constrained peptides. Firstly, a constrained peptide may allow a more rigid presentation of an epitope and thus more closely mimics its state in the native molecule. Secondly, the entropic costs of binding are lowered, therefore increasing both the affinity and selectivity of peptide to its target molecule. Additionally, useful information about the structure of the selected peptide can be easily obtained, as constrained peptides possess a more defined configuration. A number of studies demonstrated that the addition of appropriate constraints to a peptide sequence might favor specific and high affinity binding (81-83). One possible drawback in the use of constrained libraries is that a peptide might be held in a conformation not suitable for high affinity binding. Although this could lead to a negative result in identifying a specific peptide from RPLs, alternative ligands or mimotopes can often be selected (84).

### 2.3 Affinity Selection

The probability of finding a ligand in RPLs is a function of its affinity for the selector molecule, as well as its frequency in the library. There are three key elements which determine the success of the combinatorial epitope discovery process: (1) the use of diverse RPLs; (2) the use of a target molecule that is specific and highly selective, for instance a mAb; and (3) the use of an efficient selection and screening procedure so that positive clones can be readily isolated and identified. Several detailed procedures regarding the affinity selection of peptide has been previously published (63,85,86).

The basic strategy of affinity selection is illustrated in Figure 1.4. Factors such as the concentration of the ligand, the stringency of washes, and the elution method, all have a great influence on the efficacy of the selection. They should be carefully chosen since it is necessary to obtain a sufficiently diverse set of positive clones for deriving a consensus sequence. Usually ELISA or colony blotting assays are used as a final screen procedure to identify reactive clones.

The use of RPLs to determine the epitope recognized by an antibody is technically simple, and if successful, it usually requires about two weeks of experimental work. This involves the identification of a consensus sequence derived from positively selected phage clones and then the comparison of this sequence to the original antigen to

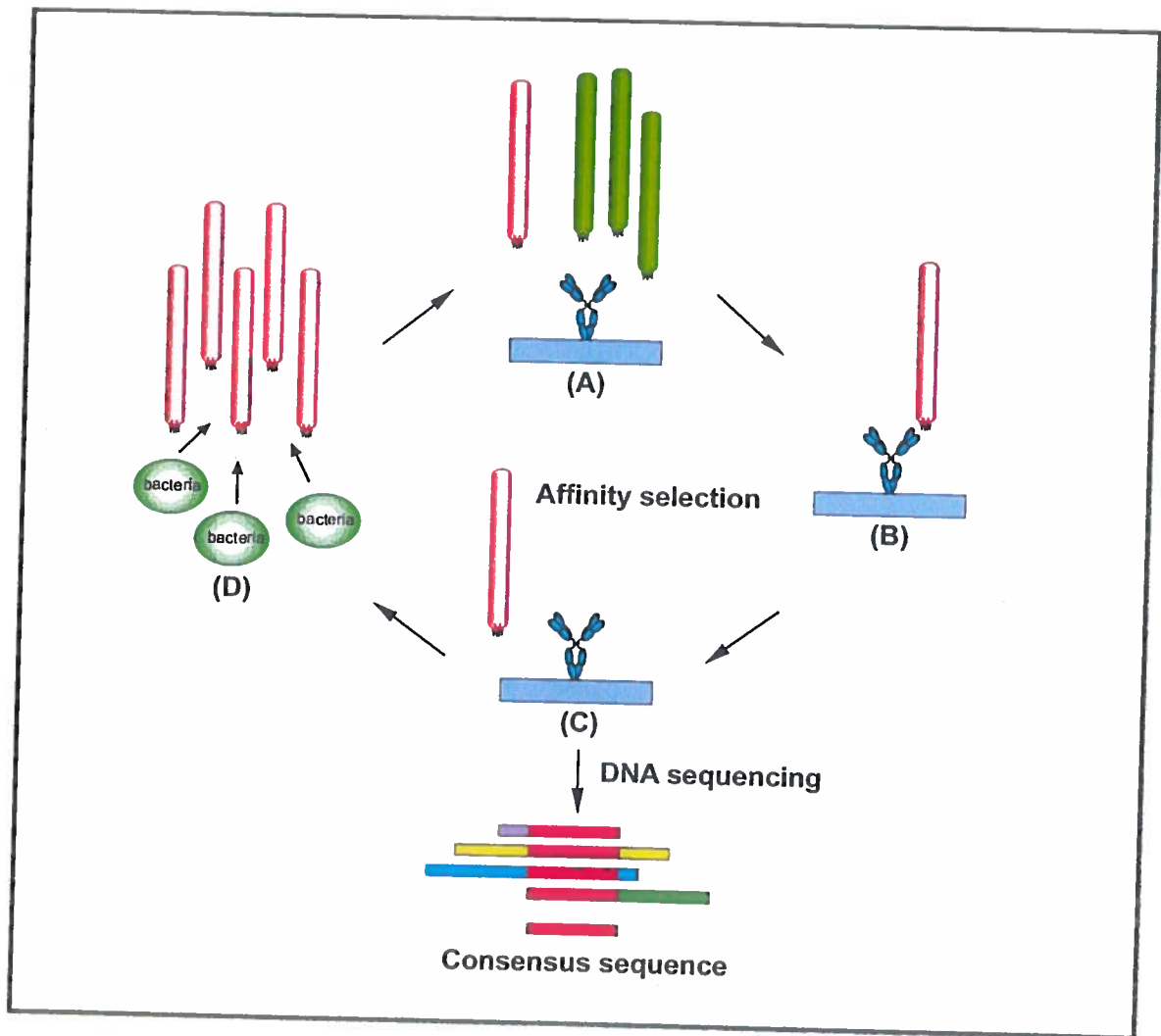


**Figure 1.4. The Principle of Epitope Mapping Using Phage RPLs.**

Affinity selection (A-D): Phage particles are allowed to bind to the immobilized mAb in the presence of blocking proteins (A). Following binding, the matrix is washed extensively to remove unbound phage (B) and bound phage are eluted from the mAb (C). The recovered phage can be used directly to infect fresh bacterial host and are amplified (D). The amplified phage can be used in a new round of affinity selection and this procedure is repeated several times. After the last round of affinity selection, immunological screening methods were used to identify the positive clones. Consensus sequence is then derived by sequencing the reactive clones.

detect similarities. Both linear and discontinuous epitopes have been successfully identified. Mimotopes that share no sequence homology to the antigen can also be discovered using this approach.

## **2.4 Epitope Discovery**

In 1990, Cwirla et al. and Scott et al. almost simultaneously reported the construction and use of RPLs for epitope mapping of mAbs. As a model system, the two groups used mAbs with known linear epitope specificity as probes and successfully selected clones displaying consensus sequences that resembled the original epitopes (65,66). The power of phage RPLs in defining an unmapped native linear epitope was demonstrated by Stephen and Lane in 1992. In their study, the authors localized the epitope of the anti-p53 mAb to a cryptic region comprising the residues RSHVV in wild type p53 (87). Subsequently, linear epitopes of mAbs, against a range of different antigens, have been identified using this method (53,88-92).

Despite these successes, a number of mAbs known to recognize linear epitopes has failed to select reactive clones from RPLs (93). Different studies reported that phage clones were only selected from long RPLs (for example 20-mer) while short RPLs yielded only mimotopes with no sequence similarity to the original antigen (94-96). These findings may be due to the fact that important contact residues could lay further apart than what is allowed by a short peptide. Alternatively, appropriate flanking residues may be needed to stabilize the conformation (94). Nevertheless, success cannot be ensured mainly because of the incompleteness of these libraries, and it may sometimes be difficult to interpret the sequence data and to unambiguously locate the epitope site.

Mapping of discontinuous or conformational epitopes represents a much more difficult task than the mapping of linear epitopes. The major problem is that in most cases, it is extremely difficult to identify homology between the selected phage clones and the antigen. Despite these difficulties, there are several successful examples of the use of RPLs to identify discontinuous epitopes. For example, Luzzago et al. successfully mapped the conformational epitope of the anti-human ferritin mAb H107 by combining the information provided by the phage sequence with the antigen structural data, thus confirming the hypothesis that the epitope recognized by the mAb H107 is composed of

two discontinuous regions (59). Similarly, Ravera et al. mapped a discontinuous epitope on p53 by comparing information provided by the phage sequence to the crystal structure of p53 (96).

When the three-dimensional structure of the antigen is not available, mapping usually depends on the alignment of the consensus sequences to two or more linear regions of the primary sequence of the antigen. When successful, this information provides valuable insights into the folded structure of the antigen. Poloni et al. identified the epitope of the anti-P-gp mAb MC57 by using RPLs (97). The authors found that the epitope was formed by regions localized on the predicted two extracellular loops of the P-gp, as well as by a third region, postulated to be intracellular in the current structural model. Their finding supports the existence of a new structural model of P-gp. Using similar methodology, Orlandi et al. partially mapped the conformational epitope of the mAb MGr6, which recognizes the extracellular domain of the HER2/neu oncoprotein (98).

## 2.5 Mimotope Discovery

Epitope mapping using RPLs can, in many cases, lead to the isolation of mimotopes that bear no sequence similarity to the antigen. These peptides can interact with mAbs that recognize either linear or discontinuous epitopes of protein. For example, peptides that mimic a linear region of the *Plasmodium vivax* merozoite surface protein 1 were selected using RPLs (91). There are also numerous examples where mimotopes of conformational epitopes were identified (58,60,99-101).

Peptides can mimic native epitopes, either because of conformational or amino acid sequence similarity. In the latter, the peptide mimotope could contain residues corresponding to those brought together by proper folding of the protein. This folding may only involve 4-6 residues, and without the three-dimensional structure of the protein, it may be impossible to precisely assign these residues to the corresponding antigen (58).

In the majority of cases, peptides seem to mimic the binding properties of the native antigen, mainly because of sufficient similarity in chemistry and shape. For example, hydrophobic residues have been found to be important in the binding of several mAbs. Orlandi et al. isolated two consensus sequences that mimic the epitope of the

HER2/neu reactive mAb MGr2. However, this consensus sequence could not be found in the amino acid sequence of the neu polypeptide chain. Residues of the consensus sequences were all hydrophobic and the sequence contained a conserved proline and leucine residue (100).

Actually, proline and hydrophobic residues were shown to be involved in the interaction of mAbs with Na, K-ATPase and the guanylyl cyclase C receptor (102,103). In the latter, Nandi et al. reported that both mimotopes and native epitopes contained hydrophobic and proline residues, thus supporting the hypothesis that peptides might mimic the mode of interaction between the native epitope and the mAb. In fact, when epitope sequences contain proline residues, it is likely that a turn motive is required for the interaction with the antibody. Interestingly, by using a 6-mer phage display library, Deroo et al. isolated several mimotopes all containing a consensus proline residue instead of a serine. The authors suggested that the proline residue could be important in placing peptides into the correct spatial orientation so that it could mimic the helical turn of the native antigen sequence (104). In other cases, the presence of aromatic or basic residues was shown to be important for the binding of mAbs (60,101).

Even though it seems unlikely that peptides can mimic non-peptidic structures, different groups have successfully isolated peptides that mimic carbohydrate or oligonucleotide epitopes. In fact, several studies have shown that peptide mimotopes can be found for most, if not all, anti-carbohydrate mAbs (80,105,106). For example, the mAb B3, which reacts with the Lewis Y antigen found on the surface of a number of tumor cells, was used to select peptides that mimic the carbohydrate structure. The selected mimotope was found to specifically inhibit the binding of B3 to tumor cells, thus demonstrating the efficacy of peptides in mimicking complex carbohydrate epitopes (77). Peptide epitopes have also been shown to mimic glycosphingolipids and oligonucleotides structures (106-109).

Mimotopes are usually of little value in mapping natural epitopes, but they may have several important uses. For example, mimotopes selected from random repertoires could provide alternative ligand structures with functional effects. Mimotopes could also replace the original antigen for vaccine development (106,110,111). The latter is

particularly important in cases where the antigen is toxic or crossreactive with host proteins. These potential applications will be discussed in the following section.

## 2.6 Immunogenic Mimics and Vaccine Design

Phage display technology has considerable potential in the area of vaccine design development. Immunogenic peptides can be identified by screening RPLs against antibodies with reactivity to the antigen of interest. Furthermore, the phage itself is an excellent immunogen and can be used as a carrier, thus potentially obviating the need for conjugation of peptides to carrier particles. A peptide ligand that has been isolated *in vitro* by phage display can be subsequently screened *in vivo*, greatly reducing the time of discovery and the cost involved in evaluating a potential vaccine.

De la Cruz et al. were among the first to investigate the possibility of using phages to present peptides to the immune system. They cloned the repeats of the circumsporozoite protein of the human malaria parasite *Plasmodium falciparum* into the pIII gene of a filamentous phage, and reported that an immune response to the displayed peptide could be elicited in both rabbits and mice (112). Other groups displayed foreign peptides on the major coat protein pVIII. In this case, because of the high copy number of protein present, peptides displayed in this way appear to have greater immunogenicity (61,62,113-115). By acting as carriers, phage particles are able to present the peptide epitopes to the immune system more efficiently than a range of other carrier proteins (116). Furthermore, animals immunized with phages produce specific antibodies against both the phages and the peptide antigen without the use of adjuvants (117,118).

Phage display also facilitates the discovery of immunogenic epitopes or mimotopes. Motti *et al.* used two mAbs against the Hepatitis B surface antigen (HBsAg) to select peptides from RPL. When injected into mice, one of the selected peptides was able to elicit antibodies directed against HBsAg (119). Other groups have successfully used peptides selected from RPLs to induce immune response against viral antigens (120), tumor antigens (100) and pollen allergens (121). The ability of peptides to elicit antibodies that recognize the original antigen is particularly useful when large quantities of the native antigen is not available for use as a vaccine.

The examples cited above clearly demonstrate the close correlation between the ability of a peptide to recognize the antigen-binding site of an antibody (antigenic mimicry) and its ability to induce an immune response (immunogenic mimicry). Based on this concept, Zhong et al. used phage display to improve the immunogenicity of a peptide sequence that had previously failed to elicit antibodies cross-reactive with a native antigen. The authors constructed a RPL in which random conformational constraints were imposed on the known epitope sequence. The library was then screened against a mAb that recognized the epitope only in its native conformation. Phages selected in this manner displayed native-like peptides and hence elicited immune responses against the native antigen. More importantly, because this approach does not require the previous knowledge of the native conformation of the epitope, it may be used to improve the immunogenic profile of existing peptide vaccines (122).

Despite the successes described above, there are also reports in which peptides selected from phage RPLs only behaved as antigenic mimics, and not as immunogenic mimics. For example, Felici et al. reported that when mimotopes of a discontinuous epitope of *Bordetella pertussis* toxin (PTX) were used to immunize mice, the immune response was directed only to the peptide sequences, but not to PTX (58). In another case, peptides were found to have lost their immunogenicity, when separated from their phage carrier (121). These apparent failures may reflect the fact that phage structures can contribute to the epitope formation. It is also possible that peptides in solution are conformationally heterogeneous, and that only a portion of the peptides mimics the native epitope. The latter hypothesis is supported by data from NMR spectroscopy (121).

## 2.7 Conclusion

In summary, phage RPLs have certainly provided a rapid means for epitope and mimotope discovery. The indisputable advantage of this technology is its simplicity, minimal cost, ease of manipulation, power, and robustness. Peptides identified using this approach have a number of potential uses; including epitope mapping, drug design and vaccine development (123).



### 3. MULTIDRUG RESISTANCE

#### 3.1 Introduction

Resistance to cytotoxic chemotherapy is a common problem in patients with cancer and a major obstacle to the effective treatment of disseminated neoplasms. Resistance can be intrinsic or acquired. Intrinsic resistance seems to be associated with malignancies of specific tissues. Acquired resistance generally results from exposure of initially responsive malignant cells to various antineoplastic agents. In both cases, when tumor cells develop drug resistance, they become resistant not only to the treated drug, but also to a variety of structurally and functionally unrelated drugs of natural origin. Therefore, the tumor cell resistance is often referred to as multidrug resistance (MDR). A great variety of structurally and functionally diverse drugs, such as Anthracyclines, Epipodophyllotoxines, Actinomycin D, Vinca alkaloids, Colchicine and even Taxol are able to induce this type of resistance (124).

Several proteins have been found to be overexpressed in multidrug resistant human cancer cells, including the multidrug resistance *MDR1* gene product P-gp (125-128), the multidrug resistance-associated protein MRP (129-131), the lung resistance protein LRP which has been identified as the major vault protein (132,133), the drug resistance-associated protein DRP (134), the breast cancer resistance protein BCRP (135), the adenosine triphosphate-binding cassette protein ABCP (136), and several enzymes associated with the glutathione system (137-139). Moreover, atypical multidrug resistance has been ascribed to alterations in activity of DNA Topoisomerase II (140-142).

Clinical studies have shown that a number of these mechanisms can be detected in human tumors, and most of them have been associated with poor prognosis in particular types of cancers (143-147). Although clinical resistance to chemotherapy is likely to be multifactorial in most cancer patients, this review focuses on recent data generated by molecular genetics and biochemical analyses performed to understand the topology and structure of P-gp and to identify functionally important domains and amino acid residues within the P-gp molecule that could be involved in drug binding.

### 3.2 Structure of P-gp

P-gp was discovered 25 years ago by Juliano and Ling as an ubiquitous marker in multidrug-resistant cells (125). P-gp is a membrane bound P-ATPase encoded by the *MDR1* gene, and it is overexpressed in a wide variety of multidrug resistant cancer cell lines (148). This trans-membrane protein functions as an ATP-dependent efflux pump for a large number of drugs, thus leading to suboptimal intracellular concentrations of drugs or toxins (149). Overexpression of P-gp causes cancer cells to become resistant to a variety of anticancer drugs (e.g. Vinblastine, Vincristine, Doxorubicin, Daunorubicin, Etoposide, Teniposide, and Paclitaxel), as well as many other drugs and cytotoxic agents (150)

Ten years ago, it was recognized that the MDR gene family belongs to a larger superfamily of ATP-binding cassette (ABC) transporters or traffic ATPases (151-152). More than 100 ABC transporters have been identified from different organisms, including archaebacteria, bacteria, yeast, plants, insects, animals and humans (153-155). Although the mechanism of the inhibition of P-gp on a molecular level is still unclear, different hypotheses have been formulated. According to Gottesmann and Pastan, P-gp extrudes the toxins mainly by trapping them during their diffusion through the phospholipid bilayer, thus acting like a hydrophobic vacuum cleaner (156). The alternative hypothesis states that P-gp eliminates positively charged molecules from the cytosol by channel formation (157).

Mammalian P-gps are single chain proteins and consist of approximately 1280 amino acid residues (158-160). P-gps are composed of two homologous halves each of which contains a hydrophobic, membrane-associated domain (approximately 250 amino acid residues) followed by a hydrophilic nucleotide binding fold (approximately 300 amino acid residues). A working model for the topology of human P-gp (based entirely on hydropathy calculations) is schematically illustrated in Figure 1.5. According to this model, both the N- and C-terminal membrane-associated domains harbor six predicted trans-membrane (TM) regions (128,161). The N- and C-terminus, as well as the two nucleotide binding folds are located intra-cellularly and the first extracellular loop is glycosylated. This twelve TM region model of P-gp is supported experimentally by cellular epitope localization data obtained from several mAbs that specifically recognize

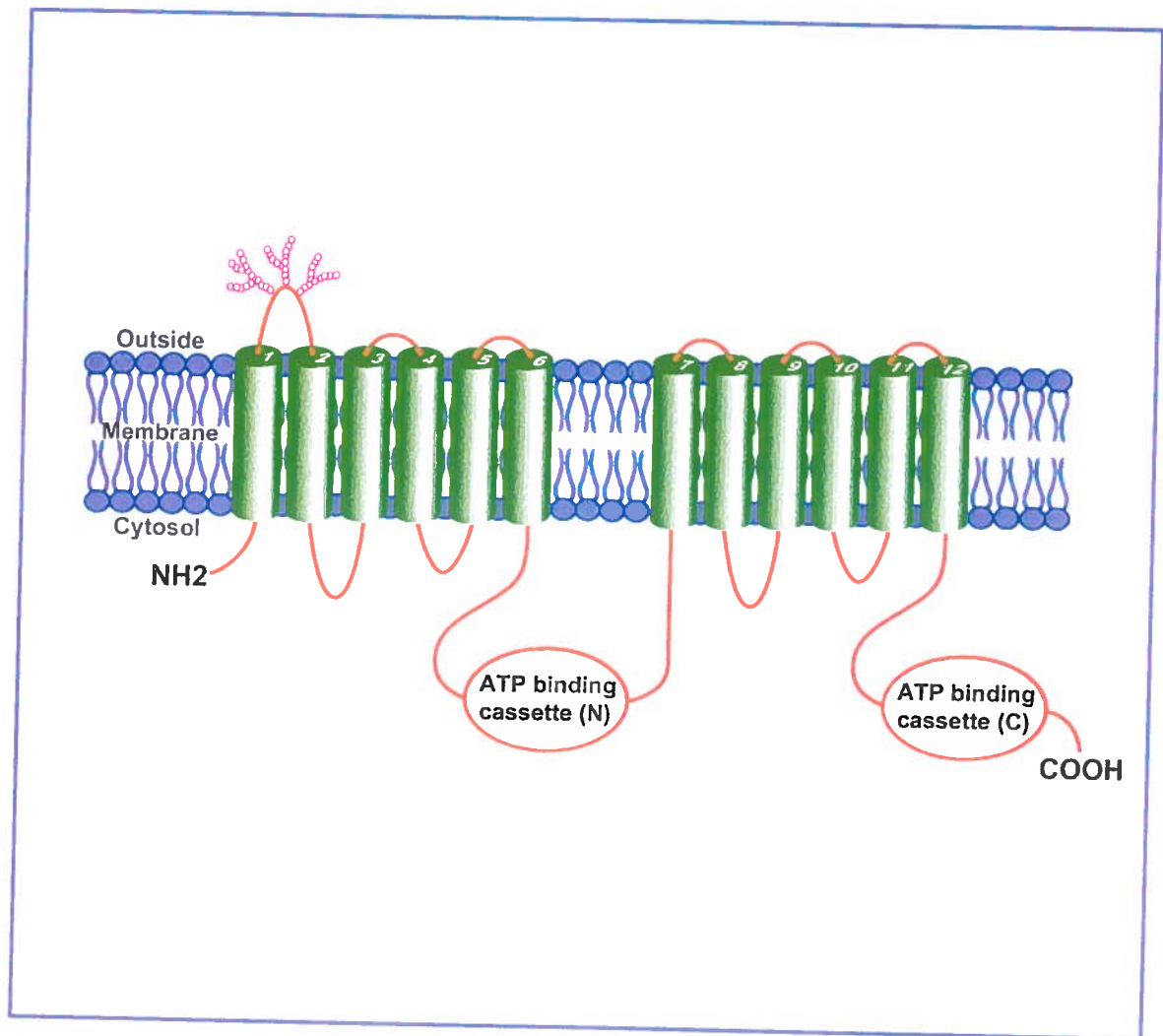


**Figure 1.5. Schematic Model of the Human P-gp and its Functional Domains.**

A twelve-TM domain model is predicted by computer-assisted hydropathy profile analysis and amino acid sequence comparison of P-gp with bacterial transport proteins. Two putative ATP binding sites are circled and putative N-linked carbohydrates are represented as wiggly lines.

(a) the N- or C-terminus of P-gp, (b) its first and fourth extracellular loop, or (c) the two ATP-binding sites (162-165). The predicted position of the glycosylated loop has been confirmed by site-directed mutagenesis and deletion analyses (166). However, the exact number of membrane-spanning regions and the orientation thereof has been a matter of many debates and several alternative models have been proposed for P-gp.

Based on the analyses of truncated P-gp molecules that were translated *in vitro* and translocated into microsomes, a topological P-gp variant was suggested that contains only four TM segments in each half (167). Moreover, expression studies in *Xenopus* oocytes of truncated P-gp fused to a reporter gene suggested a six TM domain configuration for the N-terminal half, and a four TM domain configuration for the C-terminal half (168). Analyses of the membrane polarity of bacterially expressed P-gp-alkaline phosphatase (mdr-phoA) hybrids suggested that the N-terminal half of P-gp spans the membranes six times, but in a different manner from the model presented in Figure 1.5 (169). Finally, results obtained by Poloni et al. using phage RPL to isolate antigenic mimics of P-gp for mAb MC57, indicated that one of the three distinct P-gp regions, postulated as intracellular, is a putative part of the extracellular MC57 binding domain, thus confirming the ten TM model proposed by the Germann group (97,170). Conversely, all studies performed with full-length, functional P-gp mutants or epitope-tagged P-gp variants in intact mammalian cells have corroborated the twelve TM model shown in Figure 1.5 (171,172). The reasons for the discrepancies have been hypothesized by Zhang et al. to be due to the fact that alternate topological forms of P-gp reflect different functional phenotypes (167).

Twelve TM domains and two nucleotide-binding folds constitute a minimal functional unit for many mammalian ABC transporters and, generally, it has been assumed that the multidrug transporter acts as a monomer. However, the existence of oligomeric forms of P-gp has been demonstrated in multidrug resistant cells. This raises the possibility that the functional activity of P-gp may be modulated via its incorporation into homo-oligomeric complexes. Indirect evidence for P-gp dimers in the plasma membranes has been obtained from radiation inactivation and freeze fracture studies (173-175). Data from chemical cross-linking studies are also consistent with the occurrence of P-gp dimers in multidrug resistant cells (176). The hypothesis that the

formation and dissociation of P-gp oligomers may modulate its functional activity is attractive, but clearly requires support by additional experiments.

### 3.3 Drug-Binding Site

The identification of protein domains and/or amino acid residues implicated in recognition, binding, transport through the membrane lipid bilayer, and release of drugs or MDR modulators by P-gp are a necessary prerequisite to the understanding of its structure, function and mechanisms of action. Major questions include the number, location and nature of the drug interaction sites. If both halves of the P-gp molecule are involved in drug binding, can they operate independently of each other? On the other hand, if drugs and/or modulators bind to different sites within the P-gp molecule, are there allosteric interactions between these sites? Are there central amino acid regions and/or residues within the P-gp polypeptide chain that are essential for the interaction with all substrates for transport? In particular, the exact determination of the conformation of membrane bound proteins is extremely difficult to demonstrate and to date has only been possible in the case of few selected molecules. Thus, two major approaches towards this goal have involved (1) ligand-based design of analogues of MDR drugs and modulators that can be photoactivated, and (2) site specific mutagenesis of the P-gp molecule that might demonstrate altered substrate specificity.

Attempts to map putative drug-binding sites within the primary structure of the P-gp molecule have involved the immunological identification of radioactive P-gp peptides obtained by enzymatic or chemical degradation of P-gp labeled with  $^{125}\text{I}$ -Iodoaryl azidoprazosin. Two major labeling sites have been identified within the mouse *mdr1b* P-gp: one in a region near or within TM6, and the other near or within TM12, suggesting that both halves of the P-gp molecule could contribute to drug binding (177).

Based on the observation that  $^3\text{H}$ -azidopine equally labels both halves of the human P-gp molecule, it has been suggested that amino acid residues from the N- and C-terminal halves of P-gp interact and could cooperate to form one major drug interaction pore (178). This model is also supported by the findings that both halves are required for the drug-stimulated ATPase activity of P-gp (179). However, this model still allows multiple sites for drug recognition, hence it might rather constitute a three dimensional

structural pocket within the P-gp molecule through which drugs pass during the transport process and from which they are released again.

Many different radioactive photo-affinity analogues of drugs and MDR-reversing agents have been used to prove the drug-binding capacity of P-gp, including derivatives of Vinblastine, Colchicine, Verapamil, Daunomycin, Azidopine and other drugs (180-186). Results generated from such analyses suggested that different drugs bind to separate, possibly overlapping, or allosterically coupled sites. Alternatively, P-gp harbors a common drug-acceptor site that displays variable affinity for different agents (187).

Data obtained from mutational analyses provided further evidence of the importance of the TM5-6 and TM11-12 regions for drug interactions. Substitution of Phe335 in TM6 by Ala strongly altered the substrate specificity of human P-gp and impaired its ability to confer resistance to Vinblastine or Actinomycin D, while the ability to confer resistance to Colchicine and Doxorubicin was retained (188).

More dramatically, mutation of Ser344 in TM6 to Ala, Thr, Cys, or Tyr completely abrogated the ability of human P-gp to confer drug resistance (179). A human P-gp mutant carrying a Phe to Ala or Ser mutation at position 978 in TM12 was shown to lower the capacity to confer resistance to Vinblastine and Actinomycin D and conferred no detectable resistance to Colchicine and Doxorubicin (188). Moreover, an *MDR1* mutant in which the extra-cytoplasmic loop between TM11 and TM12 was replaced with that of *MDR2* conferred increased resistance to Actinomycin D, Colchicine, and Doxorubicin, but not to Vincristine (189). Thus, several key amino acid residues are present within the TM5-6 and TM11-12 regions, which when altered, could change the drug substrate specificity of P-gp. Additional amino acid residues within other membrane-spanning segments may also play a role in determining the cross-resistance pattern conferred by P-gp. A mutational analysis of thirteen proline residues implicated two of these, Pro223 in TM4 and Pro866 in TM10, as being critical for the drug substrate specificity of human P-gp (188).

Taken together, point mutations that are scattered throughout the primary structure, but reside within or in close proximity to membrane-spanning segments, contribute to the drug substrate specificity of P-gp. It remains to be determined which one of these amino acid residues interact with drug and/or modulator substrate(s) and which

ones act indirectly, for example by contributing to conformational changes upon binding of drug and/or ATP, or upon ATP hydrolysis.

### **3.5 Conclusion**

MDR has been one of the more intensely investigated fields of cancer research during the last three decades, mainly because of its close association with the failure of chemotherapy leading to increased morbidity and mortality in cancer patients. Molecular investigations in MDR have identified many drug transporter genes and established the role of these marker genes in the refractory status of cancer patients. Although the true clinical relevance of MDR is still heavily debated, P-gp is believed to be one of the key molecules which cause MDR in cancer (190,191). Many efforts have been made to understand its mechanism and develop specific inhibitors. Recent observations have challenged the notion that P-gp has evolved merely to efflux xenotoxins out of healthy cells and raised the possibility that P-gp and related transporter molecules might play a fundamental role in regulating cell differentiation, proliferation and survival (192). However, additional research including clinical trials is needed before molecular diagnostic assays of MDR are translated to clinical oncology.

#### 4. REFERENCES

1. Kohler G. and C. Milstein. 1975. "Continuous cultures of fused cells secreting antibody of predicted specificity". Nature, vol. 256, p. 495-496.
2. Waldmann, T. A. 1991. "Monoclonal antibodies in diagnosis and therapy". Science, vol. 252, p. 1657-1662.
3. Kavanaugh, A. F. 1998. "Anti-tumor necrosis factor-alpha monoclonal antibody therapy for rheumatoid arthritis". Rheum. Dis. Clin. North Am., vol. 24, p. 593-614.
4. Moss, T. J. 1999. "Clinical relevance of minimal residual cancer in patients with solid malignancies". Cancer Metastasis Rev., vol. 18, p. 91-100.
5. Bociek, R.G. and J. O. Armitage. 1999. "Hodgkin's disease and non-Hodgkin's lymphoma". Curr. Opin. Hematol., vol. 6, p. 205-215.
6. Kon, O. M. and A. B. Kay. 1999. "Anti-T cell strategies in asthma". Inflamm. Res., vol. 48, p. 516-523.
7. Houghton, A. N. and D. A. Scheinberg. 2000. "Monoclonal antibody therapies – a constant threat to cancer". Nature Medicine, vol. 6, p. 373-374.
8. Breedveld, F. C. 2000. "Therapeutic monoclonal antibodies". Lancet, vol. 355, p. 735-740.
9. Farah, R. A., B. Clinchy, L. Herrera, and E. S. Vitetta. 1998. "The development of monoclonal antibodies for the therapy of cancer". Critical Reviews in Eukaryotic Gene Expression, vol. 8, p. 321-356.
10. Dalgleish, A. G. 2000. "Cancer vaccines". Br. J. Cancer, vol. 82, p. 1619-1624.
11. Wang, R.-F. and S. A. Rosenberg. 1999. "Human tumor antigens for cancer vaccine development". Immunol. Rev., vol. 170, p. 85-100.
12. Brown, S. L., R. A. Miller, and R. Levy. 1989. "Antiidiotype antibody therapy of B-cell lymphoma". Semin. Oncol., vol. 16, p. 199-210.
13. Dillman, R. O. 1994. "Antibodies as cytotoxic therapy". J. Clin. Oncol., vol. 12, p. 1497-1514.
14. Choy, E. H. S., G. S. Panayi, and G. H. Kingsley. 1995. "Therapeutic monoclonal antibodies". Br. J. Rheumatol., vol. 34, p. 707-715.



15. Schlom, J., P. H. Hand, J. W. Greiner, D. Colcher, S. Shrivastav, J. A. Carrasquillo, J. C. Reynolds, S. M. Larson, and A. Raubitschek. 1990. "Innovations that influence the pharmacology of monoclonal antibody guided tumor targeting". Cancer Res., vol. 50 (suppl. 3), p. 820s-887s.
16. Pietersz, G. A., L. Wenjun, V. R. Sutton, J. Burgess, I. F. C. McKenzie, H. Zola, and J. A. Trapani. 1995. "*In vitro* and *in vivo* antitumor activity of a chimeric anti-CD19 antibody". Cancer Immunol. Immunother., vol. 41, p. 53-60.
17. Dyer, M. J. S., G. Hale, F. G. J. Hayhoe, and H. Waldmann. 1989. "Effects of CAMPATH-1 antibodies *in vivo* in patients with lymphoid malignancies: influence of antibody isotype". Blood, vol. 73, p. 1431-1439.
18. Lobuglio, A. F. and M. N. Saleh. 1992. "Advances in monoclonal antibody therapy of cancer". Am. J. Med. Sci., vol. 304, p. 214-224.
19. Wallace, P. M., J. F. MacMaster, V. F. Smith, D. E. Kerr, P. D. Senter, and W. L. Cosand. 1994. "Intratumoral generation of 5-fluorouracil mediated by an antibody cytosine deaminase conjugate in combination with 5-fluorocytosine". Cancer Res., vol. 54, p. 2719-2723.
20. Seino, J., P. Eveleigh, S. Warnaar, L. J. van Haarlem, L. A. van Es, and M. R. Daha. 1993. "Activation of human complement by mouse and mouse/human chimeric monoclonal antibodies". Clin. Exp. Immunol., vol. 94, p. 291-296.
21. Trauth, B. C., C. Klas, A. M. J. Peters, S. Matzku, S. Moller, W. Falk, K.-M. Debatin, and P. H. Krammer. 1989. "Monoclonal antibody-mediated tumor regression by induction of apoptosis". Science, vol. 245, p. 301-305.
22. Debatin, K. M. and P. H. Krammer. 1995. "Resistance to APO-1 (CD95) induced apoptosis in T-ALL is determined by a BCL-2 independent anti-apoptotic program". Leukemia, vol. 9, p. 815-820.
23. Pan, G., K. O'Rourke, A. M. Chinnaiyan, R. Gentz, R. Ebner, J. Ni, and V. M. Dixit. 1997. "The receptor for the cytotoxic ligand TRAIL". Science, vol. 276, p. 111-113.
24. Pan, G., J. Ni, Y. F. Wci, G. Yu, R. Gentz, and V. M. Dixit. 1997. "An antagonist decoy receptor and a death domain-containing receptor for TRAIL". Science, vol. 277, p. 815-818.
25. Mitsiades, N., V. Poulaki, S. Tseleni-Balafouta, D. A. Koutras, and I. Stamenkovic. 2000. "Thyroid carcinoma cells are resistant to FAS-mediated apoptosis but sensitive to tumor necrosis factor-related apoptosis-inducing ligand". Cancer Res., vol. 60, p. 4122-4129.

26. Ghetie, M. A., V. Ghetie, and E. S. Vitetta. 1999. "Anti-CD19 antibodies inhibit the function of the P-gp pump in multidrug-resistant B lymphoma cells". Clin. Cancer Res., vol. 5, p. 3920-3927.
27. Ghetie, M.-A., L. J. Picker, J. A. Richardson, K. Tucker, J. W. Uhr, and E. S. Vitetta. 1994. "Anti-CD19 inhibits the growth of human B-cell tumor lines *in vitro* and of Daudi cells in SCID mice by inducing cell cycle arrest". Blood, vol. 83, p. 1329-1336.
28. Chaouchi, N. A., A. Vazquez, P. Galanaud, and C. Leprince. 1995. "B cell antigen receptor-mediated apoptosis: importance of accessing molecules CD19 and CD22, and of surface IgM cross-linking". J. Immunol., vol. 154, p. 3096-3104.
29. Vuist, W. M. J., R. Levy, and D. G. Maloney. 1994. "Lymphoma regression induced by monoclonal anti-idiotypic antibodies correlates with their ability to induce Ig signal transduction and is not prevented by tumor expression of high levels of Bcl-2 protein". Blood, vol. 83, p. 899-906.
30. Rodeck, U., K. Melber, R. Kath, H. D. Menssen, M. Varello, B. Atkinson, and M. Herlyn. 1991. "Constitutive expression of multiple growth factor genes by melanoma cells but not normal melanocytes". J. Invest. Dermatol., vol. 97, p. 20-26.
31. Baselga, J. and J. Mendelsohn. 1994. "Receptor blockade with monoclonal antibodies as anticancer therapy". Pharmacol. Ther., vol. 64, p. 127-154.
32. Shepard, H. M., G. D. Lewis, J. C. Sarup, B. M. Fendly, D. Maneval, J. Mordenti, I. Figari, C. E. Kotts, M. A. Palladino, A. Ullrich, and D. Slamon. 1991. "Monoclonal antibody therapy of human cancer: taking the HER2 protooncogene to the clinic". J. Clin. Immunol., vol. 11, p. 117-127.
33. Shan, D., J. A. Ledbetter, and O. W. Press. 1998. "Apoptosis of malignant human B cells by ligation of CD20 with monoclonal antibodies". Blood, vol. 91, p. 1644-1652.
34. Wu X, Z. Fan, H. Masui, S. Rosen, and J. Mendelsohn. 1995. "Apoptosis induced by an anti-epidermal growth factor receptor monoclonal antibody in a human colorectal carcinoma cell line and its delay by insulin". J. Clin. Invest., vol. 95, p. 1897-1905.
35. von Mehren, M. and L. M. Weiner. 1996. "Monoclonal antibody-based therapy". Curr. Opin. Oncol., vol. 8, p. 493-498.

36. Peterson, N. C. 1996. "Recombinant antibodies: alternative strategies for developing and manipulating murine derived monoclonal antibodies". Lab Anim. Sci., vol. 46, p. 8-14.
37. Owens, R. J. and R. J. Young. 1994. "The genetic engineering of monoclonal antibodies". J. Immunol. Methods, vol. 168, p. 149-165.
38. Kozarsky, K. F., C. Tsai, C. M. Bott, G. Allada, L. L. Li, and D. A. Fox. 1993. "An anti-CD2 monoclonal antibody that both inhibits and stimulates T cell activation recognizes a subregion of CD2 distinct from known ligand-binding sites". Cell. Immunol., vol. 150, p. 235-246.
39. Rapley, R. 1995. "The biotechnology and applications of antibody engineering". Mol. Biotechnol., vol. 3, p. 139-154.
40. Khazaeli, M. B., M. N. Saleh, T. P. Liu, R. A. Reisfield, and A. F. LoBuglio. 1991. "Pharmacokinetics and immune response of <sup>131</sup>I-chimeric mouse/human B72.3 (human gamma4) monoclonal antibody in humans". Cancer Res., vol. 51, p. 5461-5466.
41. Porter, R. R. 1958. "Separation of fraction of rabbit gamma-globulin containing the antibody and antigenic combining sites". Nature, vol. 182, p. 670-671.
42. Nisonoff, A., F. C. Wissler, and L. N. Lipman. 1960. "Properties of the major component of a peptic digest of rabbit antibody". Science, vol. 132, p. 1770-1771.
43. Huston, J. S., M.-S. Tai, M. Mudgett-Hunter, J. McCartney, F. Warren, E. Haber, and H. Opperman. 1991. "Protein engineering of single-chain Fv analogs and fusion proteins". Methods Enzymol., vol. 203, p. 46-88.
44. Bird, R. E., K. D. Hardman, J. W. Jacobson, S. Jonson, B. M. Kaufman, S. M. Lee, T. Lee, S. H. Pope, G. S. Riordan, and M. Whitlow. 1988. "Single-chain antigen-binding proteins". Science, vol. 242, p. 423-426.
45. Huston, J. S., J. McCartney, M.-S. Tai, C. Mottola-Hartshorn, D. Jin, F. Warren, P. Keck, and H. Opperman. 1993. "Medical applications of single-chain antibodies". Int. Rev. Immunol., vol. 10, p. 195-217.
46. Renner, C., L. Trumper, and M. Pfreundschuh. 1997. "Monoclonal antibodies in the treatment of non-Hodgkin's lymphoma: recent results and future prospects", Leukemia, vol. 11, p. S55-S59.
47. Riethmuller, G., E. Schneidergadicke, G. Schlimok, W. Schmiegell, R. Raab, K. Hoffken, R. Gruber, H. Pichlmaier, H. Hirche, R. Pichlmayr, P. Buggisch, J. Witte, F. W. Eigler, I. Facklerschwalbe, I. Funke, C. G. Schmidt, H. Schreiber, L. Schweiberer, and B. Eibleibesfeldt. 1994. "Randomised trial of monoclonal

- antibody for adjuvant therapy of resected Dukes C colorectal carcinoma". Lancet, vol. 343, p. 1177-1183.
48. Weiner, L. M. 1999. "Monoclonal antibody therapy of cancer". Semin. Oncol., vol. 26, p. 43-51.
  49. Buske, C., M. Feuring-Buske, M. Unterhalt, and W. Hiddem. 1999. "Monoclonal antibody therapy for B cell non-Hodgkin's lymphomas: emerging concepts of a tumour-targeted strategy". Eur. J. Cancer, vol. 35, p. 549-557.
  50. Link, B. K. and G. J. Weiner. 1998. "Monoclonal antibodies in the treatment of human B-cell malignancies". Leuk. Lymphoma, vol. 31, p. 237-249.
  51. Ouwehand, W. H. and N. Watkins. 1998. "Novel diagnostic and therapeutic strategies with genetically engineered human antibodies". Vox.Sang., vol. 74, p. 223-232.
  52. Adams, G. P. and R. Schier. 1999. "Generating improved single-chain Fv molecules for tumor targeting". J. Immunol. Methods, vol. 231, p. 249-260.
  53. Cabilly, S. 1999. "The basic structure of filamentous phage and its use in the display of combinatorial peptide libraries". Mol. Biotechnol., vol. 12, p. 143-148.
  54. Johnson, K. and L. Ge. 1999. "Phage display of combinatorial peptide and protein libraries and their applications in biology and chemistry". Curr. Top. Microbiol. Immunol., vol. 243, p. 87-105.
  55. Forrer, P., S. Jung, and A. Pluckthun. 1999. "Beyond binding: using phage display to select for structure, folding and enzymatic activity in proteins". Curr. Opin. Struct. Biol., vol. 9, p. 514-520.
  56. Yip, Y. L. and R. L. Ward. 1999. "Epitope discovery using monoclonal antibodies and phage peptide libraries". Comb. Chem. High Throughput Screen, vol. 2, p. 125-138.
  57. Cortese, R., F. Felici, G. Galfre, A. Luzzago, P. Monaci, and A. Nicosia. 1991. "Epitope discovery using peptide libraries displayed on phage". Tibtech, vol. 12, p. 262-267.
  58. Felici, F., A. Luzzago, A. Folgori, and R. Cortese. 1993. "Mimicking of discontinuous epitopes by phage-displayed peptides, II. Selection of clones recognized by a protective monoclonal antibody against the *Borotella pertussis* toxin from phage peptide libraries". Gene, vol. 128, p. 21-27.
  59. Luzzago, A., F. Felici, A. Tramontano, A. Pessi, and R. Cortese. 1993. "Mimicking of discontinuous epitopes by phage-displayed peptides, I. Epitope

- mapping of human H ferritin using a phage library of constrained peptides". Gene, vol. 128, p. 51-57.
60. Balass, M., Y. Heldman, S. Cabilly, D. Givol, E. Katchalski-Katzir, and S. Fuchs. 1993. "Identification of a hexapeptide that mimics a conformation-dependent binding site of acetylcholine receptor by use of a phage-epitope library". Proc. Natl. Acad. Sci. USA, vol. 90, p. 10638-10642.
  61. Greenwood, J., A. E. Willis, and R. N. Perham. 1991. "Multiple display of foreign peptides on a filamentous bacteriophage". J. Mol. Biol., vol. 220, p. 821-827.
  62. Willis, A. E., R. N. Perham, and D. Wraith. 1993. "Immunological properties of foreign peptides in multiple display on a filamentous bacteriophage: peptides from *Plasmodium falciparum* circumsporozoite as antigens". Gene, vol. 128, p. 79-83.
  63. Smith, G. P. and V. A. Petrenko. 1997. "Phage display". Chem. Rev., vol. 97, p. 391-410.
  64. Smith, G. P. 1985. "Filamentous fusion phage: novel expression vectors that display cloned antigens on the virion surface". Science, vol. 228, p. 1315-1316.
  65. Scott, J. K. and G. P. Smith. 1990. "Searching for peptide ligands with an epitope library". Science, vol. 249, p. 386-390.
  66. Cwirla, S. E., E. A. Peters, R. W. Barrett, and W. J. Dower. 1990. "Peptides on phage: A vast library of peptide for identifying ligands". Proc. Natl. Acad. Sci. USA, vol. 87, p. 6378-6382.
  67. Devlin, J. J., L. C. Panganiban, and P. E. Devlin. 1990. "Random peptide libraries: A source of specific protein binding molecules". Science, vol. 249, p. 404-406.
  68. Felici, F., L. Castagnoli, A. Musacchio, R. Jappelli, and G. Cesareni. 1991. "Selection of antibody ligands from a large library of oligopeptides expressed on a multivalent expression vector". J. Mol. Biol., vol. 222, p. 301-310.
  69. Felici, F., A. Luzzago, P. Monaci, A. Nicosia, M. Sollazzo, and C. Traboni. 1995. "Peptide and protein display on the surface of filamentous bacteriophage". Biotechnol. Annu. Rev., vol. 1, p. 149-183.
  70. Koscielska, K., L. Kiczak, M. Kasztura, O. Wesolowska, and L. Otlewski. 1998. "Phage display of proteins". Acta Biochim. Pol., vol. 45, p. 705-720.
  71. Wilson, D. R. and B. B. Finlay. 1998. "Phage display: applications, innovations, and issues in phage and host biology". Can. J. Microbiol., vol. 44, p. 313-329.

72. Hoess, R. H., A. J. Mack, H. Walton, and T. M. Reilly. 1994. "Identification of a structural epitope by using a peptide library displayed on filamentous bacteriophage". J. Immunol., vol. 153, p. 724-729.
73. Koivunen, E., B. Wang, and E. Ruoslahti. 1994. "Isolation of a highly specific ligand for the  $\alpha_5\beta_1$  integrin from a phage display library". J. Cell. Biol., vol. 124, p. 373-380.
74. Jellis, C. L., T. J. Cradick, P. Rennert, P. Salinas, J. Boyd, T. Amirault, and G. S. Gray. 1993. "Defining critical residues in the epitope for HIV-neutralizing monoclonal antibody using phage display and peptide array technologies". Gene, vol. 137, p. 63-68.
75. McConnell, S. J., A. J. Uveges, D. M. Fowlkes, and D. G. Spinella. 1996. "Construction and screening of M13 phage libraries displaying long random peptides". Mol. Divers., vol. 1, p. 165-176.
76. Smith, G. P. 1991. "Surface presentation of protein epitopes using bacteriophage expression systems". Curr. Opin. Biotechnol., vol. 2, p. 668-673.
77. Hoess, R. H., U. Brinkmann, T. Handel, and I. Pastan. 1993. "Identification of a peptide which binds to the carbohydrate-specific monoclonal antibody B3". Gene, vol. 128, p. 43-49.
78. O'Neil, K.T. and R. H. Hoess. 1995. "Phage display: protein engineering by directed evolution". Curr. Opin. Struct. Biol., vol. 5, p. 443-449.
79. Koivunen, E., B. Wang, and E. Ruoslahti. 1995. "Phage libraries displaying cyclic peptides with different ring sizes: ligand specificities of the RGD-directed integrins". Biotechnology, vol. 13, p. 265-270.
80. Bonnycastle, L. L., J. S. Mehroke, M. Rashed, X. Gong, and J. K. Scott. 1996. "Probing the basis of antibody reactivity with a panel of constrained peptide libraries displayed by filamentous phage". J. Mol. Biol., vol. 258, p. 747-762.
81. McLafferty, M. A., R. B. Kent, R. C. Ladner, and W. Markland. 1993. "M13 bacteriophage displaying disulfide-constrained microproteins". Gene, vol. 128, p. 29-36.
82. Lundin, K., A. Samuelsson, M. Jansson, J. Hinkula, B. Wahren, H. Wigzell, and M. A. Persson. 1996. "Peptides isolated from random peptide libraries on phage elicit a neutralizing anti-HIV-1 response: analysis of immunological mimicry". Immunology, vol. 89, p. 579-586.

83. Demangel, C., S. Rouyre, P. M. Alzari, F. Nato, S. Longacre, P. Lafaye, and J. C. Mazie. 1996. "Phage-displayed mimotopes elicit monoclonal antibodies specific for a malaria vaccine candidate". J. Biol. Chem., vol. 379, p. 65-70.
84. McConnell, S. J., M. L. Kendall, T. M. Reilly, and R. H. Hoess. 1994. "Constrained peptide libraries as a tool for finding mimotopes". Gene, vol. 151, p. 115-118.
85. Gordon, E. M., R. W. Barrett, W. J. Dower, S. P. Fodor, and M. A. Gallop. 1994. "Applications of combinatorial technologies to drug discovery. 2. Combinatorial organic synthesis, library screening strategies, and future directions". J. Med. Chem., vol. 37, p. 1385-1401.
86. Kay, B. K., G. Winter, and J. McCafferty (eds.). 1996. Phage Display of Peptides and Proteins. A Laboratory Manual, San Diego: Academic Press.
87. Stephen, C. W., and D. P. Lane. 1992. "Mutant conformation of p53: precise epitope mapping using a filamentous phage epitope library". J. Mol. Biol., vol. 225, p. 577-583.
88. Schellekens, G. A., E. Lasonder, M. Feijibrief, D. G. Koedijk, J. W. Drijfhout, A. J. Scheffer, S. Welling-Wester, and G. Welling. 1994. "Identification of the core residues of the epitope of a monoclonal antibody raised against glycoprotein D of herpes simplex virus type 1 by screening of a random peptide library". Eur. J. Immunol., vol. 24, p. 3188-3193.
89. Bottger, V. and E. B. Lane. 1994. "A monoclonal antibody epitope on keratin 8 identified using a phage peptide library". J. Mol. Biol., vol. 235, p. 61-67.
90. James, M., N. T. Man, Y. H. Edwards, and G. E. Morris. 1997. "The molecular basis for cross-reaction of an anti-dystrophin antibody with alpha-actinin". Biochim. Biophys. Acta, vol. 1360, p. 169-176.
91. Demangel, C., P. Lafaye, and J. C. Mazie. 1996. "Reproducing the immune response against the *Plasmodium vivax* merozoite surface protein 1 with mimotopes selected from a phage-displayed peptide library". Mol. Immunol., vol. 33, p. 909-916.
92. Morishita, E., H. Narita, M. Nishida, N. Kawashima, K. Yamagishi, S. Masuda, M. Nagao, H. Hatta, and R. Sasaki. 1996. "Anti-erythropoietin receptor monoclonal antibody: epitope mapping, quantification of the soluble receptor, and detection of the solubilized transmembrane receptor and the receptor-expressing cells". Blood, vol. 88, p. 465-471.
93. Lane, D. P. and C. W. Stephen. 1993. "Epitope mapping using bacteriophage peptide libraries". Curr. Opin. Immunol., vol. 5, p. 268-271.

94. Bottger, V., P. C. Stasiak, D. L. Harrison, D. M. Mellerick, and E. B. Lane. 1995. "Epitope mapping of monoclonal antibodies to keratin 19 using keratin fragments, synthetic peptides and phage peptide libraries". Eur. J. Biochem., vol. 231, p. 475-485.
95. Stephen, C. W., P. Helminen, and D. P. Lane. 1995 "Characterization of epitopes on human p53 using phage-displayed peptide libraries: insights into antibody-peptide interactions". J. Mol. Biol., vol. 248, p. 58-78.
96. Ravera, M. W., J. Carcamo, R. Brissette, A. Alam-Moghe, O. Dedova, W. Cheng, K. C. Hsiao, D. Klebanov, H. Shen, P. Tang, A. Blume, and W. Mandecki. 1998. "Identification of an allosteric binding site on the transcription factor p53 using a phage-displayed peptide library". Oncogene, vol. 16, p. 1993-1999.
97. Poloni F., G. Romagnoli, M. Cianfriglia, and F. Felici. 1995. "Isolation of antigenic mimics of *MDR1*-P-glycoprotein by phage-displayed peptide libraries". Int. J. Cancer, vol. 61, p. 727-731.
98. Orlandi, R., C. Formantici, S. Menard, C. M. Boyer, J. Wiener, and M. Colnaghi. 1997 "A linear region of a monoclonal antibody conformational epitope mapped on p185HER2 oncoprotein". J. Biol. Chem., vol. 378, p. 1387-1392.
99. Barchan, D., M. Balass, M. C. Souroujon, E. Katchalski-Katzir, and S. Fuchs. 1995. "Identification of epitopes within a highly immunogenic region of acetylcholine receptor by a phage epitope library". J. Immunol., vol. 155, p. 4264-4269.
100. Orlandi, R., S. Menard, M. I. Colnaghi, C. M. Boyer, and F. Felici. 1994. "Antigenic and immunogenic mimicry of the HER2/neu oncoprotein by phage-displayed peptides". Eur. J. immunol., vol. 24, p. 2868-2873.
101. Cook, A., J. M. Davies, M. A. Myers, I. R. Mackay, and M. J. Rowley. 1998. "Mimotopes identified by phage display for the monoclonal antibody CII-C1 to type II collagen". J. Autoimmun., vol. 11, p. 205-211.
102. Pacholczyk, T. and K. J. Sweadner. 1997. "Epitope and mimotope for an antibody to the Na/K-ATPase". Protein Sci., vol. 6, p. 1537-1548.
103. Nandi, A., K. Suguna, A. Surolia, and S. S. Visweswariah. 1998. "Topological mimicry and epitope duplication in the guanylyl cyclase C receptor". Protein Sci., vol. 7, p. 2175-2183.
104. Deroo, S., K. C. El Kasmi, P. Fournier, D. Theisen, N. H. Brons, M. Herrmann, J. Desmet, and C. P. Muller. 1998. "Enhanced antigenicity of a four-contact-residue epitope of the measles virus hemagglutinin protein by phage display libraries: evidence of a helical structure in the putative active site". Mol. Immunol., vol. 35, p. 435-443.



105. Harris, S. L., L. Craig, J. S. Mehroke, M. Rashed, M. B. Zwick, K. Kenar, E. J. Toone, N. Greenspan, F. I. Auzanneau, J. R. Marino-Albernas, B. M. Pinto, and J. K. Scott. 1997. "Exploring the basis of peptide-carbohydrate crossreactivity: evidence for discrimination by peptides between closely related anti-carbohydrate antibodies". Proc. Natl. Acad. Sci. USA, vol. 94, p. 2454-2459.
106. Gaynor, B., C. Putterman, P. Valadon, L. Spatz, M. D. Scharff, and B. Diamond. 1997. "Peptide inhibition of glomerular deposition of an anti-DNA antibody". Proc. Natl. Acad. Sci. USA, vol. 94, p. 1955-1960.
107. Taki, T., D. Ishikawa, H. Hamasaki, and S. Handa. 1997. "Preparation of peptides which mimic glycosphingolipids by using phage peptide library and their modulation on beta-galactosidase activity". FEBS Lett., vol. 418, p. 219-223.
108. Sibille, P., T. Ternynck, F. Nato, G. Buttin, D. Strosberg, and A. Avrameas. 1997. "Mimotopes of polyreactive anti-DNA antibodies identified using phage-display peptide libraries". Eur. J. Immunol., vol. 27, p. 1221-1228.
109. Moe, G. R., S. Tan, and D. M. Granoff. 1999. "Molecular mimetics of polysaccharide epitopes as vaccine candidates for prevention of *Neisseria meningitidis* serogroup B disease". FEMS Immunol. Med. Microbiol., vol. 26, p. 209-226.
110. Oggioni, M. R., D. Medaglini, T. Magg, and G. Pozzi. 1999. "Engineering the gram-positive cell surface for construction of bacterial vaccine vectors". Methods, vol. 19, p. 163-173.
111. Oiu, J., P. Luo, K. Wasmund, Z. Steplewski, and T. Kieber-Emmons. 1999. "Towards the development of peptide mimotopes of carbohydrate antigens as cancer vaccines". Hybridoma, vol. 18, p. 103-112.
112. de la Cruz, V. F., A. A. Lai, and T. F. McCutchan. 1988. "Immunogenicity and epitope mapping of foreign sequences via genetically engineered filamentous phage". J. Biol. Chem., vol. 263, p. 4318-4322.
113. Minenkova, O.O., A. A. Ilyichev, G. P. Kishchenko, and V. A. Petrenko. 1993. "Design of specific immunogens using filamentous phage as the carrier". Gene, vol. 128, p. 85-88.
114. di Marzo Veronese, F., A. E. Willis, C. Boyer-Thompson, E. Appella, and R. N. Perham. 1994. "Structural mimicry and enhanced immunogenicity of peptide epitopes displayed on filamentous bacteriophage. The V3 loop of HIV-1 gp120". J. Mol. Biol., vol. 243, p. 167-172.

115. Delmastro, P., A. Meola, P. Monaci, R. Cortese, and G. Galfre. 1997. "Immunogenicity of filamentous phage displaying peptide mimotopes after oral administration. Vaccine, vol. 15, p. 1276-1285.
116. Meola, A., P. Delmastro, P. Monaci, A. Luzzago, A. Nicosia, F. Felici, R. Cortese, and G. Galfre. 1995. "Derivation of vaccines from mimotopes. Immunologic properties of human hepatitis B virus surface antigen mimotopes displayed on filamentous phage". J. Immunol., vol. 154, p. 3162-3172.
117. Perham, R. N., T. D. Terry, A. E. Willis, J. Greenwood, F. di Marzo Veronese, and E. Appella. 1995. "Engineering a peptide epitope display system on filamentous bacteriophage". FEMS Microbiol. Rev., vol. 17, p. 25-31.
118. Engberg, J., M. Krogsgaard, and L. Fugger. 1999. "Recombinant antibodies with the antigen-specific, MHC restricted specificity of T cells: novel reagents for basic and clinical investigations and immunotherapy". Immunotechnology, vol. 4, p. 273-278.
119. Motti, C., M. Nuzzo, A. Meola, G. Galfre, F. Felici, R. Cortese, A. Nicosia, and P. Monaci. 1994. "Recognition by human sera and immunogenicity of HbsAg mimotopes selected from an M13 phage display library". Gene, vol. 146, p. 191-198.
120. D'Mello, F., C. D. Partidos, M. W. Steward, and C. R. Howard. 1997. "Definition of the primary structure of hepatitis B virus (HBV) pre-S hepatocyte binding domain using random peptide libraries". Virology, vol. 237, p. 319-326.
121. Jensen-Jarolim, E., A. Leitner, H. Kalchhauser, A. Zurcher, E. Ganglberger, B. Bohle, O. Scheiner, G. Boltz-Nitulescu, and H. Breiteneder. 1998. "Peptide mimotopes displayed by phage inhibit antibody binding to Bet v1, the major birch pollen allergen, and induce specific IgG response in mice". FASEB J., vol. 12, p. 1635-1642.
122. Zhong, G., G. P. Smith, J. Berry, and R. C. Brunham. 1994. "Conformational mimicry of a chlamydial neutralization epitope on filamentous phage". J. Biol. Chem., vol. 269, p. 24183-24188.
123. Cesareni, G., L. Castagnoli, and G. Cestra. 1999. "Phage displayed peptide libraries". Comb. Chem. High Throughput Screen, vol. 2, p. 1-17.
124. Bradley, G., P. F. Juranka, and V. Ling. 1988. "Mechanism of multidrug resistance". Biochim. Biophys. Acta, vol. 948, p. 87-128.
125. Juliano R. I. and V. Ling. 1976. "A surface glycoprotein modulating drug permeability in Chinese hamster ovary cell mutants". Biochim. Biophys. Acta, vol. 455, p. 152-162.

126. Skovsgaard, T. 1978. "Mechanisms of resistance to daunorubicin in Ehrlich ascites tumour cells". Cancer Res., vol. 38, p. 1785-1791.
127. Beck, W. T., T. J. Mueller, and L. R. Tanzer. 1979. 'Altered surface membrane glycoprotein in vinca alkaloid-resistant human leukemic lymphoblasts'. Cancer Res., vol. 39, p. 2070-2076.
128. Gros, P., Y. B. Neriah, J. M. Croop, and D. E. Housman. 1986. "Isolation and expression of a cDNA (*mdr*) that confers multidrug resistance". Nature, vol. 323, p. 728-731.
129. Cole, S. P. C., G. Bhardwaj, J. H. Gerlach, et al. 1992. "Overexpression of a transporter gene in a multidrug-resistant human lung cancer cell line". Science, vol. 258, p. 1650-1654.
130. Grant, C.E., G. Valdimarsson, D. R. Hiphler, K. C. Almquist, S. P. C. Cole, and R. G. Deeley. 1994. "Overexpression of multidrug resistance-associated protein (MRP) increases resistance to natural product drugs". Cancer Res., vol. 54, p. 357-361.
131. Zaman, G. J. R., M. J. Flens, M. R. van Leusden, M. de Haas, H. S. Mulder, J. Lankelma, H. M. Pinedo, R. J. Scheper, F. Baas, and H. J. Broxterman. 1994. "The human multidrug resistance-associated protein MRP is a plasma membrane drug-efflux pump". Proc. Natl. Acad. Sci. USA, vol. 91, p. 8822-8826.
132. Scheper, R. J., H. J. Broxterman, G. L. Scheffer, P. Kaaijk, W. S. Dalton, T. H. van Heijningen, C. K. van Kalken, M. L. Slovak, E. G. de Vries, and P. van der Valk. 1993. "Overexpression of a M<sub>r</sub> 110,000 vesicular protein in non-P-glycoprotein-mediated multidrug resistance". Cancer Res., vol. 53, p. 1475-1479.
133. Scheffer, G. L., P. L. J. Wijngaard, M. J. Flens, M. A. Izquierdo, M. L. Slovak, H. M. Pinedo, C. J. Meijer, H. C. Clevers, and R. J. Scheper. 1995. "The drug resistance-related protein LRP is the human major vault protein". Nature Med., vol. 1, p. 578-582.
134. Ramachandran, C., W. You, and A. Krishan. 1998. "Characterization of a novel drug resistance-associated protein (DRP)". Proc. Am. Assoc. Cancer Res., vol. 39, p. 557.
135. Ross, D. D., J. Karp, and W. Yang. 1998. "Expression of breast cancer resistance protein (BCRP) in blast cells from patient with acute myeloid leukemia (AML)". Blood, vol. 92S, p. 396a.
136. Allikmets, R., L. M. Schriml, A. Hutchinson, V. Romano-Spica, and M. Dean. 1998. "A human placenta-specific ATP-binding cassette gene (ABCP) on chromosome 4q22 that is involved in multidrug resistance". Cancer Res., vol. 58, p. 5337-5339.

137. Peters, W. H. M. and H. M. J. Roelofs. 1992. "Biochemical characterization of resistance to mitoxantrone and adriamycin in Caco-2 human colon adenocarcinoma cells: a possible role for glutathione S-transferases". Cancer Res., vol. 52, p. 1886-1890.
138. Meijer, C., N. H. Mulder, H. Timmer-Bosscha, W. J. Sluiter, G. J. Meersma, and E. G. E. de Vries. 1992. "Relationship of cellular glutathione to the cytotoxicity and resistance of seven platinum compounds". Cancer Res., vol. 52, p. 6885-6589.
139. Hao, X.-Y., J. Bergh, O. Brodin, U. Hellman, and B. Mannervik. 1994. "Acquired resistance to cisplatin and doxorubicin in a small lung cancer cell line is correlated to elevated expression of glutathione-linked detoxification enzymes". Carcinogenesis, vol. 15, p. 1167-1173.
140. Glisson, B., R. Gupta, P. Hodges, and W. Ross. 1986. "Cross-resistance to intercalating agents in an epipodophyllotoxin-resistant Chinese hamster ovary cell line: evidence for a common intracellular target". Cancer Res., vol. 46, p. 1939-1942.
141. Pommier, Y., D. Kerrigan, R. E. Schwartz, J. A. Swack, and A. McCurdy. 1986. "Altered DNA topoisomerase II activity in Chinese hamster cells resistant to topoisomerase II inhibitors". Cancer Res., vol. 46, p. 3075-3081.
142. Beck, W. T., M. C. Cirtain, M. K. Danks, R. L. Felsted, A. R. Safa, J. S. Wolverton, D. P. Suttle, and J. M. Trent. 1987. "Pharmacological, molecular, and cytogenetic analysis of atypical multidrug-resistant human leukemic cells". Cancer Res., vol. 5455-5460.
143. Van der Zee, A. G. J., B. van Ommen, C. Meijer, H. Hollema, P. J. Bladeren, and E. G. E. de Vries. 1992. "Glutathione S-transferase activity and isoenzyme composition in benign ovarian tumors, untreated malignant ovarian tumors, and malignant ovarian tumors after platinum/cyclophosphamide chemotherapy". Br. J. Cancer., vol 66, p. 930-936.
144. Arceci, R. J. 1993. "Clinical significance of P-glycoprotein in multidrug resistance malignancies". Blood, vol. 81, p. 2215-2222.
145. Beck, J., D. Niethammer, and V. Gekeler. 1994. "High *mdr1*- and MRP-, but low topoisomerase II $\alpha$ -gene expression in B-cell chronic lymphocytic leukemias". Cancer Lett., vol. 86, p. 135-142.
146. Izquierdo, M. A., A. G. J. van der Zee, J. B. Vermorken, P. van der Valk, J. A. Belien, G. Giaccone, G. L. Scheffer, M. J. Flens, H. M. Pinedo, and P. Kenemans. 1995. "Drug resistance-associated marker Lrp for prediction of response to chemotherapy and prognosis in advanced ovarian carcinoma". J. Natl. Cancer Inst., vol. 87, p. 1230-1237.

147. Schneider, E., H. Yamazaki, B. K. Sinha, and K. H. Cowan. 1995. "Buthionine sulfoximine-mediated sensitization of etoposide-resistant human breast cancer MCF7 cells overexpressing the multidrug resistance-associated protein involves increased drug accumulation". Br. J. Cancer, vol. 71, p. 738-743.
148. Ueda, K., M. M. Cornwell, M. M. Gottesman, I. Pastan, I. B. Roninson, V. Ling, and J. R. Riordan. 1986. "The *mdr1* gene, responsible for multidrug-resistance, codes for P-glycoprotein". Biochem. Biophys. Res. Commun., vol. 141, p.956-962.
149. Horio, M., M. M. Gottesman, and I. Pastan. 1988. "ATP-dependent transport of vinblastine in vesicles from human multidrug-resistant cells". Proc. Natl. Acad. Sci. USA, vol. 86, p. 3580-3584.
150. Yu, D. K. 1999. "The contribution of P-glycoprotein to pharmacokinetic drug-drug interactions". J. Clin. Pharmacol., vol. 39, p. 1203-1211.
151. Hyde, S. C., P. Emsley, M. J. Hartshorn, M. M. Mimmack, U. Gileadi, S. R. Pearce, M. P. Gallagher, D. R. Gill, R. E. Hubbard, and C. F. Higgins. 1990. "Structural model of ATP-binding proteins associated with cystic fibrosis, multidrug resistance, and bacterial transport". Nature, vol. 346, p. 362-365.
152. Mimura, C. S., S. R. Holbrook, and G. F.-L. Ames. 1991. "Structural model of the nucleotide-binding conserved component of periplasmic permeases". Proc. Natl. Acad. Sci. USA, vol. 88, p. 84-88.
153. Ames, G. F.-L., C. S. Mimura, S. R. Holbrook, and V. Shyamala. 1992. "Traffic ATPases: a superfamily of transport proteins operating from Escherichia coli to humans". Adv. Enzymol., vol. 65, p. 1-47.
154. Higgins, C. F. 1992. "ABC transporters – from microorganism to man". Ann Rev. Cell. Biol., vol. 8, p. 67-113.
155. Konig, J., A. T. Nies, Y. Cui, I. Leier, and D. Keppler. 1999. "Conjugate export pumps of the multidrug resistance protein (MRP) family: localization, substrate specificity, and MRP2-mediated drug resistance". Biochim. Biophys. Acta, vol. 1461, p. 377-394.
156. Gottesmann, M. M. and I. Pastan. 1993. "Biochemistry of multidrug resistance mediated by the multidrug transporter". Ann. Rev. Biochem., vol. 62, p. 385-427.
157. Roepe, P. D. 1992. "Analysis of the steady-state and initial rate of doxorubicin efflux from a series of multidrug-resistant cells expressing different levels of P-glycoprotein". Biochemistry, vol. 31, p. 12555-12564.
158. Endicott, J. A. and V. Ling. 1989. "The biochemistry of P-glycoprotein-mediated multidrug resistance". Ann. Rev. Biochem., vol. 58, p. 137-171.

159. Roninson, I. B. (ed.). 1991. Molecular and Cellular Biology of Multidrug Resistance in Tumor Cells. New York: Plenum Press. 406 p.
160. Gottesman, M. M., P. V. Schoenlein, S. J. Currier, E. P. Bruggemann, and I. Pastan. 1991. "Biochemical basis for multidrug resistance in cancer". In T. Pretlow (ed.). Biochemical and Molecular Aspects of Selected Cancer, vol. 1, San Diego: Academic Press, p. 339-371.
161. Chen, C., J. E. Chin, K. Ueda, D. P. Clark, I. Pastan, M. M. Gottesman, and I. B. Roninson. 1986. "Internal duplication and homology with bacterial transport proteins in *MDR1* (P-glycoprotein) gene from multidrug-resistant human cells". Cell, vol. 47, p. 381-389.
162. Kartner, N., D. Evernden-Porelle, G. Bradley, and V. Ling. 1985. "Detection of P-glycoprotein in multidrug-resistant cell lines by monoclonal antibodies". Nature, vol. 316, p. 820-823.
163. Yoshimura, A., Y. Kuwazuru, T. Sumizawa, et al. 1989. "Cytoplasmic orientation and two-domain structure of the multidrug transporter, P-glycoprotein, demonstrated with sequence-specific antibodies". J. Biol. Chem., vol. 264, p. 16282-16291.
164. Georges, E., G. Bradley, J. Gariepy, and V. Ling. 1990. "Detection of P-glycoprotein isoform by gene-specific monoclonal antibodies". Proc. Natl. Acad. Sci. USA, vol. 87, p. 152-156.
165. Cianfriglia, M., M. C. Willingham, M. Tombesi, G. V. Scagliotti, G. Frasca, and A. Chersi. 1994. "P-glycoprotein epitope mapping. II. The murine monoclonal antibody MM6.15 to human multidrug-resistant cells binds with three distinct loops in the *MDR1*-P-glycoprotein extracellular domain". Int. J. Cancer, vol. 56, p. 153-160.
166. Schinkel, A. H., S. Kemp, M. Dolle, G. Rudenko, and E. Wagenaar. 1993. "N-glycosylation and deletion mutants of the human *MDR1* P-glycoprotein". J. Biol. Chem., vol. 268, p. 7474-7481.
167. Zhang, J.-T., M. Duthie, and V. Ling. 1993. "Membrane topology of the N-terminal half of the hamster P-glycoprotein molecule". J. Biol. Chem., vol. 268, p. 15101-15110.
168. Skach, W. R. and V. R. Lingappa. 1994. "Transmembrane orientation and topogenesis of the third and fourth membrane-spanning regions of human P-glycoprotein (*MDR1*)". Cancer Res., vol. 54, p. 3202-3209.
169. Bibi, E. and O. Beja. 1994. "Membrane topology of multidrug resistance protein expressed in *Escherichia coli*. N-terminal domain". J. Biol. Chem., vol. 269, p. 19910-19915.

170. Germann, U. A., I. Pastan, and M. M. Gottesman. 1993. "P-glycoproteins: mediators of multidrug resistance". Semin. Cell Biol., vol. 4, p. 63-76.
171. Loo, T. W. and D. M. Clarke. 1995. "Membrane topology of a cysteine-less mutant of human P-glycoprotein". J. Biol. Chem., vol. 270, p. 843-848.
172. Kast, C., V. Canfield, R. Levenson, and P. Gros. 1995. "Membrane topology of P-glycoprotein as determined by epitope insertion: transmembrane organization of the N-terminal domain of mdr3". Biochemistry, vol. 34, p. 4402-4411.
173. Wright, L. C., M. Dyne, K. T. Holmes, and C. E. Mountford. 1985. "Phospholipid and ether linked phospholipid content alter with cellular resistance to vinblastine". Biochem. Biophys. Res. Commun., vol. 133, p. 539-545.
174. Arsenault, A. L., V. Ling, and N. Kartner. 1988. "Altered plasma membrane ultrastructure in multidrug-resistant cells". Biochim. Biophys. Acta, vol. 938, p. 315-321.
175. Boscoboinik, D., M. T. Debanne, A. R. Stafford, C. Y. Jung, R. S. Gupta, and R. M. Epand. 1990. "Dimerization of the P-glycoprotein in membranes". Biochim. Biophys. Acta, vol. 1027, p. 225-228.
176. Naito, M. and T. Tsuruo. 1992. "Functionally active homodimer of P-glycoprotein in multidrug-resistant tumor cells". Biochem. Biophys. Res. Commun., vol. 185, p. 284-290.
177. Greenberger, L. M. 1993. "Major photoaffinity drug labeling sites for iodoaryl azidoprazosin in P-glycoprotein are within, or immediately C-terminal to, transmembrane domain-6 and domain-12". J. Biol. Chem., vol. 268, p. 11417-11425.
178. Bruggemann, E. P., S. G. Currier, M. M. Gottesman, and I. Pastan. 1992. "Characterization of the azidopine and vinblastine binding site of P-glycoprotein". J. Biol. Chem., vol. 267, p. 21020-21026.
179. Loo, T. W., and D. M. Clarke. 1994. "Functional consequences of glycine mutations in the predicted cytoplasmic loops of P-glycoprotein". J. Biol. Chem., vol. 269, p. 7243-7248.
180. Cornwell, M. M., M. M. Gottesman, and I. Pastan. 1986. "Increased vinblastine binding to membrane vesicles from multidrug resistant KB cells". J. Biol. Chem., vol. 262, p. 7921-7928.
181. Safa, A. R., R. K. Stern, K. Choi, M. Agresti, I. Tamai, N. D. Mehta, and I. B. Roninson. 1990. "Molecular basis of preferential resistance to colchicine in multidrug-resistant human cells conferred by Gly to Val-185 substitution in P-glycoprotein". Proc. Natl. Acad. Sci. USA, vol. 87, p. 7225-7229.

182. Safa, A. R. 1988. "Photoaffinity labeling of the multidrug-resistance-related P-glycoprotein with photoactive analogs of verapamil". Proc. Natl. Acad. Sci. USA, vol. 85, p. 7187-7191.
183. Busche, R., B. Tummler, J. R. Riordan, and D. F. Cano-Gauci. 1989. "Preparation and utility of a radioiodinated analogue of daunomycin in the study of multidrug resistance". Mol. Pharmacol., vol. 35, p. 414-421.
184. Greenberger, L. M., C. H. Yang, E. Gindin, and S. B. Horwitz. 1990. "Photoaffinity probes for the alpha 1-adrenergic receptor and the calcium channel bind to a common domain in P-glycoprotein". J. Biol. Chem., vol. 265, p. 4394-4401.
185. Morris, D. I., L. A. Speicher, A. E. Ruoho, K. D. Tew, and K. B. Seamon. 1991. "Interaction of forskolin with the P-glycoprotein multidrug transporter". Biochemistry, vol. 30, p. 8371-8379.
186. Borchers, C., W. R. Ulrich, K. Klemm, W. Ise, V. Gekeler, S. Haas, A. Schodl, J. Conrad, M. Przybylski, and R. Boer. 1995. "B9209-005, an azido derivative of the chemosensitizer dexniguldipine-HCl, photolabels P-glycoprotein". Mol. Pharmacol., vol. 48, p. 21-29.
187. Safa, A. R. 1993. "Photoaffinity labeling of P-glycoprotein in multidrug resistant cells". Cancer Invest., vol. 11, p. 46-56.
188. Loo, T. W. and D. M. Clarke. 1993. "Functional consequences of phenylalanine mutations in the predicted transmembrane domain of P-glycoprotein". J. Biol. Chem., vol. 268, p. 19965-19972.
189. Zhang, X., K. I. Collins, and L. M. Greenberger. 1995. "Functiond evidence that transmembrane 12 and the loop between transmembrane 11 and 12 form part of the drug-binding domain in P-glycoprotein encoded by *MDR1*". J. Biol. Chem., vol. 270, p. 5441-5448.
190. Ueda, K., A. Yoshida, and T. Amachi. 1999. "Recent progress in P-glycoprotein research". Anti-Cancer Drug Design, vol. 14, p. 115-121.
191. Ramachandran, C. and S. J. Melnick. 1999. "Multidrug resistance in human tumors – molecular diagnosis and clinical significance". Molecular Diagnosis, vol. 4, p. 81-94.
192. Johnstone, R. W., A. A. Ruefli, and M. J. Smyth. 2000. "Multiple physiological functions for multidrug transporter P-glycoprotein?". Trends. Biochem. Sci., vol. 25, p. 1-6.



## **CHAPTER 2**

### **Inhibition of Tumor Growth and Metastasis of Human Fibrosarcoma Cells HT-1080 by Monoclonal Antibody BCD-F9**

## RÉSUMÉ TRADUIT

BCD-F9 est un anticorps monoclonal murin de type IgG2a qui reconnaît un épitope conformationnel présent à la surface de plusieurs cellules tumorales. Le but de ce travail était de caractériser l'habileté de l'anticorps BCD-F9 à reconnaître une variété de lignées cellulaires néoplasiques et de tester *in vivo* l'activité anti-tumorale de BCD-F9 sur des modèles de tumeur sous-cutanée et métastatique. L'administration intraveineuse de BCD-F9 à des souris nude CD-1 auxquelles des cellules HT1080 ont été préalablement inoculées a entraîné une inhibition significative de la croissance tumorale. Nous avons démontré que BCD-F9 administré *i.v.* prolongeait de manière significative la vie des souris CD-1 auxquelles étaient inoculées des cellules HT-1080 pouvant induire le développement de métastases pulmonaires agressives chez des souris non-traitées. Nous avons aussi étudié l'activité anti-tumorale *in vitro* de BCD-F9 au moyen d'essais de cytotoxicité cellulaire anticorps-dépendante (ADCC) et de cytotoxicité anticorps-dépendante médiée par le complément (ADCMC). Les sous-populations de cellules effectrices ont été obtenues par stimulation des macrophages (thioglycollate) ou par enrichissement des cellules Natural Killer (NK) (sélection négative). BCD-F9 s'est révélé efficace dans la médiation de la lyse *in vitro* de cellules tumorales, tel que démontré par les techniques d'ADCC et d'ADCMC. Ces résultats suggèrent que le mAb BCD-F9 pourrait être utile dans le traitement immunothérapeutique de tumeurs d'origine diverse.

## **Inhibition of Tumor Growth and Metastasis of Human Fibrosarcoma Cells HT-1080 by Monoclonal Antibody BCD-F9**

Mikhail Popkov<sup>1</sup>, Salwa Sidrac-Ghali<sup>1</sup>, Yvette Lusignan<sup>1</sup>, Suzanne Lemieux<sup>1</sup>, and Rosemonde Mandeville<sup>2,3\*</sup>

<sup>1</sup>INRS-Institut Armand-Frappier, University of Quebec, 531 Blvd. des Prairies, Laval, QC, Canada H7V 1B7

<sup>2</sup>Department of Biological Sciences, UQAM, University of Quebec, Montreal, QC, Canada

<sup>3</sup>BIOPHAGE Inc., 6100 Royalmount Avenue, Montreal, QC, Canada H4P 2R2

**\*Corresponding author:** Rosemonde Mandeville

BIOPHAGE Inc.,

6100 Royalmount Avenue, Montreal, QC, Canada H4P 2R2

E-mail: Rosemonde.Mandeville @ nrc.ca

Tel.: (514) 496-7722; Fax: (514) 496-1521

## ABSTRACT

BCD-F9 is a murine IgG<sub>2a</sub> monoclonal antibody (mAb) that recognizes a conformational epitope found on the surface of many tumor cells. The aim of this study was to investigate the ability of BCD-F9 to recognize a variety of neoplastic cell lines and to test BCD-F9 *in vivo* for anti-cancer activity in subcutaneous and metastatic tumor models. Intravenous administration of BCD-F9 in CD-1 nude mice xenografted s.c. with human HT-1080 cells led to a significant inhibition of tumor growth. We demonstrate that BCD-F9 administered i.v. significantly prolonged the life span of CD-1 nude mice inoculated i.v. with the same tumor cell line that induces an aggressive lung metastasis development in untreated mice. We also investigated the antitumor activity of BCD-F9 *in vitro* in antibody-dependent cellular cytotoxicity (ADCC) and antibody-dependent complement-mediated cytotoxicity (ADCMC) assays. The effector cell subpopulations were obtained by macrophage stimulation (thioglycollate) or natural killer (NK) cell enrichment (negative selection). BCD-F9 was found to be effective in mediating tumor cell killing *in vitro* by ADCC and ADCMC mechanisms. These results suggest that the mAb BCD-F9 can have a potential use in immunotherapy for treatment of tumors of different origin.

**Keywords:** cancer, immunotherapy, mAb, *in vivo* animal models

## INTRODUCTION

In oncology, tumor-associated antigens are considered as good targets for the delivery of anti-cancer therapy, and mAbs directed at such antigens are increasingly being seen as important immunotherapeutic reagents. There is a consensus that target antigens in general are essentially normal structures that are expressed in higher density, in an overt fashion, and in an atypical tissular context on tumor cells (1). A variety of cell surface proteins have been used as targets for mAbs. In the case of cancer cells, the only truly tumor-specific antigens are the clonally expressed receptor idiotypes on B lymphoma cells. Unfortunately, the use of anti-Id mAbs to treat lymphoid cancers is limited by the need to create custom-made mAbs against the tumor from each patient or small group of patients (2). Thus, most investigators considered other targets such as differentiation antigens, growth factor receptors, oncofetal antigens, unique carbohydrate antigens, or altered normal antigens (3-5). Such antigens are tumor selective rather than tumor specific, that is, they are present in higher densities on tumor cells when compared with normal cells.

Whatever is their specificity, mAbs in general rarely have the capacity to eradicate large tumor masses. Several factors such as affinity and the number of binding sites on the target cell, antigen expression on tumor versus normal tissue, tumor size and the degree of vascularisation can limit the access of mAbs to the target cells and therefore affect their cytotoxic potential in vivo (6). Moreover, immunotherapy requires injection of relatively high doses of mAb, which leads in most patients to the development of an immune response against the injected rodent mAb with possible side effects (4,7). Targeting a highly expressed cell surface antigen, preferentially present on a wide range of neoplastic cells, might improve the efficacy of mAbs in therapy.

Most of the unconjugated mAbs displaying anti-neoplastic properties require the contribution of either complement (6,8) or Fc $\gamma$  receptor (Fc $\gamma$ R)-expressing effector cells (9,10) in order to achieve tumor cell killing. The presence in tumors, surgically removed from mAb-treated patients, of infiltrating NK cells and macrophages (11,12) as well as of complement deposits (11) are consistent with ADCC and ADCMC playing a role in tumor cell destruction in vivo. However, because most tumor cells express large amounts

of complement-inhibiting regulators, which protect the cells against lysis by autologous complement (13,14), the main antitumor mechanism of therapeutic antibodies in vivo is considered to be ADCC.

The murine mAb BCD-F9 was obtained by immunizing BALB/c mice with the human breast carcinoma cell line BT-20 (15). This mAb recognizes an antigen localized on the surface of most neoplastic, and to a lesser extent, normal mammary epithelial cells. In previous studies, BCD-F9 was shown to be a useful tool for the preoperative detection of axillary lymph nodes metastasis in over 30 breast cancer patients with minimal cancer (16). Moreover, BCD-F9 was shown to be a potential plasmatic marker that correlates with Ki 67 immunoreactivity and tumor aneuploidy (17). The antigen recognized by BCD-9 has not been identified yet.

In this study, the ability of BCD-F9 to recognize a wide variety of neoplastic cell lines was investigated. The reactivity of the mAb with the human fibrosarcoma HT-1080 enabled us to use this cell line to investigate the antitumor properties of BCD-F9 in an experimental animal model, where either subcutaneous or metastatic tumors can be induced depending on the site of injection (18). Our results show that repeated i.v. inoculation of BCD-F9 in HT-1080-transplanted CD-1 nude mice significantly reduced tumor growth rate in animals transplanted s.c. and completely abrogated the development of lung metastases in mice transplanted intravenously. In vitro studies of BCD-F9-dependent killing of HT-1080 cells confirm ADCC and ADCMC as two potential mechanisms for the antitumor activity observed in BCD-F9-treated animals. These properties, together with the reactivity of BCD-F9 with several tumor cell lines of different lineages, identify this mAb as a potentially useful immunotherapeutic reagent.

## MATERIAL AND METHODS

**Antibodies.** The BCD-F9 antibody-producing hybridoma was derived from the fusion of NS-1 myeloma cells with spleen cells from BALB/c mice hyperimmunized with the human breast carcinoma cell line BT-20 (15). The mAb BCD-F9 is an IgG2a that was purified from ascitic fluid collected from BALB/c mice inoculated i.p. with the hybridoma cell line. A protein-G Sepharose column (Pharmacia, Uppsala, Sweden) was used for that purpose. The mAb BCD-F9 was biotinylated according to a conventional procedure (19). Fluoroisothiocyanate (FITC)-labeled mouse anti-human CD3 (IgG2a), CD14 (IgG2a), CD15 (IgM), CD40 (IgG1), and all FITC-labeled mAbs used for isotype controls were purchased from Cedarlane (Hornby, Ontario). The anti-human HLA-ABC class I mAb and the guinea pig complement were also purchased from Cedarlane. FITC-conjugated sheep anti-mouse IgG antibody was purchased from Roche Diagnostics (Laval, Quebec). The anti-PLC $\gamma$ 1 rabbit polyclonal IgG was purchased from Santa Cruz Biotechnology (Santa Cruz, CA). Normal rabbit IgG was purchased from CALTAG Laboratories (Burlingame, CA). The anti- $\beta$ -Galactosidase mAb (mouse IgG2a, Calbiochem, Cambridge, MA) was used as isotype control for BCD-F9 in flow cytometry analysis and immunoprecipitation assays.

**Mice and Tumor Cells.** Female athymic CD-1 nude mice were obtained from Charles River, Canada. The mice were maintained in sterilized cages under sterile filter top conditions and were handled in a laminar airflow. They were 6-week old when transplanted with the human fibrosarcoma cell line, HT-1080, that was purchased from the American Type Culture Collection (ATCC, Rockville, MD) and maintained in DMEM supplemented with 10% of fetal bovine serum (FBS). Cells were cultured at 37°C in a 5% CO $_2$  humidified atmosphere. Other human tumor cell lines, BT-20, MCF-7, MDA/MB-231, SW480, LoVo, Mes-sa, U937, HL-60, Jurkat, and Raji used for the cell distribution analysis of the antigen recognized by BCD-F9 were also purchased from ATCC and were maintained in culture according to supplier recommendations.

**Metabolic Labeling of HT-1080 Cells.** For metabolic incorporation of radioactive precursors into proteins, confluent HT-1080 cells were harvested by incubation with phosphate-buffered saline (PBS) containing 0.5 mM EDTA. Cells were

washed twice in conical tube with 50 ml of methionine-free DMEM by centrifugation. Cells were placed (a) in 20 ml of methionine-free DMEM ( $2 \times 10^8$  cells) containing 5% of complete DMEM and 5% of dialyzed FBS, in the presence of [ $^{35}\text{S}$ ]-Methionine (80  $\mu\text{Ci/ml}$ , ICN Pharmaceuticals, Irvin, CA), for 20 h at  $37^\circ\text{C}$  or (b) in 20 ml of complete DMEM ( $2 \times 10^6$  cells) containing 10% of dialyzed FBS, in the presence of [ $^3\text{H}$ ]-glucosamine (12.5  $\mu\text{Ci/ml}$ , ICN Pharmaceuticals, Irvin, CA), for 72 h at  $37^\circ\text{C}$ . After metabolic labeling, the cells were harvested and washed twice with PBS by centrifugation. The cell pellets were resuspended by Vortex mixing at room temperature in 1 ml of lysis buffer (25 mM Tris-HCl pH 8.0, 0.15 M NaCl, 5 mM  $\text{MgCl}_2$ , 0.5% NP-40 (vol/vol), 2 mM EDTA, 1 mM phenylmethylsulfonyl fluoride) and centrifuged at  $14\,500 \times g$  for 10 min. The supernatants were incubated with 20  $\mu\text{l}$  of a 50% suspension of protein G-Sepharose beads (vol/vol) and 10  $\mu\text{g}$  of anti- $\beta$ -Galactosidase control mAb for 1 h at  $4^\circ\text{C}$  on a rotary wheel. The beads were removed by centrifugation and kept as a control for non-specific adsorption. Aliquots of the supernatants (250-500  $\mu\text{l}$ ) were incubated with 25  $\mu\text{g}$  of mAb BCD-F9 or 10  $\mu\text{l}$  of anti-PLC $\gamma$ 1 positive control polyclonal antiserum and 30  $\mu\text{l}$  of protein G-Sepharose beads for 4 h at  $4^\circ\text{C}$  on a rotary wheel. The beads were collected by centrifugation and washed four times with lysis buffer and twice with 50 mM Tris-HCl, pH 8.0/0.15 M NaCl. The immunoadsorbed proteins were released from the protein G-Sepharose by boiling for 10 min in 60  $\mu\text{l}$  of 1% NaDodSO $_4$ /2% 2-mercaptoethanol and analyzed by 12% polyacrylamide gel electrophoresis and autoradiography according to Mahony et al. (20).

**In vivo Tumor Growth.** Confluent cultured HT-1080 cells were harvested by incubation with PBS containing 0.5 mM EDTA. Viable cells were counted by trypan blue exclusion. Fractions containing over 95% of viable cells were used in this study. Cells ( $1.5 \times 10^7$  cells/ml) were suspended in PBS, and 0.2 ml of the suspension was inoculated s.c. into right flanks of 2 groups of 5 CD-1 nude mice on day 0. Normal rabbit IgG (100  $\mu\text{g}$ ) or mAb BCD-F9 (100  $\mu\text{g}$ ) was administrated i.v. in 0.2 ml of PBS on days 1-4, 7-10, and 13-14. The resulting tumor was measured over the skin in two dimensions using a slide caliper, and the tumor volume was calculated according to the following formula,  $(\text{width})^2 \times \text{length}/2$ . All animals were sacrificed after 30 days, their tumor dissected and weighted.



**Experimental Metastasis.** For the experimental metastasis model, HT-1080 cells ( $2 \times 10^7$  cells/ml) were harvested in PBS containing 0.5 mM EDTA, centrifuged and resuspended in PBS, and 0.1 ml of the suspension was inoculated i.v. into the tail vein of 2 groups of 5 CD-1 nude mice (day 0). Normal rabbit IgG (100  $\mu$ g) or mAb BCD-F9 (100  $\mu$ g) was administrated i.v. in 0.2 ml of PBS on days 1-2, 5-9, 12-16, and 19-21 and the lungs were recovered from recently deceased animals or from sacrificed survivors on day 61. Lungs were fixed in 10% buffered formalin, embedded in parafin, sectioned, and stained with H&E for routine histological examination by light microscopy.

**Preparation of Effector Cells.** Splenic NK cells from nude mice were enriched by a single filtration through nylon wool column. Effector cells for macrophage-mediated cytotoxicity were thioglycollate-elicited peritoneal exudate cells harvested from CD-1 nude mice (21).

**Antibody-Dependent Cytotoxicity Assays.** For use as targets in ADCC assays,  $3 \times 10^6$  HT-1080 cells were labeled with 150  $\mu$ Ci of  $\text{Na}_2^{51}\text{CrO}_4$  (ICN Biomedical, Costa Mesa, CA) for 1 h at  $37^\circ\text{C}$  and washed 4 times in DMEM. Fifty  $\mu$ l of  $^{51}\text{Cr}$ -radiolabeled HT-1080 cells ( $2 \times 10^5$ /ml) were distributed into U-bottomed 96-well microtiter plates and incubated for 1 h at  $37^\circ\text{C}$  with 50  $\mu$ l of protein G-purified mAb BCD-F9 at the concentration of 80  $\mu$ g/ml. Then 100  $\mu$ l of various concentrations of murine effector cells prepared as described above were added in quadruplicates to each well. After plates were incubated in  $\text{CO}_2$  incubator at  $37^\circ\text{C}$  for 8 h, they were centrifuged for 5 min at  $250 \times g$  and supernatants were collected with the Titertek supernatant collection system (Skatron, Oslo, Norway). Radioactivity was measured in a Beckman 7000 gamma counter. Percent specific lysis was calculated with the following formula:

$$\% \text{ specific lysis} = \frac{\text{cpm (test)} - \text{cpm (spontaneous)}}{\text{cpm(max)} - \text{cpm (spontaneous)}} \times 100$$

in which spontaneous release (12-17%) was measured by incubating radiolabeled cells in the absence of effector cells and maximum release was obtained by adding 1% Triton X-100 to radiolabeled cells.

For ADCMC, 50  $\mu$ l of  $^{51}\text{Cr}$ -radiolabeled HT-1080 tumor cells ( $2 \times 10^5$ /ml) and 50  $\mu$ l of various concentrations of protein G-purified mAb BCD-F9 were distributed in triplicates into U-bottomed 96-well microtiter plates. Then 100  $\mu$ l (1:5 dilution) of Low-

Tox guinea pig complement was added to each well and plates were incubated for 45 min at 37°C in a 5% CO<sub>2</sub> humidified atmosphere. Plates were centrifuged for 5 min at 250 x g and culture supernatants were harvested as described above for the ADCC assay. Spontaneous release was measured by incubating radiolabeled cells in the absence of complement and maximum release was obtained by adding 1% Triton X-100 to radiolabeled cells. The anti-human HLA-ABC class I mAb was used as a positive control in the ADCMC assay.

**Flow Cytometry.** Various tumor cell lines were stained with protein G-purified mAb BCD-F9. Binding of mAb BCD-F9 was detected with FITC-conjugated sheep anti-mouse IgG antibody. Control samples were incubated with anti-β-Galactosidase mAb (mouse IgG2a) as primary antibody.

Fresh heparinized blood samples were obtained from healthy donors and processed immediately. First, unwashed blood samples (100 µl) were incubated with biotin-conjugated mAb BCD-F9 (1 µg total) for 20 min at room temperature and washed once in PBS containing 0.1% BSA. Then, 10 µl of each undiluted FITC-labeled CD3, CD14, CD15, and CD40 antibody were added to different tubes. Binding of biotinylated mAb was detected with phycoerythrin (PE)-labeled streptavidin (Beckton Dickinson, Mountain View, CA). For each mAb, control samples were stained with a non-reactive FITC-labeled primary mAb of the same isotype, and the biotinylated anti-β-Galactosidase IgG2a mAb was used as negative control for PE-labeled streptavidin staining. Samples were incubated for 20 min at room temperature and washed once in PBS containing 0.1% BSA. Then, 0.5 ml of OptiLyse C solution (Immunotech, Marseille, France) was mixed with pelleted cells and samples were incubated for 15 min at room temperature. Finally, 0.5 ml of PBS containing 0.5% formaldehyde was added to each sample.

Stained samples were analyzed on a Epics XL-MCL flow cytometer (Coulter, Hialeah, FL) equipped with a 488 nm argon laser. Tumor cell populations were gated on the basis of forward and side scatter parameters. T and B blood lymphocytes were gated on the basis of CD3 and CD40 fluorescence and side-scattering characteristics, whereas monocytes and granulocytes were gated on the basis of CD14 and CD15 fluorescence, respectively. Data analysis based on collection of 10 000 events/sample was performed

using XL software. The degree of reactivity of tumor cells or blood leukocyte populations with BCD-F9 is expressed as the mean fluorescence intensity (MFI) of the positive cells after subtraction of nonspecific binding of anti- $\beta$  galactosidase isotype control on the same cell population.

**Statistical Analysis.** Unpaired two-tailed Student's *t*-test and Cox-Mantel logrank test were performed using INSTAT software. A *P*-value < 0.05 was considered significant.

## RESULTS

*BCD-F9 Recognition of Neoplastic Cell Lines and Peripheral Blood Mononuclear Cells (PBMC).* Eleven human cell lines harvested when confluent were examined by flow cytometry analysis for the binding of the mAb BCD-F9. As shown in Figure 2.1A, BCD-F9 recognizes an epitope expressed on the surface of all cell lines tested. Low reactivity was detected in almost half of them including the BT-20 cell line used for BALB/c immunization. Significant binding of BCD-F9 was observed with MDA/MB-231, SW480, HT-1080, and HL-60, the highest reactivity being found in LoVo and Raji. No obvious correlation was observed between the level of BCD-F9 staining and neoplastic cell origin. No fluorescence was detected when human blood cells were stained with BCD-F9 and FITC-conjugated anti-mouse IgG antibody (data not shown).

In order to obtain greater sensitivity, human PBMC were stained with FITC-conjugated mAbs specific for leukocyte populations and biotinylated mAb BCD-F9 followed by incubation with PE-labeled streptavidin for the detection of BCD-F9 binding. Under these conditions, BCD-F9 positively stained monocytes (CD14<sup>+</sup>) while weak staining was observed in lymphocytes (CD3<sup>+</sup>, CD40<sup>+</sup>) and no staining on granulocytes (CD15<sup>+</sup>) (Fig. 2.1B). The human colon carcinoma cell line SW480 expressing the BCD-F9 epitope at intermediate level was used for positive control staining with the biotinylated mAb. The MFI observed with the tumor cells was more than 4 fold higher than with monocytes.

*Characterization of the BCD-F9 Reactive Antigen.* To confirm the flow cytometry data, lysates from metabolically labeled HT-1080 cells were immunoprecipitated with mAb BCD-F9. A predominant band with molecular mass of about 57 kDa was detected (Fig. 2.2, lanes 2). The antigen in HT-1080 cell lysates is a glycoprotein, since it was labeled by both [<sup>35</sup>S]-Methionine and [<sup>3</sup>H]-Glucosamine. In addition, mAb BCD-F9 precipitated two secondary proteins with molecular masses of about 80 and 25 kDa, respectively (Fig. 2.2, lanes 2). All other bands were nonspecific reactions with negative control mAb and /or Protein G-Sepharose beads (Fig. 2.2A, lane 1). PLC $\gamma$ 1, a 145 kDa intracellular signal transduction protein was used as a positive control (Fig. 2.2, lanes 3).

It remains to be determined whether 80 and 25 kDa coprecipitates are physically associated with the 57 kDa BCD-F9 antigen or if they are cross-reactive with mAb BCD-F9.

*Antitumor Activity of BCD-F9.* Among cell lines stained with mAb BCD-F9, the fibrosarcoma HT-1080 was selected for in vivo model because of the rather short time for tumor growth and metastasis development (three weeks), and its ability to produce tumors in all injected animals (18). In order to evaluate the antitumor efficacy of BCD-F9 for in vivo tumor cell eradication, CD-1 nude mice were injected s.c. on day 0 with  $3 \times 10^6$  HT-1080 cells into the right flank, followed by 10 i.v. administrations of the mAb BCD-F9. The mean tumor size of all treated mice was monitored from day 9 to 30 after which all mice were sacrificed mainly because of large tumor volumes. As depicted in Figure 2.3 all injected animals developed palpable tumors within 9 days; however, starting from day 12, a reduced tumor growth rate in the BCD-F9-treated group was observed when compared to control group. Repeated inoculation of BCD-F9 in mice bearing HT-1080 tumors resulted in significantly lower tumor sizes as compared with the control group, which had been treated with normal rabbit IgG ( $P < 0.01$ , from days 15 to 30 versus control). Starting from day 15, in all of the BCD-F9-treated mice, clear signs of tumor necrosis were visible in the center of the tumor, surrounded by a rim of viable tumor cell mass. These signs of necrosis were only observed in the BCD-F9-treated mice but not in the control group. Moreover, one tumor in the BCD-F9 treated animals showed clear signs of regression and totally disappeared within 18 days. Tumor weights, as determined after sacrifice of all animals on day 30 after tumor cell inoculation, were compared. In the group given BCD-F9, the mean tumor weight was  $0.25 \pm 0.1$  g as compared to  $1.16 \pm 0.22$  g in the control group, a finding that corresponds to a 78.45% reduction in tumor growth in the BCD-F9 treated group ( $P < 0.001$  versus control). These data rule out the possibility that the antitumor activity of BCD-F9 could be due to nonspecific action of the administration of IgG. At no time during the period of observation, side effects such as a loss of body weight were observed in mice treated with either antibody.

*Effect of BCD-F9 on the Experimental Metastasis.* We also examined the antitumor activity of BCD-F9 in an experimental metastasis model. In this case, HT-1080

cells were injected i.v. into CD-1 nude mice for the formation of metastatic foci in the lung. Survival curves show that animals treated with rabbit IgG started to die at 21 days after tumor cell inoculation, apparently due to lung colonization inducing difficulties in breathing. Mean survival time for the group of mice treated with rabbit IgG was  $25 \pm 1$  days (Fig. 2.4). All animals treated with BCD-F9 survived the experimental period thus confirming the antitumor activity of BCD-F9 even in an aggressive tumor model. Survivors were sacrificed after 60 days of observation. Histological examination of the lungs of all animals showed diffuse metastases in the case of control animals (Fig. 2.5A) and no metastatic foci at all in the case of BCD-F9-treated animals (Fig. 2.5B). No toxic reactions were observed in mice treated with BCD-F9 throughout the experimental period, thus suggesting that no serious side effects were caused by the i.v. injection of BCD-F9.

*BCD-F9 Antibody-Dependent Complement- or Cell-Mediated Cytotoxicity.* Two potential effector mechanisms that might contribute to the efficacy of BCD-F9 in vivo were investigated in vitro. We first examined the ability of mAb BCD-F9 to kill HT-1080 tumor cells by ADCMC. Figure 2.6 shows that mAb BCD-F9 produced substantial cytotoxicity against HT-1080 cells in the presence of guinea-pig complement. Significant lysis of tumor cells was observed at an antibody concentration between 6 and 50  $\mu\text{g/ml}$ . As ADCMC is not detected at lower antibody concentration, it suggests that a minimal number of antibody molecules had to be bound to its epitope to induce ADCMC. There was no direct cytotoxicity of BCD-F9 for HT-1080 tumor cells, which were not killed by the mAb at the concentration of 50  $\mu\text{g/ml}$  in the absence of complement. Complement-dependent lysis of HT-1080 tumor cells by anti-human HLA-ABC class I mAb was the positive control in the ADCMC assay.

Another mechanism through which antibodies can destroy tumor cells is ADCC. Experiments with splenic NK cells and peritoneal cells from nude mice were performed against BCD-F9 antibody-coated HT-1080 cells at different effector-target ratios. The results show that the HT-1080 tumor cell line is not susceptible to spontaneous killing by these effector cells, which however lysed BCD-F9-coated targets in a dose-dependent manner (Fig. 2.7)

## DISCUSSION

The use of mAbs in immunotherapy was demonstrated previously for various types of tumors (3-5); however, major improvement is still needed before this therapy reaches its full potential. Selection of the optimal mAb for the treatment of some cancers is still in its early phases and depends on many factors, notably its specificity, affinity and avidity for the target antigen (22). Access to a homogeneously expressed cell surface antigen as a target is also of good prognostic for successful mAb-mediated therapy.

The mAb BCD-F9 raised originally against breast carcinoma (BT-20) was originally shown to recognize a cell surface antigen of mammary tumors and, to a lesser extent, of normal breast tissue (23). The present data demonstrate that the epitope recognized by the mAb BCD-F9 was not restricted to the breast cancer cell lines. It is also present to various degree on other neoplastic cell lines from different origin: colon carcinoma, sarcoma, lymphoma, and leukemia. A common reactivity with BCD-F9 implies that these cell lines share a common surface antigen or express different molecules with common or cross-reactive epitopes.

The ability of BCD-F9 to recognize the human fibrosarcoma cell line HT-1080 enables us to use it for experimental antibody-mediated therapy in a xenograft tumor model. Although BCD-F9 was reacting more strongly with LoVo and Raji cell lines, HT-1080 was preferred for *in vivo* studies because of the rapid tumor growth in nude mice transplanted subcutaneously and the production of lung metastases when the tumor was injected *i.v.* The antitumor activity of the mAb BCD-F9 is supported by the reduced growth rate of the tumor in BCD-F9-treated mice transplanted *s.c.*, the survival of all mice inoculated *i.v.* with tumor cells, and the absence of detectable metastatic foci following histological examination of the lung of sacrificed animals at 60 days post tumor transplantation. As *in vitro* analyses showed that BCD-F9 has the ability to kill HT-1080 tumor cells by ADCC or ADCMC, these mechanisms may contribute to the *in vivo* antitumor activity of the mAb. These same mechanisms can explain the presence of necrosis in the center of subcutaneous tumors in BCD-F9-treated group. Usually, rapidly growing masses show central necrosis due to insufficient neovascularisation (24), while in our study only smaller subcutaneous tumors had necrotic foci and only when treatment

with BCD-F9 was administrated. This suggests that BCD-F9 can elicit a specific cytotoxic response that is not observed following the inoculation of nonspecific IgG. As no killing was observed after tumor cells were incubated for up to 9 h with BCD-F9 in the absence of effector cells or complement, the mAb alone is unlikely to be efficient in inducing tumor cell apoptosis.

The mechanism of tumor eradication mediated by antibodies *in vivo* is thought to be mainly ADCC, because macrophage and NK cell depletion resulted in 100% increase in tumor take in mAb-treated xenografted nude mice (9). Although mAb BCD-F9 elicits ADCC by murine effector cell *in vitro*, this finding does not imply that ADCC is the only important mechanism for the inhibition of tumor growth *in vivo*. Another possible mechanism of cytotoxicity in a xenograft model is complement activation. Considering the strong complement-mediated cytotoxicity of BCD-F9 *in vitro*, the participation of complement-mediated mechanism in the antitumor activity of this antibody *in vivo* cannot be ruled out. Usually, autologous cells will not be killed by complement-mediated mechanisms because they express complement down-regulating factors (13,25,26). However, this tumor evasion mechanism should not occur in nude mice as xenografted human cells lacks inhibitors of murine complement. Therefore, although ADCMC may be involved in control of HT-1080 tumor growth in nude mice, the capacity of BCD-F9 to activate complement component cascade would probably be of limited interest for clinical use.

The immunoprecipitation of cell lysates after metabolic staining with radiolabelled methionine or glucosamine allowed the identification of a 57 kDa glycoprotein as the major molecule expressing the BCD-F9 epitope. Although less intensively, the mAb reacts with other proteins, for instance with some of 25 and 80 kDa, respectively. Whether the detected proteins coprecipitate with the predominant protein of 57 kDa or share with it a common epitope has to be established. It is conceivable that different band patterns might even be detected after immunoprecipitation of lysates from the other tumor cell lines that reacted with BCD-F9 in flow cytometry analysis. However, the fact that the mAb binds to several proteins does not limit its interest for immunotherapy. A good example for that is the mouse mAb 17-1A, a reagent well known for its therapeutic effect in colorectal cancer patients with minimal residual disease (27).



This mAb not only detects an epithelial cell adhesion molecule of 33-40 kDa but also immunoprecipitates other proteins of 50 and 65 kDa from different cell lysates (28). Whether these secondary antigens play a role in antitumor activity of mAb 17-1A has not been determined yet.

Taken together, findings reported in this study suggest that broad recognition of neoplastic cell lines from different origin identifies mAb BCD-F9 as a potentially useful immunotherapeutic reagent. It is worthwhile to study whether mAb BCD-F9 will be capable to suppress the tumor cells growth and metastasis of other human tumor cells as it did against HT-1080 fibrosarcoma. Should this be the case, the contribution of ADCC to the *in vivo* antitumor activity of the mAb will have to be confirmed and the effector cells involved will have to be identified. It will then be possible to consider combine treatment with mAb and cytokines to improve the therapeutic effect of BCD-F9. Successes with such a strategy were recently reported for different mAbs, in particular, mAb 14.G2A (29), which reacts with the GD2 ganglioside expressed on several tumors including neuroblastoma and melanoma, and mAb 17-1A (30-32) already used for treatment of minimal residual disease of colon cancer patients.

## ACKNOWLEDGEMENTS

The authors thank Michel Houde, BIOPHAGE Inc., for critical reading of the manuscript and Marie Desy, INRS - Institut Armand-Frappier, for statistical analysis. M.P. was supported by scholarships from FCAR and INRS – Institut Armand-Frappier.

## REFERENCES

1. Farah, R. A., B. Clinchy, L. Herrera, and E. S. Vitetta. 1998. "The development of monoclonal antibodies for the therapy of cancer". Critical Reviews in Eukaryotic Gene Expression, vol. 8, p. 321-356.
2. Brown, S. L., R. A. Miller, and R. Levy. 1989. "Antiidiotype antibody therapy of B-cell lymphoma". Semin. Oncol., vol. 16, p. 199-210.
3. Waldmann, T. A. 1991. "Monoclonal antibodies in diagnosis and therapy". Science, vol. 252, p. 1657-1662.
4. Dillman, R. O. 1994. "Antibodies as cytotoxic therapy". J. Clin. Oncol., vol. 12, p. 1497-1514.
5. Choy, E. H. S., G. S. Panayi, and G. H. Kingsley. 1995. "Therapeutic monoclonal antibodies". Br. J. Rheumatol., vol. 34, p. 707-715.
6. Velders, M. P., S. V. Litvinov, S. O. Warnaar, A. Gorter, G. J. Fleuren, V. R. Zurawski Jr, and L. R. Coney. 1994. "New chimeric anti-pancarcinoma monoclonal antibody with superior cytotoxicity-mediating potency". Cancer Res., vol. 54, p. 1753-1759.
7. LoBuglio, A. F. and M. N. Saleh. 1992. "Monoclonal antibody therapy of cancer". Crit. Rev. Oncol. Hematol., vol. 13, p. 271-282.
8. Orlandi, R., M. Figini, A. Tomassetti, S. Canevari, and M. I. Colnaghi. 1992. "Characterization of a mouse-human chimeric antibody to a cancer-associated antigen". Int. J. Cancer, vol. 52, p. 588-593.
9. Herlyn, D. and H. Koprowski. 1982. "IgG2a monoclonal antibodies inhibit human tumor growth through interaction with effector cells". Proc. Natl. Acad. Sci. USA, vol. 79, p. 4761-4765.
10. Steplewski, Z., L. K. Sun, C. W. Shearman, J. Ghayeb, P. Daddona, and H. Koprowski. 1988. "Biological activity of human-mouse IgG1, IgG2, IgG3 and IgG4 chimeric monoclonal antibodies with anti-tumor specificity". Proc. Natl. Acad. Sci. USA, vol. 85, p. 4852-4856.
11. Adams, D.O., T. Hall, Z. Steplewski, and H. Koprowski. 1984. "Tumors undergoing rejection induced by monoclonal antibodies of the IgG2a isotype contain increased numbers of macrophages activated for a distinctive form of antibody-dependent cytotoxicity". Proc. Natl. Acad. Sci. USA, vol. 81, p. 3506-3510.
12. Shetye, J., J. E. Frodin, B. Christensson, C. Grant, B. Jacobsson, S. Sundelius, M. Sylven, and H. Mellstedt. 1988. "Immunohistochemical monitoring of metastatic

- colorectal carcinoma in patients treated with monoclonal antibodies (Mab 17-1A)". Cancer Immunol. Immunother., vol. 27, p. 154-162.
13. Kumar, S., J. M. Vinci, B. A. Pytel, and C. Baglioni. 1993. "Expression of messenger RNAs for complement inhibitors in human tissues and tumors". Cancer Res., vol. 53, p. 348-353.
  14. Gorter, A., V. T. Block, W. H. B. Haasnoot, N. G. Ensink, M. R. Daha, and G. J. Fleuren. 1996. "Expression of CD46, CD55, and CD59 on renal tumor cell lines and their role in preventing complement-mediated tumor cell lysis". Lab. Invest., vol. 74, p. 1039-1049.
  15. Mandeville, R., L. Giroux, J. Lecomte, J.-P. Chausseau, F. Dumas, I. Ajdukovic, I., D. Vidal, and F. Boury. 1987. "Production and characterization of monoclonal antibodies showing a different spectrum of reactivity to human breast tissue". Cancer Detect. Prev., vol. 10, p. 89-100.
  16. Mandeville, R., C. Schatten, N. Pateisky, M.-J. Dicaire, B. Barbeau, and B. Grouix. 1989. "Immunolymphoscintigraphy with BCD-F9 monoclonal antibody and its F(ab')<sub>2</sub> fragments for the preoperative staging of breast cancers". In: R. L. Ceriani (ed.). Breast Cancer Immunodiagnosis and Immunotherapy, New York: Plenum Press, 203p.
  17. Charpin, C., M.-J. Dicaire, B. Barbeau, M. N. Lavaut, C. Andonian, B. Devictor, C. Allasia, P. Bonnier, and R. Mandeville. 1991. "Monoclonal 3C6F9 distribution in human breast carcinomas: image cytometry of immunocytochemical assays". Med. Oncol. Tumor Pharmacother., vol. 8, p. 243-251.
  18. Asano, M., A. Yukita, T. Matsumoto, S. Kondo, and H. Suzuki. 1995. "Inhibition of tumor growth and metastasis by an immunoneutralizing monoclonal antibody to human vascular endothelial growth factor/vascular permeability factor121". Cancer Res., vol. 55, p. 5296-5301.
  19. Goding, J. W. (ed.). 1986. Monoclonal Antibodies: Principles and Practice, San Diego: Academic Press, 241p.
  20. Mahony, J., A. Bose, D. Cowdrey, T. Nusair, M. Lei, J. Harris, A. Marks, and R. Bauml. 1981. "A monoclonal antiidiotypic antibody to MOPC 315 IgA inhibits the growth of MOPC 315 myeloma cells in vitro". J. Immunol., vol. 126, p. 113-117.
  21. Takahashi, H. T. Nakada, M. Nakaki, and J. R. Wands. 1995. "Inhibition of hepatic metastases of human colon cancer in nude mice by a chimeric SF-25 monoclonal antibody". Gastroenterology, vol. 108, p. 172-182.
  22. Schlom, J., D. Colcher, K. Siler, A. Thor, G. Bryant, W. W. Johnston, C. A. Szpak, P. Sugarbaker, J. A. Carrasquillo, and J. C. Reynolds. 1990. "Tumor

- targeting with monoclonal antibody B72.3: experimental and clinical results". Cancer Treat. Res., vol. 51, p. 313-335.
23. Zelechowska, M. G. and R. Mandeville. 1989. "Immunogold and immunogold/silver staining in the ultrastructural localization of target molecules identified by monoclonal antibodies". Anticancer Res., vol. 9, p. 53-57.
  24. Folkman, J. 1990. "What is the evidence that tumors are angiogenesis dependent?" J. Natl. Cancer. Inst., vol. 82, p. 4-6.
  25. Finberg, R.W., W. White, and A. Nicholson-Weller. 1992. "Decay-accelerating factor expression on either effector or target cells inhibits cytotoxicity by human natural killer cells". J. Immunol., vol. 149, p. 2055-2060.
  26. Gorter, A. and S. Meri. 1999. "Immune evasion of tumor cells using membrane-bound complement regulatory proteins". Immunol. Today, vol. 20, p. 576-582.
  27. Balzar, M., M. J. Winter, C. J. de Boer, and S. V. Litvinov. 1999. "The biology of the 17-1A antigen (Ep-CAM)". J. Mol. Med., vol. 77, p. 699-712.
  28. Chen, Y. H., T. Yu, Y. Bai, and N. Zhao. 1999. "Two proteins share immunological epitopes on the tumor-associated antigen 17-1A". Cancer Lett., vol. 144, p. 101-105.
  29. Sondel, P. M. and J. A. Hank. 1997. "Combination therapy with interleukin-2 and antitumor monoclonal antibodies". Cancer J. Sci. Am., vol. 3, p. S121-S127.
  30. Shetye, J., P. Ragnhammar, M. Liljefors, B. Christensson, J. E. Frodin, P. Biberfeld, and H. Mellstedt. 1998. "Immunopathology of metastases in patients of colorectal carcinoma treated with monoclonal antibody 17-1A and granulocyte macrophage colony-stimulating factor". Clin. Cancer Res., vol. 4, p. 1921-1929.
  31. Bungard, S., D. Flieger, S. Schweitzer, T. Sauerbruch, and U. Spengler. 1998. "The combination of interleukin-2 and interferon alpha effectively augments the antibody-dependent cellular cytotoxicity of monoclonal antibodies 17-1A and BR55-2 against the colorectal carcinoma cell line HT29". Cancer Immunol. Immunother., vol. 46, p. 213-220.
  32. Flieger, D., U. Spengler, I. Beier, R. Kleinschmidt, A. Hoff, M. Varvenne, T. Sauerbruch, and I. Schmidt-Wolf. 1999. "Enhancement of antibody dependent cellular cytotoxicity (ADCC) by combination of cytokines". Hybridoma, vol. 18, p. 63-68.

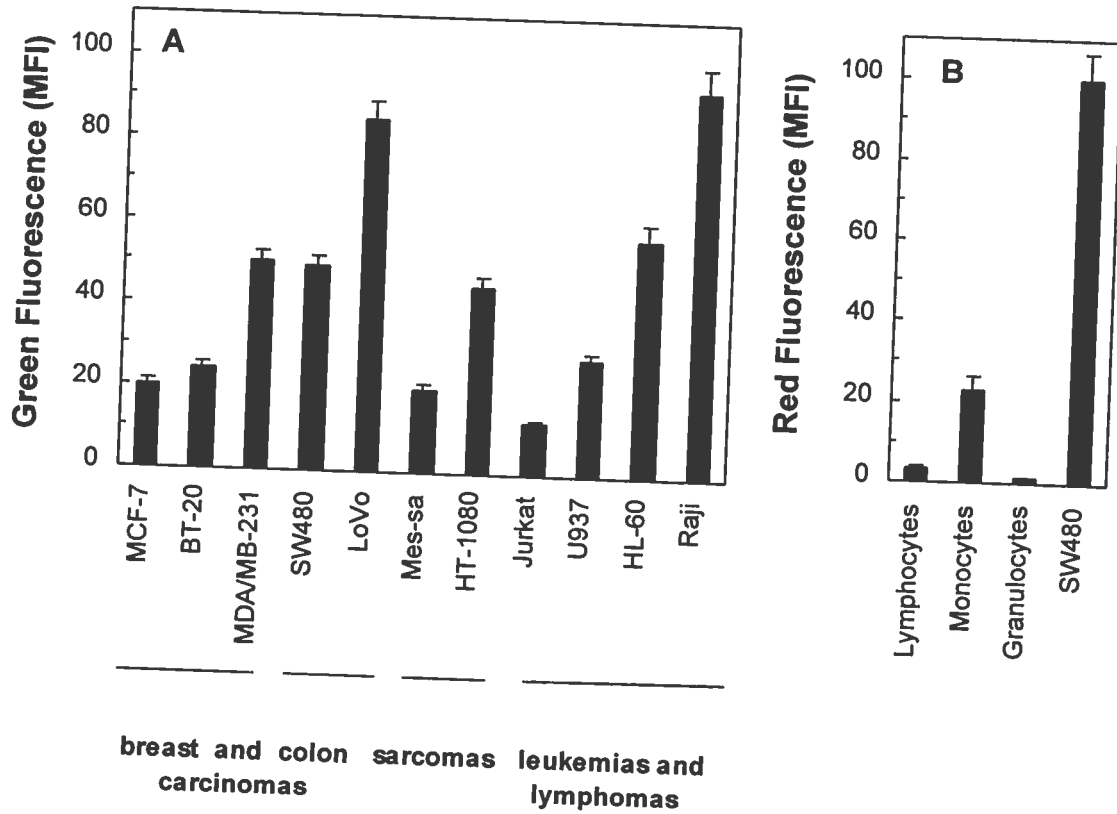


**Figure 2.1. Reactivity of mAb BCD-F9 with Various Neoplastic Cell Lines and PBMC.**

Expression of BCD-F9 epitope on cultured tumor cell lines (A) and on freshly collected PBMC (B) was analyzed by flow cytometry as described in Materials and Methods. Data correspond to the MFI of positive cells after staining with unconjugated BCD-F9 and FITC-labeled sheep antimouse IgG (green fluorescence) or biotinylated-BCD-F9 and PE-labeled streptavidin (red fluorescence). The results illustrated represent mean values  $\pm$  SD of three independent experiments.

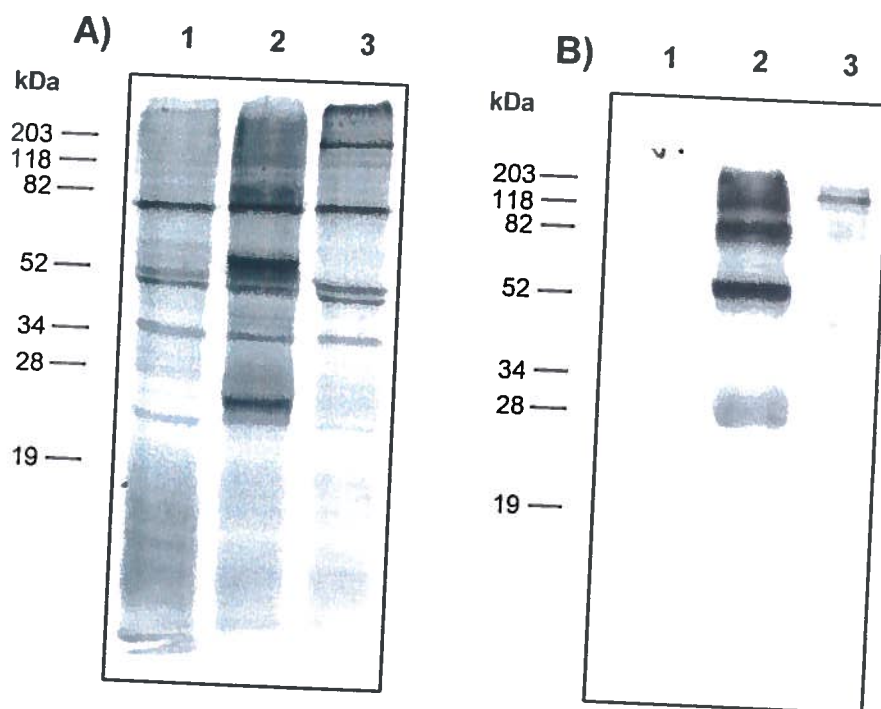


**Figure 2.2. Characterization of the BCD-F9-Reactive Antigen.**

Aliquots of lysates of HT-1080 cells labeled metabolically with  $[^{35}\text{S}]$ -Methionine (A) or  $[^3\text{H}]$ -Glucosamine (B) were immunoprecipitated with anti- $\beta$ -Galactosidase IgG2a isotype control mAb (lanes 1), mAb BCD-F9 (lane 2), or anti-PLC $\gamma$ 1 rabbit polyclonal IgG (lanes 3) and analyzed by electrophoresis in 12% polyacrylamide slab gels under reducing conditions, followed by autoradiography as described in Material and Methods.

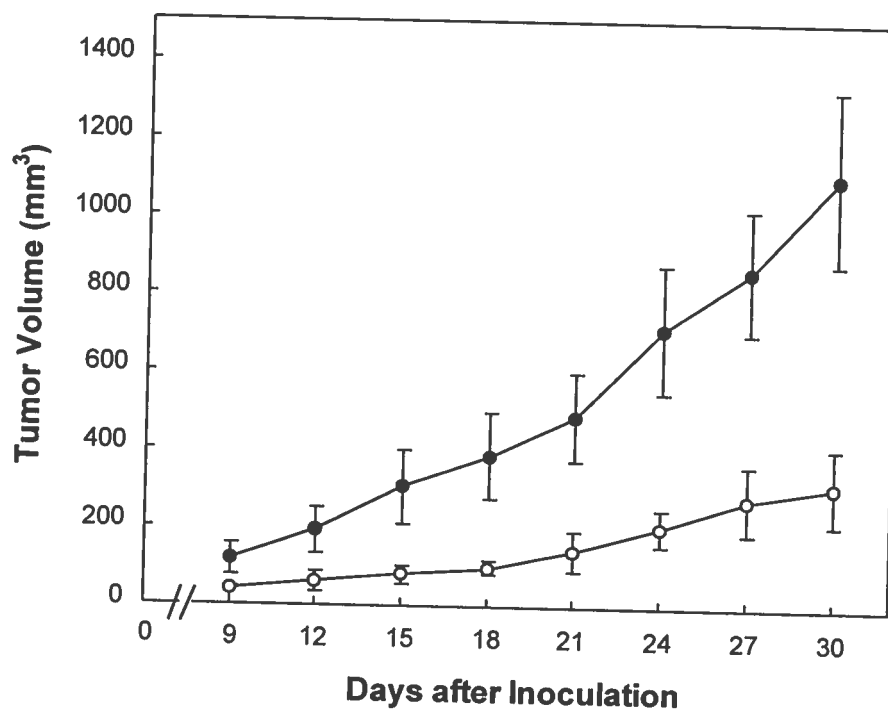


**Figure 2.3. Antitumor Activity of BCD-F9 in HT-1080-Xenografted Nude Mice.**

Cultured HT-1080 cells were inoculated s.c. into CD-1 nude mice on day 0. Normal rabbit IgG (●) or mAb BCD-F9 (○) was administered i.v. according to a schedule described in Material and Methods. Results expressed as mean tumor volume  $\pm$  SD were calculated from 5 growing tumors/group measured at 3-day intervals from 9 to 30 days post-grafting. Statistical significance:  $P < 0.01$  versus normal IgG, calculated using the Student's  $t$ -test.

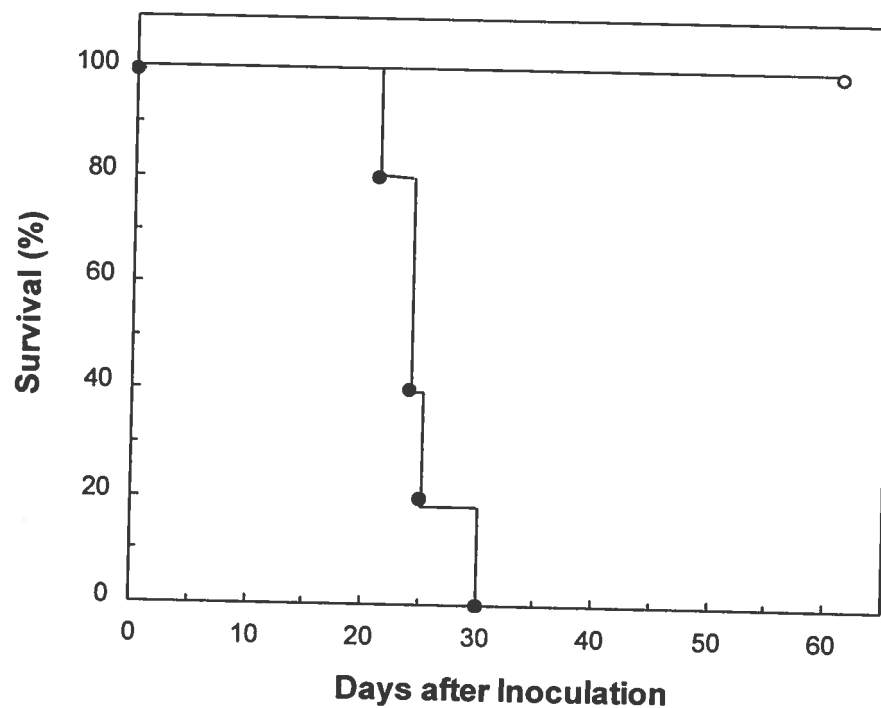


**Figure 2.4. Prolonged Survival Time of HT-1080 Tumor-Bearing Mice after Treatment with BCD-F9.**

Cultured HT-1080 cells were inoculated i.v. into 2 groups of 5 CD-1 nude mice on day 0. Rabbit IgG (●) or BCD-F9 (○) was administered i.v. according to a schedule described in Material and Methods. Statistical significance:  $P < 0.05$  versus normal IgG, calculated using the Cox-Mantel test.



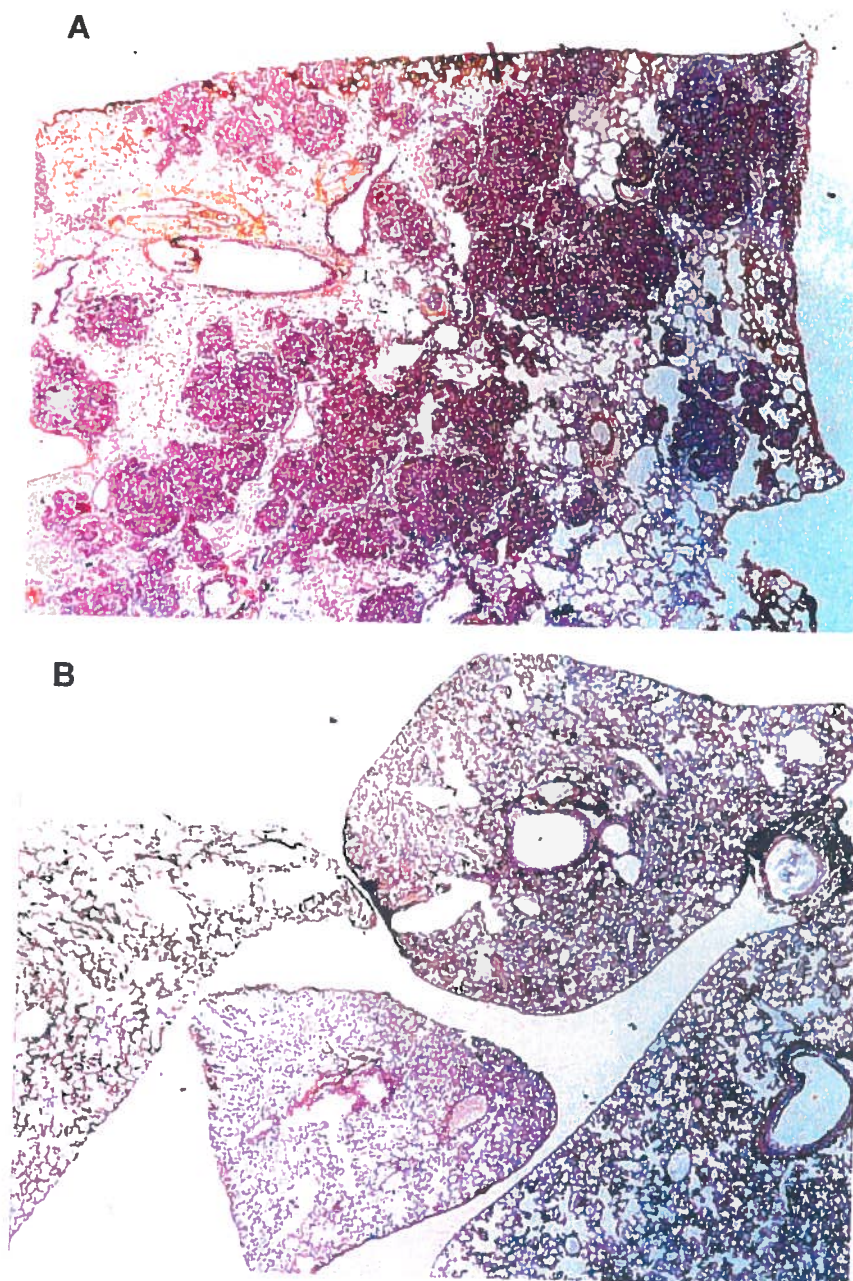


**Figure 2.5. Tumor Histology.**

Photomicrographs demonstrating histological features of tumors formed in mouse lung after i.v. injection of human HT-1080 cells. Representative lung colony of HT-1080 tumor cells in mice treated with normal rabbit IgG (A) or mAb BCD-F9 (B) x 100.

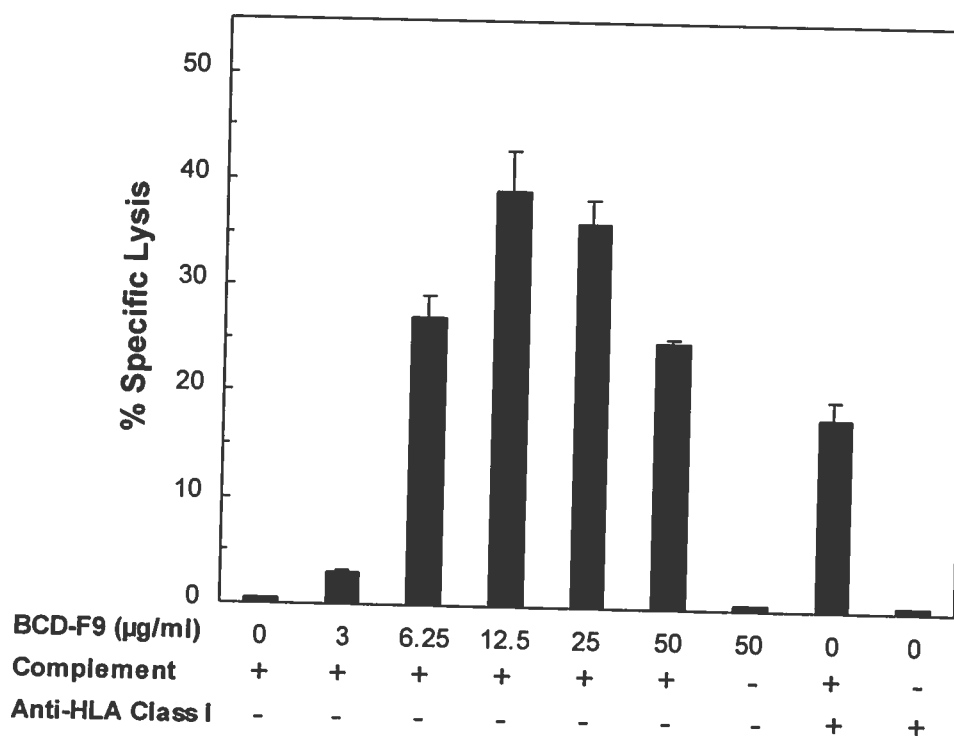


**Figure 2.6. Capacity of mAb BCD-F9 to Kill HT-1080 Cells by ADCMC.**

Lysis of radiolabeled tumor cells was measured in a standard  $^{51}\text{Cr}$ -release assay after cells were incubated for 45 min at  $37^\circ\text{C}$  with various concentrations of protein G-purified mAb BCD-F9 with or without guinea-pig complement. The values shown are means of triplicate samples  $\pm$  SD

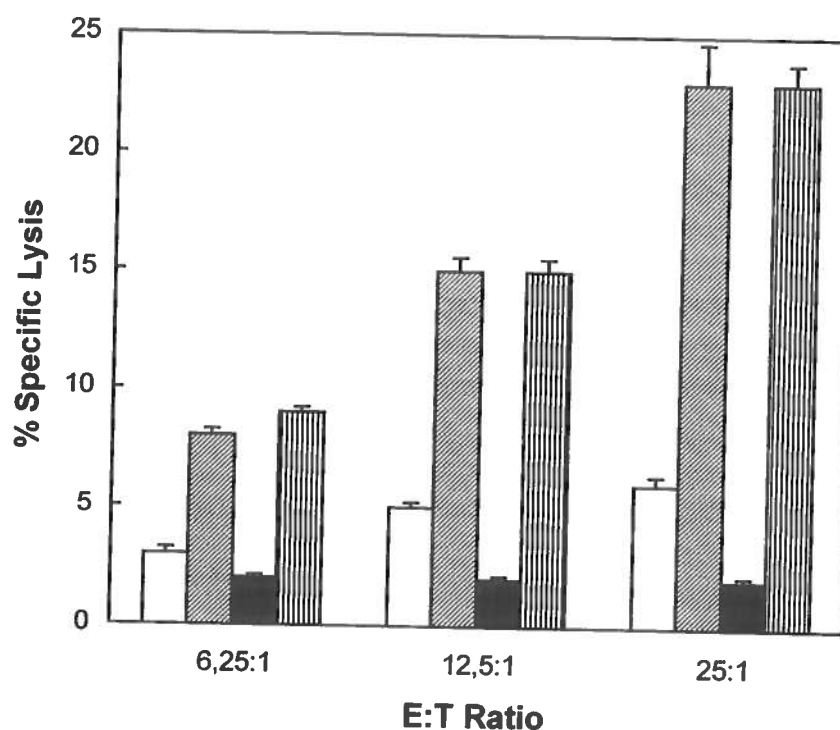


**Figure 2.7. Capacity of mAb BCD-F9 to Kill HT-1080 Tumor Cells by ADCC.**

The capacity of protein G-purified mAb BCD-F9 to lyse radiolabeled HT-1080 tumor cells by ADCC was evaluated in a standard  $^{51}\text{Cr}$ -release assay using as effector cells NK-enriched spleen cells (hatched bars) or thioglycollate-elicited peritoneal cells (lined bars) harvested from CD-1 nude mice. Open bars and solid bars show the resistance of HT-1080 target cells to lysis by splenic NK-enriched cells and peritoneal cells in the absence of antibodies, respectively. The values shown are mean of quadruplicate samples  $\pm$  SD containing cells at indicated E:T ratios.

## **CHAPTER 3**

### **Epitope-Specific Antibody Response to HT-1080 Fibrosarcoma Cells by Mimotope Immunization**

## RÉSUMÉ TRADUIT

Le mAb murin BCD-F9, reconnaissant un antigène non-identifié à la surface de plusieurs cellules tumorales, a servi au criblage d'une banque de phages exprimant des peptides décimères de manière aléatoire. Le phage sélectionné comportait une séquence unique GRRPGGWMMR représentant le peptide pouvant se lier au BCD-F9. Le peptide a été synthétisé et a inhibé de manière spécifique la liaison du mAb à des cellules de fibrosarcome HT1080. Une mutagenèse de type «alanine» de la séquence du peptide a indiqué que la présence de trois résidus, PXXWW, était cruciale pour la liaison au BCD-F9. Des anticorps polyclonaux produits par immunisation de lapins avec le peptide synthétique GRRPGGWMMR (antisérum anti-mimotope ou AM-F9) se sont liés de manière spécifique aux cellules HT1080 et ont inhibé la liaison de l'anticorps BCD-F9 à ces cellules. Un modèle expérimental murin dans lequel des souris CD-1 nues sont inoculées i.v. avec des cellules HT1080, développent des métastases pulmonaires et meurent à l'intérieur d'une période de 30 jours nous a permis de montrer que le AM-F9 pouvait prolonger de manière significative la vie de ces animaux. Ces résultats suggèrent qu'un mimotope peptidique pourrait être utilisé en tant que nouvel outil immunothérapeutique pour susciter une réponse anti-tumorale bénéfique.

## **Epitope-Specific Antibody Response to HT-1080 Fibrosarcoma Cells by Mimotope Immunization**

Mikhail Popkov<sup>1</sup>, Salwa Sidrac-Ghali<sup>1</sup>, Valery Alakhov<sup>1,2</sup>, and Rosemonde Mandeville<sup>3,4\*</sup>

<sup>1</sup>INRS - Institute Armand-Frappier, University of Quebec, 531 Blvd. des Prairies, Laval, Quebec, Canada H7V 1B7

<sup>2</sup>Supratek Pharma Inc., 531 Blvd. des Prairies, Laval, Quebec, Canada H7V 1B7

<sup>3</sup>Department of Biological Sciences, UQAM, University of Quebec, Montreal, QC, Canada

<sup>4</sup>Biophage Inc., 6100 Royalmount Avenue, Montreal, Quebec, Canada H4P 2R2

**\*Corresponding author:** Rosemonde Mandeville, MD, PhD

Biophage Inc.,

6100 Royalmount Avenue, Montreal, Quebec, Canada H4P 2R2

Tel.: (514) 496-1488; Fax: (514) 496-1521

E-mail: Rosemonde.Mandeville@nrc.ca

**Running title:** Peptide inducing anti-cancer immune response

**Key words:** phage, monoclonal antibody, mimotope, immunization, mouse model

**Research support:** M.P. was supported by scholarships from NSERC and FCAR.

## ABSTRACT

The mouse mAb<sup>1</sup> BCD-F9 that recognizes an unknown antigen found on the surface of many tumor cells was used to screen a phage display library expressing random peptide decamers. The phage that was selected encoded for the unique sequence GRRPGGWWMR representing the peptide capable of binding to the BCD-F9 mAb. The peptide was synthesized and found to specifically inhibit the binding of mAb to HT-1080 fibrosarcoma cells. Alanine mutagenesis of the sequence encoding for this peptide indicated that three residues, PXXWW, were critical for its binding to the BCD-F9 mAb. Polyclonal antibodies generated by immunization of rabbits with the synthetic peptide GRRPGGWWMR (anti-mimotope antiserum or AM-F9) specifically bound to HT-1080 cells and inhibited the binding of the BCD-F9 antibody to these cells. Using an experimental animal model where CD-1 nude mice are inoculated i.v. with HT-1080 cells develop lung metastasis and die within 30 days, we have shown that AM-F9 could significantly prolong the life span of these animals. Our results suggest that a peptide mimotope can be potentially used as a novel immunotherapy to induce a beneficial antitumor response.

## INTRODUCTION

Since the development of the hybridoma approach (1), a large number of rodent mAbs with specificity for antigens of therapeutic interest have been generated and characterized. However, the fact that rodent antibodies are highly immunogenic in humans severely limits their clinical applications, especially when repeated administrations are required. It was therefore suggested that passive immunization using humanized or reshaped mouse mAbs could have clinical application, and several of these mAbs are now in clinical trials (2). Ideally, antibody humanization should not diminish their specificity and affinity toward the antigen, whereas immunogenicity must be completely eliminated. However, it has become apparent that the accomplishment of both aims is usually time-consuming and costly. Another approach is the use of synthetic peptides (mimotopes) corresponding to the sequence of the native antigen that can induce antibodies *in vivo* (3-5). Furthermore, protective immune reactions were elicited by mimotope immunization for several infectious agents (6-8). Therefore, the use of peptide mimotopes might be a valuable approach to develop vaccines for the induction of a defined antibody response to cancer antigens.

Phage display technology is a powerful tool for identifying peptide structures that mimic natural epitopes, including both linear and conformational epitopes expressed on a variety of cell types (9-13). Phage peptide libraries consist of filamentous phages displaying random peptides of defined length on their surface. The peptides are usually fused to the phage minor coat protein pIII (14-15), which is expressed at low density (3-5 molecules per phage particle) or to the major coat protein pVIII (16), which is represented at a higher copy number. Such libraries have been successfully screened with a variety of mAbs, and the peptides selected have been shown to mimic linear, assembled and nonpeptidic epitopes (12,13,17). In all these methodologies, the selection of mimotopes (molecules of the repertoire able to bind to the ligate) does not necessarily require that the original ligand be known. The mimotopes have been shown to effectively induce a specific immune response directed against the epitope recognized by the mAb used for the affinity selection of phage clones (4,7), which has suggested a new way to induce epitope-specific antibody responses against unknown epitopes (5,18,19).



However, there are limited data on whether the antibodies generated by mimotopes can recognize native antigens on tumor cells and much less is even known about the antitumor activity of anti-mimotope antibodies.

Recent findings in a nude xenograft mouse model have shown that mAb BCD-F9 (20), when administrated i.v. is able to reduce growth and metastasis of human HT-1080 tumor cells<sup>2</sup>. Because of the ability of BCD-F9 to recognize a wide variety of neoplastic cell lines as opposed to normal tissues (21), this mAb could potentially be used for antitumor immunotherapy. In this study, we used phage-displayed peptide libraries to identify ligands mimicking an epitope for BCD-F9, presented on the cancer cells, and we analyzed the anti-cancer activity of antiserum generated against the discovered ligand.

## MATERIAL AND METHODS

**Cell Line and Monoclonal Antibody.** The human fibrosarcoma cell line, HT-1080, was purchased from the American Type Culture Collection (ATCC, Rockville, MD) and maintained in DMEM supplemented with 10% FBS. The cells were cultured at 37 °C in 5% CO<sub>2</sub> under a humidified atmosphere.

The mAb BCD-F9 was obtained from the fusion of NS-1 myeloma cells with spleen cells from BALB/c mice hyperimmunized with the human breast carcinoma cell line BT-20 (20). BALB/c mice were inoculated i.p. with hybridoma, and the BCD-F9 mAb was purified from ascetic fluid using a protein-G Sepharose column (Pharmacia, Baie-Durfe, Quebec).

**Phage Libraries and Biopanning.** BCD-F9 ligands were selected from random phage libraries expressing linear (pIII-10aa) or circular (pIII-10aa.Cys) decapeptides fused to pIII filamentous bacteriophage fd (22).

The mAb BCD-F9 was biotinylated by incubation of 100 µg of the antibody with 5 µg of NHS-LC-Biotin in 50 µl of 0.1 M NaHCO<sub>3</sub> for 2 hr at room temperature followed by dialysis against PBS<sup>1</sup> (23). For panning, Nunc Maxisorb microtiter plates were coated with streptavidin at 20 µg/ml in 0.1 M NaHCO<sub>3</sub> overnight at 4°C and then blocked with 350 µl of blocking solution (1% powdered milk in PBS) for 1 hr at room temperature. The biotinylated mAb BCD-F9 was diluted to 10 µg/ml in blocking solution, and 25 µl were added to each well. The mAb was bound to the plate for 2 hr at room temperature, and the wells were washed six times with PBS. Then, 10<sup>10</sup> phages were added in 50 µl of 0.1% milk/PBS and bound to the mAb for 1 hr at room temperature. The plates were washed twelve times with PBS to remove non-specific phages while bound phages were eluted by treatment with 50 µl of 0.1 M glycine/HCL buffer, pH 2.2, containing 1 mg/ml of BSA. Neutralization of the eluate, titration and amplification on agar medium were carried out essentially as previously described (15). The binding and elution steps were repeated four times. Viral DNA was sequenced with fUSE <sup>32</sup>P primer 5'-TGAATTTTCTGTATGAGG-3' (kindly provided by Dr. George Smith) by using the Sequenase T7 kit (Pharmacia, Baie-Durfe, Quebec) as recommended by the supplier.

**Alanine Substitutions and Phage Attachment Assay.** Mutants of the phage selected for its binding to the BCD-F9 mAb were produced as previously described (18). Briefly, a series of complementary oligonucleotides in which a given non-Ala residue of DNA encoding for the peptide was changed so as to encode for Ala were used in the construction of mutant phages. Complementary oligonucleotides  $\gamma 2^{\text{for}}$  (5'-TGGCTTCTAAAGAGCCGGGGGGGTGGTGAAGGGGGCGGCCTCTG-3') and  $\gamma 2^{\text{rev}}$  (5'-AGGCCGCCCCCTTCCACCACCCCCCGGCTCTTTAGAAGCCACGT-3') were used in the construction of the phage  $\gamma 2$ . All mutants were purified and verified by DNA sequencing as described above.

To test the ability of each phage to be recognized by the BCD-F9 mAb, approximately  $10^8$  virions of a given mutant were incubated for 1 hr at room temperature with the biotinylated antibody previously immobilized on microtiter plates as described above. Following ten washes, phages were eluted with 0.1 M glycine/HCL pH 2.2, neutralized, and tittered on strain K91 (15). The percentage of attachment was calculated as the number of the eluted phages divided by the input phages x 100.

**Synthetic Peptides.** The mimotope sequence GRRPGGWWMR (designated M-F9) was synthesized as linear free peptides by standard solid-phase method Fmoc<sup>1</sup> chemistry and TGA (24). The purity of peptides was assessed by reverse-phase high-pressure liquid chromatography and mass spectrometry. The complete peptide GRRPGGWWMRAASYC contains five additional residues at the C terminus. Three of them (AAS) represent the linker fusing the peptide and gIII protein as expressed on the phage, a Tyr residue was added for possible radiolabeling, and a Cys residue for coupling to KLH<sup>1</sup>. P- $\gamma 2$  peptide was synthesized as a NVSKEPGGWKGDYC sequence corresponding to the native PLC- $\gamma 2$  sequence with the exception of the C-terminal Cys residue added for coupling. For immunization, the peptides were conjugated to KLH via the carboxyl terminus as previously described (3).

**Rabbit Immunization.** New Zealand white female rabbits were given a primary i.m. immunization with 100  $\mu$ g of the peptide-KLH solution emulsified 1:1 in Freund's complete adjuvant and subsequently boosted with 150  $\mu$ g of antigen emulsified 1:1 in Freund's incomplete adjuvant at biweekly intervals. The rabbits were boosted three times

and bled 5 days after the last boost at week 7. The serum samples from rabbits were tested by ELISA as previously described (3). The synthetic peptides M-F9 and P- $\gamma$ 2 were used as capture antigens (1  $\mu$ g per well). All ELISA experiments were performed at least twice in triplicates.

**Cell Binding and Inhibition Assays.** For the preparation of cells, 10 ml of PBS were added to HT-1080 cell culture, and the cells were washed, harvested by incubation with PBS containing 0.5 mM EDTA and transferred to 15-ml centrifuge tubes. Viable cells were then counted using the Trypan Blue dye exclusion technique. The concentration of cells was adjusted to  $10^7$  cells per ml, and 100  $\mu$ l were used for each sample. The BCD-F9 mAb (1  $\mu$ g) was then added to the sample tubes and incubated on ice for 45 min, washed twice with 2 ml of BSA/PBS and centrifuged for 5 min at 1,500 rpm. A total of 10  $\mu$ l of antibody [goat anti-mouse IgG FITC<sup>1</sup>-labeled (Roche Diagnostics, Laval, Quebec) diluted 1:25 with PBS] was added to the sample and incubated on ice for 45 min and again washed twice with BSA/PBS. The cells were fixed using 0.5 ml of 1% paraformaldehyde in PBS and the percentage of cells binding the antibody was analysed on a Epics XL-MCL flow cytometer (Coulter, Hialeah, FL) equipped with a 488 nm argon laser.

For phage inhibition assay, 0.5  $\mu$ g of the BCD-F9 mAb was preincubated for 2 hr at room temperature with 100  $\mu$ l of BSA/PBS containing various concentrations of phage particles: F9,  $\gamma$ 2, and W7 expressing the VCDWWGWGIC peptide. Aliquots were then added to HT-1080 cells ( $10^6$  cells/sample), and the cells were treated as described above.

For peptide inhibition assay, 0.5  $\mu$ g of the BCD-F9 mAb was pre-incubated for 2 hr at room temperature with 100  $\mu$ l of BSA/PBS containing various concentrations of the synthetic peptides: M-F9, P- $\gamma$ 2, and VCDWWGWGIC. Aliquots were then added to HT-1080 cells ( $10^6$  cells/sample), and the cells were treated as described above.

For antisera inhibition assay, HT-1080 cells ( $10^6$  cells/sample) were pre-incubated for 45 min on ice with different dilutions of antisera: AM-F9, AP- $\gamma$ 2, or pre-immune rabbit serum. Then, 1  $\mu$ g of the BCD-F9 mAb was added to the sample tubes and treatment proceeded as described above.

**Experimental Metastasis.** Confluent monolayers of HT-1080 cells were harvested by incubation with PBS containing 0.5 mM EDTA. Viable cells were counted by the Trypan Blue exclusion dye method. Aliquots containing over 95% of viable cells were used in this experiment. The cells ( $2 \times 10^7$  cells/ml) were suspended in PBS, and 0.1 ml of the suspension was inoculated i.v. into the tail vein of CD-1 nude mice (Day 0). Rabbit pre-immune serum (100  $\mu$ l), or AM-F9 polyserum (100  $\mu$ l) was administered i.v. in 0.2 ml of PBS on days 1 and 2, 5 to 9, 12 to 16, and 19 to 21, and the lungs were recovered from recently deceased animals. The lungs were fixed in 10% buffered formalin, embedded in paraffin, sectioned and stained with H&E for routine histological examination by light microscopy.

**Statistical Analysis.** Cox-Mantel logrank test was performed using INSTAT software. A *P*-value of  $< 0.05$  was considered significant.

## RESULTS

*Identification of BCD-F9-Specific Mimotopes.* To search for a peptide that is able to bind with BCD-F9, we screened two phage peptide libraries. One of these libraries displays linear decapeptides that are fused to the minor coat protein pIII, while the second has additional two cysteines flanking the random decapeptide sequence, leading to formation of circular peptides through the creation of a disulfide bridge. After four rounds of biopanning using mAb BCD-F9 as a target, we observed an approximately 33,000-fold increase in the number of eluted phages in the case of the linear library (Fig. 3.1). The circular library showed a marginal enrichment of about 100-fold following the third round of selection. Therefore, no further manipulations were continued with this library.

After the fourth round of selection with the linear library, sixteen independent phage isolates were amplified and sequenced. All isolates yielded the identical DNA sequence encoding for the amino acid sequence GRRPGGWWMR. Additional eight independent isolates were chosen from the second round and were sequenced. All the phages from the second round encoded for the same sequence as was obtained from the fourth round isolates. The comparison of the identified peptide sequence with protein sequences available in Gene Bank showed the homology of five amino acid residues (PGGWW) to six SH3 domain-containing proteins (NCBI accession no. AAD29953, AAC78610, Q15811, AAD29952, NP\_003015, NP\_002652). These proteins are all intracellular signal transducers and therefore, it is unlikely that they contain the BCD-F9 reactive epitope.

*Determination of Critical Amino Acids Necessary for Binding to the BCD-F9 mAb.* In order to determine which residues were critical for the binding, a series of mutant phages were constructed in which residues inside the PGGWW block were individually changed to Ala. Phage  $\gamma 2$  expressing the sequence corresponding to that of PLC- $\gamma 2$ , one of the six proteins identified in the Gene Bank (NCBI accession no. NP\_002652), was also constructed in order to determine the effect of the remaining residues N- or C-terminal to this block. Each of the resulting phages was then tested for its ability to bind to the BCD-F9 mAb. Results shown in Figure 3.2 indicate that

mutations of three residues Pro (4<sup>th</sup> position), Trp (7<sup>th</sup> position), and Trp (8<sup>th</sup> position) led to a significant reduction in binding of the peptide to the BCD-F9 mAb. The remaining residues had no effect on the peptide binding when changed all at once in phage  $\gamma$ 2. We did not change two Gly residues inside the PGGWW block, mainly because it was previously shown that Gly residues do not usually contribute directly to the binding but rather serve as structural linkers to position the critical residues (18).

*Binding of Phage F9 and Mimotope (M-F9) to the BCD-F9 mAb.* To confirm the specificity of the peptide represented on phage F9, we analyzed its ability to inhibit binding of the BCD-F9 mAb to HT-1080 cells i.e., cells that express a high level of the BCD-F9-specific antigen. Phages  $\gamma$ 2 and W7 were used as controls mainly because they show the highest and the lowest binding to the BCD-F9 mAb, respectively (Fig. 3.2). BCD-F9 was incubated with the serial dilutions of phages and then assayed for its ability to bind to HT-1080 cells. The results shown in Figure 3.3A demonstrate that phage F9 induced a 47% inhibition at the  $10^{13}$  virions/ml concentration while phage  $\gamma$ 2 was less potent inducing 38% inhibition at the same virion concentration. The phage W7 did not show any specific binding to the BCD-F9 mAb.

A peptide corresponding to the sequence presented on phage F9 (M-F9 peptide) was then synthesized and tested for its binding to the BCD-F9 mAb. We also synthesized a peptide corresponding to the phage  $\gamma$ 2 (P- $\gamma$ 2 peptide) and an unrelated (VCDWWGWGIC) peptide. These three peptides were tested for their ability to bind to the BCD-F9 mAb. Briefly, BCD-F9 was incubated with the peptides at various concentrations of the synthetic peptides and then assayed for its ability to bind to HT-1080 cells. Figure 3.3B shows that the M-F9 bound specifically to the antibody and blocked its subsequent binding to HT-1080 cells. The highest potency of the M-F9 peptide was  $IC_{50}$  of  $2 \times 10^{-6}$  M, as compared to the P- $\gamma$ 2 peptide that showed inhibitory effect only at concentrations higher than 100  $\mu$ M. The peptide VCDWWGWGIC had no inhibitory effect (Fig. 3.3B).

*Induction of an Epitope-Specific Immune Response.* To investigate whether the mimotope represents an immunogenic structure corresponding to the natural epitope expressed on cancer cells, rabbits were immunized either with the M-F9 peptide or the P- $\gamma$ 2 peptide conjugated with KLH. After a primary immunization and three boosts, the sera

from individual rabbits were separately collected and tested for anti-peptide antibodies using an ELISA technique. All the sera collected showed an ability to bind to peptides at 1:2000 dilution, whereas the pre-immune serum showed no anti-peptide reactivity. We then investigated the specificity of the rabbit anti-mimotope antisera by inhibiting the binding of the BCD-F9 mAb to HT-1080 cells. As shown in Figure 3.4, serum from the rabbit immunized with M-F9 peptide (AM-F9) inhibited the binding of BCD-F9 to HT-1080 cells by 75%, suggesting that the rabbit anti-mimotope antiserum was directed against the epitope of these tumor cells. In contrast, the serum from rabbit immunized with the P- $\gamma$ 2 peptide, as well as rabbit pre-immune serum, did not inhibit the binding of the BCD-F9 mAb to HT-1080 cells.

*Effect of AM-F9 on Experimental Lung Metastasis.* Finally, we examined the antitumor activity of AM-F9 in an experimental metastasis model. In this model, HT-1080 cells injected i.v. into CD-1 nude mice induce the formation of metastatic foci in the lung, and 100% of the animals die within 30 days after inoculation. After 50 days of observation, the MST values were calculated for groups of mice injected with AM-F9 and mice treated with pre-immune serum. These were  $47 \pm 2$  and  $25 \pm 1$ , respectively (Fig. 3.5). The animals treated with AM-F9 had significantly prolonged life span ( $T/C = 188\%$ ), suggesting that the antitumor activity of AM-F9 was not dependent on the nonspecific action of the rabbit serum. Histological examination of the lungs showed diffuse metastasis in the case of control animals and more localized metastatic foci in the case of animals treated with anti-mimotope antisera. In-life observations showed that mice treated with AM-F9 appeared as healthy as the control mice during the duration of the experiment, suggesting that no severe side effects were caused by AM-F9.



## DISCUSSION

Several authors have previously demonstrated that peptide mimotopes can be obtained from phage epitope libraries (9-11) or by chemical synthesis (25-27) and that these sequences bind antibodies raised against native structures. In fact, several studies have shown that peptide mimotopes can be found for most, if not all, anti-carbohydrate mAbs (28-30). Peptide epitopes have also been shown to mimic glycosphingolipids and oligonucleotides structures (30-32). In the case of mimotope immunization, several investigators showed that synthetic peptides could induce an epitope-specific immune response *in vivo* (3-5). Furthermore, protective immune reactions by mimotope immunizations have been shown for several infectious agents (6-8), viral antigens (33), and pollen allergens (34). The larger issue of whether such mimotopes can be exploited to elicit functional antibody response against tumor cells has yet to be fully resolved.

In this study, we chose a well-characterized functional mAb, BCD-F9, and used it to identify peptides that mimic the epitope recognized by this antibody. The BCD-F9 mAb is a murine mAb (IgG2a) that recognizes an antigen present on the surface of many tumor cell lines. Because of its high selectivity towards tumor cells as opposed to normal tissues, this mAb could be potentially used for killing tumor cells (35). Whereas the tumor antigen that is recognized by BCD-9 has not been isolated, our unpublished data demonstrates that this mAb recognizes a conformational epitope on 57 kDa glycoprotein<sup>2</sup>.

Although we expected to identify several mimotopes, only one sequence was selected from a linear random decapeptide library while a circular library did not generate any specific phages. Despite the great number of independent clones in these libraries ( $>10^9$ ), they cover only a small percentage of all theoretically possible decapeptides. Therefore, it is possible that the circular library does not contain peptides mimicking the most optimal structure of the native epitope. It is also possible that there is a bias against particular sequences because the need to maintain phage infectivity, resulting in the absence of those sequences from the library.

Mutational analysis indicated that specificity is likely to reside in the PGGWW block of the amino acids (Fig. 3.2). This block is common to several SH3 domain-

containing regulatory proteins involved in signal transduction (36). The intracellular localization of these signaling proteins suggest that the F9 peptide mimics the native tumor-specific epitope despite the fact that they have different amino acid sequences. Binding studies and immunization experiments confirmed the specificity of the mimotope for the BCD-F9 mAb. In addition, the mimotope was specifically recognized by BCD-F9 without the phage carrier, indicating that the mimotope alone is responsible for the interaction with BCD-F9 without the involvement of structure entities from the phage particle. Another indication for the correct mimicking of the epitope by F9 peptide was obtained by the immunization experiments. We demonstrated that rabbits immunized with peptide-KLH could elicit an IgG response to the natural antigen on tumor cells.

On the other hand, results obtained with the peptide  $\gamma 2$  were surprising and we cannot reasonably explain their poor binding. However, it cannot be excluded that the amino acid residues flanking the PGGWW block can interfere with the binding when the peptide is isolated from the phage carrier. A similar situation has been previously reported in which the peptides were able to mimic the natural epitope only when presented on the phage surface (19,34).

In summary, this report describes the isolation of mimotope corresponding to the epitope of the BCD-F9 mAb. Inhibition studies either with mimotope-displaying phage particles or with synthetic peptides proved the specificity of the isolated mimotope. Immunization of rabbits with the mimotope induced polyclonal antibodies capable of blocking the binding of the BCD-F9 mAb to HT-1080 tumor cells. Finally, we assessed the effect of AM-F9 serum on tumor metastasis in an experimental animal model and showed that i.v. treatment with anti-mimotope antisera (15 injections of 100  $\mu$ l/mouse) significantly prolonged the life span of nude mice (Fig. 3.5). However, the beneficial effects of this passive immunotherapy are only achieved if relatively large amounts of antibody are applied, making this treatment very expensive. Thus, it would be an advantage to replace or combine the passive treatment with an active immunization using a mimotope. The success of such an approach has already been demonstrated with the use of mimotopes as experimental oral anti-IgE vaccines (37).

The properties of AM-F9 were further investigated in a separate study<sup>3</sup>. It was found that (a) treatment with AM-F9 significantly inhibited the growth of HT-1080 tumor

cells inoculated s.c. into CD-1 nude mice, (b) AM-F9 elicited ADCC<sup>1</sup> by splenic NK cells and by peritoneal cells, and (c) AM-F9 mediated complement-dependent cytotoxicity.

The results of this study suggest that phage epitope libraries may have broad application for the design of anti-cancer vaccines. We believe that this strategy may allow the design of immunogenic peptides without prior knowledge of the target antigen. A new generation of anti-cancer vaccines could consist of a mixture of mimotopes, including peptides that mimic the carbohydrates and complex epitopes, selected using tumor-specific mAbs.

## ACKNOWLEDGEMENTS

We would like to thank Dr G. P. Smith for providing the fUSE<sup>32</sup>P primer; Dr F. Shareck for the oligonucleotide synthesis; Dr J. Hu for peptide synthesis; and Mrs L. Labrie and L. Forget for DNA sequence analysis.

## REFERENCES

1. Kohler G. and C. Milstein. 1975. "Continuous cultures of fused cells secreting antibody of predicted specificity". Nature, vol. 256, p. 495-496.
2. Hollinger, P. and H. Hoogenboom. 1998. "Antibodies come back from the brink". Nature Biotechnol., vol. 16, p. 1015-1016.
3. Willis, A. E., R. N. Perham, and D. Wraith. 1993. "Immunological properties of foreign peptides in multiple display on a filamentous bacteriophage: peptides from *Plasmodium falciparum* circumsporozoite as antigens". Gene, vol. 128, p. 79-83.
4. Meola, A., P. Delmastro, P. Monaci, A. Luzzago, A. Nicosia, F. Felici, R. Cortese, and G. Galfre. 1995. "Derivation of vaccines from mimotopes. Immunologic properties of human hepatitis B virus surface antigen mimotopes displayed on filamentous phage". J. Immunol., vol. 154, p. 3162-3172.
5. Rudolf, M., M. Vogel, F. Kricek, C. Ruf, A. Zurcher, R. Reuschel, M. Auer, S. Miescher, and B. M. Stadler. "Epitope-specific antibody response to IgE by mimotope immunization". J. Immunol., vol. 160, p. 3315-3321.
6. Motti, C., M. Nuzzo, A. Meola, G. Galfrè, F. Felici, R. Cortese, A. Nicosia, and P. Monaci. 1994. "Recognition by human sera and immunogenicity of HbsAg mimotopes selected from an M13 phage display library". Gene, vol. 146, p. 191-198.
7. Stoute, J. A., W. R. Ballou, N. Kolodny, C. D. Deal, R. A. Wirtz, and L. E. Lindler. "Induction of humoral immune response against *Plasmodium falciparum* sporozoites by immunization with a synthetic peptide mimotope whose sequence was derived from screening a filamentous phage epitope library". Infection and immunity, vol. 63, p. 934-939.
8. Prezzi, C., A. Nuzzo, A. Meola, P. Delmastro, G. Galfrè, R. Cortese, A. Nicosia, and P. Monaci. "Selection of antigenic and immunogenic mimics of Hepatitis C virus using sera from patients". J. Immunol., vol. 156, p. 4504-4513.
9. Scott, J. K. and G. P. Smith. "Searching for peptide ligands with an epitope library". Science, vol. 249, p. 386-390.
10. Devlin, J. J., L. C. Panganiban, and P. E. Devlin. 1990. "Random peptide libraries: A source of specific protein binding molecules". Science, vol. 249, p. 404-406.

11. Cwirla, S. E., E. A. Peters, R. W. Barrett, and W. J. Dower. 1990. "Peptides on phage: A vast library of peptide for identifying ligands". Proc. Natl. Acad. Sci. USA, vol. 87, p. 6378-6382.
12. Luzzago, A., F. Felici, A. Tramontano, A. Pessi, and R. Cortese. 1993. "Mimicking of discontinuous epitopes by phage-displayed peptides, I. Epitope mapping of human H ferritin using a phage library of constrained peptides". Gene, vol. 128, p. 51-57.
13. Felici, F., A. Luzzago, A. Folgori, and R. Cortese. 1993. "Mimicking of discontinuous epitopes by phage-displayed peptides, II. Selection of clones recognized by a protective monoclonal antibody against the *Bordetella pertussis* toxin from phage peptide libraries". Gene, vol. 128, p. 21-27.
14. Smith, G. P. 1985. "Filamentous fusion phage: novel expression vectors that display cloned antigens on the virion surface". Science, vol. 228, p. 1315-1316.
15. Parmley, S. F. and G. P. Smith. "Antibody-selectable filamentous fd phage vector: Affinity purification of target genes". Gene, vol. 73, p. 305-318.
16. Felici, F., L. Castagnoli, A. Musacchio, R. Jappelli, and G. Cesareni. 1991. "Selection of antibody ligands from a large library of oligopeptides expressed on a multivalent expression vector". J. Mol. Biol., vol. 222, p. 301-310.
17. Balass, M., Y. Heldman, S. Cabilly, D. Givol, E. Katchalski-Katzir, and S. Fuchs. "Identification of a hexapeptide that mimics a conformation-dependent binding site of acetylcholine receptor by use of a phage-epitope library". Proc. Natl. Acad. Sci. USA, vol. 90, p. 10638-10642.
18. Hoess, R. H., U. Brinkmann, T. Handel, and I. Pastan. 1993. "Identification of a peptide which binds to the carbohydrate-specific monoclonal antibody B3". Gene, vol. 128, p. 43-49.
19. Chargelegue, D., O. E. Obeid, S.-C. Hsu, M. Shaw, A. N. Denbury, G. Taylor, and M. W. Steward. 1998. "A peptide mimic of a protective epitope of respiratory syncytial virus selected from a combinatorial library induces virus-neutralizing antibodies and reduces viral load in vivo". J. Virol., vol. 72, p. 2040-2046.
20. Mandeville, R., J. Lecomte, F. Dumas, L. Giroux, J.-P. Chausseau, I. Ajdukovic, and F. Boury. 1987. "Production and characterization of monoclonal antibodies showing a different spectrum of reactivity to human breast tissue". Cancer Detection and Prevention, vol. 10, p. 89-100.
21. Zelechowska, M. G. and R. Mandeville. 1989. "Immunogold and immunogold/silver staining in the ultrastructural localization of target molecules identified by monoclonal antibodies". Anticancer Res., vol. 9, p. 53-58.

22. Popkov, M., I. Lussier, V. Medvedkine, P.-O. Estève, V. Alakhov, and R. Mandeville. 1998. "Multidrug-resistance drug-binding peptides generated by using a phage display library". Eur. J. Biochem., vol. 251, p. 155-163.
23. Gretch, D. R., M. Suter, and M. F. Stinski. 1987. "The use of biotinylated monoclonal antibodies and strepavidin affinity chromatography to isolate herpesvirus hydrophobic proteins or glycoproteins". Anal. Biochem., vol. 163, p. 270-277.
24. Atherton, E., D. L. Clive, and R. C. Sheppard. 1975. "Letter: Polyamide supports for polypeptide synthesis". J. Am. Chem. Soc., vol. 97, p. 6584-6585.
25. Geysen, H. M., S. J. Rodda, and T. J. Mason. 1986. "A priori delineation of a peptide which mimics a discontinuous antigenic determinant". Mol. Immunol., vol. 23, p. 709-715.
26. Houghten, R. A., C. Pinilla, S. E. Blondelle, J. R. Appel, C. T. Dooley, and H. Cuervo. 1991. "Generation and use of synthetic peptide combinatorial libraries for basic research and drug discovery". Nature, vol. 354, p. 84-86.
27. Lam, K. S., S. E. Salmon, E. M. Hersh, V. J. Hruby, W. M. Kazmierski, and R. J. Knapp. 1991. "A new type of synthetic peptide library for identifying ligand-binding activity". Nature, vol. 354, p. 82-84.
28. Bonnycastle, L. L., J. S. Mehroke, M. Rashed, X. Gong, and J. K. Scott. 1996. "Probing the basis of antibody reactivity with a panel of constrained peptide libraries displayed by filamentous phage". J. Mol. Biol., vol. 258, p. 747-762.
29. Harris, S. L., L. Craig, J. S. Mehroke, M. Rashed, M. B. Zwick, K. Kenar, E. J. Toone, N. Greenspan, F. I. Auzanneau, J. R. Marino-Albernas, B. M. Pinto, and J. K. Scott. 1997. "Exploring the basis of peptide-carbohydrate crossreactivity: evidence for discrimination by peptides between closely related anti-carbohydrate antibodies". Proc. Natl. Acad. Sci. USA, vol. 94, p. 2454-2459.
30. Moe, G. R., S. Tan, and D. M. Granoff. 1999. "Molecular mimetics of polysaccharide epitopes as vaccine candidates for prevention of *Neisseria meningitidis* serogroup B disease". FEMS Immunol. Med. Microbiol., vol. 26, p. 209-226.
31. Taki, T., D. Ishikawa, H. Hamasaki, and S. Handa. 1997. "Preparation of peptides which mimic glycosphingolipids by using phage peptide library and their modulation on beta-galactosidase activity". FEBS Lett., vol. 418, p. 219-223.
32. Sibille, P., T. Ternynck, F. Nato, G. Buttin, D. Strosberg, and A. Avrameas. 1997. "Mimotopes of polyreactive anti-DNA antibodies identified using phage-display peptide libraries". Eur. J. Immunol., vol. 27, p. 1221-1228.

33. D'Mello, F., C. D. Partidos, M. W. Steward, and C. R. Howard. 1997. "Definition of the primary structure of hepatitis B virus (HBV) pre-S hepatocyte binding domain using random peptide libraries". Virology, vol. 237, p. 319-326.
34. Jensen-Jarolim, E., A. Leitner, H. Kalchhauser, A. Zurcher, E. Ganglberger, B. Bohle, O. Scheiner, G. Boltz-Nitulescu, and H. Breiteneder. 1998. "Peptide mimotopes displayed by phage inhibit antibody binding to Bet v1, the major birch pollen allergen, and induce specific IgG response in mice". FASEB J., vol. 12, p. 1635-1642.
35. Mandeville, R., C. Schatten, N. Pateisky, M.-J. Dicaire, B. Barbeau, and B. Grouix. 1989. "Immunolymphoscintigraphy with BCD-F9 monoclonal antibody and its F(ab')<sub>2</sub> fragments for the preoperative staging of breast cancers". In: R. L. Ceriani (ed.). Breast Cancer Immunodiagnosis and Immunotherapy, New York: Plenum Press, 203p.
36. Cohen, G. B., R. Ren, and D. Baltimore. 1995. "Modular binding domains in signal transduction proteins". Cell, vol. 80, p. 237-248.
37. Zuercher, A. W., S. M. Miescher, M. Vogel, M. P. Rudolf, M. B. Stadler, and B. M. Stadler. 2000. "Oral anti-IgE immunization with epitope-displaying phage". Eur. J. Immunol., vol. 30, p. 128-135.

**FOOTNOTES**

1. Abbreviations used: mAb, monoclonal antibody; PBS, phosphate-buffered saline; Fmoc, 9-fluorenylmethoxycarbonyl; KLH, keyhole limpet haemocyanin; FITC, fluoroisothiocyanate; ADCC, antibody-dependent cellular cytotoxicity
2. Popkov, M., Sidrac-Ghali, S., Lusignan, Y., Lemieux, S., and Mandeville, R. Inhibition of Tumor Growth and Metastasis of Human Fibrosarcoma Cells HT-1080 by Monoclonal Antibody BCD-F9. Submitted for publication.
3. Popkov, M., Lusignan, Y., Lemieux, S., and Mandeville, R. Immunotherapy with Anti-Mimotope Polyclonal Antibodies in a Nude Mouse Xenograft Model: Mechanisms of Action. Submitted for publication.



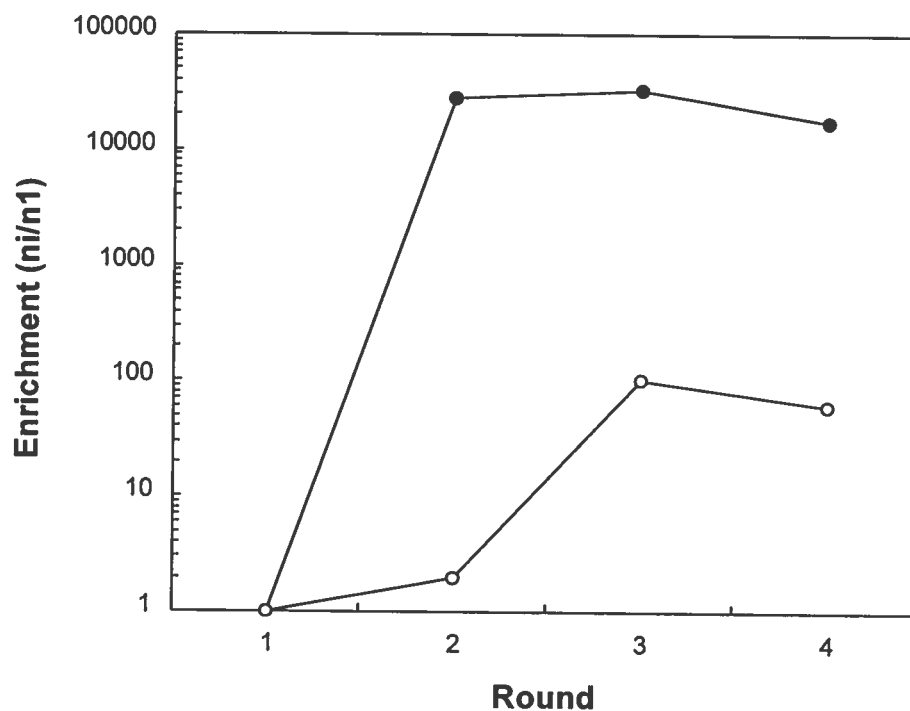


**Figure 3.1. Selection of Phages that Bind to mAb BCD-F9.**

Phages from linear (●) or circular (○) decapeptide libraries were bound to mAb-coated microtiter wells as described in Materials and Methods and eluted with glycine/HCl buffer, pH 2.2. Enrichment ( $n_i/n_1$ ) was calculated as the total number of phages recovered after elution ( $n_i$ , number of transducing units recovered after "i" round of selection) divided by the number of transducing units recovered after the first round of selection ( $n_1$ ). Data represent mean values from plating in triplicate.

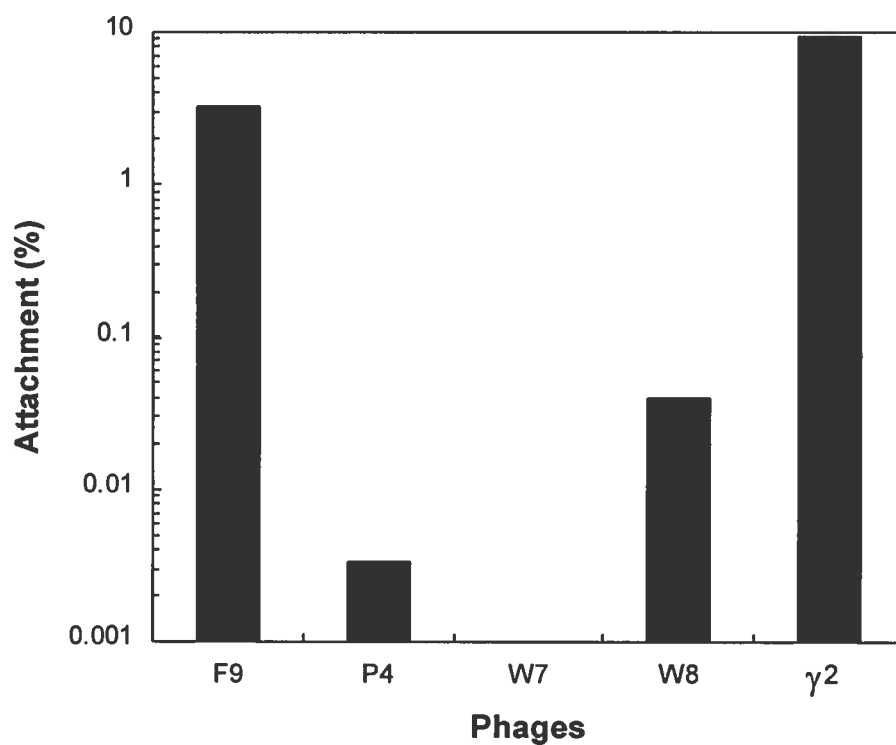


**Figure 3.2. Binding of Ala Phage Mutants and Phage  $\gamma 2$  to mAb BCD-F9.**

The effect is shown of Ala substitutions of three residues the peptide GRRPGGWWMR, starting with Pro in the fourth positions from the N terminus, following with Trp in the seventh position and ending with Trp in the eight position. F9 phage served as a positive control for binding to mAb BCD-F9. The percentage of attachment is the number of eluted phages divided by the input phage x 100. Data represent mean values from plating in triplicate.

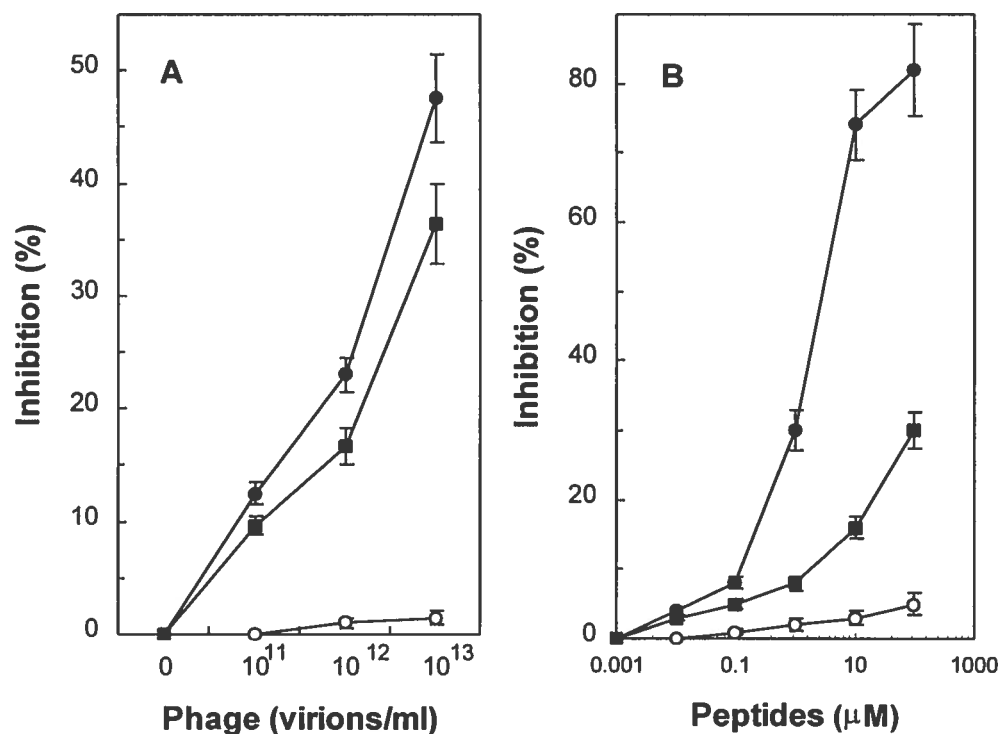


**Figure 3.3. Inhibition of BCD-F9 Binding to HT-1080 Cells by Phages and by Synthetic Peptides.**

Binding of BCD-F9 to HT-1080 cells was studied in the presence of the competing phages (A) F9 (●), γ2 (■), and W7 (○) or in the presence of the competing peptides (B) M-F9 (●), P-γ2 (■), and VCDWWGWGIC irrelevant peptide (○) as described in Materials and Methods. The Y-axis shows inhibition (%) of binding of BCD-F9 to HT-1080 cells as a function of the phage (A) or of the free peptide (B) concentration (X-axis). The data represents means  $\pm$  SD from three independent experiments.

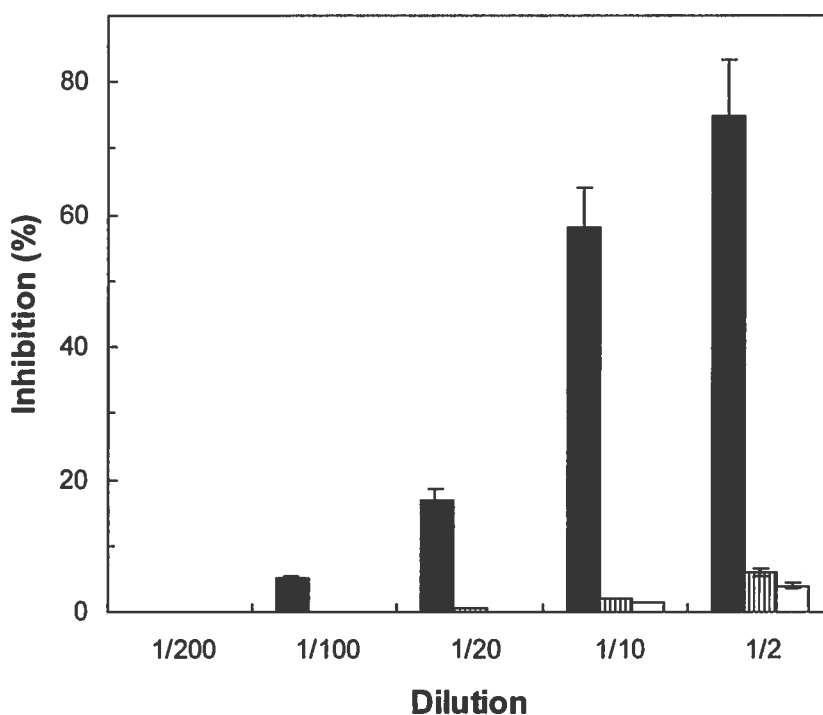


**Figure 3.4. Inhibition of Binding of the BCD-F9 mAb to HT-1080 Cells by Polyclonal Antisera.**

Inhibition of binding of the BCD-F9 mAb to HT-1080 cells by polyclonal antisera. The binding of BCD-F9 to HT-1080 cells was studied in the presence of the competing polyclonal antisera AM-F9 (solid bars), AP-γ2 (lined bars), and pre-immune serum (open bars) as described in Materials and Methods. The Y-axis shows inhibition (%) of binding of BCD-F9 to HT-1080 cells as a function of the rabbit polyclonal antiserum dilution (X-axis). The data represents means  $\pm$  SD from three independent experiments.

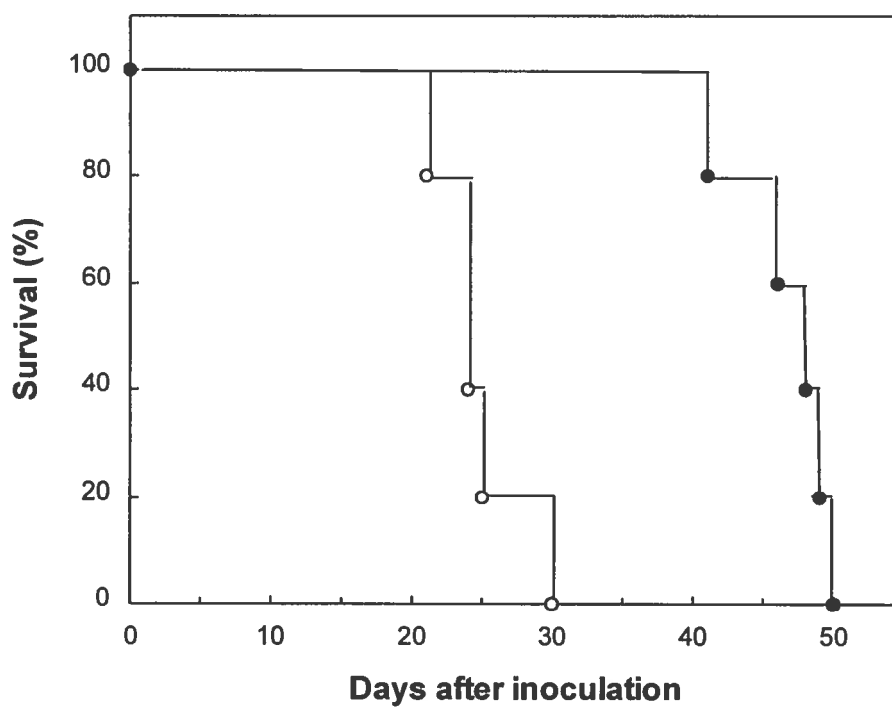


**Figure 3.5. Survival Analysis of HT-1080 Tumor-Bearing Nude Mice.**

HT-1080 cells were inoculated i.v. into CD-1 nude mice on day 0. Rabbit pre-immune serum (○) or AM-F9 (●) was administered i.v. on days 1-2, 5-9, 12-16, and 19-21. Each group comprised 5 mice. Statistical significance:  $P < 0.05$  versus pre-immune serum, calculated using the Cox-Mantel test.

## **CHAPTER 4**

### **Immunotherapy with Anti-Mimotope Polyclonal Antibodies in a Nude Mouse Xenograft Model**

## RÉSUMÉ TRADUIT

BCD-F9 est un mAb murin de type IgG2a reconnaissant un epitope conformationnel présent à la surface de plusieurs cellules tumorales. Nous avons précédemment identifié un mimotope de BCD-F9, appelé M-F9, à partir d'une banque de phages exprimant des décamères peptidiques de manière aléatoire; ce mimotope a par la suite été utilisé pour générer des anticorps polyclonaux (anti-mimotope ou AM-F9) chez le lapin. Nous avons démontré à l'aide d'un modèle de tumeurs métastatiques agressives que l'administration i.v. de AM-F9 prolongeait de manière significative la vie de souris CD-1 nues inoculées i.v. avec des cellules de fibrosarcome humain HT1080. Dans le présent travail, l'activité anti-tumorale de AM-F9 a été testée à l'aide d'un modèle de tumeur sous-cutanée. L'administration de AM-F9 à des souris CD-1 nues auxquelles des cellules HT1080 ont été inoculées par voie s.c. a provoqué une inhibition significative de la croissance tumorale. Nous avons aussi étudié l'activité anti-tumorale in vitro de AM-F9 à l'aide d'essais ADCMC<sup>3</sup> et ADCC<sup>3</sup>. Les populations de cellules effectrices ont été obtenues par déplétion des macrophages (adhérence au plastique) ou par enrichissement des cellules NK (sélection négative). AM-F9 s'est montré efficace dans la médiation de la lyse des cellules tumorales in vitro par ADCMC et ADCC. L'utilisation de différentes populations de cellules effectrices suggère que le mécanisme d'action préférentiel de l'ADCC est vraisemblablement médié par les cellules NK. Cependant, l'activité protectrice de AM-F9 dans le modèle tumoral in vivo n'a pas été abrogée par la déplétion des cellules NK provoquée par un antisérum anti-asialo GM1. Il semble donc que dans ce modèle, l'ADCMC représente un acteur important dans la lyse des cellules tumorales. Ces résultats indiquent aussi qu'un peptide mimotope peut potentiellement être utilisé en tant qu'agent immunothérapeutique pour induire une réponse anti-tumorale bénéfique.

## **Immunotherapy with Anti-Mimotope Polyclonal Antibodies in a Nude Mouse Xenograft Model: Mechanisms of Action<sup>1</sup>**

Mikhail Popkov<sup>\*</sup>, Yvette Lusignan<sup>\*</sup>, Suzanne Lemieux<sup>\*</sup>, and Rosemonde Mandeville<sup>†,‡,2</sup>

<sup>\*</sup>Human Health Research Center, INRS - Institut Armand-Frappier, University of Quebec, Laval, QC, Canada

<sup>†</sup>Department of Biological Sciences, UQAM, University of Quebec, Montreal, QC, Canada

<sup>‡</sup>BIOPHAGE Inc., Montreal, QC, Canada

**Running title:** Anti-tumor Activity of Anti-Mimotope Polyclonal Antibodies

**Keywords:** in vivo animal models, antibodies, NK cells, complement

**Corresponding author:** Rosemonde Mandeville, BIOPHAGE Inc.,

6100 Royalmount Avenue, Montreal, QC, Canada H4P 2R2,

E-mail: Rosemonde.Mandeville @ nrc.ca,

Tel.: (514) 496-7722; Fax: (514) 496-1521

**Abbreviations used:** ADCMC, antibody-dependent complement-mediated cytotoxicity;

ADCC, antibody-dependent cellular cytotoxicity

**Footnotes:** M.P. was supported by scholarships from FCAR and INRS – Institut Armand-Frappier



## ABSTRACT

BCD-F9 is a murine IgG2a mAb, which recognizes a conformational epitope found on the surface of many tumor cells. We have previously selected a mimotope of BCD-F9, designated M-F9, from a phage display library expressing random peptide decamers and used it to generate polyclonal antibodies (anti-mimotope or AM-F9) by immunization of rabbits. Using an aggressive lung metastatic model, we demonstrated that AM-F9 administered i.v. significantly prolonged the life span of CD-1 nude mice inoculated i.v. with HT-1080 human fibrosarcoma cells. In this study, we report that AM-F9 also inhibited tumor growth in CD-1 nude mice inoculated s.c. with HT-1080 cells, thus further supporting the potential usefulness of a peptide mimotope as a novel antitumor immunotherapy. In vitro assays, AM-F9 was found to be effective in mediating tumor cell killing by both antibody-dependent complement-mediated cytotoxicity (ADCMC) and antibody-dependent cellular cytotoxicity (ADCC). Splenic NK cells were more efficient effector cells than peritoneal cells in ADCC assay. Furthermore, only low lysis of AM-F9-coated HT-1080 cells was observed when effector cells were plastic-adherent thioglycolate-elicited peritoneal macrophages. These findings suggested a putative contribution of NK cells in AM-F9-dependent inhibition of tumor cell growth in vivo. Surprisingly, the protective activity of AM-F9 in the s.c. tumor model was enhanced rather than abrogated in NK cell-depleted mice. AM-F9-dependent tumor cell killing in this model would thus either be complement-mediated or require the implication of another cytotoxic effector cell population yet to be identified.

## INTRODUCTION

Peptide libraries displayed on filamentous phages have proven to be powerful tools to define specific epitopes for mAbs, polyclonal sera, or receptor molecules on various cell types [1-4]. Phage display-derived peptides isolated by affinity selection from linear or circular libraries are often called mimotopes, mainly because they show significant sequence divergence from the native antigens and only mimic their conformation [5,6].

Peptide mimotopes are of considerable interest because of their potential use in vaccine development. Upon immunization, mimotopes have been shown to induce an antigen-specific immune response directed against the epitope recognized by the mAb used for affinity selection of phage clones [7,8]. Mimotope immunizations could therefore be a novel way to induce epitope-specific Ab responses *in vivo* especially when the original antigen is unknown or induces Ab of undesired specificity. However, there are limited data on whether anti-mimotope Ab so derived can be effective against tumor cells expressing the original antigen and less is known about the mechanisms of their anti-tumor activity.

Antibody-mediated effector mechanisms against tumor cells, of which the activity has been shown *in vitro*, are ADCMC [9,10] and ADCC [11,12]. The presence, of infiltrating NK cells, macrophages, and complement deposits in tumors removed from mAb-treated patient, suggests that both ADCMC and ADCC may play a role in tumor cell destruction *in vivo* [13,14]. However, as many tumor cells express increased amounts of complement-inhibiting regulators which protect them against lysis by autologous complement [15,16], the main anti-tumor mechanism of therapeutic antibodies *in vivo* is considered to be mediated by ADCC [17].

BCD-F9 is a murine mAb (IgG2a) which recognizes an antigen present on the surface of many tumor cell lines and in 100% of breast cancer biopsies [18]. BCD-F9 also reacts with an integral membrane glycoprotein highly expressed on colon, ovary, and lung carcinomas. Radiolabeled BCD-F9 was successfully used for the detection of axillary lymph node metastasis in over 30 breast cancer patients with minimal cancer [19]. Recent findings in a nude xenograft mouse model have shown that BCD-F9, when

administrated i.v. is able to reduce growth and metastasis of human HT-1080 tumor cells (\*). Because of the ability of BCD-F9 to recognize a wide variety of neoplastic cell lines as opposed to normal tissues, this mAb could potentially be used for killing tumor cells.

We have previously shown that a peptide mimic of the tumor antigen recognized by the BCD-F9 mAb can induce antibodies (AM-F9) that react with the HT-1080 tumor cell line and prolong the life span of mice inoculated i.v. with HT-1080 cells [20]. The objectives of the present study were to evaluate the capacity of anti-mimotope antibodies AM-F9 to inhibit the subcutaneous growth of HT-1080 tumor cells in nude mice, and to determine the polyclonal anti-mimotope antibody capacity to induce ADCMC and ADCC by NK cells or macrophages. We report that the polyclonal anti-mimotope antibodies, AM-F9, significantly reduced tumor cell growth in vivo. AM-F9 is efficient in both complement-mediated and NK cell-mediated killing of HT-1080 tumor cells in vitro. However, because of the lack of effect of NK cell removal by anti-asialo GM1, ADCC mediated by NK cells does not appear to contribute to the reduced tumor growth observed in vivo. Whether the therapeutic effect of AM-F9 depends only on ADCMC or may involve ADCC by other effector cell populations is discussed.

---

\* Popkov, M., Sidrac-Ghali, S., Lusignan, Y., Lemieux, S., and Mandeville, R. Inhibition of Tumor Growth and Metastasis of Human Fibrosarcoma Cells HT-1080 by Monoclonal Antibody BCD-F9. Submitted for publication.

## RESULTS

*Anti-tumor activity of AM-F9.* We have recently shown that the peptide GRRPGGWWMR, which was selected from a random decapeptide phage library that mimics a conformational epitope found on tumor cells, induces rabbit antiserum AM-F9 that is specific for tumor cells [20]. To evaluate the efficacy of AM-F9 in mediating anti-tumor activity, CD-1 nude mice were injected s.c. on day 0 with  $3 \times 10^6$  HT-1080 cells into the right flank, followed by 10 i.v. injections of the AM-F9 antiserum. Control animals were injected with pre-immune serum. The mean tumor size was monitored daily in all mice starting at day 9 post-inoculation (first sign of tumor growth) until sacrifice (day 30). Tumors grew very rapidly; however, at day 12, we observed a reduced growth rate in the AM-F9-treated group as compared to control group. As depicted in Figure 4.1, treatment of HT-1080 tumor-bearing mice with the AM-F9 antiserum resulted in a significantly lower mean tumor size compared with the control group treated with rabbit pre-immune serum ( $p < 0.01$ , versus control from days 15 to 30). On day 15, in all AM-F9-treated mice, clear signs of tumor necrosis were visible at the tumor center. This area was surrounded by a rim of viable tumor cell mass. Tumor necrosis persisted until animal sacrifice but these tumors did not disappear completely. Signs of necrosis were totally absent in the control group. On day 30 after tumor cell inoculation, mean tumor weights in the experimental and in the control groups were  $0.46 \pm 0.1$  g and  $1.16 \pm 0.22$  g, respectively demonstrating a 60% reduction in tumor growth in the AM-F9 treated group ( $p < 0.001$  versus control). This finding suggests that the anti-tumor activity of AM-F9 was not a nonspecific effect due to the administration of a rabbit serum. Throughout the observation period, side effects such as loss of body weight and moribundity were not observed in all groups of animals.

*Complement-mediated cytotoxicity by AM-F9.* Two of the potential effector mechanisms (ADCMC and ADCC) that could mediate the anti-tumor activity of AM-F9 were investigated in vitro. We first examined the ability of AM-F9 to mediate ADCMC of HT-1080 human fibrosarcoma cells. As shown in Figure 4.2, rabbit AM-F9 polyclonal antiserum and the BCD-F9 mAb (used as a positive control) induced significant complement-dependent lysis of HT-1080 cells. In the absence of complement, neither

BCD-F9 nor AM-F9 could induce lysis of HT-1080 cells at all the antibody concentrations tested (data not shown).

*Phenotypic characterization and control of cytotoxic activity of splenic NK cells.*

NK-enriched spleen cells from CD-1 or CD-1 nude mice were analyzed by flow cytometry after labeling with biotin-conjugated anti-NK1.1 mAb and FITC-conjugated anti-TCR $\alpha\beta$  mAb. As shown in Figure 4.3, the majority of NK cells enriched from the spleen of CD-1 mice express NK1.1 (82%). Low expression of TCR $\alpha\beta$  was detected on a small population of freshly harvested NK1.1<sup>+</sup> cells, corresponding to the recently discovered NKT cell population mostly constituted of CD4<sup>-</sup>CD8<sup>-</sup> and CD4<sup>+</sup>CD8<sup>-</sup> cells [21]. In the spleen, the size of the CD4<sup>+</sup>CD8<sup>-</sup> cell subset is three times less than double negative CD4<sup>-</sup>CD8<sup>-</sup> cells [22]. Therefore, even though CD4<sup>+</sup>CD8<sup>-</sup> NKT cells are expected to have been depleted along with T cells during the NK cell enrichment procedure, the residual CD4<sup>-</sup>CD8<sup>-</sup> NKT cells remain in sufficient number and they should have been enriched with NK cells. TCR $\alpha\beta$  was also detected on a small population of NK cells isolated from CD-1 nude mice. This is an unexpected finding since nude mice have been shown not to express NKT cells [23]. Even more surprising was the fact that NK1.1 was not detected on NK cells in CD-1 nude mice (Fig. 4.3).

In order to evaluate whether the NK cell phenotype would change after stimulation, NK-enriched spleen cells from normal and nude CD-1 mice were incubated for 5 days with IL-2. Equivalent numbers of LAK cells were harvested from cultures of both normal and nude NK cell suspensions (data not shown). Flow cytometry analysis revealed that in the cell suspension from normal CD-1 mice, the growth of NK1.1<sup>+</sup> cells was preferentially stimulated as their numbers increased from 82% to 95%. However, when NK-enriched spleen cells from nude mice were incubated with IL-2, the expression of NK1.1 was not induced on these cells. At the same time, a loss of TCR $\alpha\beta$ <sup>+</sup> cells was observed in suspensions from both mouse strains.

Having observed that NK and LAK cells from normal and nude mice do not share similar phenotypic characteristics, it was of interest to compare the efficacy of these cell subsets in mediating target cell lysis. The capacity of NK and LAK cells from normal and nude CD-1 mice to lyse HT-1080 target cells was thus tested (Fig. 4.4). Even though both NK cell suspensions were efficient in lysing susceptible YAC-1 target cells, normal NK

cells were undoubtedly more lytic than nude NK cells (Fig. 4.4A). Unstimulated NK cells from normal and nude CD-1 mice were unable to lyse HT-1080 target cells, but both LAK cell suspensions were active in lysing the same target cells (Fig. 4.4A and B). These results indicate that nylon wool-filtered populations of cells harvested from the spleen of nude CD-1 mice indeed contain LAK cell precursors, thus NK cells, although their percentage in the suspension remained unknown.

*Antibody-dependent cellular cytotoxicity by AM-F9.* ADCC experiments with splenic NK cells and peritoneal cells from nude mice were performed using both AM-F9 and BCD-F9-coated HT-1080 cells at effector-target ratios (E:T) of 6.25, 12.5, and 25:1. In all experiments, the increase of E:T ratios enhanced tumor cell killing (Fig. 4.5). These results indicate that both AM-F9 and BCD-F9 could induce NK and peritoneal cell-mediated killing of HT-1080 tumor cells, although the percentage of lysis obtained with peritoneal cells was lower for AM-F9 than for BCD-F9 (Fig. 4.5B). Splenic NK cell-mediated ADCC with AM-F9 and with BCD-F9 was equivalent, however, in this experiment splenic NK cells showed higher spontaneous (i.e. Ab-independent) cytotoxic activity than peritoneal cells (Fig. 4.5A).

Peritoneal cell fractions, either depleted or enriched in plastic-adherent macrophages, were used as effector cells against AM-F9-coated HT-1080 cells. The labeling with F4/80 mAb confirmed that the percentages of macrophages was enriched in the adherent cell fraction and that the non-adherent cell fraction recovered contains a mixture of F4/80<sup>-</sup> and F4/80<sup>+</sup> cells (Fig. 4.6). Results shown in Figure 4.7 indicate that AM-F9 could trigger lysis of HT-1080 target cells by any peritoneal cell fraction. However, the percentage of lysis obtained with unfractionated cells was lower than with non-adherent cells, possibly due to macrophage depletion in the non-adherent cell fraction. Macrophage-rich effectors exerted only weak anti-tumor AM-F9-dependent cytotoxicity.

*Effect of NK cell-depletion on anti-tumor activity of AM-F9.* In vitro experiments reported in the above sections suggested that NK cells could be the major effectors in the mediation of AM-F9-dependent cytotoxicity towards HT-1080 tumor cells. To evaluate the contribution of this mechanism to the in vivo anti-tumor activity of AM-F9, NK-cell-depleted animals were used. Our results show that depletion of NK cells did not abrogate

the protective activity of AM-F9 antiserum. Furthermore, the reduced growth rate of HT-1080 tumors in AM-F9-treated mice was even more pronounced in mice inoculated with rabbit anti-asialo GM1 antiserum (Fig. 4.8). The absence of asialo GM1 on HT-1080 cells was confirmed in flow cytometry assays under conditions where this molecule was detected on 90% of NK-enriched spleen cells. Furthermore, unlike NK cells, HT-1080 cells were totally resistant to killing when incubated with anti-asialo GM1 antiserum and guinea pig or mouse complement (data non shown). At necropsy, tumor weights determined on day 33 after tumor cell inoculation in the groups treated with AM-F9, anti-asialo GM1/AM-F9, and pre-immune serum were  $0.57 \pm 0.14$  g,  $0.33 \pm 0.08$  g, and  $1.40 \pm 0.37$  g respectively, leading to a 59% and 76% reduction in tumor growth during AM-F9 and anti-asialo GM1/AM-F9 treatments ( $p < 0.01$  and  $p < 0.001$  versus control, respectively). Anti-asialo GM1/AM-F9 treatment significantly reduced the weight of the tumors not only when compared to controls, but also with tumors from AM-F9 treated mice ( $p < 0.01$ ). This finding excludes NK cell-mediated ADCC as a major mechanism of anti-tumor activity of AM-F9 in vivo.

## DISCUSSION

In a previous study, we described the generation of rabbit anti-mimotope antiserum AM-F9 by immunization with the synthetic peptide (GRRPGGWWMR) selected from a decapeptide phage display library using the BCD-F9 mAb. We also demonstrated that AM-F9 inhibited the binding of BCD-F9 to the HT-1080 human fibrosarcoma cells and prolonged the life span of CD-1 nude mice injected i.v. with HT-1080 [20]. The properties of AM-F9 were further investigated in the present study. It was found that (a) treatment with AM-F9 significantly inhibited the growth of HT-1080 tumor cells inoculated s.c. into CD-1 nude mice, (b) AM-F9 elicited ADCC by both splenic NK cells and peritoneal cells, (c) AM-F9 mediated complement-dependent cytotoxicity, and (d) the in vivo depletion of NK cells did not abrogate the protective activity of AM-F9 in this experimental animal model. These properties of AM-F9 antibodies are of importance mainly because they suggest that anti-mimotope antiserum may be a potential immunotherapeutic agent.

The use of experimental animal models to study treatment of established tumors with antibodies is not ideal. For efficient tumor take in our model, mice were inoculated with high numbers of cells using an aggressively growing tumor HT-1080. In this model, within a month, tumors reach about 1.2 g; this is approximately 1/15 of the total weight of the mice. This type of aggressiveness is seldom observed in humans and mean tumor growth rates in this model are clearly different from those observed in cancer patients. This accelerated growth rate might overwhelm the host defense system, such as ADCMC and ADCC. However, in CD-1 nude mice the immunologic defect is limited to T lymphocytes; accordingly, NK cells and macrophage functions including the capacity to mediate ADCC are intact [24,25]. Therefore, both effector cell populations could contribute to tumor cell lysis in our experimental model.

Because macrophage and NK cell depletion severely abrogates mAb-mediated lysis of xenograft tumor uptake in nude mice, it is a general agreement that the major mechanism of tumor eradication by antibodies is through ADCC [11,26]. Although AM-F9 antiserum elicited ADCC by murine effector cells in vitro, it is rather an unexpected finding that depletion of NK cells did not increase tumor growth in vivo. This



observation may suggest an important role for non-NK cells in the induction or enhancement of ADCC, probably because of the release of promoting cytokines [27,28]. For example, the ability of normal neutrophils, which express various FcγR on their cell surface, to exert ADCC towards certain human tumor cells is well-documented [29-31]. It has also been shown that in vitro IFN-γ-activated neutrophils as well as neutrophils derived from patients treated with G-CSF efficiently kill tumor cells by ADCC through inducible FcγRI [32-34]. Our in vivo experimental conditions do not exclude that IFN-γ and/or G-CSF-activated neutrophils might be used, through FcγRI recruitment by AM-F9 antibodies, as effector cells for immune intervention.

Another possible mechanism of cytotoxicity in a xenograft model is complement activation. Autologous cells are usually not killed by complement since they express complement down-regulating factors [15,35]. However, xenografted human cells lack inhibitors of murine complement; this property would therefore allow ADCMC upon treatment with antibodies in the mouse. The strong complement cytotoxicity of AM-F9 as well as the depletion studies of NK cells are consistent with the anti-tumor effects of this antiserum in vivo being by a complement-dependent mechanism.

It is also possible that AM-F9 could enhance the tumoricidal properties of effector cells through unknown mechanisms different from the tested ADCC and ADCMC. It is well documented that NK1.1<sup>+</sup> T cells could mediate anti-tumor effects under certain experimental conditions [36-38]. However, the number NK1.1<sup>+</sup> T cells are very low in nude mice; moreover, these cells demonstrate low expression of CD16 in the absence of activation [39,40]. These observations suggest that the population of NK1.1<sup>+</sup> T cells may contribute very little to AM-F9-dependent cell-mediated killing of HT-1080 tumor cells in this model. On the other hand, it is also possible that the NK1.1<sup>+</sup> T cell population may have expanded in tumor-bearing mice as a consequence of IL-12 production by antigen-presenting cells, such as macrophages or dendritic cells, activated by antibody-coated tumor cells. It has been previously shown that the presence of IL-12 in the environment of NK1.1<sup>+</sup> T cells induces these cells to produce IFN-γ [41] that could act as a killing factor. Such a mechanism was recently reported to participate in the control of the growth of solid tumors [42]. Therefore, NK1.1<sup>+</sup> T cells remain a putative effector cell population in our experimental model. It is also possible that NK cells and NK1.1<sup>+</sup> T cells affect

each other and that activation of NK1.1<sup>+</sup> T cells may be enhanced in the absence of NK cells (anti-asialo GM1 depletion).

Furthermore, data generated in a nude mouse model could possibly underestimate or overestimate what may be achieved with this antibody in humans. The use of nude mice, necessary to avoid rejection of human cells, does not allow for a direct interaction of the injected antibodies with all the effectors of an intact immune system. For example, no anti-idiotypic antibody response is expected to be generated in a nude mouse model, which might also be correlated with the clinical outcome [43]. Finally, in the ADCC assay human effector cells are more cytotoxic to human tumor cells than those of nude mice, suggesting that eradication of human xenografts from mice is biased by species differences [44]. Accordingly, there are several limitations inherent to the nude mouse xenograft model: nevertheless, this experimental animal model has provided a functional system in order to elucidate some of the *in vivo* anti-tumor properties of the AM-F9 anti-mimotope antibody.

## MATERIAL AND METHODS

**Antibodies.** The AM-F9 rabbit anti-mimotope antiserum was produced as previously described [20]. The anti-asialo GM1 antiserum was purchased from Wako (Richmond, VA). The mAb BCD-F9 was obtained from the fusion of NS-1 myeloma cells with spleen cells from BALB/c mice hyperimmunized with human breast carcinoma cell line BT-20 [18]. Hybridomas producing anti-NK1.1 (mouse IgG2a, clone PK136), anti-TCR $\alpha\beta$  (hamster IgG), anti-CD8 (rat IgG2a), anti-CD24 (rat IgG2b, clone M1/69), and anti-macrophage (rat IgG2b, clone F4/80) mAbs were purchased from the American Type Culture Collection (ATCC, Rockville, MD). Hybridoma producing anti-CD4 (rat IgG2b) was kindly provided by Dr. E.F. Potworowski (INRS – Institut Armand-Frappier). All mAbs were purified on Protein G Sepharose column (Pharmacia Biotech, Baie d'Urfé, Quebec). The PK136 and F4/80 mAbs were biotinylated and anti-TCR $\alpha\beta$  was FITC-conjugated using conventional procedures described in Goding et al. [45]. FITC-labeled goat anti-rabbit IgG (Fc specific) and FITC-labeled goat anti-mouse IgG (Fc specific) antibodies were purchased from BIO/CAN Scientific (Mississauga, Ontario).

**Mice and tumor cells.** Five-week-old female CD-1 mice and age-matched athymic CD-1 nude mice were obtained from Charles River Canada (St-Constant, Quebec). The nude mice were maintained in sterilized cages under sterile filter top conditions and were handled in a laminar flow. Normal mice were kept under standard conditions. The human fibrosarcoma cell line HT-1080 was purchased from ATCC and maintained in DMEM supplemented with 10% Fetal Bovine Serum (Canadian Life, Burlington, Ontario). The YAC-1 cell line, a mouse lymphoma of A/Sn origin also purchased from ATCC, was maintained in RPMI 1640 medium supplemented with 10% FBS, 100 U/ml Penicillin, 100  $\mu$ g/ml Streptomycin, and 25 mM HEPES (thereafter indicated as complete medium). Cells were grown at 37°C in a humidified 5% CO<sub>2</sub> atmosphere. When used as targets in cytotoxicity assays, 3 x 10<sup>6</sup> HT-1080 or YAC-1 cells were labeled with 150  $\mu$ Ci of Na<sub>2</sub><sup>51</sup>CrO<sub>4</sub> (ICN Biomedical, Costa Mesa, CA) for 1 h and washed 4 times before mixing with effector cells.

**In vivo tumor growth.** The cultured HT-1080 cells were harvested with PBS containing 0.5 mM EDTA. Fractions containing over 95% of viable cells as assessed with Trypan Blue were used in this study. Six-week old CD-1 nude mice were inoculated s.c. into the right flanks with  $3 \times 10^6$  cells in 0.2 ml of PBS on day 0. Treated and control mice were injected i.v. with 0.2 ml of AM-F9 antiserum or rabbit pre-immune serum diluted 1:2 in PBS on day 1-4, 7-10, and 13-14. One group of AM-F9-treated mice was depleted of NK cells by injecting i.p. 50  $\mu$ l of rabbit anti-asialo GM1 antiserum (diluted in 0.2 ml of PBS) 1 day prior to tumor cell inoculation and thereafter on day 5, 10, and 15. Tumor growth was monitored daily by measuring tumor size over the skin in two dimensions using a slide caliper. Tumor volume was calculated according to the formula:  $(\text{width})^2 \times \text{length}/2$ .

**Effector cells preparation.** Splenic NK cells were enriched by negative selection according to a previously described procedure [46]. Briefly: spleen cells from normal mice were depleted of erythrocytes by osmotic shock, filtered twice through a nylon wool column (Fisher Scientific, Montreal, Quebec) and then depleted of T cells and residual non-NK cells using a mixture of rat anti-CD4, anti-CD8 and anti-CD24 (Heat Stable Antigen) mAbs and sheep anti-rat IgG-coated magnetic beads (Dynal Inc, Great Neck, NY). Splenic NK cells from nude mice were enriched by a single filtration through a nylon wool column. For the production of LAK cells, NK-enriched cells at  $1 \times 10^6$  cells/ml were cultured for 5 days at 37°C in a humidified 5% CO<sub>2</sub> atmosphere in complete RPMI 1640 medium supplemented with 300 U/ml of mouse recombinant IL-2 (Roche Diagnostics, Laval, Quebec) and 50 mM 2-Mercaptoethanol (Fisher Scientific, Montreal, Quebec). For macrophage-mediated cytotoxicity, effector cells were thioglycollate-elicited peritoneal exudate cells harvested from CD-1 nude mice. The macrophage-rich fraction was separated by adherence to plastic culture flask for 1 h at 37°C and subsequent detachment [47]. Accordingly, non-adherent cells represented a macrophage-depleted fraction of peritoneal cells.

**Cell cytotoxicity assays.** Susceptibility of HT-1080 tumor cells to lysis by NK-enriched spleen cells or LAK cells was measured at different effector:target ratios in a standard <sup>51</sup>Cr-release assay using radiolabeled YAC-1 cells as control targets. Briefly, different concentrations of effector cells in 100  $\mu$ l of complete medium were distributed

in quadruplicate into U-bottomed 96-well microtiter plates and then 100  $\mu$ l of radiolabeled target cells ( $1 \times 10^5$ /ml) were added. After 4 h incubation of the co-cultures at 37°C in a 5% CO<sub>2</sub> humidified atmosphere, the plates were centrifuged for 5 min at 250 x g and culture supernatants were harvested using the Titertek Supernatant Collection System (Skatron, Oslo, Norway). Radioactivity was measured in a Beckman 7000 gamma counter. Specific lysis (%) was calculated using the following formula:

$$\% \text{ specific lysis} = \frac{\text{cpm (test)} - \text{cpm (spontaneous)}}{\text{cpm(max)} - \text{cpm (spontaneous)}} \times 100$$

in which the spontaneous release (12-17%) was measured by incubating radiolabeled cells in the absence of effector cells and the maximum release was obtained by incubating radiolabeled cells with 1% Triton X100.

For ADCC, 50  $\mu$ l of radiolabeled HT-1080 tumor cells ( $2 \times 10^5$ /ml) were distributed in triplicate into U-bottomed 96-well microtiter plates and incubated for 1 h at 37°C with 12.5  $\mu$ g/ml of protein G-purified AM-F9 or BCD-F9. Then, 100  $\mu$ l of various concentrations of murine effector cells were prepared as described above and added to each well. The plates were then incubated in a CO<sub>2</sub> incubator at 37°C for 8 h, and the radioactivity released in the supernatant determined with a gamma counter. The percent specific lysis was calculated as described above.

For ADCMC, 50  $\mu$ l of radiolabeled HT-1080 tumor cells ( $2 \times 10^5$ /ml) and 50  $\mu$ l of various concentrations of protein G-purified AM-F9 antibodies, BCD-F9 mAb, or 50  $\mu$ l of 1:50 dilution of anti-asialo GM1 antibodies were distributed in triplicate into U-bottomed 96-well microtiter plates, and then 100  $\mu$ l of Low-Tox guinea pig complement (Cedarlane, Hornby, Ontario) diluted 1:5 in DMEM was added to each well. The plates were incubated in a CO<sub>2</sub> incubator at 37°C for 45 min, and the radioactivity released in the supernatant determined in a gamma counter. The specific lysis (%) was calculated as described above.

**Flow cytometry analysis.** NK and LAK cells from normal and nude mice were labeled with FITC-conjugated anti-mouse TCR $\alpha\beta$  and biotin-conjugated anti-NK1.1 (PK136). Biotin-conjugated F4/80 mAb was used for the evaluation of the percentage of macrophages in thioglycollate-elicited peritoneal cell suspensions. Binding of biotinylated mAbs was detected with phycoerythrin-labeled Streptavidin (Beckton

Dickinson, Mountain View, CA). Lymphocytic and monocytic cell populations gated on the basis of forward and side scatter parameters were analyzed on a Epics XL-MCL flow cytometer (Coulter, Hialeah, FL) equipped with a 488 nm argon laser. Data analysis based on collection of 10 000 events/sample was performed using XL software.

**Statistical analysis.** Unpaired two-tailed Student's *t*-test was performed using INSTAT software. A *p*-value of  $< 0.05$  was considered significant.

## ACKNOWLEDGEMENTS

The authors thank Michel Houde, BIOPHAGE Inc., for critical reading of the manuscript and Marie Desy, INRS-Institut Armand-Frappier, for statistical analysis.

## REFERENCES

1. Yayon, A., D. Aviezer, M. Safran, J. L. Gross, Y. Heldman, S. Cabilly, D. Givol, and E. Katchalski-Katzir. 1993. "Isolation of peptides that inhibit binding of basic fibroblast growth factor to its receptor from a random phage-epitope library". Proc. Natl. Acad. Sci. USA, vol. 90, p. 10643-10647.
2. Cortese, R., F. Felici, G. Galfré, A. Luzzago, P. Monaci, and A. Nicosia. 1994. "Epitope discovery using peptide libraries displayed on phage". Tibtech, vol. 12, p. 262-267.
3. Dybwad, A., B. Bogen, J. B. Natvig, O. Forre, and M. Sioud. 1995. "Peptide phage libraries can be an efficient tool for identifying antibody ligands for polyclonal antisera". Clin. Exp. Immunol., vol. 102, p. 438-442.
4. Pasqualini, R., and E. Ruolahti. 1996. "Organ targeting in vivo using phage display peptide libraries". Nature, vol. 380, p. 364-366.
5. Hoess, R. H., A. J. Mack, H. Walton, and T. M. Reilly. 1994. "Identification of a structural epitope by using a peptide library displayed on filamentous bacteriophage". J. Immunol., vol. 153, p. 724-729.
6. Zhong, G., G. P. Smith, J. Berry, and R. C. Brunham. 1994. "Conformational mimicry of a chlamydial neutralization epitope on filamentous phage". J. Biol. Chem., vol. 269, p. 24183-24188.
7. Stoute, J. A., W. R. Ballou, N. Kolodny, C. D. Deal, R. A. Wirtz, and L. E. Lindler. 1995. "Induction of humoral immune response against *Plasmodium falciparum* sporozoites by immunization with a synthetic peptide mimotope whose sequence was derived from screening a filamentous phage epitope library". Infect. Immun., vol. 63, p. 934-939.
8. Meola, A., P. Delmastro, P. Monaci, A. Luzzago, A. Nicosia, F. Felici, R. Cortese, and G. Galfré. 1995. "Derivation of vaccines from mimotopes. Immunologic properties of human hepatitis B virus surface antigen mimotopes displayed on filamentous phage". J. Immunol., vol. 154, p. 3162-3172.
9. Orlandi, R., M. Figini, A. Tomassetti, S. Canevari, and M. I. Colnaghi. 1992. "Characterization of a mouse-human chimeric antibody to a cancer-associated antigen". Int. J. Cancer, vol. 52, p. 588-593.
10. Velders, M. P., S. V. Litvinov, S. O. Warnaar, A. Gorter, G. J. Fleuren, V. R. Zurawski Jr, and L. R. Coney. 1994. "New chimeric anti-pancarcinoma monoclonal antibody with superior cytotoxicity-mediating potency". Cancer Res., vol. 54, p. 1753-1759.

11. Herlyn, D., and H. Koprowski. 1982. "IgG2a monoclonal antibodies inhibit human tumor growth through interaction with effector cells". Proc. Natl. Acad. Sci. USA, vol. 79, p. 4761-4765.
12. Steplewski, Z., L. K. Sun, C. W. Shearman, J. Ghayeb, P. Daddona, and H. Koprowski. 1988. "Biological activity of human-mouse IgG1, IgG2, IgG3 and IgG4 chimeric monoclonal antibodies with anti-tumor specificity". Proc. Natl. Acad. Sci. USA, vol. 85, p. 4852-4856.
13. Adams, D. O., T. Hall, Z. Steplewski, and H. Koprowski. 1984. "Tumors undergoing rejection induced by monoclonal antibodies of the IgG2a isotype contain increased numbers of macrophages activated for a distinctive form of antibody-dependent cytotoxicity". Proc. Natl. Acad. Sci. USA, vol. 81, p. 3506-3510.
14. Shetye, J., J. E. Frodin, B. Christensson, C. Grant, B. Jacobsson, S. Sundelius, M. Sylven, and H. Mallstedt. 1988. "Immunohistochemical monitoring of metastatic colorectal carcinoma in patients treated with monoclonal antibodies (Mab 17-1A)". Cancer Immunol. Immunother., vol. 27, p. 154-162.
15. Kumar, S., J. M. Vinci, B. A. Pytel, and C. Baglioni. 1993. "Expression of messenger RNAs for complement inhibitors in human tissues and tumors". Cancer Res., vol. 53, p. 348-353.
16. Gorter, A., V. T. Blok, W. H. B. Haasnoot, N. G. Ensink, M. R. Daha, and G. J. Fleuren. 1996. "Expression of CD46, CD55, and CD59 on renal tumor cell lines and their role in preventing complement-mediated tumor cell lysis". Lab. Invest., vol. 74, p. 1039-1049.
17. Velders, M. P., C. M. van Rhijn, E. Oskam, G. J. Fleuren, S. O. Warnaar, and S. V. Litvinov. 1998. "The impact of antigen density and antibody affinity on antibody-dependent cellular cytotoxicity: relevance for immunotherapy of carcinomas". Brit. J. Cancer, vol. 78, p. 478-483.
18. Mandeville, R., L. Giroux, J. Lecomte, J.-P. Chausseau, F. Dumas, I. Ajdukovic, I., D. Vidal, and F. Boury. 1987. "Production and characterization of monoclonal antibodies showing a different spectrum of reactivity to human breast tissue". Cancer Detect. Prev., vol. 10, p. 89-100.
19. Mandeville, R., C. Schatten, N. Pateisky, M.-J. Dicaire, B. Barbeau, and B. Grouix. 1989. "Immunolymphoscintigraphy with BCD-F9 monoclonal antibody and its F(ab')<sub>2</sub> fragments for the preoperative staging of breast cancers". In: R. L. Ceriani (ed.). Breast Cancer Immunodiagnosis and Immunotherapy, New York: Plenum Press, 203p.
20. Popkov, M., S. Sidrac-Ghali, V. Alakhov, and R. Mandeville. 2000. "Epitope-specific antibody response to HT-1080 fibrosarcoma cells by mimotope



- immunization". Clinical Cancer Res., vol. 6, p. 3629-3635.
21. Vicari, A. P. and A. Zlotnik. 1996. "Mouse NK1.1<sup>+</sup> T cells: a new family of T cells". Immunol. Today, vol. 17, p. 71-76.
  22. Watanabe H., C. Miyaji, Y. Kawachi, T. Iiai, K. Ohtsuka, T. Iwanaga, H. Takahashi-Iwanaga, and T. Abo. 1995. "Relationship between intermediate TCR cells and NK1.1<sup>+</sup> T cells in various immune organs. NK1.1<sup>+</sup> T cells are present within a population of intermediate TCR cells". J. Immunol., vol. 155, p. 2972-2983.
  23. Bendelac, A., M. N. Rivera, S.-H. Park, and J. H. Roark. 1997. "Mouse CD1-specific NK1 T cells: development, specificity, and function". Annu. Rev. Immunol., vol. 15, p. 535-562.
  24. Cheers, C. and R. Waller. 1975. "Activated macrophages in congenitally athymic nude mice and in lethally irradiated mice". J. Immunol., vol. 115, p. 844-847.
  25. Habu, S., H. Fukui, K. Shimamura, M. Kasai, Y. Nagai, K. Okumura, and N. Tamaoki. 1981. "In vivo effects of anti-asialo GM1. I. Reduction of NK activity and enhancement of transplanted tumor growth in nude mice". J. Immunol., vol. 127, p. 34-38.
  26. Eisenthal, A. and S. A. Rosenberg. 1989. "Systemic induction of cells mediating antibody-dependent cellular cytotoxicity following administration of interleukin 2". Cancer Res., vol. 49, p. 6953-6959.
  27. Vuist, W. M. J., M. J. W. Visseren, M. Otsen, K. Bos, F. A. Vyth-Dreese, C. G. Figdor, C. J. M. Melief, and A. Hekman. 1993. "Enhancement of the antibody-dependent cellular cytotoxicity of human peripheral blood lymphocytes with interleukin-2 and interferon  $\alpha$ ". Cancer Immunol. Immunother., vol. 36, p. 163-170.
  28. Ragnhammar, P. 1996. "Anti-tumoral effect of GM-CSF with or without cytokines and monoclonal antibodies in solid tumors". Med. Oncol., vol. 13, p. 167-176.
  29. Kushner, B. H. and N. K. V. Cheung. 1991. "Clinically effective monoclonal antibody 3F8 mediates nonoxidative lysis of human neuroectodermal tumor cells by polymorphonuclear leukocytes". Cancer Res., vol. 51, p. 4865-4870.
  30. Baldwin, G. C., G. Y. Chung, C. Kaslander, T. Esmail, R. A. Reinsfeld, and D. W. Golde. 1993. "Colony-stimulating factor enhancement of myeloid effector cell cytotoxicity toward neuroectodermal tumor cells". Br. J. Haematol., vol. 83, p. 545-553.

31. Ottonello, L., P. Morone, P. Dapino, and F. Dallegri. 1996. "Monoclonal Lym-1 antibody-dependent lysis of B-lymphoblastoid targets by human complement and cytokine-exposed mononuclear and neutrophilic polynuclear leukocytes". Blood, vol. 87, p. 5171-5178.
32. Perussia, B., M. Kobayashi, M. E. Rossi, I. Anegon, and G. Trinchieri. 1987. "Immune interferon enhances functional properties of human granulocytes: role of Fc receptors and effect of lymphotoxin, tumor necrosis factor, and granulocyte-macrophages colony-stimulating factor". J. Immunol., vol. 138, p. 765-774.
33. Valerius, T., R. Repp, T. P. M. de Wit, S. Berthold, E. Platzner, J. R. Kalden, M. Gramatzki, and J. G. J. van de Winkel. 1993. "Involvement of the high-affinity receptor for IgG (FcγRI; CD64) in enhanced tumor cell cytotoxicity of neutrophils during granulocyte colony-stimulating factor therapy". Blood, vol. 82, p. 931-939.
34. Michon, J., S. Moutel, J. Barbet, J.-L. Romet-Lemonne, Y. M. Deo, W. H. Fridman, and J. L. Teillaud. 1995. "In vitro killing of neublastoma cells by neutrophils derived from granulocyte colony-stimulating factor-treated cancer patients using an anti-disialoganglioside/anti-FcγRI bispecific antibody". Blood, vol. 86, p. 1124-1130.
35. Finberg, R. W., W. White, and A. Nicholson-Weller. 1992. "Decay-accelerating factor expression on either effector or target cells inhibits cytotoxicity by human natural killer cells". J. Immunol., vol. 149, p. 2055-2060.
36. Ballas, Z. K. and W. Rasmussen. 1993. "Lymphokine-activated killer cells. VII. IL-4 induces an NK1.1<sup>+</sup> CD8<sup>+</sup> αβ<sup>+</sup> TCR-αβ B220<sup>+</sup> lymphokine-activated killer subset". J. Immunol., vol. 150, p. 17-30.
37. Takeda, K. and G. Dennert. 1994. "Demonstration of MHC class I-specific cytolytic activity in IL-2-activated NK1<sup>+</sup> CD3<sup>+</sup> cells and evidence of usage of T and NK cell receptors". Transplantation, vol. 58, p. 496-504.
38. Smyth, M. J., K. Y. T. Thia, S. E. A. Street, E. Cretney, J. A. Trapani, M. Taniguchi, T. Kawano, S. B. Pelikan, N. Y. Crowe, and D. I. Godfrey. 2000. "Differential tumor surveillance by natural killer (NK) and NKT cells". J. Exp. Med., vol. 191, p. 661-668.
39. Sykes, M. 1990. "Unusual T cell populations in adult murine bone marrow. Prevalence of CD3<sup>+</sup>CD4<sup>-</sup>CD8<sup>-</sup> and αβTCR<sup>+</sup>NK1.1<sup>+</sup> cells". J. Immunol., vol. 145, p. 3209-3215.
40. Bendelac, A. 1995. Mouse NK1<sup>+</sup> T cells". Curr. Opin. Immunol., vol. 7, p. 367-374.
41. Leite-De-Moraes, M. C., G. Moreau, A. Arnould, F. Machavoine, C. Garcia, M.

- Papiernik, and M. Dy. 1998. "IL-4-producing NK T cells are biased towards IFN- $\gamma$  production by IL-12. Influence of the microenvironment on the functional capacities of NK T cells". Eur. J. Immunol., vol. 28, p. 1507-1515.
42. Kawamura, T., S. Seki, K. Takeda, J. Narita, Y. Ebe, M. Naito, H. Hiraide, and T. Abo. 1999. "Protective effect of NK1.1+ T cells as well as NK cells against intraperitoneal tumors in mice". Cell. Immunol., vol. 193, p. 219-225.
  43. Frodin, J. E., M. E. Faxas, B. Hagstrom, A. K. Lefvert, G. Masucci, B. Nilsson, M. Steinitz, P. Unger, and H. Mellstedt. 1991. "Induction of anti-idiotypic (ab2) and anti-anti-idiotypic (ab3) antibodies in patients treated with the mouse monoclonal antibody 17-1A (ab1): relation to the clinical outcome – an important anti-tumoral effector function?". Hybridoma, vol. 10, p. 421-431.
  44. Velders, M. P., C. M. van Rhijn, I. H. Briaire, G. J. Fleuren, S. O. Warnaar, and S. V. Litvinov. 1995. "Immunotherapy with low and high affinity monoclonal antibodies 17-1A and 323/A3 in a nude mouse xenograft carcinoma model". Cancer Res., vol. 55, p. 4398-4403.
  45. Goding, J. W. (ed.). 1986. Monoclonal Antibodies: Principles and Practice, San Diego: Academic Press, 241p.
  46. Depatie, C., A. Chalifour, C. Paré, S.-H. Lee, S. M. Vidal, and S. Lemieux. 1999. "Assessment of *Cmv1* candidates by genetic mapping and in vivo antibody depletion of NK cell subsets". Inter. Immunol., vol. 11, p. 1541-1551.
  47. Partridge, L. J. and I. Dransfield. 1993. "Isolation and characterization of mononuclear phagocytes". In: G. Gallagher, R. C. Rees, and Reynolds (eds.). Tumor Immunobiology. A Practical Approach, Oxford: Oxford University Press.

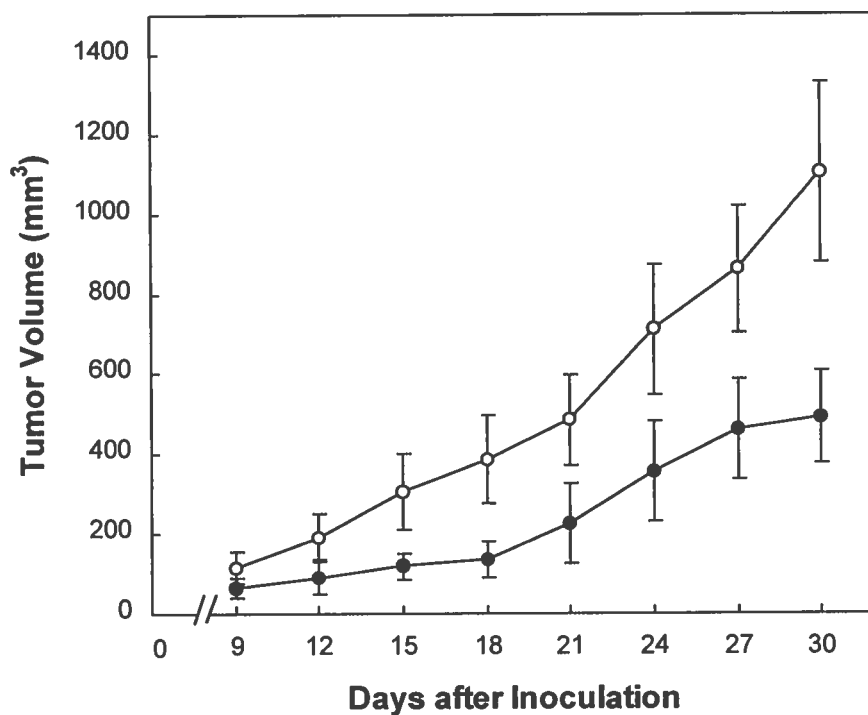


**Figure 4.1. Inhibition of Xenograft Tumor Growth in CD-1 Nude Mice Inoculated with AM-F9 Anti-Mimotope Antiserum.**

HT-1080 human tumor cells were grafted s.c. into CD-1 nude mice inoculated i.v. with rabbit pre-immune serum (○) or AM-F9 antiserum (●) according to a schedule described in Material and Methods. Results expressed as mean tumor volume  $\pm$  SD were calculated from five growing tumors/group measured at 3-day intervals from 9 to 30 days post-grafting.

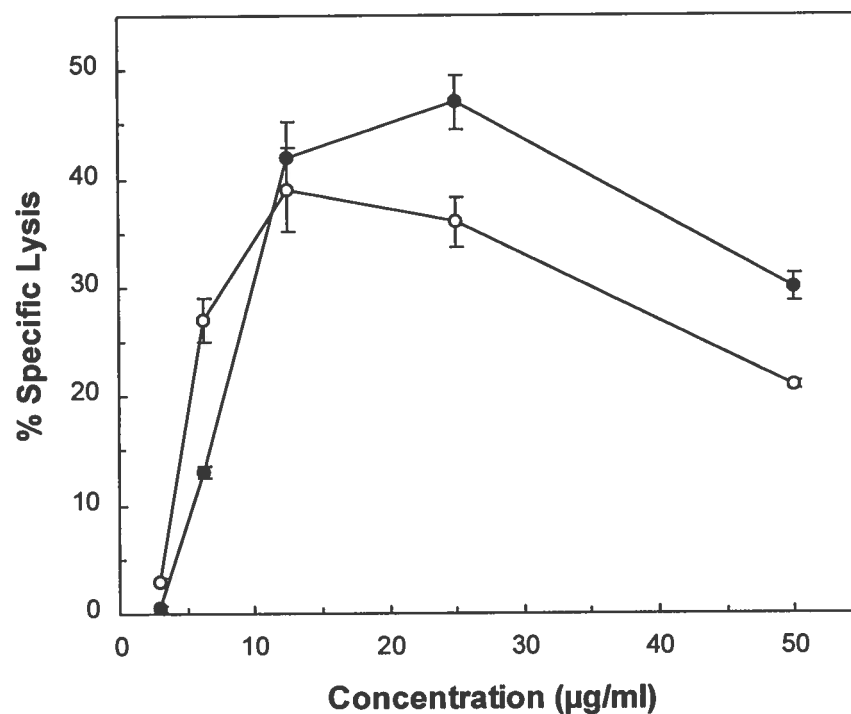


**Figure 4.2. Susceptibility of HT-1080 Cells to ADCMC.**

Lysis of radiolabeled tumor cells was measured in a  $^{51}\text{Cr}$ -release assay after cells were incubated for 45 min at 37°C with various concentrations of protein G-purified AM-F9 (●) or BCD-F9 (○) antibodies in the presence of guinea-pig complement. The values shown are means of triplicate samples  $\pm$  SD.

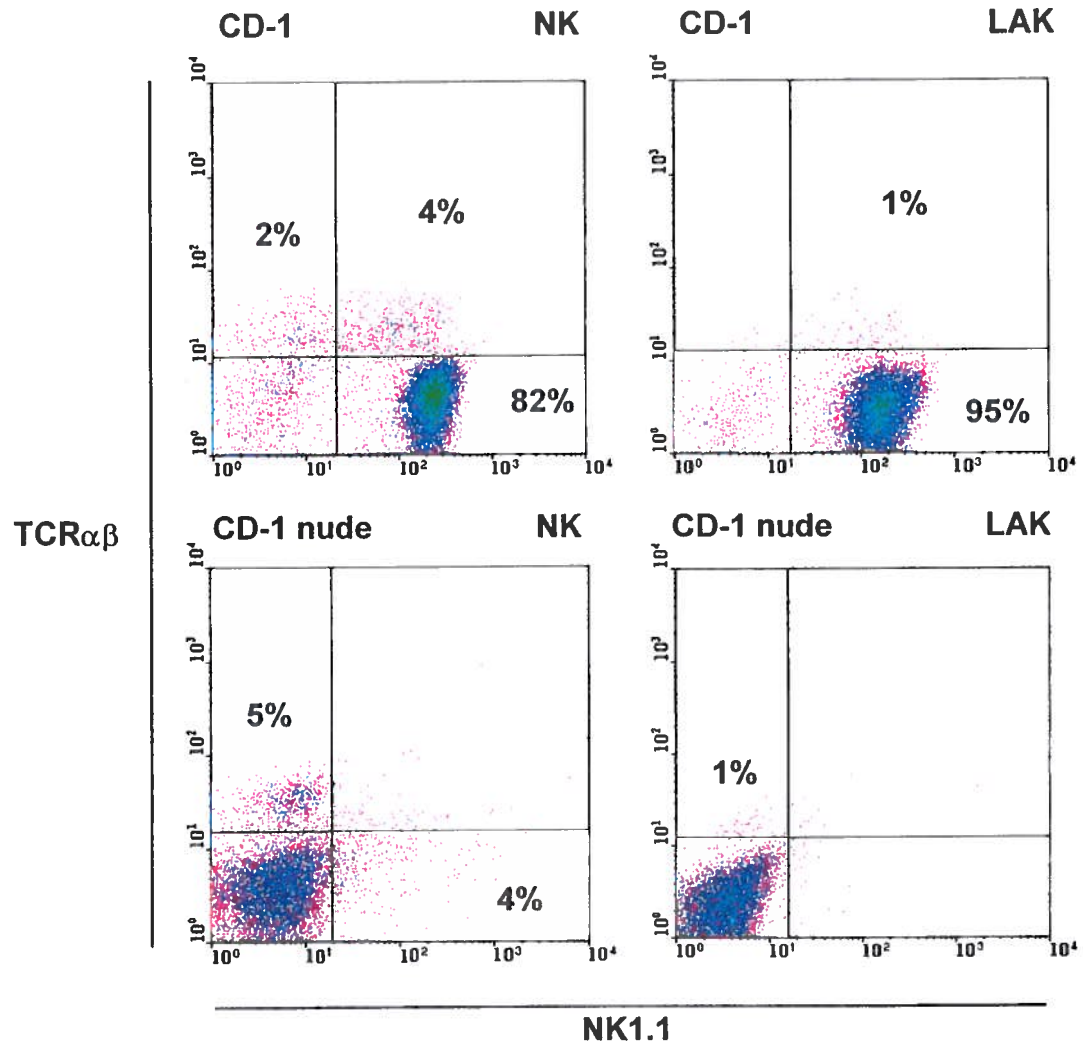


**Figure 4.3. Phenotypic Characterization of NK and LAK Cells from Normal and Athymic CD-1 Mice.**

NK-enriched spleen cells from 10-week old CD-1 mice and nylon-wool non-adherent spleen cells from age-matched CD-1 nude mice were stained for NK1.1 and TCR $\alpha\beta$  using a 2-color standard staining procedure. Cells were stained immediately after enrichment (NK) or after 5 days in culture in the presence of IL-2 (LAK). Numbers in the figure represent the percentage of stained cells in the corresponding quadrants.

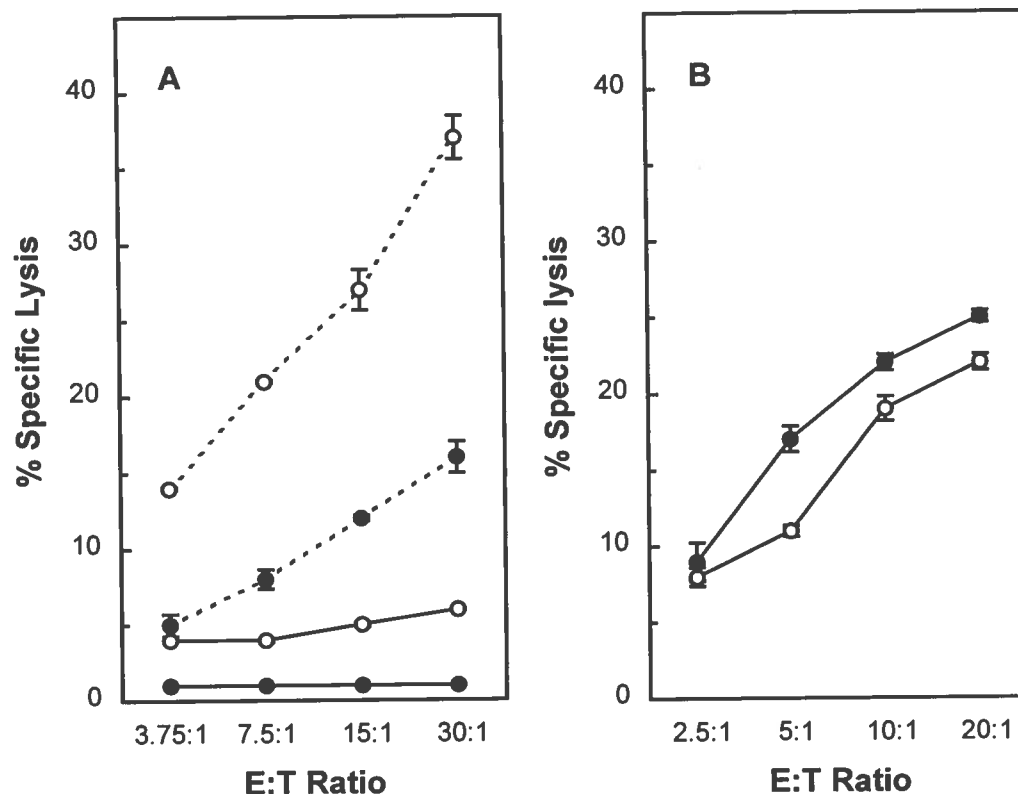


**Figure 4.4. Susceptibility of HT-1080 Cells to NK and LAK Cell-Mediated Lysis.**

Radiolabeled HT-1080 tumor cells (—) were used as targets in a standard  $^{51}\text{Cr}$ -release assay using as effector cells splenic NK (A) or LAK (B) cells from CD-1 (○) or CD-1 nude (●) mice. The radiolabeled YAC-1 prototypic target cell line (-----) was used to control NK cell activity in NK cell suspensions from normal and immunodeficient mice. The values shown are means of quadruplicate samples  $\pm$  SD containing cells at indicated E:T ratios.

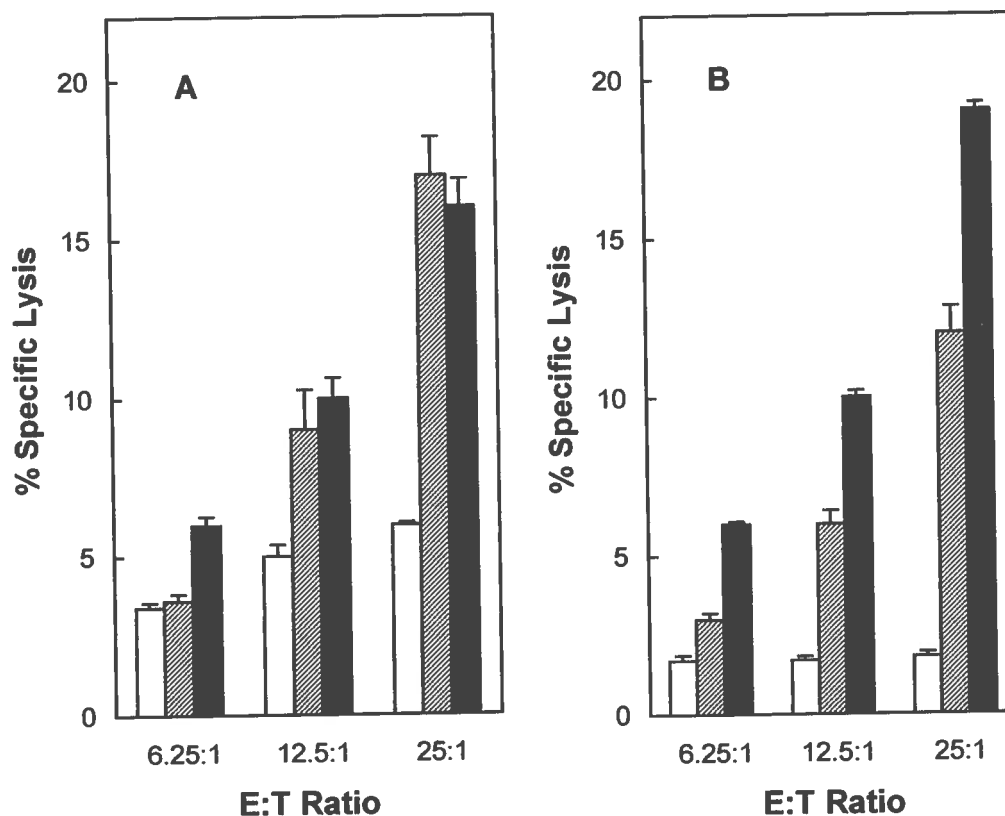


**Figure 4.5. Susceptibility of HT-1080 Tumor Cells to ADCC.**

The capacity of protein G-purified AM-F9 (hatched bars) or BCD-F9 (solid bars) antibodies to lyse radiolabeled HT-1080 tumor cells by ADCC was evaluated in a standard  $^{51}\text{Cr}$ -release assay using as effector cells (A) NK-enriched spleen cells or (B) thioglycollate-elicited peritoneal cells. Open bars in (A) and (B) show the resistance of HT-1080 target cells to lysis by splenic NK-enriched cells and unfractionated peritoneal cells in the absence of antibodies. The values shown are means of quadruplicate samples  $\pm$  SD containing cells at indicated E:T ratios.



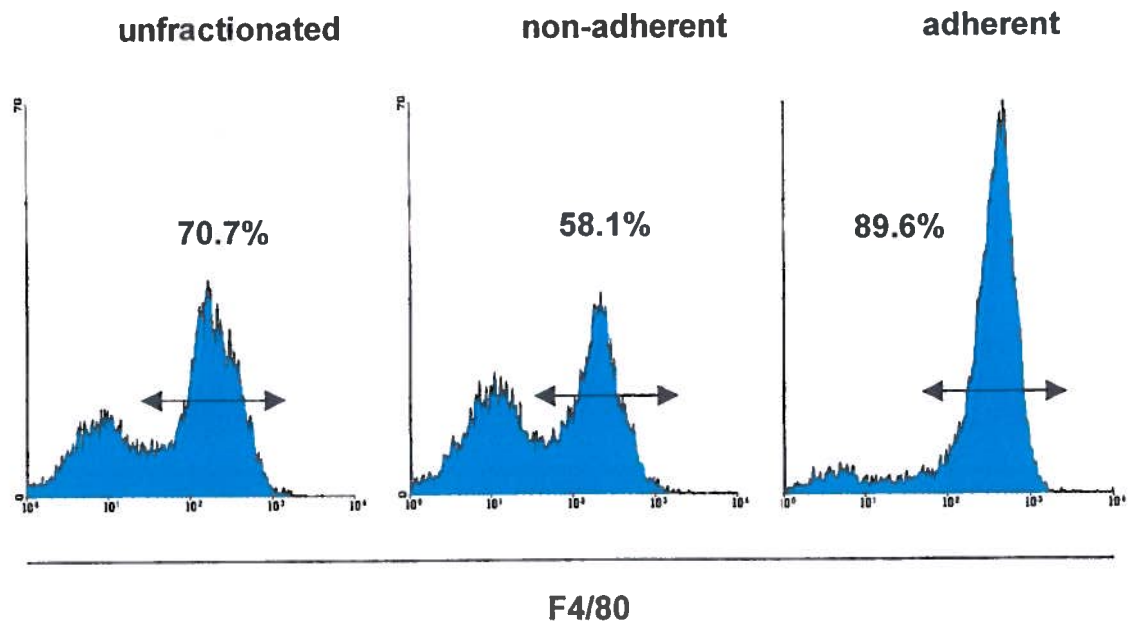


**Figure 4.6. Flow Cytometric Analysis of Thioglycollate-Elicited Peritoneal Cells.**

Macrophages in unfractionated, non-adherent, and adherent cell populations were identified by staining with F4/80 mAb.

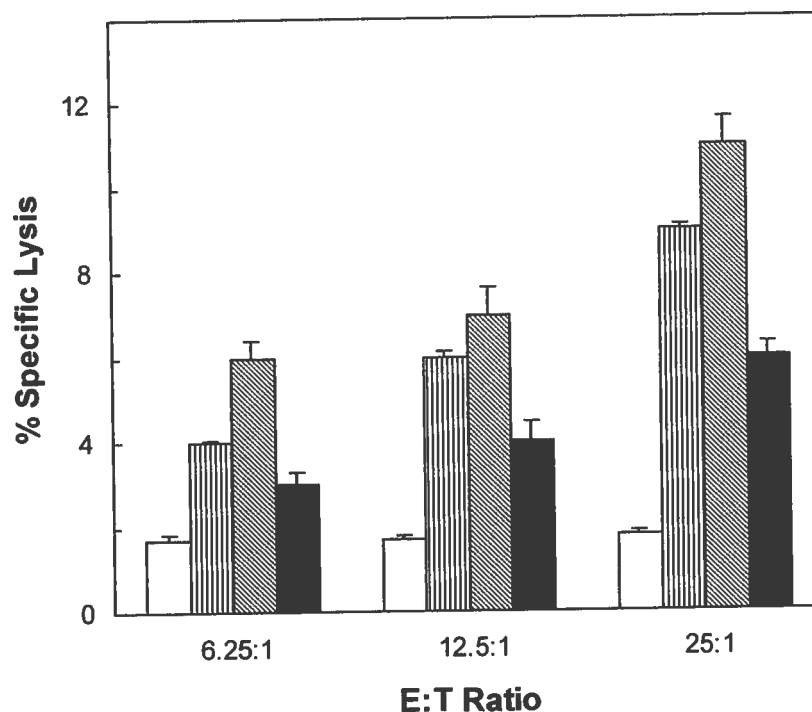


**Figure 4.7. Identification of Peritoneal Cells Mediating Antibody-Dependent Lysis of Tumor Targets.**

The capacity of protein G-purified AM-F9 antibodies to lyse radiolabeled HT-1080 tumor cells by ADCC was evaluated in a standard  $^{51}\text{Cr}$ -release assay using as effector cells thioglycollate-elicited peritoneal cells, either unfractionated (lined bars) or fractionated into non-adherent (hatched bars) and adherent (solid bars) cells. Open bars show the resistance of HT-1080 target cells to lysis by unfractionated peritoneal cells in the absence of AM-F9 antibodies. The values shown are means of quadruplicate samples  $\pm$  SD containing cells at indicated E:T ratios.

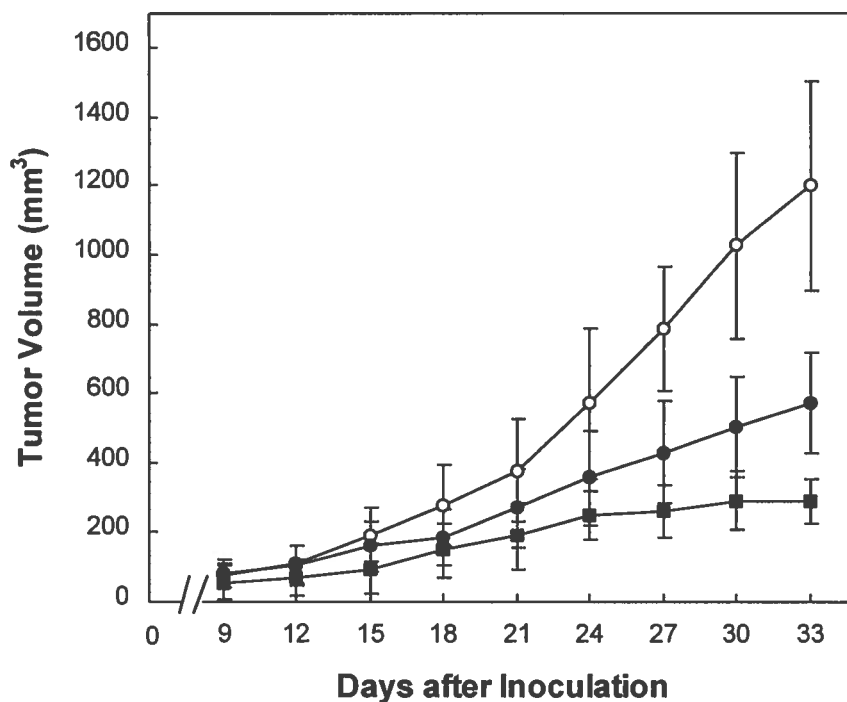


**Figure 4.8. Effect of NK Cell-Depletion on AM-F9-Mediated Inhibition of Xenograft Tumor Growth in CD-1 Nude Mice.**

One group of five CD-1 nude mice (■) were inoculated i.p. with 50  $\mu$ l of anti-asialo GM1 antiserum 1 day before and 5, 10 and 15 days after tumor grafting. These mice and another group of five mice (●) were then inoculated i.v. with AM-F9 antiserum according to the schedule described in Material and Methods. Control mice (○) were inoculated with rabbit pre-immune serum. Cultured HT-1080 were grafted s.c. in all mice on day 0. Tumor growth was followed over a 33-day period. Results are expressed as mean tumor volume  $\pm$  SD.

## **CHAPTER 5**

### **Multidrug Resistance Drug-Binding Peptides Generated by Using a Phage Display Library**

## RÉSUMÉ TRADUIT

Une banque de phages exprimant des décapeptides de manière aléatoire a été utilisée pour générer des ligands peptidiques pouvant se lier à des drogues MDR et ce, de manière à simuler l'activité de liaison de drogue de la P-glycoprotéine. Sept séquences peptidiques pouvant se lier spécifiquement à la doxorubicine ont été identifiées. Cinq de ces séquences contenaient la séquence canonique WXXW. Des essais de déplacement ont montré que les phages exprimant ces peptides se liaient aux drogues de type MDR (vinblastine, doxorubicine, verapamil et genistéine) avec la même sélectivité que la P-glycoprotéine; de plus, ces phages n'interagissaient pas avec des drogues de type non-MDR, telles que l'arabinosylcytosine (Ara-C) et le melphalan. Le peptide possédant la plus haute capacité de liaison (VCDWWGWGIC) a été synthétisé et a pu compétitionner avec le phage pour la liaison à la doxorubicine. Le modelage structurel suggère que toutes les séquences sélectionnées contiennent une enveloppe hydrophobique dans laquelle les drogues MDR peuvent se réfugier avec une substantielle minimisation d'énergie. Des tests d'immunobuvardage ont montré que l'anticorps monospécifique au phage exprimant VCDWWGWGIC pouvait spécifiquement reconnaître la P-glycoprotéine dans la fraction membranaire de cellules MCF-7ADR à phénotype MDR. Les séquences se liant aux drogues MDR que nous avons trouvées pourraient constituer un outil important pour le design et le criblage de nouveaux agents chimiothérapeutiques.

## Multidrug Resistance Drug-Binding Peptides Generated by Using a Phage Display Library

Mikhail Popkov<sup>1</sup>, Isabelle Lussier<sup>1</sup>, Viatcheslav Medvedkine<sup>2</sup>, Pierre-Olivier Estève<sup>1</sup>, Valery Alakhov<sup>1,3</sup>, and Rosemonde Mandeville<sup>1,4\*</sup>

<sup>1</sup>Institute Armand-Frappier, University of Quebec, 531 Blvd. des Prairies, Laval, QC, Canada H7N 4Z3

<sup>2</sup>Biotechnology Research Institute, 6100 Royalmount Avenue, Montreal, QC, Canada H4P 2R2

<sup>3</sup>Supratek Pharma Inc., c/o Institute Armand-Frappier, University of Quebec, 531 Blvd. des Prairies, Laval, QC, Canada H7N 4Z3

<sup>4</sup>BIOPHAGE Inc., c/o CQIB, 230 Bernard Belleau, Laval, QC, Canada H7V 4A9

**\*Corresponding author:** Rosemonde Mandeville

<sup>1</sup>Institute Armand-Frappier, University of Quebec

531 Blvd. des Prairies, Laval, QC, Canada H7N 4Z3

E-mail: Rosemonde Mandeville @ IAF.UQUEBEC.ca

Tel.: (514) 687-5010; Fax: (514) 686-5617;

**Subdivision:** Molecular cell biology and metabolism.

### Abbreviations

MDR, multidrug resistance

ABC, ATP-binding cassette

TM, transmembrane

### Enzymes

Peroxidase (EC 1.11.1.7)

Published in European Journal of Biochemistry, 1998, vol. 251, p. 155-163.

## SUMMARY

A phage display library of random decapeptides was used to generate peptide ligands that can bind MDR drugs mimicking, in this respect, the drug binding activity of P-glycoprotein. Seven peptide sequences were identified that specifically bound doxorubicin. Five of these sequences expressed the core consensus motif **WXXW**. The displacement assay showed that the phages expressing these peptides bound MDR type drugs (vinblastine, doxorubicin, verapamil, and genistein) with the same selectivity as P-glycoprotein and did not interact with non-MDR type drugs, such as arabinosylcytosine (Ara-C) and melphalan. One of the selected peptides that showed a highest capacity for the binding (VCDWWGWGIC) was synthesized and displayed competition with the phage for doxorubicin binding. The structure modeling suggested that all the selected sequences contained a hydrophobic envelope in which MDR drugs could be docked with substantial energy minimization. Western-blot analysis showed that monospecific antibody obtained against the phage expressing VCDWWGWGIC peptide could specifically recognize P-glycoprotein in the membrane fraction of MDR phenotype MCF-7ADR cells. The MDR drug-binding sequences generated during this work could provide an important tool for design and screening of new chemotherapeutical agents.

**Key words:** MDR, drug-binding peptides, P-glycoprotein, phage display library.

## INTRODUCTION

The acquisition of multidrug resistance (MDR) by cancer cells is a major clinical problem in tumor chemotherapy. This phenomenon is generally defined as selection and outgrowth of pre-existing or newly developing subpopulations of chemoresistant cells [1]. The usual pattern of cross-resistance includes a large number of lipophilic and positively charged molecules, such as anthracyclines, *Vinka* alkaloids, taxanes, epipodophylotoxines and some other structurally unrelated compounds (for review see[2]). An important role in mediation of MDR belongs to the ATP-Binding Cassette (ABC) family of transporters, such as P-glycoprotein [3], that can mediate drug resistance by acting as a drug efflux pump. The amino acid sequence analysis and hydropathy profiling indicate that P-glycoprotein is formed by two homologous halves, each composed of six transmembrane (TM) segments and one nucleotide-binding domain [4,5].

The ability of P-glycoprotein to recognize many structurally unrelated cytotoxic drugs that form the MDR drug group remains a puzzling aspect of P-glycoprotein function. In the absence of three-dimensional structural information, the identification of structure/function relationships in P-glycoprotein has relied on the scrutiny of P-glycoprotein primary sequence and on biochemical and genetic analyses. Although the exact topology of P-glycoprotein remains to be fully defined, considerable evidence indicates that the hydrophobic TM domains are intimately associated with drug binding. Indeed, the energy transfer experiments with doxorubicin have indicated that hydrophobic drug molecules are likely recognized by P-glycoprotein within the context of the membrane bilayer [6]. Furthermore, the epitope mapping studies of P-glycoprotein proteolytic fragments labeled with photoactivable drug analogs have identified two major drug-binding sites symmetrically located within or immediately C-terminal to TM6 and TM12 domains, respectively [7,8,9]. The study of naturally occurring human and hamster P-glycoprotein mutants with altered drug resistance profiles have indicated that discrete mutations near TM3 or within TM6 domains alter the substrate specificity of P-glycoprotein [10,11]. Finally, the studies of Loo and Clark, in which they used alanine-scanning mutagenesis of P-glycoprotein, have identified several residues within TM4,



TM6, TM10, and TM12 domains and in the intervening cytoplasmic loops where mutations differentially affect the capacity of P-glycoprotein to confer resistance to vinblastine, doxorubicin, colchicine, and actinomycin D [12,13,14].

However, despite numerous efforts, the precise mechanism by which P-glycoprotein recognizes a variety of structurally diverse compounds still remains unclear. In this connection, mimicking the P-glycoprotein drug-binding activity by generating functional analogues of P-glycoprotein and analysis of their interactions with MDR drugs could provide important information for design of new anticancer agents that would be effective against MDR tumors. One of the most effective ways to mimic biologically active entities such as antigenic sites, enzyme inhibitors or receptor ligands is a combinatorial phage display approach [15,16,17]. For example, a phage display technology has been recently successfully used to reveal the conformational antigenic site of P-glycoprotein that is recognized by MC57 monoclonal antibody [18], as well as to generate single-chain antibody that specifically recognizes doxorubicin [19]. In this work, we have applied the phage display technology to identify the peptide sequences that possess similar to P-glycoprotein drug-binding activity.

## MATERIAL AND METHODS

**Construction of Phage Display Library.** The decapeptide library used in this study was constructed essentially as previously described [15] using a phage vector fUSE5 (a generous gift from Dr. George Smith, University of Missouri, Columbia, MO). The fUSE5 vector was prepared for ligation by digesting 100 µg of RF DNA with 100 Units of *Sfi*I {Boehringer Mannheim Biochemica (BMB)} in 200 µl of the buffer, as recommended by the supplier. After extraction with phenol and chloroform [20], the volume was brought to 810 µl with 10 mM Tris/HCl pH 8.0, 1 mM EDTA buffer (Tris/EDTA), and DNA was precipitated with 90 µl of sodium acetate buffer (3 M sodium acetate pH 6.0) and 540 µl of isopropanol. The mixture was incubated for 20 min on ice, then centrifuged for 30 min at 4°C. The pellet was washed with 70% (v/v) ethanol, redissolved in Tris/EDTA, ethanol-precipitated [20] and dissolved in 120 µl of Tris/EDTA (final yield 60 µg). The DNA obtained could not be self-ligated, indicating complete removal of the 14 bp spacer sequence that lies between the *Sfi*I sites. The insert was prepared essentially as previously described [21]. Briefly: (i) a collection of oligonucleotides encoding all possible decapeptides was synthesized with self-complementary 3'-terminus {5'-CGCTGGCCGACGTGGCC(NNG/T)<sub>10</sub>GCGGCCTCTGAGGCCTCTGAGGCCACGTAATACACGTGGCCTCAGAGGCCGC-3'; where N indicates that an equimolar mixture of all four nucleotides was used in the position during oligonucleotide synthesis}. The complementary strand was synthesized by extension of the 3'-end with Klenow fragment (BMB); (ii) the *Sfi*I compatible ends were generated by restriction of 5 µg of fill-in product with 400 units of *Bgl*I (BMB) in 50 µl, as recommended by the supplier; (iii) the desired fragment was electrophoresed on 15% (w/v) polyacrylamide gel. The DNA of the correct size was then excised, recovered and purified according to conventional techniques [20]. A total of 20 µg of *Sfi*I digest of fUSE5 was then ligated with 200 ng of the purified oligonucleotide insert (molar ratio 1:2) by overnight incubation at 15°C in the volume of 1 ml using 4000 units of T4 DNA ligase (New England Biolabs). The product was extracted with phenol/chloroform, precipitated with ethanol, washed twice with 70% (v/v) ethanol, dried and resuspended in 40 µl of water. The transformation of 4 µl of the ligation mixture into 80 µl of

electrocompetent MC1061 cells was performed by electroporation using a Gene Pulser electroporation apparatus (Biorad) at 1.8 kV/cm, 200 ohms, 25 mF in 0.2 cm cuvettes for a total of 10 transformation mixes [22]. Ten transformation mixtures were separated into 5 pairs, and each pair diluted in 1 L of LB medium (with 20 mg/ml tetracycline and 100 mg/ml streptomycin) and allowed to grow for 18 h at 37°C at 300 revs/min. Phages from liquid culture were obtained by clearing the supernatant twice by centrifugation at 8000 revs/min for 10 min at 4°C, precipitating phage particles twice with polyethylene glycol (3.3% PEG 8000 in 0.4 M NaCl) and recentrifuging as described above. The phage pellets were resuspended in 50 mM Tris/HCl pH 7.5, 150 mM NaCl buffer (Tris/NaCl) and stored at 4°C. This linear library consisted of  $1.4 \times 10^9$  independent recombinant phages recovered as tetracycline-resistant colonies. The majority of these phages (>90%) contained inserts as was indicated by sequencing of randomly selected clones.

**Selection of Doxorubicin-Binding Phage.** Doxorubicin was conjugated with BSA by using the glutaraldehyde method [20], diluted to a final concentration of 100 µg/ml in 15 mM Na<sub>2</sub>HPO<sub>4</sub>, 1,5 mM KH<sub>2</sub>PO<sub>4</sub>, 150 mM NaCl, 2,5 mM KCl pH 7.4 buffer (NaCl/P<sub>i</sub>) and placed on Nunc Maxisorb microtiter plates (50 µl per well). The conjugate was allowed to bind to the plates overnight at 4°C, the wells were then washed with NaCl/P<sub>i</sub> and blocked with 1% BSA in NaCl/P<sub>i</sub> (NaCl/P<sub>i</sub>/BSA) for 1 h at room temperature. After blocking, the wells were washed six times with NaCl/P<sub>i</sub> and the primary decapeptide library was then added to the plates ( $10^{10}$  phage particles per well in 50 µl of NaCl/P<sub>i</sub>/BSA). To allow the binding with doxorubicin, the plates were incubated for 1 h at room temperature. The unbound phages were washed 12 times with NaCl/P<sub>i</sub>, and the bound phages were eluted with 50 µl of 0.1 M glycine/HCl buffer pH 2.2, containing 1 mg/ml BSA, or with 50 µl of 50 mM of verapamil in NaCl/P<sub>i</sub>/BSA, a competitive inhibitor of doxorubicin binding with P-glycoprotein. Neutralization of the eluate, titration and amplification on agar medium were carried out essentially as previously described [23]. The binding and elution steps were repeated several times. Viral DNA was sequenced with the fUSE <sup>32</sup>P primer 5'-TGAATTTTCTGTATGAGG-3' (kindly provided by Dr. George Smith) by using the Sequenase T7 kit (Pharmacia) as recommended by the supplier.

**Phage Attachment Assay.** To characterize binding of the individual clones, doxorubicin-BSA was immobilized on microtiter plates as described above. The purified phages [23] were then added ( $10^{10}$  phage particles per well in 50  $\mu$ l of NaCl/ $P_i$ /BSA) and incubated for 1 h at room temperature. After extensive washing with Tris/NaCl containing 0.05% Tween20 (Tris/NaCl/T), 100  $\mu$ l of rabbit wild-type fd phage antiserum {generated by immunization following standard procedures [20]}, diluted at the ratio 1:1000 in the blocking solution (Tris/NaCl/T containing 5% dry fat-free milk) was added to the wells and allowed to react overnight at 4°C. The plates were washed seven times with Tris/NaCl/T and once with Tris/NaCl and incubated for 2 h at room temperature with 100  $\mu$ l of peroxidase-conjugated goat anti-rabbit immunoglobulin [Kirkegaard & Perry Labs (KPL)], diluted at the ratio 1:1000 in the blocking solution. The plates were then washed seven times with Tris/NaCl/T and once with Tris/NaCl, incubated for 30 min at room temperature with 100  $\mu$ l of 2,2'-azinobis(3-ethylbenzothiazoline-6-sulfonoc acid) solution (KPL), and the absorbance (A) was read by using a microplate ELISA reader at 405 nm wavelength.

**Competitive Displacement Assay.** V6 phage ( $10^9$  transducing units) was preincubated for 2 h at room temperature in 100  $\mu$ l of NaCl/ $P_i$ /BSA containing various concentrations of free drugs: doxorubicin, vinblastine, genistein, melphalan, verapamil, and Ara-C, or of VCDWWGWGIC synthetic peptide. Aliquots were then added to microtiter wells precoated with doxorubicin-BSA as described above. After 1 h incubation at room temperature, the plates were washed 12 times with NaCl/ $P_i$ , and the bound phages were eluted with 100  $\mu$ l of 0.1 M glycine/HCl buffer pH 2.2. The phages were quantitated by titrating on log phage *E. coli* K91Kan plated on LB plates containing 40 mg/ml tetracycline [23].

**Antibodies and Immunoblotting Analysis.** Monoclonal anti-P-glycoprotein antibody C219 was purchased from Centocor, Malvern, PA. Rabbit anti-wild-type fd phage and anti-V6 phage polyclonal antibodies were prepared by immunizing rabbits with corresponding phages following standard procedures [20]. Antisera were first pre-adsorbed with wild-type phage particles [24], and antibodies were then affinity-purified on AffinityPak Immobilized Protein A columns using the procedure recommended by the manufacturer (Pierce).

Membrane-enriched fractions of MCF-7 and MCF-7ADR cells were prepared as previously described [25] and resuspended in Tris/sucrose buffer (10 mM Tris/HCl pH 7.5, 0.25 M sucrose) containing protease inhibitors. Samples containing 50  $\mu$ g of protein were subjected to SDS-polyacrylamide gel electrophoresis on 7% gel and then electrophoretically transferred to nitrocellulose membranes (Hybond-ECL, Amersham Corp.) in the transfer buffer, consisting of 48 mM Tris, 39 mM glycine, 20% methanol pH 9.2, and 0.0375% SDS or 0.1% Empigen BB. The membranes were blocked with Tris/NaCl/T containing 5% dry fat-free milk and further incubated with primary antibody for 1 h at room temperature. Immunodetection was performed with horseradish peroxidase-conjugated goat anti-rabbit or anti-mouse IgG using enhanced chemiluminescence according to the manufacturer's instructions (Amersham Corp.).

**Mass-Spectrometry Analysis.** VCDWWGWGIC peptide was purchased as a custom order from Anaspec Inc. (San Jose, CA). The complete peptide VCDWWGWGICG contains additional Gly residues at the C terminus to improve solubility. The mass-spectra of synthetic peptide were measured using a Perkin-Elmer Sciex API III triple quadrupole mass spectrometer (Norwalk, CT). The samples were dissolved in 50% MeOH and injected at a flow rate of 2  $\mu$ l/min.

**Molecular Modeling.** SYBYL Molecular Graphics (version 6.1, Tripos Inc., St. Louis, Missouri) software was used for molecular modeling and energy minimization experiments. The Powell method with Tripos force field and the Gasteiger-Huckel method for charge calculation [26] were used for energy minimization. The dielectric constant,  $E=80$ , was used for solvent simulation. The modeling program was run on Silicon Graphics GTX4, Indigo, and Indigo II workstations. Each structure was taken through conjugate gradient energy minimization to find the approximate starting structure. Initially, energy minimization was carried out on the peptide alone. Then, after having achieved the energy gradient of 0.21 kJ/mol, the MDR drug molecules (doxorubicin, vinblastine, and verapamil) were docked to the tryptophane pocket and energy minimization was repeated again. The initial orientation of the drugs was chosen in a way that allowed reaching maximum surface contact between the drug and peptide molecules.

## RESULTS

*Selection of Doxorubicin-Binding Phages.* To ensure a high level of the drug absorption on polystyrene, doxorubicin was conjugated to BSA, and the conjugate was immobilized on polystyrene ELISA plates that were used to select drug-binding clones by successive rounds of biopanning. Displacement with verapamil, a competitive inhibitor of doxorubicin binding with P-glycoprotein (protocol A) or treatment with low pH buffer which is usually used for phage panning [16] (protocol B) were used to elute the phages that bound to the doxorubicin-BSA coated plates. After four rounds of panning using protocol A and five rounds of that using protocol B, the percentage of phage particles in the output reached the maximum and remained unchanged during further rounds suggesting that the highest enrichment of the library by the drug-binding phages was achieved (Fig. 5.1). To analyze the selected phages, 26 individual clones were randomly chosen for sequencing. The results shown in Table 5.1 demonstrate that of these 26 clones, 24 (96%) contained tryptophane residues within the consensus motif WXXW distributed among five different sequences represented in the template with the ratio 9:6:5:3:1. Two sequences represented by single clones did not contain the WXXW motif, but had other hydrophobic residues at the tryptophane position. All the peptides showed a high hydrophobic index; one of them, VCDWWGWGIC, contained two cysteine residues suggesting that this peptide could be of a cyclic structure. Four clones (V6, V10, V12, and A4) displaying the highest frequency of distribution in the template were analyzed for doxorubicin binding using a phage attachment assay. The results of this experiment demonstrated that the selected clones could specifically bind the doxorubicin-BSA conjugate (Table 5.1), while none of these clones bound BSA alone (data not shown).

*Binding of V6 Phage with MDR Type Drugs.* Phage V6, showing the highest binding capacity with respect to doxorubicin (Table 5.1) and apparently having a cyclic structure, was chosen for further drug binding experiments. Although the sequence presented on V6 phage was not of highest frequency in the selected template (3 of 16 or 18,8%), we have chosen V6 phage because under the same conditions it possesses higher than other phages binding with doxorubicin, which is suggestive of its higher affinity. The latter appears to be a more important parameter than frequency, taking into account

uneven distribution of peptides in the library as well as possible differences in the amplification efficacy of phages bearing different sequences.

To evaluate the affinity and selectivity of the peptide represented on V6 phage, we analyzed its binding with several drugs using a competitive displacement assay (see Materials and Methods). Vinblastine and doxorubicin were chosen as drugs possessing high affinities to P-glycoprotein [27]; verapamil which has lower affinity and genistein which preferably binds to MDR-associated protein (MRP) rather than to P-glycoprotein [28,29] were grouped as moderate and low affinity drugs, respectively; Ara-C and melphalan were selected as non-MDR drugs [30,31]. The results shown in Fig. 5.2 demonstrate that the drug concentrations that produce 50% of the inhibition effect ( $IC_{50}$ ) for vinblastine and doxorubicin were 0.15 nM and 0.45 nM, respectively. Verapamil was about 100 times less potent than vinblastine ( $IC_{50} = 20$  nM); about 1000-fold lower affinity was established for genistein ( $IC_{50} = 200$  nM). Ara-C and melphalan did not show any specific binding with V6 phage. The values of  $IC_{50}$  determined in these experiments were in general agreement with the resistance profile mediated by P-glycoprotein: high resistance to vinblastine and doxorubicin, intermediate resistance to verapamil, low resistance to genistein, and no resistance to Ara-C and melphalan [27-31].

*P-glycoprotein Recognition by Monospecific Antibodies.* To analyze the relevance of the selected peptide sequences to P-glycoprotein, antibodies were raised in rabbits against fd phage (wild-type) and V6 phage. To achieve monospecificity, the anti-V6 phage sera was purified by precipitation with fd phage for several times until it showed no binding with the wild type phage in ELISA test. The monospecificity of anti-V6 antibodies was additionally confirmed by Western blot analysis, which demonstrated that the antibodies did not interact with proteins in the wild phage lysate, while pIII protein in the V6 phage lysate, that contains the respective sequence, was specifically stained (data not shown).

The membrane fractions obtained from two human breast carcinoma cell sublines, MCF-7 and MCF-7ADR cells, were analyzed for binding with anti-V6 antibodies. MDR phenotype MCF-7ADR cells obtained by multiple passaging of parental MCF-7 cells with increasing doses of doxorubicin [32], expressed high level of P-glycoprotein that could be revealed with C219 monoclonal antibody, while MCF-7 cells were P-

glycoprotein negative (Fig. 5.3A and B, lines 1 and 2). The Western blot analysis showed that anti-V6 antibody specifically recognized a protein with Mm 170kDa in MCF-7ADR membrane fraction, that corresponded to the protein revealed by anti P-glycoprotein C-219 mAb (Fig. 5.3B, lines 2 and 6), suggesting a cross-reactivity between VCDWWGWGIC peptide and P-glycoprotein. Importantly, the binding of P-glycoprotein with anti-V6 antibody was observed only when SDS in the transfer buffer was replaced by Empigen BB (Fig. 5.3A, line 6 and Fig. 5.3B, line 6) a zwitterionic surfactant that is capable of restoring antibody-binding capacity of conformational antigenic sites in Western blot assay [33].

*Structural Characteristics of the Synthetic VCDWWGWGIC Peptid.* The synthetic VCDWWGWGIC peptide showed a tendency to spontaneous internal cyclization, which was observed during its isolation from crude reaction mixture (Fig. 5.4A). Cyclization of the peptide was more pronounced in the presence of DMSO (Fig. 5.4B) which was used as an oxidizing agent as described elsewhere [34]. The cyclic structure of the oxidized peptide was revealed by using mass-spectrum analysis (Table 2). It demonstrated a loss of two mass units in the peptide ion in comparison to the noncyclized peptide. As it is shown in Table 5.2, the first and second peaks seen on the HPLC analysis (Fig. 5.4A) correspond to the peptides with  $m/z = 1282$  and  $1280$ , respectively, where  $m$  is the mass of the protonated peptide ion  $[M^+H]^+$ , and  $z$  is its charge. The additional confirmation of internal cyclization of the peptide vs its dimerization or polymerization was obtained from the analysis of the isotopic peak distribution in a way similar to the one described for monomeric and dimeric cyclic thrombin inhibitors [35]. More specifically, in the expanded mass-spectra, corresponding to the cyclized peptide, ion with  $m/z = 1280$  shows in its molecular ion region a set of major isotopic peaks that differ by 1 Da (Table 5.2). This can only correspond to a monocharged ion ( $m = [M^+zH]^{z+}$ ,  $z=1$ ). In the case of doubly charged  $[M^+2H]^{2+}$  and any multiply charged  $[M^+zH]^{z+}$  ions, the difference between isotopic peaks should be 0.5 Da or less (due to division by  $z$ , where  $z \geq 2$ ).

*Binding of the Synthetic VCDWWGWGIC Peptide with Doxorubicin.* To verify whether the synthetic VCDWWGWGIC peptide expressed on V6 phage has itself all the necessary elements to bind MDR drugs, or a phage particle is required for this process, we analyzed the ability of the peptide to compete with V6 phage for doxorubicin binding.



The results shown in Fig. 5.5 indicate that the VCDWWGWGIC peptide was active in the competitive displacement assay, although the affinity of peptide to the drug ( $IC_{50} = 50$  nM) is lower as compared to that of V6 phage ( $IC_{50} = 0.45$  nM). The reduced affinity of synthetic peptides as compared to their phage-displayed prototypes has been reported by many authors [15,21,24]. One possible reason for that could be the absence of “supportive” conformational effect from phage protein. Another speculation can be made that decrease in the affinity of the peptide to doxorubicin in comparison to that of V6 phage could be explained by monovalency of the peptide, while phage particles are polyvalent and display up to five copies of peptide molecules [36]. Under conditions of the heterophase binding assay used in this experiment (doxorubicin is immobilized on the solid phase, while phages and the peptide are in the liquid phase), the  $IC_{50}$  value for multivalent phage particles should be significantly lower than that of the monovalent peptide due to positive cooperativity.

*Molecular Modeling of the VCDWWGWGIC Peptide.* SYBYL Molecular Graphics approach was applied to analyze possible structures of the peptides and to evaluate their stereochemical ability to form complexes with MDR drugs. Because we were concerned only about broad structural trends, numerous minimized structures that did not vary significantly in their energy range were considered as equal for our purposes of this study.

The results demonstrated that after preliminary minimization, all the peptides selected during the panning (Table 5.1) initially represented in  $\beta$ -turn conformation, accepted conformation with the same deep hydrophobic envelope formed by two tryptophane residues of the consensus motif. The cyclic VCDWWGWGIC peptide was chosen for further modeling. Cyclization of the disulfide bond in the VCDWWGWGIC peptide resulted in four conformers with different orientation of bulky tryptophane indole rings in relation to the cyclic backbone. All these conformers retained a deep hydrophobic envelope as a major structural element. According to the modeling results, the third tryptophane that was located inside the WXXW motif of the VCDWWGWGIC peptide was out of plane and neither significantly participated in the hydrophobic envelope formation, nor affected the shape of this envelope. One of these structures with indole nitrogens oriented towards the disulfide bond (Fig. 5.6) was used for the docking

experiments with the MDR drugs. The purpose of the docking experiments was to analyze whether the hydrophobic pocket in the peptide molecule fits to the planar polycyclic structural elements of the drugs. The results obtained (Fig. 5.7, A to C) suggested that doxorubicin, vinblastine and verapamil could be easily docked between the indole rings of two tryptophane residues of the consensus motif. The indole rings, while originally oriented at an angle of 30 degrees in the peptide alone, became nearly parallel upon complexing with the drug molecule. In the case of the peptide-doxorubicin complex, the distance between the two indole rings was calculated to be 5.9 Å. Interestingly, this value was similar to the width of the  $\beta$ -form of the DNA minor groove that is known to be the target during doxorubicin-DNA intercalation [37]. The values of  $\Delta\Delta G$  (Van der Waals energy) calculated as differences between  $\Delta G$  of the free peptide and  $\Delta G$  of hypothetical peptide-drug complexes were as follows: doxorubicin = -177.80 kJ/mol; vinblastine = -149.55 kJ/mol; verapamil = -96.00 kJ/mol. The relative difference between these values was in general agreement with that of  $IC_{50}$  obtained during the binding experiments (Fig. 5.2). Doxorubicin and vinblastine demonstrated higher affinity for the peptide ( $IC_{50}$  = 0.45 nM;  $\Delta\Delta G$  = -177.80 kJ/mol for doxorubicin, and  $IC_{50}$  = 0.15 nM;  $\Delta\Delta G$  = -149.55 kJ/mol for vinblastine) than verapamil ( $IC_{50}$  = 20 nM;  $\Delta\Delta G$  = -96.00 kJ/mol). The inversion in relative affinities of doxorubicin and vinblastine to peptide observed during docking indicates that additional interactions may be involved in complex formation.

## DISCUSSION

In this work, we have described peptide ligands that can specifically bind doxorubicin. The selected V6, V10, V12, and A4 phages have demonstrated specific binding with doxorubicin that can be inhibited by another P-glycoprotein substrate, verapamil (Table 5.1) that is known to be a competitive inhibitor of doxorubicin binding with the drug transporter. More detailed studies of V6 phage have revealed its ability to interact with MDR drugs of different classes with the same selectivity pattern as P-glycoprotein (Fig. 5.2). This has led us to conclude that the selected peptides are at least functionally relevant to the P-glycoprotein drug-binding site(s). The fact that the synthetic VCDWWGWGIC peptide was able to compete at a nanomolar concentration range with V6 phage for doxorubicin-binding (Fig. 5.5) indicates that the drug-binding activity is an intrinsic property of this peptide rather than that of the phage particle expressing this peptide. The VCDWWGWGIC peptide contains two cysteines separated by seven amino acid residues. This distance is considered to be highly preferable for the formation of the internal disulfide bond [38] suggesting that the peptide most likely has a cyclic structure. The HPLC and mass-spectrometry analyses of the synthetic peptide support this idea showing that it tends to spontaneous cyclization.

The molecular modeling experiments have suggested that the distance between cysteine residues is minimal when the VCDWWGWGIC peptide is in  $\beta$ -turn conformation, and that the internal cyclization of this peptide leads to additional energy minimization of the molecule. These data together with cyclization experiment findings (Fig. 5.4 and Table 5.2) imply that most likely both the synthetic peptide and its fused version expressed on V6 phage have  $\beta$ -turn conformations. Furthermore, the modeling studies have revealed that all other selected sequences bearing the WXXW motif, when presented in  $\beta$ -turn conformation, can form a hydrophobic envelope similar to that found in the synthetic peptide model, shaped by tryptophane residues of the consensus motif (Fig. 5.6). At the same time, no conformational analogy between the peptides was found when other secondary structures were used during energy minimization. The conformational similarity between  $\beta$ -turn forms of the selected peptides and the tendency of VCDWWGWGIC peptide to form an internal cycle have led us to assume that the

drug-binding activity of the selected phages is related to the tryptophane envelope predicted by the modeling experiments. The correlation between the theoretical  $\Delta\Delta G$  values calculated from the docking experiments and the experimental binding results supports this idea. Having said that we realize that energy calculations obtained by molecular modeling could yield values that do not correspond to true binding energies. Therefore, direct X-ray analysis would be required to confirm the suggested structure of the complex.

The fact that the monospecific antibody against V6 phage is cross-reactive with P-glycoprotein indicates that the VCDWWGWGIC peptide has not only functional, but also some structural analogy with the drug-binding site(s) located in the P-glycoprotein molecule. It is noteworthy that the cross-reactivity between anti-V6 antibody and P-glycoprotein was only observed when Empigen BB, a zwitterionic surfactant which provides with a high renaturation degree of proteins transferred to nitrocellulose filters, was used during the Western blot analysis (Fig. 5.3). In the presence of SDS no binding of anti-V6 antibody with P-glycoprotein was detected indicating that the antigenic site in the P-glycoprotein molecule has a conformational rather than a linear structure. In fact, the examination of the primary structure of P-glycoprotein [39] has not revealed any WXXW sequence allowing a speculation that the peptides generated using our phage display library could mimic a nonlinear site involved in the drug binding, that may be formed by two or more regions on the P-glycoprotein polypeptide chain. The hypothesis that at least two different regions of the P-glycoprotein polypeptide chain approach each other to form a single binding site during drug recognition has been recently proposed on the basis of experiments on photoaffinity labeling of this transporter with azidopine [7]. Such a cross-matching site could be involved in initial drug recognition and its further transfer to a transmembrane tunnel formed by a cassette of aromatic amino acid residues [40]. The fact that the positions of eleven tryptophane residues in the P-glycoprotein polypeptide chain are conserved among different species [41] supports the idea that these amino acid residues could be involved in the formation of functional sites on the P-glycoprotein molecule.

The peptides mimicking the drug-binding properties of P-glycoprotein represent a useful tool for identification of common features of highly diversified MDR drug

molecules. Such a tool could substantially facilitate the design of new drugs, as well as used for the screening of new chemotherapeutic agents. Further experiments using synthetic peptides containing the WXXW motif and QSAR (Quantitative Structure-Activity Relationship) approach to simulate the structural and functional relations of the drug-peptide complexes are under the way in this laboratory. We believe that, these experiments will generate new important information on the application of peptides for drug design.

## **ACKNOWLEDGEMENTS**

We would like to thank G.P. Smith for providing the fUSE5 vector and the fUSE<sup>32</sup>P primer; F. Shareck for oligonucleotide synthesis; L. Labrie and L. Forget for DNA sequence analysis.

## REFERENCES

1. Goldstein, L. J., I. Pastan, and M. M. Gottesman. 1992. "Multidrug resistance in human cancer". Crit. Rev. Oncol. Hematol., vol. 12, p. 243-253.
2. Gros, P. and E. Buschman. 1993. "The mouse multidrug resistance gene family: Structural and functional analysis". Int. Rev. Cytol., vol. 137C, p.169-197.
3. Van der Bliek, A. M., T. Van der Velde-Koerts, V. Ling, and P. Borst. 1986. "Overexpression and amplification of five genes in a multidrug-resistant chinese hamster ovary cell line". Mol. Cell. Biol., vol. 6, p. 1671-1678.
4. Chen, C., J. E. Chin, K. Ueda, D. P. Clark, I. Pastan, M. M. Gottesman, and I. B. Roninson. 1986. "Internal duplication and homology with bacterial transport proteins in MDR1 (P-glycoprotein) gene from multidrug-resistant human cells". Cell, vol. 47, p. 381-389.
5. Gros, P., J. Croop, and D. Housman. 1986. "Mammalian multidrug resistance gene: Complete cDNA sequence indicates strong homology to bacterial transport proteins". Cell, vol. 47, p. 371-380.
6. Raviv, Y., H. B. Pollard, E. P. Bruggeman, I. Pastan, and M. M. Gottesman. 1990. "Photosensitized labeling of a functional multidrug transporter in living drug-resistant tumor cells". J. Biol. Chem., vol. 265, p. 3975-3980.
7. Bruggemann, E. P., S. G. Currier, M. M. Gottesman, and I. Pastan. 1992. "Characterization of the azidopine and vinblastine binding site of P-glycoprotein". J. Biol. Chem., vol. 267, p. 21020-21026.
8. Greenberger, L. M. 1993. "Major photoaffinity drug labeling sites for iodoaryl azidoprazosin in P-glycoprotein are within, or immediately C-terminal to, transmembrane domain-6 and domain-12". J. Biol. Chem., vol. 268, p. 11417-11425.
9. Morris, D. I., L. M. Greenberger, E. P. Bruggemann, C. Cardarelli, M. M. Gottesman, I. Pastan, and K. B. Seamon. 1994. "Localization of the forskolin labeling sites to both halves of P-glycoprotein: Similarity of the sites labeled by forskolin and prazosin". Mol. Pharmacol., vol. 46, p. 329-337.
10. Choi, K., C.-J. Chen, M. Kriegler, and I. B. Roninson. 1988. "An altered pattern of cross-resistance in multidrug-resistant human cells results from spontaneous mutations in the *mdr1* (P-glycoprotein) gene". Cell, vol. 53, p. 519-529.
11. Devine, S. E., V. Ling, and P. W. Melera. 1992. "Amino acid substitutions in the sixth transmembrane domain of P-glycoprotein alter multidrug resistance". Proc. Natl. Acad. Sci. USA, vol. 89, p. 4564-4568.

12. Loo, T. W. and D. M. Clarke. 1993. "Functional consequences of proline mutations in the predicted transmembrane domain of P-glycoprotein". J. Biol. Chem., vol. 268, p. 3143-3149.
13. Loo, T. W. and D. M. Clarke. 1993. "Functional consequences of phenylalanine mutations in the predicted transmembrane domain of P-glycoprotein". J. Biol. Chem., vol. 268, p. 19965-19972.
14. Loo, T. W. and D. M. Clarke. 1994. "Functional consequences of glycine mutations in the predicted cytoplasmic loops of P-glycoprotein". J. Biol. Chem. Vol. 269, p. 243-7248.
15. Scott, J. K. and G. P. Smith. 1990. "Searching for peptide ligands with an epitope library". Science, vol. 249, p. 386-390.
16. Cwirla, S. E., E. A. Peters, R. W. Barrett, and W. J. Dower. 1990. "Peptides on phage: A vast library of peptide for identifying ligands". Proc. Natl. Acad. Sci. USA, vol. 87, p. 6378-6382.
17. Devlin, J. J., L. C. Panganiban, and P. E. Devlin. 1990. "Random peptide libraries: A source of specific protein binding molecules". Science, vol. 249, p. 404-406.
18. Poloni F., G. Romagnoli, M. Cianfriglia, and F. Felici. 1995. "Isolation of antigenic mimics of *MDR1*-P-glycoprotein by phage-displayed peptide libraries". Int. J. Cancer, vol. 61, p. 727-731.
19. Vaughan, T. J., A. J. Williams, K. Pritchard, J. K. Osbourn, A. R. Pope, J. C. Earnshaw, J. McCafferty, R. A. Hodits, J. Wilton, and K. S. Johnson. 1996. "Human antibodies with sub-nanomolar affinities isolated from a large non-immunized phage display library". Nature Biotech., vol. 14, p.309-314.
20. Ausubel, F. M., R. E. Kingston, D. D. Moore, J. G. Seidman, J. A. Smith, and K. Struhl, (eds.). 1994. Current Protocols in Molecular Biology. New York: John Wiley & Sons.
21. Christian, R. B., R. N. Zuckermann, J. M. Kerr, L. Wang, and B. A. Malcolm. 1992. "Simplified methods for construction, assessment and rapid screening of peptide libraries in bacteriophage". J. Mol. Biol., vol. 227, p. 711-718.
22. Dower, W. J., J. F. Miller, and C. W. Ragsdale. 1988. "High efficiency transformation of *E. coli* by high voltage electroporation". Nucl. Acids Res., vol. 16, p. 6127-6145.
23. Parmley, S. F. and G. P. Smith. 1988. "Antibody-selectable filamentous fd phage vector: Affinity purification of target genes". Gene, vol. 73, p. 305-318.

24. Felici, F., A. Luzzago, A. Folgori, and R. Cortese. 1993. "Mimicking of discontinuous epitopes by phage-displayed peptides, II. Selection of clones recognized by a protective monoclonal antibody against the *Bordetella pertussis* toxin from phage peptide libraries". Gene, vol. 128, p. 21-27.
25. Almquist, K. C., D. W. Loe, D. R. Hipfner, J. E. Mackie, S. P. C. Cole, and R. G. Deeley. 1995. "Characterization of the M(r) 190,000 multidrug resistance protein (MRP) in drug-selected and transfected human tumor cell". Cancer Res., vol. 55, p. 102-110.
26. SYBYL Force Field Manual. Version 6.1. Tripos Inc. 1995.
27. Ferry, D. R., P. J. Malkhandi, M. A. Russell, and D. J. Kerr. 1995. "Allosteric regulation of [<sup>3</sup>H]vinblastine binding to P-glycoprotein of MCF-7 ADR cells by dexniguldipine". Biochem. Pharmacol., vol. 49, p. 1851-1861.
28. Malkhandi, P. J., D. R. Ferry, R. Boer, V. Gekeler, W. Ise, and D. J. Kerr. 1994. "Dexniguldipine-HCl is a potent allosteric inhibitor of [<sup>3</sup>H]vinblastine binding to P-glycoprotein of CCRF ADR 5000 cells". Eur. J. Pharmacol., vol. 288, p. 105-114.
29. Feller, N., C. M. Kuiper, J. Lankelma, J. K. Ruhdal, R. J. Scheper, H. M. Pinedo, and H. J. Broxterman. 1995. "Functional detection of MDR1/P170 and MRP/P190-mediated multidrug resistance in tumor cells by flow cytometry". Brit. J. Cancer, vol. 72, p. 543-549.
30. Bhalla, K., Y. Huang, C. Tang, S. Self, S. Ray, M. E. Mahoney, V. Ponnathpur, E. Tourkina, A. M. Ibrado, and G. Bullock. 1994. "Characterization of a human myeloid leukemia cell line highly resistant to taxol". Leukemia, vol. 8, p. 465-475.
31. Binaschi, M., R. Supino, R. A. Gambetta, G. Giaccone, E. Prosperi, G. Capranico, I. Cataldo, and F. Zunino. 1995. "MRP gene overexpression in a human doxorubicin-resistant SCLC cell line: Alterations in cellular pharmacokinetics and in pattern of cross-resistance". Int. J. Cancer, vol. 62, p. 84-89.
32. Fairchild, C. R., S. P. Ivy, C. S. Kao-Shan, J. Whang-Peng, N. Rosen, M. A. Israel, P. W. Melera, K. H. Cowan, and M. E. Goldsmith. 1987. "Isolation of amplified and overexpressed DNA sequences from adriamycin-resistant human breast cancer cells". Cancer Res., vol. 47, p. 5141-5148.
33. Mandrell, R. E. and W. D. Zollinger. 1984. "Use of a zwitterionic detergent for the restoration of the antibody-binding capacity of electroblotted meningococcal outer membrane proteins". J. Immunol. Methods, vol. 67, p. 1-11.



34. Tam, J. P., C. R. Wu, W. Liu, and J. W. Zhang. 1991. "Disulfide bond formation in particles by dimethylsulfoxide. Scope and applications". J. Am. Chem. Soc., vol. 113, p. 6657-6662.
35. Szewczuk, Z., B. F. Gibbs, S. Y. Yue, E. Purisima, and Y. Konishi. 1992. "Conformationally restricted thrombin inhibitors resistant to proteolytic degradation". Biochemistry, vol. 31, p. 9132-9140.
36. Lin, T.-C., R. Webster, and W. Konigsberg. 1980. "Isolation and characterization of the C and D proteins coded by gene IX and gene VI in the filamentous bacteriophage f1 and fd". J. Biol. Chem., vol. 255, p. 10331-10337.
37. Williams, L. D., C. A. Frederick, G. Ughetto, and A. Rich. 1990. "Ternary interactions of spermine with DNA: 4'-epiadriamycin and other DNA:anthracycline complexes". Nucl. Acids Res., vol. 8, p. 5533-5541.
38. Zhang, R. and G. Snyder. 1991. "Factors governing selective formation of specific disulfides in synthetic variants of  $\alpha$ -conotoxin". Biochemistry, vol. 30, p. 11343-11348.
39. Zhang, J.-T., M. Duthie, and V. Ling. 1993. "Membrane topology of the N-terminal half of the hamster P-glycoprotein molecule". J. Biol. Chem., vol. 268, p. 15101-15110.
40. Pawagi, A. B., J. Wang, M. Silverman, R. A. F. Reithmeier, and C. M. Deber. 1994. "Transmembrane aromatic amino acid distribution in P-glycoprotein". J. Mol. Biol., vol. 235, p. 554-564.
41. Roninson, I. B. (ed.). 1991. Molecular and Cellular Biology of Multidrug Resistance in Tumor Cells. New York: Plenum Press. 406 p.
42. Adey, N. B., A. H. Mataragnon, J. E. Rider, J. M. Carter, and B. K. Kay. 1995. "Characterization of phage that bind plastic from phage-displayed random peptide libraries". Gene, vol. 156, p. 27-31.

**Table 5.1. Peptide Sequences and Binding Characteristics of Affinity-Purified Clones.**

Phages from a decapeptide display library were subjected up to five rounds of selection on doxorubicin-BSA immobilized on polystyrene ELISA plates. The sequences have been aligned on the common WXXW motif, where X is any of all 20 possible amino acid residues. The number of times each sequence occurred in the 26 isolates is given in the frequency column. The relative hydrophobic (HP) index was calculated as described [42]. Specific binding is expressed as the absorbance (A) units  $\times 10^{-3}$  at 405 nm (mean $\pm$ SEM) as described in Materials and Methods after subtraction of background reading obtained with the non-relevant phage (background reading was less than 10% of the sample reading).

Isolates	Elution	Displayed Peptides			Frequency	HP Index	Specific Binding
V12	Verapamil	WGRF	WGRW	LA	5	31	590 $\pm$ 23
V6		VCD	WWGW	GIC	3	29	700 $\pm$ 32
V10		Y	WMGW	KWEGE	6	26	560 $\pm$ 17
V15			WWDF	LQGSR	1	24	nd
V2			FAMW	YPLGWR	1	31	nd
A6	Acid	TW	WWTW	AGKH	1	33	nd
A4		L	WSPW	YGGSW	9	30	640 $\pm$ 19
Motif			WXXW		26		

**Table 5.2. Molecular Ion Masses and Isotopic Compositions of Reduced and Oxidized Forms of VCDWWGWGIC Peptide Determined by Mass Spectrometry.**

The retention times of reduced and oxidized forms of peptide were determined by HPLC as described in the legend to Fig. 5.4. The molecular ion masses (MS) and isotopic compositions were determined by using triple quadrupole mass spectrometry as described in Materials and Methods.

Peptide	HPLC	Mass Spectrometry	
	Retention Time	Major MS Peak	Isotopic Peaks
	min	m/z	m/z
Reduced form	30.79	1282	1282.6, 1283.5, 1284.5
Oxidized form	31.47	1280	1279.6, 1280.7, 1281.5

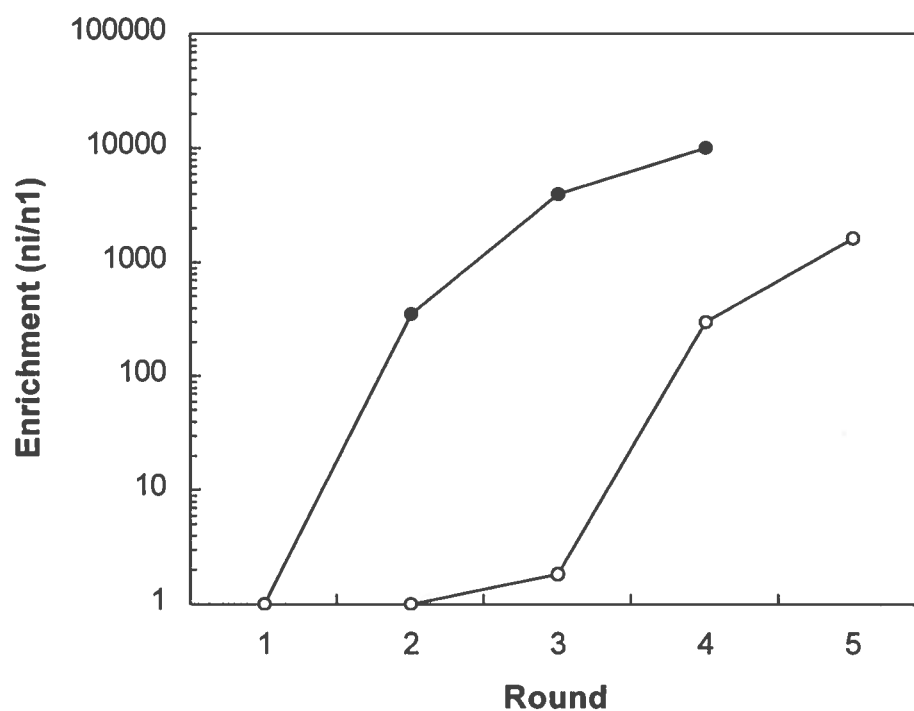


**Figure 5.1. Selection of Phages that Bind to Doxorubicin-BSA.**

Phages from a decapeptide library were bound to doxorubicin-BSA coated microtiter wells as described in Materials and Methods and eluted with 50 mM verapamil (●) or with glycine/HCl buffer pH 2.2 (○). Enrichment was calculated as the total number of phage recovered after elution ( $n_i$ , measured in transducing units) divided by the number of transducing units recovered after first round of selection ( $n_1$ ). The data represents mean values from plating in triplicate.

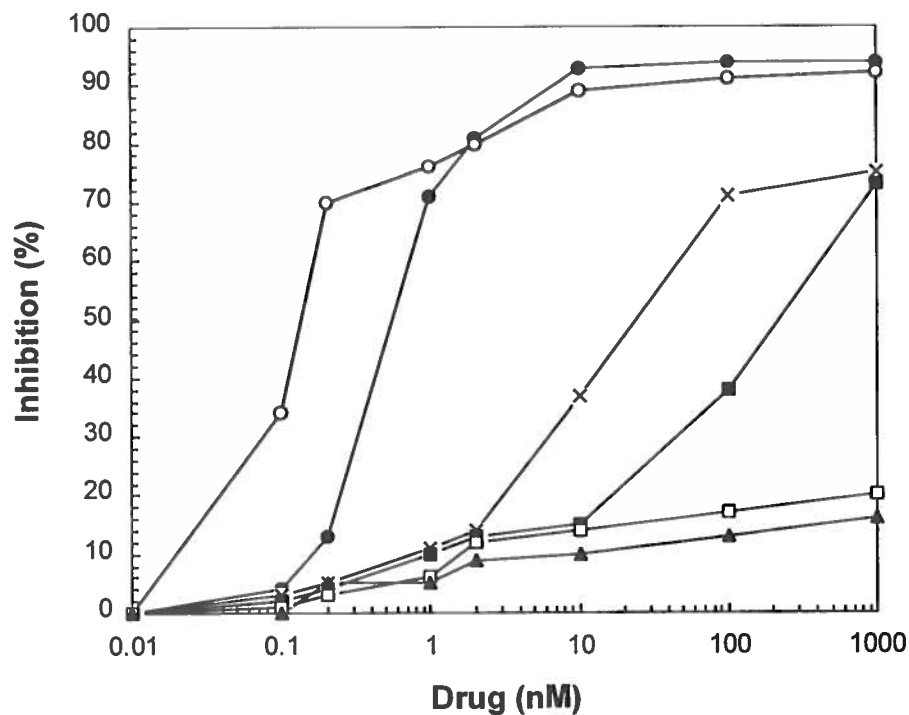


**Figure 5.2. Displacement Assay of Binding of Various Anti-Cancer Drugs with V6 Phage.**

V6 phage containing the VCDWWGWGIC peptide was bound to microtiter wells precoated with doxorubicin-BSA. The bound phages were eluted with glycine/HCl buffer pH 2.2 and quantitated by infection of bacteria as described in Materials and Methods. The Y-axis shows inhibition (%) of binding of V6 phage to doxorubicin-BSA as a function of the free drug concentration (X-axis). The drugs tested were doxorubicin (●); vinblastine (○); verapamil (x); genistein (■); melphalan (□); Ara-C (▲). The data represents means values of three independent experiments (SEM was less than 10 %,  $p < 0.05$ ).

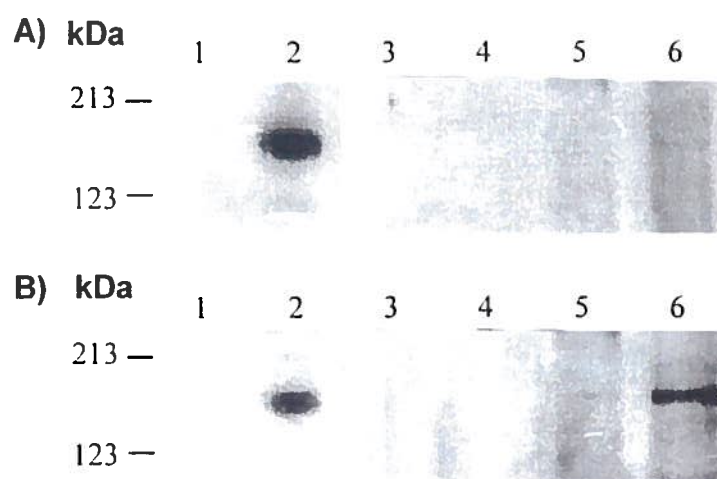


**Figure 5.3. Immunoblot Analysis.**

Membrane-enriched fractions from MCF-7 (lanes 1, 3, and 5) and MCF-7ADR (lanes 2, 4, and 6) cells were resolved by SDS-polyacrylamide gel electrophoresis and were electroblotted onto nitrocellulose membrane in the presence of either SDS (3A) or Empigen BB (3B). The membranes were then probed with monoclonal anti-P-glycoprotein antibody C219 (lanes 1 and 2), or with polyclonal anti-wild-type phage (lanes 3 and 4) and anti-V6 phage (lanes 5 and 6) antibodies. The membranes were washed, incubated with horseradish peroxidase-conjugated anti-IgG antibodies, and the blots were developed using an enhanced chemiluminescence detection kit as described in Materials and Methods.

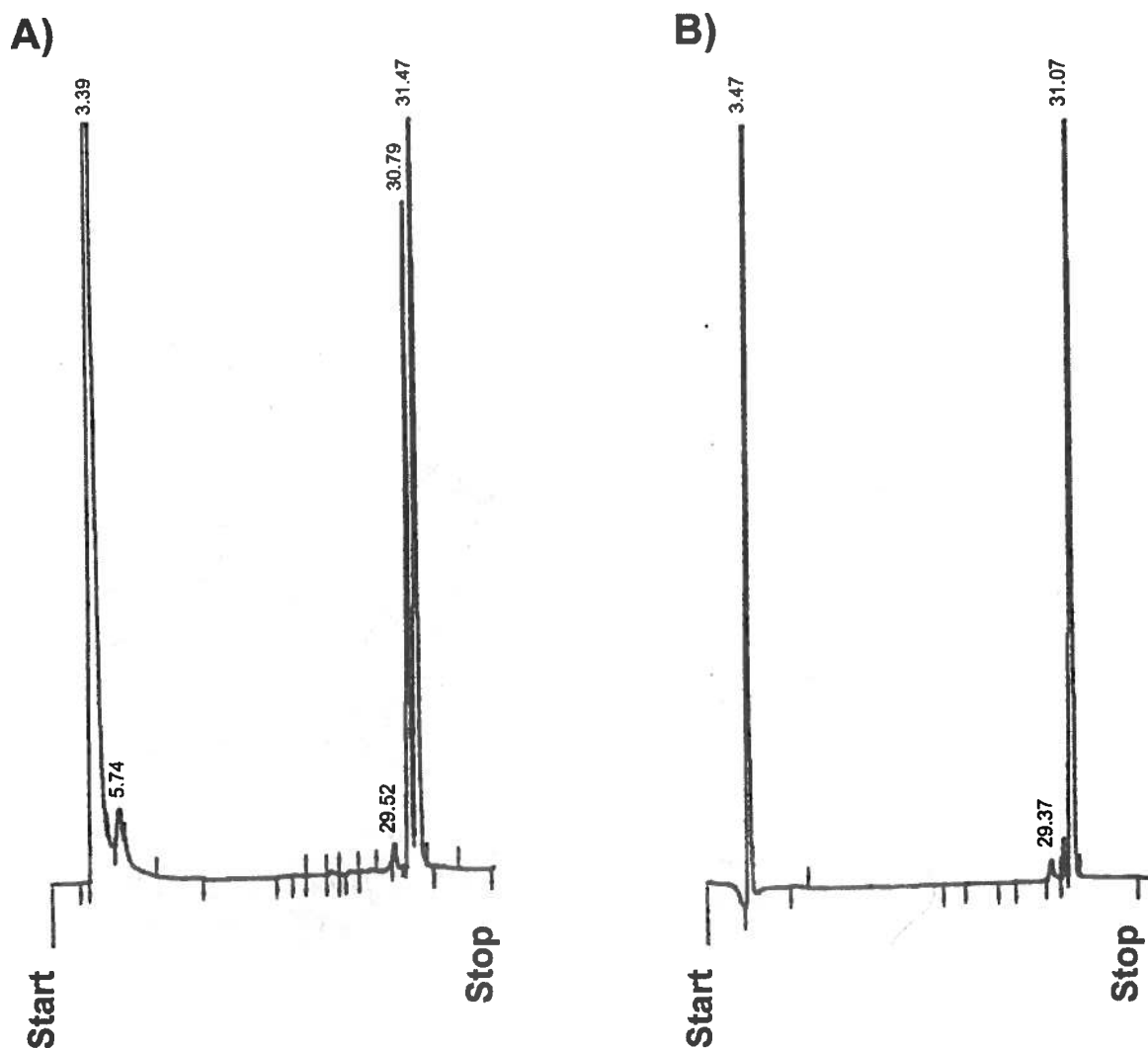


**Figure 5.4. HPLC of VCDWWGWGIC Peptide.**

Peptide was obtained from deprotection cocktail as a mixture of reduced and oxidized forms (A) and after additional oxidation with DMSO (B) under following conditions: Vydac 218TP54 Peptide and Protein column (5 $\mu$ M, C18, 4.6x250 mm), flow rate 1 ml/min, monitoring at 280 nm. Gradient 0-100% was developed 35 min using 0.1% TFA as buffer A and 0.1% TFA in acetonitrile as buffer B.

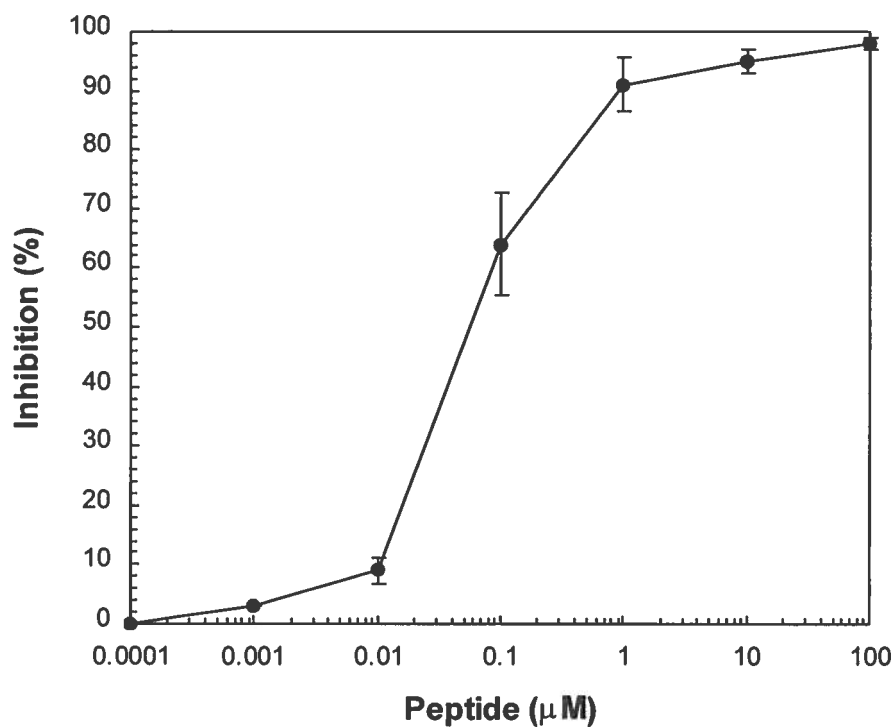


**Figure 5.5. Inhibition of V6 Phage Binding to Doxorubicin by the VCDWWGWGIC Peptide.**

Binding of V6 phage to doxorubicin-BSA was studied as described in the legend to Fig. 2 in the presence of the competing peptide. The Y-axis shows inhibition (%) of binding of V6 phage to doxorubicin-BSA as a function of the free peptide concentration (X-axis). The data represents means  $\pm$  SEM from three independent experiments.



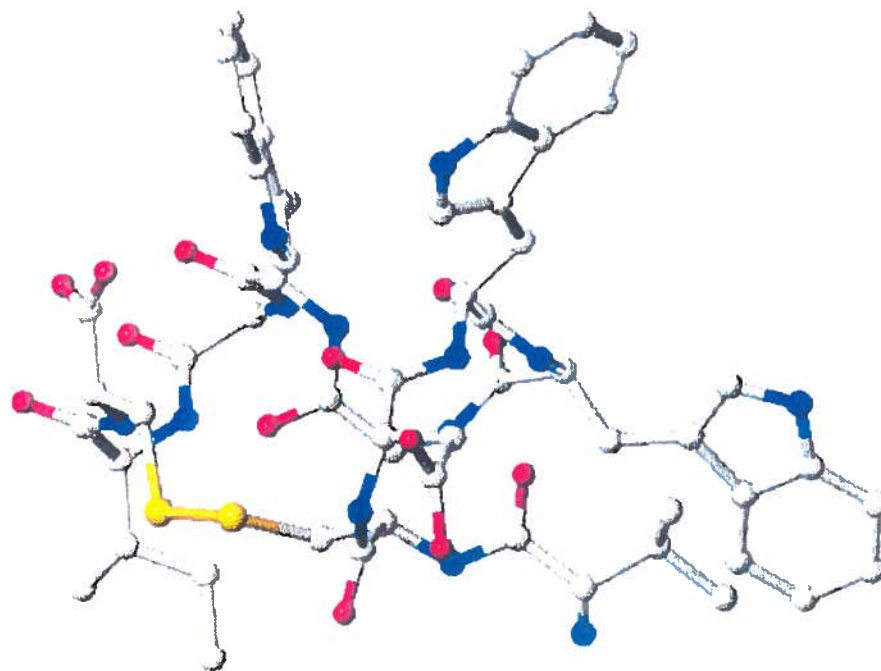


**Figure 5.6. Molecular Structure of VCDWWGWGIC Peptide Predicted by SYBYL Molecular Graphics (version 6.1a).**

The energy minimization of the peptide was performed as described in Materials and Methods. The following colors are used for the different atoms: carbon - gray; nitrogen - dark blues; oxygen - red; sulfur - yellow. The hydrogen atoms are omitted for clarity.

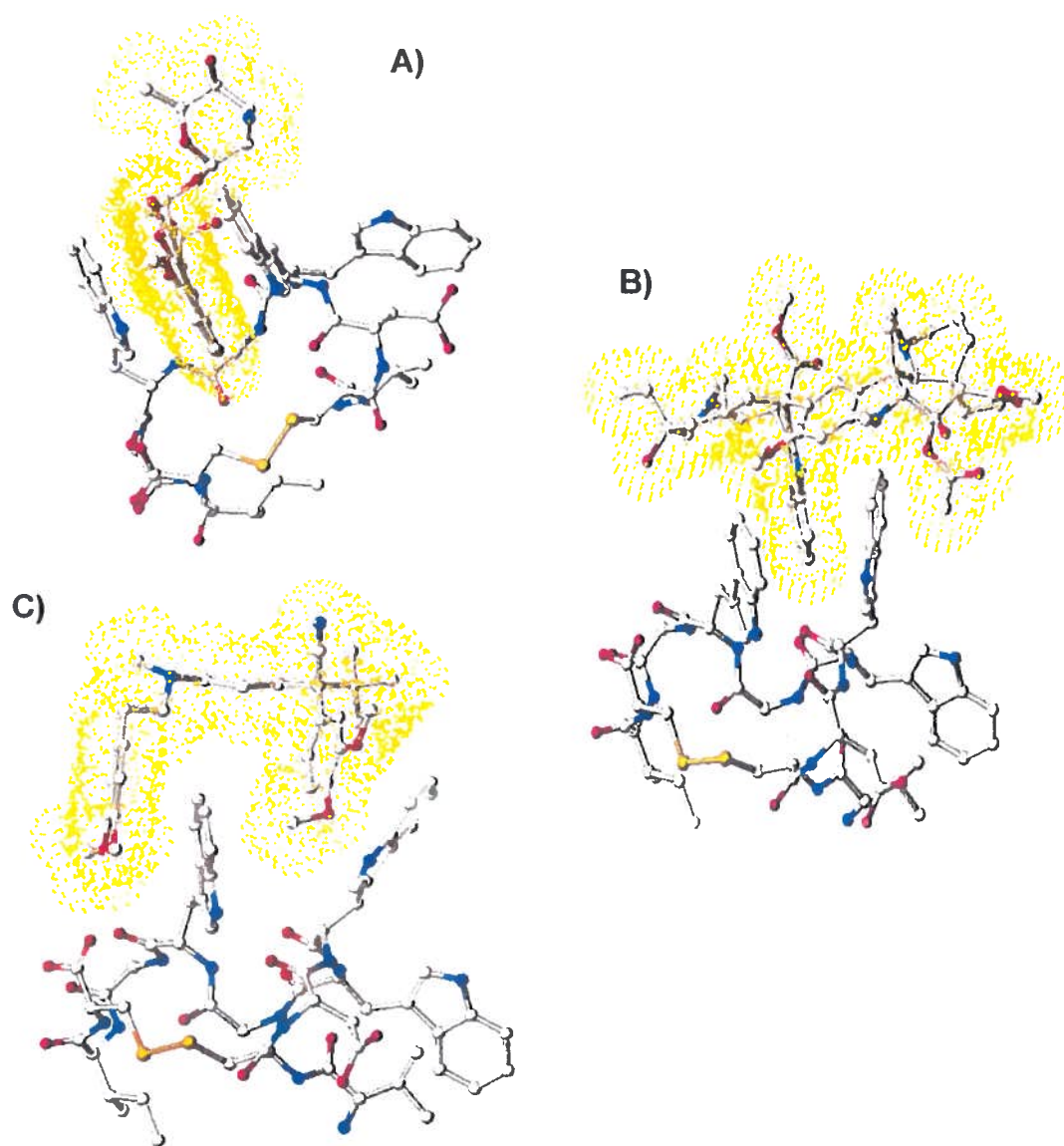


**Figure 5.7. Molecular Docking of Anti-Cancer Drug Molecules into the Tryptophane Envelope of VCDWWGWGIC Peptide.**

The drugs docked were doxorubicin (A); vinblastine (B); verapamil (C). The drug molecules are drawn with solid bonds and dashed surfaces; the peptide molecules are drawn with solid bonds.

## **CHAPTER 6**

### **General Discussion**

The aim of this chapter is to integrate our observation with the most recently published literature and with some additional personal observations.

## 1. MIMOTOPE DISCOVERY

Theoretically it seems highly unlikely that relatively small peptides could mimic functionally discontinuous epitopes of antigens. Nevertheless various recent reports show this to be the case. Peptide mimics of protein-, polysaccharide- and DNA-epitopes have been shown to be able to replace the native epitope (1). Moreover, some of them are able to induce, when used in a vaccine, antibodies with the same activity as that of the antibody used as a template (2,3). These mimics, called mimotopes, can be used in vaccines and diagnostics and can be developed more or less systematically using solely antibodies and RPLs.

Chapter 3 describes the screening of RPLs with the mAb BCD-F9 that resulted in the sequence deduced to be GRRPGGWMMR. This sequence was deduced to be a mimotope, a sequence capable of mimicking the natural epitope of the mAb BCD-F9. Mutational analysis indicated that specificity is likely to reside in the PGGWW block of the amino acids. The query of the SwissProt databank revealed that this block is common to many SH3 domain-containing regulatory proteins involved in signal transduction (4). This finding suggest that over-expression of tumor-specific antigen recognized by the BCD-F9 mAb in malignant cells may have a functional role in their status.

A major question raised by this result is why the selected sequence was unique. Although the library used here is highly diverse ( $>10^9$  independent clones), it is possible that it does not contain a close enough match to GRRPGGWMMR. It is also possible that there is a bias against particular sequences because the need to maintain phage infectivity, resulting in the absence of those sequences from the library.

Examination of the literature describing mimotopes suggests that a high frequency proline, glycine, and hydrophobic amino acids, particularly aromatic amino acids, is the norm. Examples include YPY for Concanavalin (5), PWLY for a carbohydrate-binding mAb (6), HPQF for streptavidin (7-9), SSLRGF for an anti-galactosyl antibody (10), and YYLH for an anti-biotin antibody (11). These are all binding sites that normally

recognize non-peptidic ligands, but examples of peptidic binding site mimotopes can also be found: DLVWLL for acetylcholine receptor antibody for example (12). Although the presence of helix-disrupting residues and aromatic residues appears to be important, each mimotope listed is unique in its structure.

Binding studies and immunization experiments confirmed the specificity of the mimotope for the BCD-F9 mAb. In addition, the mimotope was specifically recognized by BCD-F9 without the phage carrier, indicating that the mimotope alone is responsible for the interaction with BCD-F9 without the involvement of structure entities from the phage particle. Another indication for the correct mimicking of the epitope by F9 peptide was obtained by the immunization experiments. We demonstrated that rabbits immunized with peptide-KLH could elicit an IgG response to the natural antigen on tumor cells.

Peptide mimotopes are also of importance in mimicking the binding of non-proteinaceous substances as, for example, low molecular weight drugs. Chapter 5 describes a peptidic mimicry of drug-binding site, as seen by a routinely used in a chemotherapy drug, doxorubicin. It was shown that phages selected here with doxorubicin show remarkable sequence similarities with each other. Results shown in Table 5.1 demonstrate that of these 26 clones, 24 (96%) contained tryptophane residues within the consensus motif WXXW. Two sequences represented by single clones did not contain the WXXW motif, but had other hydrophobic residues at the tryptophane position. All the peptides showed a high hydrophobic index, confirming the previously mentioned observation about high frequency of hydrophobic amino acids, particularly aromatic amino acids in the mimotopes.

The modeling studies have revealed that all selected sequences bearing the WXXW motif, when presented in  $\beta$ -turn conformation, can form a hydrophobic envelope similar to that found in the synthetic peptide model, shaped by tryptophane residues of the consensus motif. At the same time, no conformational analogy between the peptides was found when other secondary structures were used during energy minimization. The conformational similarity between  $\beta$ -turn forms of the selected peptides and the tendency of VCDWWGWGIC peptide to form an internal cycle have led us to assume that the drug-binding activity of the selected phages is related to the tryptophane envelope predicted by the modeling experiments. The correlation between the theoretical  $\Delta\Delta G$

values calculated from the docking experiments and the experimental binding results supports this idea. However, conclusive evidence can only be obtained by NMR studies or X-ray crystallography of the structure of the complex.

In addition to an antigen-antibody system, the strategy demonstrated here might also be applicable to other systems where a low molecular weight substance is bound by a protein. It could, therefore, be very promising to substantially facilitate the design of new drugs, as well as use RPLs for the screening of new chemotherapeutic agents and other medically interesting substances.

## 2. IMMUNOTHERAPY

The development of mAbs displaying some degree of specificity for tumors allowed the concepts of immunological targeting of tumors to be readily explored, with studies demonstrating that xenogenic mAbs could not only be safely administered to patients and can localize on tumors (13), but could also have a therapeutic effect on their own in xenograft models (14) and in patients with leukemia and lymphoma (15). Passive immunization with antibodies may have an advantage in the initiation of tumor destruction, since it can occur within minutes to hours of antibody infusion. The use of specific immunoglobulins that are capable of activating NK cells through ADCC appears to be a method successfully used for treatment of solid tumors.

The mAb BCD-F9, as it was shown in this study, has these advantageous characteristics. The antitumor activity of the mAb BCD-F9 is supported by the reduced growth rate of solid tumor in BCD-F9-treated mice transplanted s.c. with HT1080 tumor cells. Moreover, the survival of all mice inoculated i.v. with tumor cells and the absence of detectable metastatic foci following histological examination of the lung of sacrificed animals at 60 days post tumor transplantation are also good indications of successful immunotherapy. Although, there are several antitumor mAbs that are already approved for clinical use or are currently in clinical trials (16,17), there is a need for development of new mAbs for anti-cancer immunotherapy. The findings reported in this study suggest that BCD-F9 might have an advantage as a potentially useful immunotherapeutic reagent

by recognizing the epitope that is also present to various degree on several neoplastic cell lines from different origin.

In the present study, we also demonstrated that anti-mimotope antibodies AM-F9 are able to target the BCD-F9 antigen-expressing human fibrosarcoma xenograft in nude mice. The capability of tumor targeting by AM-F9 was demonstrated by the experiment in which this antibody was injected into nude mice bearing solid HT-1080 tumors in the flanks (Fig. 3.1). Treatment with AM-F9 significantly inhibited the growth of HT-1080 tumor cells inoculated s.c. into CD-1 nude mice. Additionally, we assessed the effect of AM-F9 serum on tumor metastasis in an experimental animal model and showed that i.v. treatment with anti-mimotope antibody prolonged the life span of nude mice (Fig. 2.5). This incomplete inhibition, when compare to the fact that all animals injected with BCD-F9 survived, suggests that insufficient amounts of injected AM-F9 antibodies could be a factor.

In summary, this study demonstrated that both antibodies exhibited very similar antitumor activities against the proliferation of highly metastatic human HT-1080 tumor cells *in vivo*. However, the beneficial effects of this passive immunotherapy are only achieved if relatively large amounts of antibody are applied, making this treatment very expensive. Thus, it would be an advantage to replace or combine the passive treatment with an active immunization using a mimotope. The success of such an approach has already been demonstrated with the use of mimotopes as experimental oral anti-IgE vaccines (18) and as minigenes of carbohydrate antigens to induce functional anti-carbohydrate response (19).

### 3. ANTIBODY-DEPENDENT CYTOTOXICITY

Despite the clinical success of several antibodies, such as the anticolorectal mAb 17-1A (20), we still know surprisingly little about how mAbs operate. In the 1980s, following extensive work *in vitro* and in animals, most workers accepted that opsonisation and ADCC were the major mechanisms operating in mAb-mediated immunotherapy. During this period, studies showed that mouse IgG2a was the most active subclass in ADCC, especially with activated macrophages, and it was IgG2a that

was most effective at prolonging survival of tumor-bearing mice (21-23). This strong correlation between therapeutic performance *in vivo* and ADCC activity *in vitro* helped establish the hypothesis that cytotoxic cellular effectors provided the main arm of mAb activity.

Results of the present study appeared to confirm the importance of ADCC in cancer immunotherapy when it was found that the mAb BCD-F9 as well as AM-F9 antiserum have both the ability to kill HT-1080 tumor cells by ADCC (Fig.2.7 and Fig.4.5). Throughout these *in vitro* investigations, conclusive evidence was also found that implicated complement as an important cytotoxic effector for antitumor activity for both antibodies (Fig.4.2). The later mechanism, however, has an important obstacle to mAb therapy since most tumor cells express complement down-regulating factors (24,25).

In the last experiment, it was rather an unexpected finding that although AM-F9 antiserum elicits ADCC by murine effector cells *in vitro*, depletion of NK cells did not increase tumor growth *in vivo* (Fig.4.8). Although, the possible mechanisms of action that can explain this discrepancy have been vigorously discussed in Chapter 4, some mAbs may operate via other mechanisms. In particular, it now appears that by crosslinking or blocking membrane receptors, mAbs may generate transmembrane signals that directly alter or control tumor growth - potentially leading to apoptosis (26). In this way, the anti-idiotypic mAbs appears to be acting as a surrogate antigen that binds to the variable regions of the B cell antigen-receptor and mimics or modulates its signaling activity. Anti-idiotypic mAbs are not ideal for ADCC because they tend to be internalized by lymphoma cells but they remain the most effective mAb treatment for NHL to date (27,28). There is also evidence that anti-CD19 and anti-CD20 mAbs exert their antitumor activities predominantly, if not exclusively, by signaling growth arrest and apoptosis (29,30). These observations have important implications for mAb immunotherapy since they underline the importance of FcR-bearing cells, not as cytotoxic effectors but as multivalent surfaces that provide hyper-crosslinking to mAb-coated target cells. Such crosslinking increases the likelihood of transmembrane signaling and is also known to enhance antigenic modulation and the release of cytokines such as IL-2.



Although AM-F9 antiserum was efficient at recruiting natural effectors for ADCC *in vitro*, it was clearly also capable of controlling tumor cell growth *in vivo* by another, unfortunately unidentified mechanism. Nevertheless, given the success of AM-F9 and BCD-F9 antibodies in human xenograft nude mouse models, one would suggest that the mAb BCD-F9 and AM-F9 antiserum could potentially both be used to induce a beneficial anti-tumor response.

#### 4. ELUCIDATION OF DRUG-BINDING SITE

Defining the number and the characteristics of the binding sites of P-gp represents an important step in understanding how this protein can handle so many different ligands. Several groups have investigated the way two different compounds interfere with each other, as regards to their interaction with P-gp, using binding studies or P-gp ATPase assays. All kinds of interactions have been reported, including competitive, noncompetitive or mixed inhibition. These results indicate presence of several binding sites or one large complex binding domain (31-34). These data would appear to be consistent with a model offering multiple binding points on the lipid-exposed brace of P-gp. Binding could occur through hydrophobic interactions or through hydrogen bonding, especially near the of interfaces. Indeed, the capacity to form hydrogen bonds has been pointed out as a distinctive feature of P-gp-interacting compounds (35). Additionally, the presence of polar groups on steroids affects binding to P-gp, and amino acids critical to this interaction appear to be located near the interface (36).

Results, presented in Chapter 5 of the present work, describe peptide ligands that can specifically bind doxorubicin (Table 5.1). More detailed studies of selected V6 phage have revealed its ability to interact with MDR drugs of different classes with the same selectivity pattern as P-gp (Fig. 5.2). This has led us to conclude that the selected peptides are at least functionally relevant to the P-gp drug-binding domain. The fact that the monospecific antibody against V6 phage is cross-reactive with P-gp indicates that the VCDWWGWGIC peptide has not only functional, but also some structural analogy with the drug-binding site located in the P-gp molecule (Fig. 5.3).

The examination of the primary structure of P-gp has not revealed any WXXW sequence allowing a speculation that the peptides generated using our phage display library could mimic a nonlinear site involved in the drug binding, that may be formed by two or more regions on the P-gp polypeptide chain. The fact that the positions of eleven tryptophane residues in the P-gp polypeptide chain are conserved among different species supports the idea that these amino acid residues could be involved in the formation of functional sites on the P-gp molecule. The model illustrated in Figure 6.1, where at least two different regions of the P-gp polypeptide chain approach each other to form a single binding site during drug recognition has been presented during 21<sup>th</sup> Meeting of the International Association for Breast Cancer Research (Paris, July, 1996). This schematic 3-D representation of P-gp was based on a possible organization of 12 TM  $\alpha$ -helices, in which the two related halves of P-gp are organized in twofold symmetry (37). The orientation of symmetry was based on cross-linking studies showing proximity between helix 6 and helix 12 (38).

Other evidence, however, suggests that certain substrates can be extracted directly from the cellular membrane into the external phase. Stein proposed that the P-gp tertiary structure displays a water-accessible cavity into which substrates would be moved, prior to being released by P-gp into the external medium (39). This model supported by the published low resolution structure of P-gp, which displays a large solvent-accessible cavity in the core of the protein (40). Finally, the unusual and elusive nature of P-gp as a membrane transporter has led to the abandoning of the idea that P-gp is a pump. In this case, the necessity for P-gp to compete with relatively fast diffusion kinetics and the energetic cost required removing a hydrophobic drug from the lipid phase towards aqueous medium, along with the broad substrate specificity of P-gp, are considered as strong arguments against P-gp being a primary transporter (41,42).

Results, presented in Chapter 5, suggest that the peptides mimicking the drug-binding properties of P-gp represent a useful tool for identification of common features of highly diversified MDR drug molecules. Such a tool could substantially facilitate the design of new drugs, as well as generate new important information on the application of peptides for drug design.

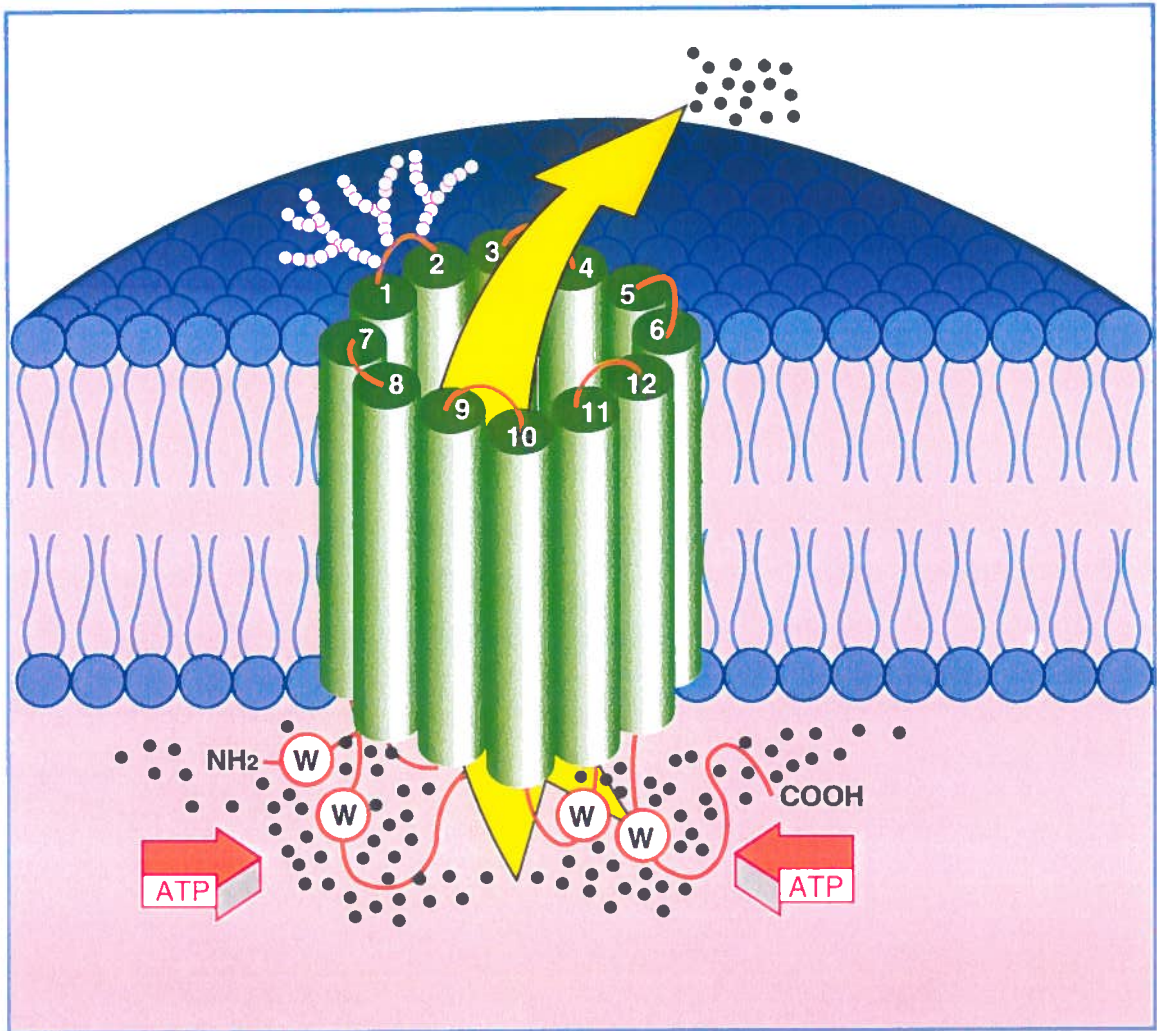


**Figure 6.1. Schematic 3-D Representation of the Human P-glycoprotein.**

## 5. REFERENCES

1. Meloen, R. H., W. C. Puijk, and J. W. Slootstra. 2000. "Mimotopes: realization of an unlikely concept". J. Mol. Recognit., vol. 13, p. 352-359.
2. Stoute, J. A., W. R. Ballou, N. Kolodny, C. D. Deal, R. A. Wirtz, and L. E. Lindler. 1995. "Induction of humoral immune response against *Plasmodium falciparum* sporozoites by immunization with a synthetic peptide mimotope whose sequence was derived from screening a filamentous phage epitope library". Infect. Immun., vol. 63, p. 934-939.
3. Meola, A., P. Delmastro, P. Monaci, A. Luzzago, A. Nicosia, F. Felici, R. Cortese, and G. Galfre. 1995. "Derivation of vaccines from mimotopes. Immunologic properties of human hepatitis B virus surface antigen mimotopes displayed on filamentous phage". J. Immunol., vol. 154, p. 3162-3172.
4. Cohen, G. B., R. Ren, and D. Baltimore. 1995. "Modular binding domains in signal transduction proteins". Cell, vol. 80, p. 237-248.
5. Oldenberg, K. R., D. Loganathan, I. J. Goldstein, P. G. Schultz, and M. A. Gallop. 1992. "Peptide ligands for a sugar-binding protein isolated from a random peptide library". Proc. Natl. Acad. Sci. USA, vol. 89, p. 5393-5397.
6. Hoess, R. H., U. Brinkmann, T. Handel, and I. Pastan. 1993. "Identification of a peptide which binds to the carbohydrate-specific monoclonal antibody B3". Gene, vol. 128, p. 43-49.
7. Devlin, J. J., L. C. Panganiban, and P. E. Devlin. 1990. "Random peptide libraries: A source of specific protein binding molecules". Science, vol. 249, p. 404-406.
8. Kay, B. K., N. B. Adey, Y.-S. He, J. P. Manfredi, A. H. Mataragnon, and D. M. Fowlkes. 1993. "An M13 phage library displaying random 38-amino-acid peptides as a source of novel sequences with affinity to selected targets". Gene, vol. 128, p. 59-65.
9. McLafferty, M. A., R. B. Kent, R. C. Ladner, and W. Markland. 1993. "M13 bacteriophage displaying disulfide-constrained microproteins". Gene, vol. 128, p. 29-36.
10. Kooyman, D. L., S. B. McClellan, W. Parker, P. L. Avissar, M. A. Velardo, J. L. Platt, and J. S. Logan. 1996. "Identification and characterization of a galactosyl peptide mimetic. Implications for use in removing xenoreactive anti-A Gal antibodies". Transplantation, vol. 61, p. 851-855.
11. Roberts, D., K. Gueler, and J. Winter. 1993. "Antibody as a surrogate receptor in

the screening of a phage display library". Gene, vol. 128, p. 67-69.

12. Balass, M., Y. Heldman, S. Cabilly, D. Givol, E. Katchalski-Katzir, and S. Fuchs. 1993. "Identification of a hexapeptide that mimics a conformation-dependent binding site of acetylcholine receptor by use of a phage-epitope library". Proc. Natl. Acad. Sci. USA, vol. 90, p. 10638-10642.
13. Schroff, R.W., K. A. Foon, R. J. Billing, and J. L. Fahey. 1982. "Immunologic classification of lymphocytic leukemias based on monoclonal antibody-defined cell surface antigens". Blood, vol. 59, p. 207-215.
14. Bodey, B., B. Bodey Jr., S. E. Siegel, and H. E. Kaiser. 2000. "Genetically engineered monoclonal antibodies for direct anti-neoplastic treatment and cancer cell specific delivery of chemotherapeutic agents". Curr. Pharm. Des., vol. 6, p. 261-276.
15. Maloney, D. G. 1999. "Advances in the immunotherapy of hematologic malignancies: cellular and humoral approaches". Curr. Opin. Hematol., vol. 6, p. 222-228.
16. Holliger, P. and H. Hoogenboom. 1998. "Antibodies come back from the brink". Nature Biotech., vol. 16, p. 1015-1016.
17. Panousis, C. and G. A. Pietersz. 1999. "Monoclonal antibody-directed cytotoxic therapy: potential in malignant diseases of aging". Drugs Aging, vol. 15, p. 1-13.
18. Zuercher, A. W., S. M. Miescher, M. Vogel, M. P. Rudolf, M. B. Stadler, and B. M. Stadler. 2000. "Oral anti-IgE immunization with epitope-displaying phage". Eur. J. Immunol., vol. 30, p. 128-135.
19. Kieber-Emmons, T., B. Monzavi-Karbassi, B. Wang, P. Luo, and D. Weiner. 2000. "DNA immunization with minigenes of carbohydrate mimotopes induce functional anti-carbohydrate antibody response". J. Immunol., vol. 165, p. 623-627.
20. Riethmuller, G., E. Holz, G. Schlimok, W. Schmiegel, R. Raab, K. Hoffken, R. Gruber, I. Funke, H. Pichlmaier, H. Hirche, P. Buggisch, J. Witte, and R. Pichlmayr. 1998. "Monoclonal antibody therapy for resected Dukes' C colorectal cancer: seven-year outcome of a multicenter randomized trial". J. Clin. Oncol., vol. 16, p. 1788-1794.
21. Herlyn, D. and H. Koprowski. 1982. "IgG2A monoclonal antibodies inhibit human tumor growth through interaction with effector cells". Proc. Natl. Acad. Sci. USA, vol. 79, p. 4761-4765.
22. Denkers, E. Y., C. C. Badger, J. A. Ledbetter, and I. D. Bernstein. 1985.

- "Influence of antibody isotype on passive serotherapy of lymphoma". J. Immunol., vol. 135, p. 2183-2186.
23. Kaminski, M. S., K. Kitamura, D. G. Maloney, M. J. Campbell, and R. Levy. 1986. "Importance of antibody isotype in monoclonal anti-idiotypic therapy of a murine B cell lymphoma. A study of hybridoma class switch variants". J. Immunol., vol. 136, p. 1123-1130.
  24. Morgan, B. P. 1999. "Regulation of the complement membrane attack pathway". Crit. Rev. Immunol., vol. 19, p. 173-198.
  25. Gorter, A. and S. Meri. 1999. "Immune evasion of tumor cells using membrane-bound complement regulatory proteins". Immunol. Today, vol. 20, p. 576-582.
  26. O'Hagan, R. C. and J. A. Hassell. 1998. "The PEA3 Ets transcription factor is a downstream target of the HER2/Neu receptor tyrosine kinase". Oncogene, vol. 16, p. 301-310.
  27. Vuist, W. M. J., R. Levy, and D. G. Maloney. 1994. "Lymphoma regression induced by monoclonal anti-idiotypic antibodies correlates with their ability to induce Ig signal transduction and is not prevented by tumor expression of high levels of Bcl-2 protein". Blood, vol. 83, p. 899-906.
  28. Davis, T. A. and S. J. Horning. 1998. "Advances in the management of Hodgkin's and non-Hodgkin's lymphoma". Curr. Opin. Hematol., vol. 5, p. 259-263.
  29. Ghetie, M.-A., L. J. Picker, J. A. Richardson, K. Tucker, J. W. Uhr, and E. S. Vitetta. 1994. "Anti-CD19 inhibits the growth of human B-cell tumor lines *in vitro* and of Daudi cells in SCID mice by inducing cell cycle arrest". Blood, vol. 83, p. 1329-1336.
  30. Shan, D., J. A. Ledbetter, and O. W. Press. 1998. "Apoptosis of malignant human B cells by ligation of CD20 with monoclonal antibodies". Blood, vol. 91, p. 1644-1652.
  31. Dey, S., M. Ramachandra, I. Pastan, M. M. Gottesman, and S. V. Ambudkar. 1997. "Evidence for two nonidentical drug-interaction sites in the human P-glycoprotein". Proc. Natl. Acad. Sci. USA, vol. 94, p. 10594-10599.
  32. Pascaud, C., M. Garrigos, and S. Orlowski. 1998. "Multidrug resistance transporter P-glycoprotein has distinct but interacting binding sites for cytotoxic drugs and reversing agents". Biochem. J., vol. 333, p. 351-358.
  33. Shapiro, A. B., K. Fox, P. Lam, and V. Ling. 1999. "Stimulation of P-glycoprotein-mediated drug transport by prazosin and progesterone. Evidence for a third drug-binding site". Eur. J. Biochem., vol. 259, p. 841-850.

34. Sonveaux, N., C. Vigano, A. B. Shapiro, V. Ling, and J. M. Ruyschaert. 1999. "Ligand-mediated tertiary structure changes of reconstituted p-glycoprotein". J. Biol. Chem., vol. 274, p. 17649-17654.
35. Ecker, G., M. Huber, D. Schmid, and P. Chiba. 1999. "The importance of a nitrogen atom in modulators of multidrug resistance". Mol. Pharmacol., vol. 56, p. 791-796.
36. Vo, Q. D. and D. J. Gruol. 1999. "Identification of p-glycoprotein mutations causing a loss of steroid recognition and transport". J. Biol. Chem., vol. 274, p. 20318-20327.
37. Higgins, C. F., R. Callaghan, K. J. Linton, M. F. Rosenberg, and R. C. Ford. 1997. "Multidrug resistance protein – structure of the multidrug resistant P-glycoprotein". In P. Borst (ed.). Seminars in Cancer Biology, London: Academic Press.
38. Loo, T. W. and D. M. Clarke. 1996. "Inhibition of oxidative cross-linking between engineered cysteine residues at position 332 in predicted transmembrane segments (TM) 6 and 975 in predicted TM12 of human P-glycoprotein by drug substrates". J. Biol. Chem., vol. 271, p. 27482-27487.
39. Stein, W. D. 1997. "Kinetics of the multidrug transporter (P-glycoprotein) and its reversal". Physiol. Rev., vol. 77, p. 545-590.
40. Rosenberg, M. F., R. Callaghan, R. C. Ford, and C. F. Higgins. 1997. "Structure of the multidrug resistance P-glycoprotein to 2.5 nm resolution determined by electron microscopy and image analysis". J. Biol. Chem., vol. 272, p. 10685-10694.
41. Wadkins, R. M. and P. D. Roepe. 1997. "Biophysical aspects of P-glycoprotein-mediated multidrug resistance". Int. Rev. Cytol., vol. 171, p. 121-165.
42. Roepe, P. D. 1998. "The P-glycoprotein efflux pump: how does it transport drugs?". J. Membr. Biol., vol. 166, p. 71-73.

## **CONCLUSION**



The work described in this thesis has attempted to identify the peptide molecules with potential in anti-cancer therapy. We have demonstrated that the epitope recognized by the mAb BCD-F9 was not restricted to the breast cancer cell lines. The findings reported in this study suggest that it is also present to various degrees on other neoplastic cell lines from different origin: colon carcinoma, sarcoma, lymphoma, and leukemia. A common reactivity with BCD-F9 implies that these cell lines share a common surface antigen or express different molecules with common or cross-reactive epitopes.

The reactivity of the mAb BCD-F9 with the human fibrosarcoma HT-1080 enabled us to use this cell line to investigate the antitumor properties of BCD-F9 in an experimental animal model. The obtained results showed that repeated i.v. inoculation of BCD-F9 in HT-1080-transplanted CD-1 nude mice significantly reduced tumor growth rate in animals transplanted s.c. and completely abrogated the development of lung metastases in mice transplanted intravenously. Our in vitro studies of BCD-F9-dependent killing of HT-1080 cells confirmed that ADCC and ADCMC are the two potential mechanisms for the antitumor activity observed in BCD-F9-treated animals. These results suggest that broad recognition of neoplastic cell lines from different origin identifies mAb BCD-F9 as a potentially useful immunotherapeutic reagent. It is worthwhile to study whether mAb BCD-F9 will be capable to suppress the tumor cells growth and metastasis of other human tumor cells as it did against HT-1080 fibrosarcoma.

We have further used the mAb BCD-F9 to identify peptides that mimic the epitope recognized by this antibody. The selected phage encoded for the unique sequence GRRPGGWWMR expressing the peptide capable of binding to the mAb BCD-F9. Immunization of rabbits with this synthetic peptide-mimotope induced polyclonal antibodies (AM-F9) capable of blocking the binding of the mAb BCD-F9 to HT-1080 tumor cells. Using an aggressive lung metastatic model, we have demonstrated that AM-F9 administrated i.v. significantly prolonged the life span of CD-1 nude mice inoculated i.v. with HT-1080 human fibrosarcoma cells.

These initial findings have since been followed by an additional study that has started to further investigate the properties of AM-F9 antiserum. We have found that treatment with AM-F9 significantly inhibited the growth of HT-1080 tumor cells inoculated s.c. into CD-1 nude mice. We have also investigated the antitumor activity of

AM-F9 in vitro in ADCMC and ADCC assays, and demonstrated that, in this model, ADCMC is likely to be a major mechanism responsible for tumor cell killing. These findings suggest that a peptide mimotopes can be potentially used as a novel immunotherapy to induce a beneficial anti-tumor response.

Finally, we have used phage display libraries to generate peptide ligands that can bind MDR drugs mimicking, in this respect, the drug binding activity of P-glycoprotein. We have showed that the phages expressing the peptides, which contain the core consensus motif WXXW, bound MDR type drugs (vinblastine, doxorubicin, verapamil, and genistein) with the same selectivity as P-glycoprotein and did not interact with non-MDR type drugs, such as arabinosylcytosine (Ara-C) and melphalan. We have also demonstrated that monospecific antibody obtained against the phage expressing VCDWWGWGIC peptide could specifically recognize P-glycoprotein in the membrane fraction of MDR phenotype MCF-7ADR cells. The MDR drug-binding sequences generated during this work could provide an important tool for design and screening of new chemotherapeutical agents.

## **Appendix A**

### **List of Communications**

1. Popkov, M., Y. Lusignan, S. Lemieux et R. Mandeville. 1999. "Immunothérapie antitumorale avec antisérum anti-mimotope chez la souris nude: analyse de mécanismes d'action". In 1<sup>er</sup> Congrès Interne INRS-Institut Armand-Frappier (Magog-Orford, Novembre 1999).
2. Popkov, M., S. Sidrac-Ghali, V. Alakhov, and R. Mandeville. 1999. "Identification of a peptide mimotope capable of inducing anti-tumor immune response using a phage display library". In Molecular Library Technilgies at the Millennium (San Francisco, October 1999).
3. Mandeville, R., Y. Lusignan, S. Lemieux, and M. Popkov. 1999. "Immunotherapy with anti-mimotope polyclonal antibodies in a nude mouse xenograft model: mechanisms of action". In Molecular Library Technilgies at the Millennium (San Francisco, October 1999).
4. Popkov, M., S. Sidrac-Ghali, V. Alakhov, and R. Mandeville. 1999. "Identification of a peptide mimotope capable of inducing anti-tumor immune response using a phage display library". In IBC's 4<sup>th</sup> Annual International Conference on Phage Display (Brussels, September 1999).
5. Popkov, M., P.-O. Esteve, V. Medvedkine, V. Alakhov, and R. Mandeville. 1996. "Elucidation of an MDR drug-binding site using a phage display library". In 21<sup>th</sup> Meeting of the International Association for Breast Cancer Research (Paris, July 1996).
6. Mandeville, R., M. Popkov, and S. Sidrac-Ghali. 1996. "Identification and molecular characterization of an antigen-binding site recognized by BCD-F9 monoclonal antibody using phage display technology". In 13<sup>th</sup> International Hammersmith Conference: Advances in the Applications of Monoclonal Antibodies in Clinical Oncology (Crete, May 1996).
7. Lussier, I., M. Popkov, and R. Mandeville. 1996. "Development of specific antisera to the extracellular domain of the P-gp molecule" In 10<sup>th</sup> Spring Meeting of the Canadian Society for Immunology (Sainte-Adele, March 1996).
8. Popkov, M., M. Houde, and R. Mandeville. 1994. "Construction d'une banque peptidique de dix acides aminés avec un bactériophage" In 62 Congrès de l'ACFAS (Montréal, Mai 1994).

**Appendix B**  
**Copies of Articles**

Pour des raisons de droits d'auteur, les pages des articles suivants ont été retirées de ce document.

POPKOV, M., LUSSIER, I., MEDVEDKINE, V., ESTÈVE, P. O., ALAKHOV, V. & MANDEVILLE, R. (1998) Multidrug-resistance drug-binding peptides generated by using a phage display library. European Journal of Biochemistry, 251, 1-2, 155-163

L'article se trouve à l'adresse URL suivante :

<http://dx.doi.org/10.1046/j.1432-1327.1998.2510155.x>

POPKOV, M., SIDRAC-GHALI, S., ALAKHOV, V. & MANDEVILLE, R. (2000) Epitope-specific antibody response to HT-1080 fibrosarcoma cells by mimotope immunization. Clinical Cancer Research, 6, 9, 3629-3635,

L'article se trouve à l'adresse URL suivante :

<http://clincancerres.aacrjournals.org/cgi/pmidlookup?view=long&pmid=10999755>